UNIVERSITY OF THE
WITWATERSRAND,
JOHANNESBURG

Design and Optimization of a Bioprocess to Simultaneously Produce Biochemicals and Remediate Acid Mine Drainage Using Indigenous South African Grasses

PhD Dissertation

Prepared by

Nicholas W. Burman (1474213)

Submitted to

School of Chemical and Metallurgical Engineering, Faculty of Engineering and the Built Environment, University of the Witwatersrand, Johannesburg, South Africa

Supervisor(s):

Kevin Harding

Craig Sheridan

June 2020

Declaration

I declare that this dissertation is my own unaided work. It is being submitted for the degree of Doctor of Philosophy in Engineering to the University of the Witwatersrand, Johannesburg. It has not been submitted before for any degree or examination to any other university.

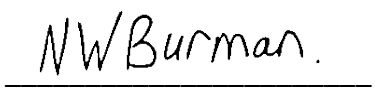

Nicholas Westley Burman

10th of June 2020

Summary

Acid mine drainage (AMD) is highly acidic water, with a high dissolved sulfate and metal concentration, that is produced through mining activity. AMD has a negative effect on natural ecosystems into which it flows and negatively impacts national water security. The impacts of AMD are widespread in the Witwatersrand mining area and Mpumalanga coalfields in South Africa. As South Africa is a water-scarce country it is imperative to efficiently remediate AMD and protect natural water resources. One method that has been investigated for AMD remediation is dissimilatory sulfate reduction (DSR), which is catalyzed through sulfate-reducing bacteria (SRB). DSR converts highly acidic sulfuric acid into weaker hydrogen sulfide, which raises the pH and results in the precipitation of metals. SRB require a carbon source that can be supplied in the form of lignocellulosic biomass. The acidity present in the AMD breaks apart the lignocellulosic biomass, releasing xylose into the water, which can then be utilized by the SRB.

Lignocellulosic biomass has also been identified as a good source of biomass for the production of biochemicals. One of the main drawbacks of using lignocellulosic biomass as a feedstock is that the presence of the ligno-hemicellulosic matrix prevents cellulase enzymes from accessing the cellulose fibrils, which are broken down to glucose and subsequently fermented to biochemicals. To overcome this the biomass first needs to be pre-treated to break apart the ligno-hemicellulosic matrix. Various pre-treatment methods have been investigated (physical, chemical, physico-chemical, biological) but pre-treatment with sulfuric acid has been identified as the most commercially feasible pre-treatment.

As the breakdown of lignocellulose for DSR remediation of AMD is similar to the pre-treatment of lignocellulosic biomass, there is the potential to combine these two processes. Biomass can undergo pre-treatment with AMD, releasing xylose into the AMD which can be utilized by SRB for DSR. The biomass can then undergo enzymatic hydrolysis to release glucose that can be fermented to produce various biochemicals. This study investigated the design, optimization, and feasibility of this simultaneous process.

The investigation started with the evaluation of different biorefinery options based on the biorefinery complexity profile (BCP). Indigenous South African grass was found to be the most suitable feedstock due to its abundance in the regions where AMD is generated. The use of xylose as a substrate for SRB, and the production of bioethanol through glucose fermentation was found to be the most feasible biorefinery option. The production of additional high-value chemicals from glucose, and processing of lignin and distillery silage into valuable products were also identified as options to increase the economic feasibility of the biorefinery.

Next, the optimal configuration of reactors to pre-treat biomass and perform DSR was investigated, through developing flowsheets for three different reactor configurations. It was found that the rate of hydrolysis of biomass is severely rate-limiting, and the only process which shows any promise for commercial implementation is one in which hydrolysis of biomass is operated at elevated temperatures (~100°C), in a stand-alone hydrolysis reactor separate from the DSR reactor. Sensitivity analyses revealed that the design was highly sensitive to the kinetic data used, and the temperature at which the pre-treatment reactor operates.

As the design was found to be highly sensitive to the kinetic data used, the rate of dilute sulfuric acid hydrolysis of indigenous South African grass, at low temperatures (<100°C), was investigated. The

xylan (hemicellulose) was found to have two distinct fractions, which react at significantly different rates. The rate of reaction of one fraction was found to display Arrhenius type temperature dependence (Ea = 155.06 kJ/mol, A_0 = 1.65×10^{19}/min), whereas the rate of the reaction of the other fraction was so slow it could be considered negligible. The portion of the fraction with a slower rate of reaction was found to be 50%, which is lower than previously determined (55 – 100%).

Following this, the optimal conditions for the production of bioethanol from biomass were investigated. This included investigating the optimal pre-treatment time, the optimal pre-treatment solid loading, and the glucose and ethanol yield in both separate hydrolysis and fermentation (SHF) and simultaneous saccharification and fermentation (SSF), for biomass pre-treated with AMD or H_2SO_4. Empirical models were also developed to predict the glucose and ethanol concentration over time. In both SHF and SSF pre-treatment using AMD was found to achieve a glucose/ ethanol concentration that was 70 – 80% of that achieved from pre-treatment with H_2SO_4. The empirical models had a high correlation (r^2 = 0.87 – 0.99) to experimental data.

An Aspen Plus™ flow sheet was then developed and used to perform a techno-economic evaluation to determine the economic feasibility of a lignocellulosic bioethanol facility that uses AMD pre-treatment of biomass. Both SHF and SSF reactor configurations were considered, and evaluations with H_2SO_4 pre-treatment were also performed for comparison. Simple estimations for capital and operating costs were used to estimate the economic feasibility of all scenarios. Only the Scenario with H_2SO_4 pre-treatment and SHF was found to make a profit, although the profit was so small the payback period would be 80.7 years, making the process infeasible. SHF was found to be better suited to the process than SSF for both AMD and H_2SO_4 pre-treatment.

Finally, a techno-economic evaluation was performed on a simultaneous AMD remediation and lignocellulosic bioethanol production facility. As previous studies showed that having separate pre-treatment and DSR, as well as SHF, is more feasible the techno-economic evaluation was based on this. The minimum ethanol selling price (MESP) was calculated using discounted cash flow methods and found to be 3 114 USD/ton ethanol. Although this is higher than recent historical prices sensitivity analyses revealed that there are various opportunities to reduce the MESP substantially. The MESP was especially sensitive to the ethanol yield and the operating temperature of the pre-treatment reactor. An evaluation at ethanol yields that are considered to be achievable and slightly increased pre-treatment temperatures (+20°C) resulted in an MESP of 741 USD/ton. This is within the recent historical prices, and indicates the process could be feasible at these conditions and favorable ethanol prices.

Financial Acknowledgements

I would like to acknowledge the following for their financial support of this research:

- The National Research Foundation of South Africa (NRF);
- The German Academic Exchange Service (DAAD);
- The University of the Witwatersrand;
- The Global Change Institute (GCI); and
- The institution of Chemical Engineers – Biochemical Engineering Special Interest Group (IChemE BESIG).

Personal Acknowledgements

I would like to personally thank the following people who have enabled me to conduct this research:

- Professors Kevin Harding and Craig Sheridan for their outstanding supervision;
- Janet Smith and Mohlatsi Phala for their excellent technical support and analytical services;
- Karl Rumbald for his guidance with microbiology related queries;
- Uwe Kappelmeyer for his brilliant supervision while I was at the Helmholtz Centre for Environmental Research, in Leipzig, Germany;
- The staff of the School of Chemical and Metallurgical Engineering, for all of their assistance along the way;
- My Father, Mother and Sister for their support and guidance; and most importantly
- Samantha Robb for all the love, support and encouragement.

Table of Contents

Table of Figures

List of Tables

Nomenclature

Nomenclature used in multiple chapters of the dissertation

k_f	Rate of reaction for fast reacting fraction of xylan	kmol/hr
K_s	Rate of reaction for slow reacting fraction of xylan	kmol/hr
k_2	Rate of reaction of xylose to degradation products	kmol/hr
A_0	Pre-exponential factor	/hr
Ca	Acid concentration	wt% H_2SO_4
n	Empirical exponential	-
Ea	Activation energy	kJ/mol
T	Temperature	K
R	Universal gas constant	8.31 x 10^{-3} kJ/mol.K

Nomenclature specific to Chapter 4

ϵ_1	Extent of reaction of hydrolysis reaction	-
$X_{C_5H_8O_4}$	Conversion of xylan	%
$n_{C_5H_8O_4,i}$	Total initial moles of xylan	-
$n_{C_5H_8O_4,f}$	Number of moles of xylan remaining	-
$\dot{n}_{C_5H_{10}O_5,2.1}$	Flow rate of xylose in stream 2.1	kmol/hr
$\dot{n}_{C_5H_{10}O_5,1}$	Flow rate of xylose in stream 1	kmol/hr
t	Reaction batch time	hr
ϵ_1^*	Time dependent extent of reaction	kmol/hr
$\epsilon_{2,1,i}$	Extent of reaction for Equation 4.1 in reactor i in Process 3	kmol/hr
$X_{C_5H_8O_4,i}$	Conversion of xylan in Equation 4.1 in reactor i in Process 3	%
$\dot{n}_{C_5H_8O_4,f,G(5-i)}$	Molar flow rate of xylan entering reactor i in Process 3	
ϵ_2	Extent of reaction for Equation 4.2	kmol/hr
ϵ_3	Extent of reaction for Equation 4.3	kmol/hr
$X_{SO_4,S}$	Conversion of sulfate in Equation 4.2 in Process 3	%
$X_{Fe^{2+},S}$	Conversion of iron in Equation 4.2 in Process 3	%
$\dot{n}_{Fe^{2+},3}$	Inlet molar flow rate of iron in Process 3	kmol/hr
$\dot{n}_{SO_4,3}$	Inlet molar flow rate of sulfate in Process 3	kmol/hr
ϵ_4	Extent of reaction of the reaction consuming H^+ ions	-
X_{H^+}	Consumption of H^+ ions	%
$\dot{n}_{H^+,3}$	Number of moles of H^+ in stream 3	kmol/hr

k_f	Rate of reaction for the fast reacting fraction of xylan	kmol/hr
k_s	Rate of reaction for the slow reacting fraction of xylan	kmol/hr
k_2	Rate of reaction for xylose	kmol/hr
$C_{C_5H_8O_4f}$	Concentration of fast reacting fraction of xylan	%
$C_{C_5H_8O_4s}$	Concentration of fast reacting fraction of xylan	%
$\epsilon_{3,1f,i}$	Extent of reaction of the hydrolysis of the fast reacting fraction of xylan in reactor i, in process 3	-
$\epsilon_{3,1S,i}$	Extent of reaction of the hydrolysis of the slow reacting fraction of xylan in reactor i, in Process 3	-
$\epsilon_{p,o}$	Extent of reaction o, in Process p	kmol/hr
$\dot{n}_{n,m}$	Molar flow rate of species n, in stream m	kmol/hr
$X_{C_5H_8O_4,f,i}$	Conversion of the fast reacting fraction of xylan in reactor i, in Process 3	%
$X_{C_5H_8O_4,s,i}$	Conversion of the slow reacting fraction of xylan in reactor i, in Process 3	%
$n_{C_5H_8O_4,f,(5-i)}$	Number of moles of fast reacting xylan entering reactor i in Process 3	kmol/hr
$n_{C_5H_8O_4,s,(5-i)}$	Number of moles of slow reacting xylan entering reactor i in Process 3	kmol/hr
r_{SO_4}	Rate of sulfate reduction	kmol/hr.m^3
k	Rate constant	kmol/hr.m^3
V	Volume of DSR recator	m^3
$\dot{n}_{SO_4}$	Molar flow rate of sulfate into the sulfate-reducing reactor	kmol/hr
X_{SO_4}	Conversion of sulfate in the sulfate-reducing reactor	%
$C_{C_5H_8O_4f,0}$	Initial concentration of the fast reacting fraction of xylan	wt%
$C_{C_5H_8O_4s,0}$	Initial concentration of the slow reacting fraction of xylan	wt%
$MW_{C_5H_8O_4}$	Molecular mass of xylan	g/mol
$\dot{M}_{grass}$	Mass flow rate of grass	kg/hr
$V_{hydrolysis}$	Volume of the hydrolysis reactor	m^3
θ	Solid loading of the biomass	%
ρ_{sludge}	Density of the sludge	kg/m^3
V_i	Volume of reactor i in Process 3	m^3
$\dot{n}_{n,wi}$	Molar flow rate of species n, in the liquid phase of stream i for Process 3	kmol/hr
$\dot{n}_{n,Gi}$	Molar flow rate of species n, in the solid phase of stream G for Process 3	kmol/hr

$\dot{n}_{C_5H_8O_4,f,G(5-i)}$	Molar flow rate of fast reacting xylan entering reactor i in Process 3	kmol/hr
$\dot{n}_{C_5H_8O_4,f,G(6-i)}$	Molar flow rate of fast reacting xylan exiting reactor i in Process 3	kmol/hr
$\dot{n}_{C_5H_8O_4,s,G(5-i)}$	Molar flow rate of slow reacting xylan entering reactor i in Process 3	kmol/hr
$\dot{n}_{C_5H_8O_4,s,G(6-i)}$	Molar flow rate of slow reacting xylan exiting reactor i in Process 3	kmol/hr
$\dot{n}_{n,Wi}$	molar flow rate of liquid phase species n entering reactor i, in Process 3	kmol/hr
$\dot{n}_{n,W(i+1)}$	molar flow rate of liquid phase species n, exiting reactor i, in Process 3	kmol/hr
$X_{C_5H_8O_4,tot}$	Total Conversion of xylose across the entire process	%

Nomenclature specific to Chapter 5

$C_{xylan,f}$	Concentration of fast reacting xylose	% wt/wt
$C_{xylan,s}$	Concentration of slow reacting xylose	% wt/wt
Ca	Actual acid concentration	wt% H_2SO_4
C	Original acid Concentration	wt% H_2SO_4
Solid Loading	Solid loading of biomass	%
NC	Neutralizing capacity of the biomass	$g_{H2SO4}/g_{biomass}$
Xr	Percentage of equivalent xylose units remaining in the solid residue	%
$X_{f,0}$	Initial percentages of fast reacting fraction	%
$X_{s,0}$	Initial percentages of slow reacting fraction	%
X_0	Initial equivalent xylose units	g/L
$C_{xylan,\ total}$	Concentration of xylan in biomass	%wt/wt
X_i	Equivalent xylose units remaining in solid residue	g/L
X_t	Measured xylose concentration at time t	g/L
α	Initial percentages of fast reacting fraction	%
X_{tot}	Total equivalent concentration of xylose	g/L
X	Measured concentration of xylose	g/L
F	Measured concentration of furfural	g/L

Nomenclature specific to Chapter 6 and 7

G	Glucose concentration	g/L
t_e	Time of enzymatic hydrolysis	hr
M_1	Empirical constant	-
C_1	Empirical constant	-
$m_{1,m}$	Empirical constant	-
$c_{1,m}$	Empirical constant	-
W	Biomass solid loading in hydrolysis	wt%
r_g	Rate of reaction in fermentation growth phase	g/L.hr
r_s	Rate of reaction in fermentation stationary phase	g/L.hr
G_0	Initial glucose concentration at start of fermentation	g/L
t_f	Fermentation time	hr
E	Ethanol concentration	g/L
$Y_{\frac{A}{P}}$	Yield of ethanol from glucose consumed	g/g
M_2	Empirical constant	-
C_2	Empirical constant	-
$m_{2,C}$	Empirical constant	-
$c_{2,C}$	Empirical constant	-
t_s	Time of SSF	hr

Nomenclature specific to Chapter 8

DCF_n	Discounted cash flow in year n	MUSD
CF	Cash Flow in year n	MUSD
R	Internal rate of return	%
n	Number of years since evaluation year	-
NPV_n	Net present value at year N	MUSD
t_n	New time to achieve equivalent level of pre-treatment	hr

Acronyms

ABC	Allkali-Barium-Calcium
ABR	Anaerobic Baffled Reactors
AFEX	Ammonia Fiber Explosion Process
AIL	Acid Insoluble Lignin
AMD	Acid Mine Drainage
ASL	Acid Soluble Lignin
BCI	Biorefinery Complexity Index
BCP	Biorefinery Complexity Profile
CBH	Exo-β-1,4-cellobiohydrolase
CBP	Consolidated Bioprocessing
COD	Chemical Oxygen Demand
CSRI	Council for Scientific and Industrial Research
CSTR	Continuously Stirred Tank Reactor
DSR	Dissimilatory Sulfate Reduction
DWA	Department of Water Affairs
DWS	Department of Water and Sanitation
ECL	Environmentally Critical Level
EG	Endo-β-1,4-Glucanase
EGSB	Expended Granular Sludge Bed
FBR	Fluidized Bed Reactors
FC	Feature Complexity
FPU	Filter Paper Unit
GCI	Global Change Institute
GLB	Gas-Lift Reactor
GLR	Gas-Lift Reactor
HMF	5-hydroxymethyl-furfural
HPLC	High Performance Liquid Chromatography
HRT	Hydraulic Retention Time
IEA	International Energy Agency

ILs	Ionic Liquids
MB	Membrane Bioreactor (sulfate-reducing bioreactor)
MBR	Membrane Bioreactor (enzymatic hydrolysis and fermentation)
MESP	Minimum Ethanol Selling Price
MLST	Multi Locus Sequence Typing
NREL	The National Renewable Energy Laboratory
NRF	National Research Foundation
NSSF	Non-Isothermal Simultaneous Saccharification and Fermentation
Organosolv	Organic Solvent Process
PFD	Process Flow Diagram
PHB	Poly-B-Hydroxybutyric Acid
PRB	Permeable Reactor Barriers
SAPS	Successive Alkalinity Producing Systems
SHF	Separate Hydrolysis and Fermentation
SRB	Sulfate-reducing Bacteria
SSCF	Simultaneous Saccharification and Co-fermentation
SSF	Simultaneous Saccharification and Fermentation
UASB	Up Flow Anaerobic Sludge Blanket Reactors
YPD	Yeast Peptone Dextrose

Chapter 1: Introduction

1.1. Introduction

South Africa is a water-scarce country, so it is vital that water resources in the country are adequately protected. Acid mine drainage (AMD) is highly acidic water with high dissolved metal and sulfate concentrations. It not only poses a threat to natural water systems but also to the aquatic ecosystems that it flows into. AMD is often produced as a result of mining activity making its effects prominent in both the Witwatersrand mining area and the Mpumalanga coalfields of South Africa (McCarthy, 2011). This prompted research into strategies and technologies to treat AMD. Current AMD treatment methods typically use a chemical pH neutralizing agent, which concurrently results in the precipitation of heavy metals (Taylor et al., 2005). Although moderately effective, this method is expensive and produces large volumes of toxic waste. Therefore, a sustainable, relatively low-cost environmentally conscious process is needed.

An AMD remediation technology that has been found to be more environmentally sustainable than chemical neutralization is dissimilatory sulfate reduction (DSR). This is catalyzed through sulfate-reducing bacteria (SRB), which reduce highly acidic sulfuric acid present in the AMD, to less acidic hydrogen sulfide. This increases the pH and results in the precipitation of dissolved metals, hence remediating the water. SRB require a carbon source to act as an electron donor, which can be supplied by various organic substrates including lignocellulosic biomass (Taylor et al., 2005).

Recently, there has been research into the remediation of AMD using SRB catalyzed DSR with indigenous South African grasses as a carbon source (Magowo et al., 2015; Ramla and Sheridan, 2015; Westensee et al., 2018). This research suggests that there is significant potential for using grass as an organic substrate for AMD remediation. It was found that the acid present in the AMD hydrolyzed part of the lignocellulose structure releasing sugars that were utilized by the SRB.

Lignocellulosic biomass consists of three fractions; cellulose fibrils (chains of linearly bound glucose molecules stacked together) surrounded by a matrix of hemicellulose (consisting of amorphous polysaccharides of hexose and pentose sugars) and lignin (consisting of amorphous phenol molecules). Lignocellulosic biomass has been used as a source of biomass

for the production of 2nd generation biofuels and biochemicals. The use of 2nd generation lignocellulosic bioethanol as an alternative to fossil fuels is necessary to reduce anthropogenic carbon emissions and limit the effects of climate change (IPCC, 2018, 2014a).

Although the production of 1st generation bioethanol from sugar and starch crops is a renewable alternative to fossil fuels, its production and use have been found to be a net emitter of carbon. There are other problems associated with 1st generation biofuels including an increase in food prices, lack of available land and land degradation (Cherubini, 2010).

In the production of lignocellulosic biofuels and chemicals, cellulose is hydrolyzed to produce glucose, which can undergo fermentation to bioethanol or other biochemicals. Unfortunately, the presence of the ligno-hemicellulosic matrix prevents enzymes from accessing the cellulose making hydrolysis inefficient. To overcome this, pre-treatment of the biomass is necessary to break apart the lignocellulosic biomass structure and improve enzyme access to the cellulose. Currently dilute sulfuric acid pre-treatment is the preferred pre-treatment method (Lenihan et al., 2010; Maurya et al., 2015).

In the remediation of AMD, the breakdown of lignocellulosic biomass is similar to the pre-treatment using dilute sulfuric acid. The two processes could thus be combined into one process to simultaneously remediate AMD and produce biofuels or biochemicals. Recently, such a process, in which fermentable sugars were produced from biomass pre-treated using AMD, while simultaneous remediating the AMD with SRB, was investigated (Magowo et al., 2015). It was found that SRB could effectively be used with indigenous South African grasses to remediate the AMD. Concomitantly, the sulfuric acid present in AMD can be used to pre-treat grass for subsequent enzymatic hydrolysis. Although this research showed that such a process was possible, little work was done on the design, optimization, and feasibility of such a process.

This dissertation aims to perform all the research necessary to design, optimize and determine the feasibility of a process to produce bioethanol from indigenous South African grass pre-treated with AMD, while simultaneously remediating the AMD with SRB. This research will be conducted using a combination of lab based experimentation and desktop based techno-economic evaluations using Microsoft Excel® and Aspen Plus™.

1.2. Problem Statement

Previous work by Ramla and Sheridan (2015) and Magowo *et al.* (2014) showed that acid mine drainage (AMD) can be remediated through sulfate-reducing bacteria catalyzed dissimilatory sulfate reduction, using indigenous South African grasses as a substrate. The work by Magowo *et al* (2014) also provided evidence that AMD could be used as a pre-treatment agent on grass. The sulfuric acid within AMD breaks down the lignocellulose in grass making it more susceptible to enzymatic hydrolysis for the production of fermentable sugars that can be further utilized to produce 2nd generation bioethanol and other biochemicals.

Although this body of literature demonstrated a proof of concept, little research was conducted into the design, optimization, and feasibility of a process that can be implemented on a commercial scale. Specific areas that need further investigation for the technical development of the process are:

- reactor configuration;
- reaction yields;
- reaction kinetics;
- optimization of integrated process; and
- process feasibility

1.3. Research Objective(s):

The objective of this dissertation is to perform the following:

a. A desktop study on the simultaneous remediation of AMD and pre-treatment of biomass. This will investigate optimal reactor configuration; estimate reactor sizing; and perform sensitivity analyses on the results;
b. An experimental investigation into the rate of dilute sulfuric acid pre-treatment of indigenous South Africa grass;
c. An experimental investigation into the rate of enzymatic hydrolysis and fermentation in both separate hydrolysis and fermentation (SHF) and simultaneous saccharification and fermentation (SSF), and the optimum conditions for the pre-treatment of grass;
d. A desktop study into the enzymatic hydrolysis of biomass pre-treated with AMD. This will investigate the optimal reactor configuration between SHF and SSF, estimate

capital and operating costs, and determine the feasibility of each reactor configuration; and

e. A desktop study into the optimum overall process to simultaneously remediate AMD and produce bioethanol through enzymatic hydrolysis and fermentation of pre-treated biomass. This will entail integrating the two desktop studies performed in (a) and (d) and incorporating all new knowledge and data determined through investigation. The results of this will be to recommend a design of a process that maximizes both the remediation of AMD and the production of bioethanol and determine the feasibility of such a process.

1.4. Methodology

This research was conducted through a combination of experimental (lab-based) investigations, flowsheet development, process optimization, and economic evaluations.

Experimental investigations were conducted using known laboratory techniques in the biochemical engineering laboratory in the School of Chemical and Metallurgical Engineering, at the University of the Witwatersrand, Johannesburg. All experiments were conducted at a scale smaller than 3L.

Flowsheet development was done using mass and mole balances and known chemical reactions and stoichiometry. This was based on yields determined experimentally and found in the literature. This flowsheet development was performed using both Microsoft Excel® and Aspen Plus™ V8.4 process simulation software from AspenTech (https://www.aspentech.com).

Process optimization was performed through both lab-based experiments, through determining optimum operating conditions (time, temperature, *etc*.), and through computer-based sensitivity analyses performed on both Microsoft Excel® and Aspen Plus™.

The estimation of capital and operating costs was performed using standard chemical engineering techniques, in addition to the Capcost program. Evaluation of the feasibility of the process used capital and operating cost estimates, and was performed using discounted cash flow methods (Turton et al., 1998).

1.5. Structure of Dissertation

This dissertation has been divided into 10 chapters. Chapters 1 and 2 are the introduction and background information respectively. Chapters 3 – 8 form the body of the dissertation, where the main research is presented. Each of these chapters has been written as a standalone article. Chapters 9 presents a discussion and conclusion for the entire dissertation, and the Appendices are presented in Chapter 10.

As the body chapters have been written as standalone articles, most of which have already been published, there is some repetition of the information presented in the background chapter (Chapter 2) in the introduction of subsequent chapters (Chapters 3 – 8). A discussion and conclusion section has been presented in each chapter, however, this is only for the content of that chapter, whereas the discussion and conclusion chapter (Chapter 9) aims to give an overall discussion and conclusion for the entire dissertation.

A summary of the work presented in each chapter is presented below:

Chapter 2: Background Information This chapter provides all the necessary background information for all of the chapters to follow and has been divided into three sections. **1.** An introduction to the generation, effect, and remediation of acid mine drainage (AMD). **2.** An introduction to biofuels, the biorefinery concept, and lignocellulosic biotechnology, with detailed information on the production of lignocellulosic bioethanol. **3.** A discussion of all previous studies investigating the production of bioethanol and simultaneous remediation of AMD.

Chapter 3: Evaluation of a Combined Lignocellulosic/Wastewater Biorefinery for the Simultaneous Production of Valuable Biochemical Products and the Remediation of Acid Mine Drainage *(Published in Biofuels, Bioproducts and Biorefineries, 2018)* This chapter investigates a process for the remediation of acid mine drainage and simultaneous production of biochemicals. Different biorefinery options are evaluated based on the biorefinery complexity profile. The most feasible process configurations were determined and recommendations into further research requirements are made. This addresses all objectives pertaining to desktop studies, *i.e.* objectives a, d, and e.

Burman, N.W., Harding, K.G., Sheridan, C.M., Van Dyk, L., 2018b. Evaluation of a combined lignocellulosic / wastewater biorefinery for the simultaneous production of valuable biochemical products and the remediation of acid mine drainage. Biofuels, Bioproducts, and Biorefining. 12, 649–664. doi:10.1002/bbb.1880

Chapter 4: Flowsheet and Sensitivity Analyses for the Bioremediation of Acid Mine Drainage Using Sulfate-reducing Bacteria and South African Grasses *(Presented at the 2nd International (Presented at the 2nd International Conference on Environmental Engineering and Climate Change, Mauritius, 2017)* This chapter developed process flowsheets for the remediation of AMD using SRB and simultaneous pre-treatment of lignocellulosic biomass. Three different reactor configurations were investigated, and the most suitable process configuration was determined based on estimates of the total reactor volumes. Knowledge gaps were identified and recommendations into further research were made. This chapter addresses objective a.

Burman, N.W., van Dyk, L., Postma, F., Sheridan, C., Simate, G.S., Harding, K.G., 2017. Flowsheet and Sensitivity Analyses for the Bioremediation of Acid Mine Drainage Using Sulfate Reducing Bacteria and South African Grasses, in: 2nd International Conference on Energy, Environment and Climate Change (ICEECC). Pointe Aux Piments, Mauritius.

Chapter 5: Modelling of Low Temperature Dilute Sulfuric Acid Pre-treatment of South African Grass *(Published in Bioresource Technology Reports, 2018)* This chapter experimentally investigated and determined the kinetics of dilute sulfuric acid hydrolysis of indigenous South African grass at low temperatures (<90°C). This addresses objective b.

Burman, N.W., Sheridan, C., van Dyk, L., Harding, K.G., 2018c. Modeling of low temperature dilute sulfuric acid pre-treatment of South African grass. Bioresource Technology Reports. 4, 21–28. doi:10.1016/j.biteb.2018.08.014

Chapter 6: Lignocellulosic Bioethanol Production from Grasses Pre-treated with Acid Mine Drainage: Modelling and Comparison of SHF and SSF (*Published in Bioresource Technology Reports, 2019)* This chapter experimentally determined the optimum conditions for pre-treatment and the rate of enzymatic hydrolysis and fermentation of biomass pre-treated with acid mine drainage. Both separate hydrolysis and fermentation (SHF) and simultaneous saccharification and fermentation (SSF) were investigated. This addresses objective c.

Burman, N.W., Harding, K.G., Sheridan, C.M., 2019b. Lignocellulosic Bioethanol Production from Grasses Pre-treated with Acid Mine Drainage. Modeling and Comparison of SHF and SSF. Bioresource Technology Reports. 7. doi:10.1016/j.biteb.2019.100299

Chapter 7: Feasibility Assessment of the Production of Bioethanol from Lignocellulosic Biomass Pre-treated with Acid Mine Drainage *(Published in Renewable Energy, 2020)* This chapter developed process flowsheets for the enzymatic hydrolysis and fermentation of South African grass pre-treated with AMD to produce bioethanol. Estimates of capital and operating costs were used to determine the feasibility of both SHF and SSF process configurations. Pre-treatment with AMD was compared to pre-treatment using H_2SO_4. This addresses objective d.

Burman, N.W., Sheridan, C.M., Harding, K.G., 2020. Feasibility assessment of the production of bioethanol from lignocellulosic biomass pretreated with acid mine drainage (AMD). Renew. Energy 157, 1148–1155. doi:10.1016/j.renene.2020.05.086

Chapter 8: Techno-Economic Evaluation of the Incorporation of Biological Acid Mine Drainage Remediation into a Bioethanol Production Process *(To be submitted to Biomass and Bioenergy)* This chapter expanded the process flowsheets developed in the previous chapter to include the remediation of AMD. A full techno-economic evaluation was performed to determine the feasibility of the process. Sensitivity analyses were performed to evaluate the feasibility of the process under various conditions. This addresses objective e.

Chapter 9: Discussion and Conclusion This chapter delivers the main findings and the conclusions that can be drawn from those findings. Each objective is considered followed by a discussion of the design, optimization, and feasibility of the process investigated. Finally, recommendations into key areas that require further investigation to develop this process, and conclusions on the entire research will be made.

A schematic representation of how the different body chapters are connected is presented in Figure 1.1. Note – background information will feed into all of these chapters, and all of these chapters will feed into the discussion and conclusion chapter.

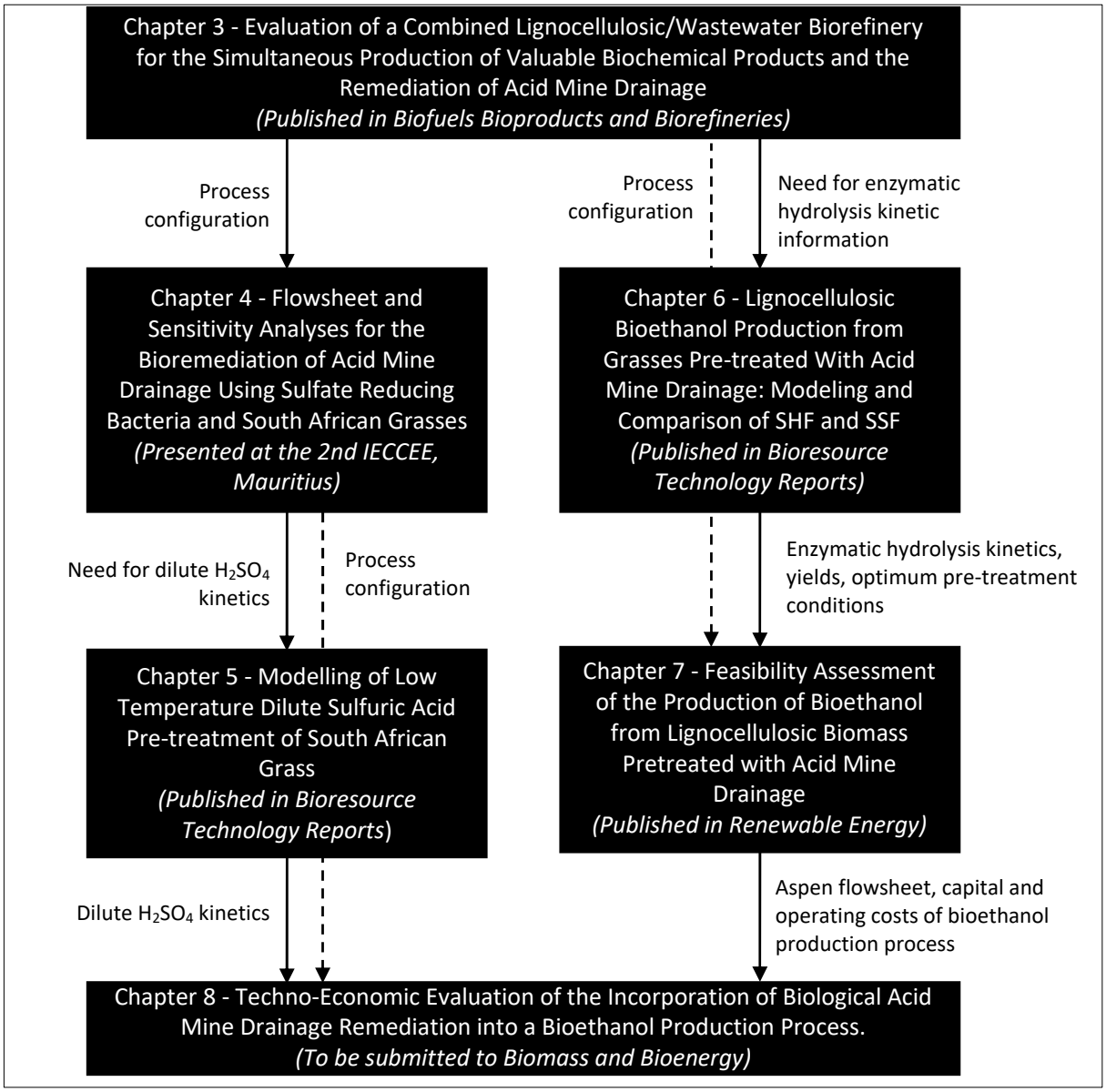

Figure 1.1: Schematic representation of the structure of the main body chapters with links between chapters indicated.

1.6. Novelty of Research

This overall process consists of four biochemical processes: pre-treatment of biomass using dilute sulfuric acid; enzymatic hydrolysis of pre-treated biomass; fermentation of glucose produced in hydrolysis; and remediation of AMD using SRB and an organic carbon source. Although these processes have been well studied; the synthesis of the four processes into one integrated process makes the proposed study novel for several reasons.

a. The determination of the optimum conditions of biomass pre-treatment using AMD is novel, as the effects that the other constituents of AMD (metals, sulfates) will have on the pre-treatment process has not been studied.
b. The performance (yield/rate) of enzymatic hydrolysis of biomass pre-treated with AMD is novel, as no studies into the effect of this pre-treatment type on the enzymatic hydrolysis have been performed.
c. The performance (yield/rate) of fermentation of glucose produced from biomass pre-treated with AMD is novel, as no studies into the effect of this pre-treatment type on the fermentation of glucose have been performed.
d. These four processes have never been integrated. The sequential optimization of these four processes which are being operated under new objectives will result in a novel study.

1.7. References

Cherubini, F., 2010. The biorefinery concept : Using biomass instead of oil for producing energy and chemicals. Energy Convers. Manag. 51, 1412–1421. doi:10.1016/j.enconman.2010.01.015

IPCC, 2018. Summary for Policy Makers, Summary for Policymakers. In: Global Warming of 1.5°C. An IPCC Special Report on the impacts of global warming of 1.5°C above pre-industrial levels and related global greenhouse gas emission pathways, in the context of strengthening the global response to. Geneva, Switzerland.

IPCC, 2014a. Climate Change 2014: Contribution of Working Groups I, II and III to the Fifth Assessment Report of the Intergovernmental Panel on Climate Change, in: Core Writing Team, Pachauri, R.K., Meyer, L.A. (Eds.), . IPCC, Geneva, Switzerland, p. 151.

Lenihan, P., Orozco, A., O'Neill, E., Ahmad, M.N.M., Rooney, D.W., Walker, G.M., 2010. Dilute acid hydrolysis of lignocellulosic biomass. Chem. Eng. J. 156, 395–403. doi:10.1016/j.cej.2009.10.061

Magowo, E., Rumbold, K., Sheridan, C., 2015. The Utilization of Cellulosic Biomass in treating AMD and the Subsequent Generation of Fermentable Sugars, in: 10th International Conference on Acid Rock Drainage and IMWA Anual Conference. pp. 1–12.

Maurya, D.P., Singla, A., Negi, S., 2015. An overview of key pretreatment processes for biological conversion of lignocellulosic biomass to bioethanol. 3 Biotech 5, 597–609. doi:10.1007/s13205-015-0279-4

McCarthy, T.S., 2011. The impact of acid mine drainage in South Africa. S. Afr. J. Sci. 107, 1–7. doi:10.4102/sajs.v107i5/6.712

Ramla, B., Sheridan, C., 2015. The potential utilisation of indigenous South African grasses for acid mine drainage remediation. Water SA 41, 247–252. doi:10.4314/wsa.v41i2.10

Taylor, J., Pape, S., Murphy, N., 2005. A Summary of Passive and Active Treatment Technologies for Acid and Metalliferous Drainage (AMD). Proc. 5th Aust. Work. Acid

Turton, R., Bailie, R.C., Whiting, W.B., Shaeiwitz, J.A., 1998. Analysis, Synthesis, and Design of Chemical Processes, 1st ed. Pretince Hall, Upper Saddle River.

Westensee, D.K., Rumbold, K., Harding, K.G., Sheridan, C.M., van Dyk, L.D., Simate, G.S., Postma, F., 2018. The availability of second generation feedstocks for the treatment of acid mine drainage and to improve South Africa's bio-based economy. Sci. Total Environ. 637–638, 132–136. doi:10.1016/j.scitotenv.2018.04.410

Chapter 2: Background Information

This chapter provides all the necessary background information for all of the chapters to follow and has been divided into three sections.

1. An introduction to the generation, effect, and remediation of acid mine drainage (AMD).
2. An introduction to biofuels, the biorefinery concept, and lignocellulosic biotechnology, with detailed information on the production of lignocellulosic bioethanol.
3. A discussion of all previous studies investigating the production of bioethanol and simultaneous remediation of AMD.

2.1. Acid Mine Drainage

South Africa is a water-scarce country. Only one-third of the countries' area receives sufficient annual rainfall for crop cultivation (Kunz and Jewitt, 2013). Therefore, any pollution of water from either domestic or industrial sources has severe negative impacts on the freshwater supply of South Africa. Recently, the adverse environmental effects of AMD on South African water systems have become visible due to the ecological collapse of various aquatic ecosystems (Durand, 2012), and has hence received considerable media coverage (McCarthy, 2011). Large scale mining in the Witwatersrand area (Eastern, Central and Western basins), as well as the Mpumalanga and KwaZulu-Natal coalfields, has indirectly caused the generation of vast amounts of AMD in these areas. This further exacerbates South Africa's water scarcity and water security for the future (McCarthy, 2011).

2.1.1 Generation of acid mine drainage

Acid mine drainage is formed through a series of geochemical reactions when sulfide rich minerals are exposed to both oxygen and water. Oxidation of pyrite (FeS_2) exposed to air and water results in the formation of ferrous iron and an increase in the acidity of the water (Equation 2.1) (Akcil and Koldas, 2006).

$$2FeS_2 + 7O_2 + 2H_20 \rightarrow 2Fe^{2+} + 4{SO_4}^{2-} + 4H^+ \qquad (2.1)$$

Ferrous iron is then converted to ferric iron (Equation 2.2). This is due to oxidation by acidophilic bacteria. This reaction consumes one mole of acidity (per mole iron) and is highly pH dependent. At low pH values (2-3) the reaction proceeds slowly while at pH 5 the reaction proceeds orders of magnitude faster (Akcil and Koldas, 2006).

$$4Fe^{2+} + O_2 + 4H^+ \leftrightarrow 4Fe^{3+} + 2H_2O \quad (2.2)$$

Subsequently, ferric iron is hydrolyzed to form ferric hydroxide ($Fe(OH)_3$) and three hydrogen ions are released (Equation 2.3) (Akcil and Koldas, 2006).

$$Fe^{3+} + 3H_2O \rightarrow Fe(OH)_3 + 3H^+ \quad (2.3)$$

The formation of ferric iron can also accelerate sulfide oxidation in the presence of fresh iron sulfide (Equation 2.4) (Akcil and Koldas, 2006).

$$FeS_2 + 14Fe^{3+} + 8H_2O \rightarrow 15Fe^{2+} + 2SO_4^{2-} + 16H^+ \quad (2.4)$$

Mining activity can lead to the increased exposure of sulfide containing rock to oxygen and water, thereby accelerating AMD production. This highly acidic metal-enriched water disrupts natural aquatic ecosystems when it decants from mining sites (Simate and Ndlovu, 2014). In the Witwatersrand mining area (Eastern, Western and Central basin) the switching off of dewatering pumps after mine closure has resulted in the flooding of shaft mines, presenting ideal conditions for the generation of AMD (McCarthy, 2011). The generation of AMD is as high as 300 ML/day in these areas (Mccarthy et al., 2010). AMD generated in underground mines flows into surface rivers through wetland systems (Figure 2.1).

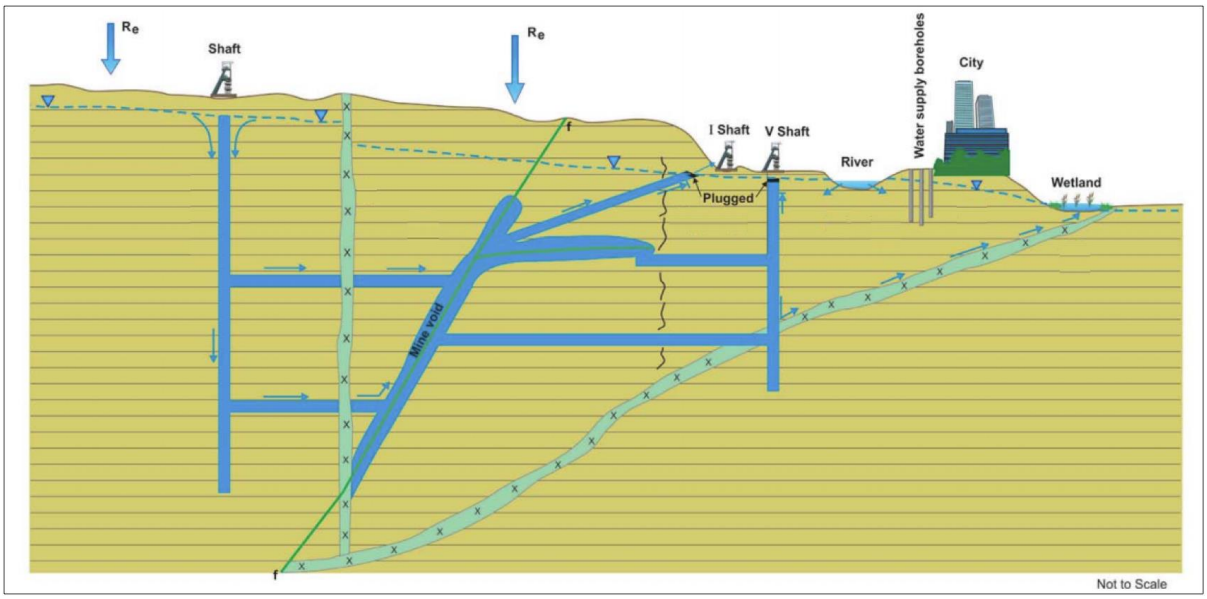

Figure 2.1: Depiction of how AMD formed underground decants into surface rivers through wetland systems (Water Research Commision, 2017)

Rainfall onto pit mines and mine tailing dumps also provide suitable conditions for the generation of AMD if sulfite rich minerals are present. This water can have a negative environmental effect when it seeps into natural water systems (Johnson and Hallberg, 2005a). The high concentration of coal pit mines in the Mpumalanga – KwaZulu Natal coalfields has resulted in the widespread generation of AMD in this area (McCarthy, 2011).

Fortunately, increased awareness of the effects of AMD on the environment and local communities has led to an amendment of legislature enforcing the indefinite treatment of all mine effluent to acceptable standards after mine closure (MPRDA, 2013). Subsequently, there is a need to develop a cheap, effective process that minimizes by-products and operational supervision.

2.1.2 Effects of acid mine drainage

AMD has a negative environmental impact on aquatic and riparian ecosystems into which it flows (Figure 2.2). The low pH can inhibit the normal physiological function of micro-organisms, such as ion exchange and respiration. These can result in both non-lethal (*i.e.* diminished growth) and lethal effects. Dissolved metals will accumulate in aquatic life both directly from the water, and indirectly from the food chain (Khayatzadeh and Abbasi, 2010). Accumulation of metals can result in both stunted growth and death of organisms (Singh and Kalamdhad, 2011).

The high concentration of sulfate and other minerals will result in the precipitation of salts (Figure 2.3), which combined with the precipitation of iron hydroxides (known as “yellow boy”) can entirely cover aquatic ecosystem floors. This prevents benthic organisms, that live and feed on the floors of aquatic ecosystems, from living in the ecosystem (Simate and Ndlovu, 2014) (Figure 2.4).

Figure 2.2: The high concentration of AMD in the Robinson Dam (source of the Tweeloopispruit), in Gauteng, South Africa, led to the collapse of aquatic and riparian ecosystems in 2007 (Durand, 2012).

Figure 2.3: Precipitation of sulfate minerals in the Tweeloopiespruit, in Gauteng, South Africa, (Durand, 2012)

Figure 2.4: Precipitation of iron hydroxide (yellow boy) in the Tweeloopiespruit, in Gauteng, South Africa, (Durand, 2012)

AMD also negatively affects agriculture. If AMD contaminated water systems are used for crop irrigation, the irrigated soil will experience an increase in the concentration of heavy metals and sulfate in the soil. This leads to oxidative stress on the crops causing cellular damage and disturbance of cellular ionic homeostasis (Singh et al., 2011; Yadav, 2010). Irrigating with AMD contaminated water systems will also result in a lowering of soil pH, which can negatively affect nutrient uptake from the soil, as well as lead to the release of toxic elements (Simate and Ndlovu, 2014). These effects will ultimately lead to lower crop yields, and hence economic productivity.

AMD can also harm rural communities if their water source is contaminated with AMD. Many rural communities live near mine tailing dumps and contaminated water sources in the Central, Eastern and Western basin of the Witwatersrand Mining Area (Figure 2.5). The spread of contaminated groundwater often leads to contaminated water being extracted at local wellpoints. In addition to this, sources of contaminated water are often not secured and are easily accessible to people not aware of the health risks associated with AMD. In addition to the toxicity of heavy metals, there is also uranium present in low quantities, which is highly toxic to human health (ATSDR, 2011).

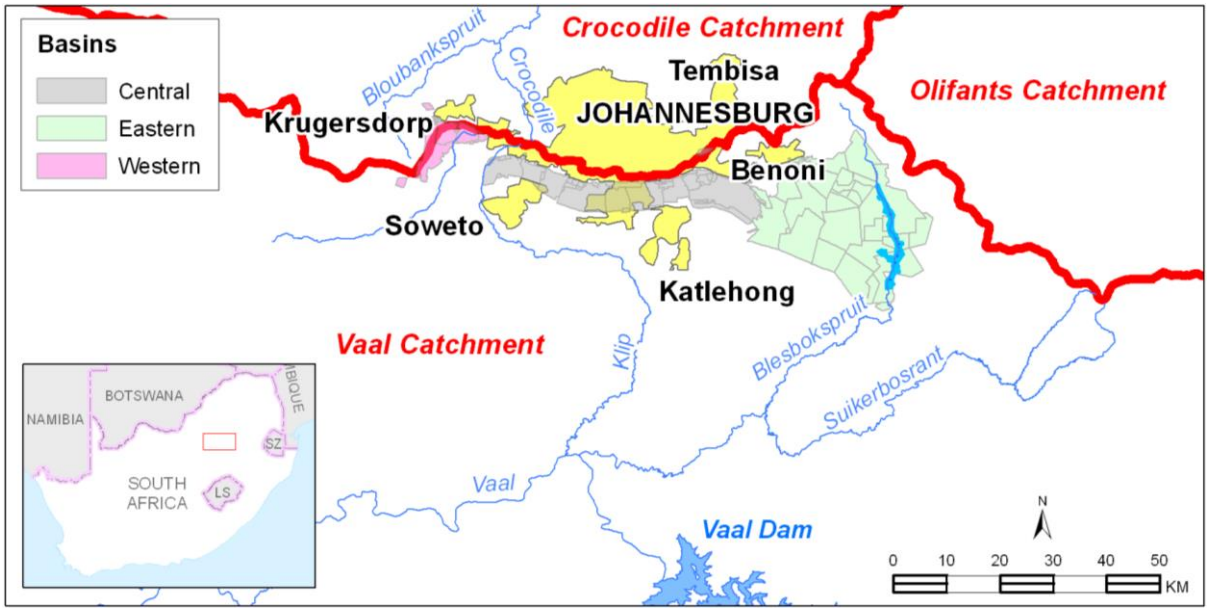

Figure 2.5: Map showing the location of the Central, Eastern, and Western basins of the Witwatersrand mining area (Department of Water and Sanitation, 2013)

2.1.3 Acid mine drainage remediation

Various technologies to remediate AMD have been developed, and the advantages and disadvantages of each need to be evaluated before implementation. The selection of the

most applicable remediation method needs to take into account several factors including the location, volume, mineral composition, and acidity of the AMD to be treated.

Remediation technologies can be broadly grouped into abiotic and biotic treatments, both of which can be applied actively in highly controlled and monitored processes, or passively in long term, low maintenance, self-sustaining processes (Johnson and Hallberg, 2005a).

2.1.3.1 Abiotic acid mine drainage remediation

Currently, the most widely used treatment is an active abiotic process, which achieves an increase in alkalinity through the addition of a neutralizing agent, such as limestone, quicklime, slaked lime, sodium hydroxide, sodium carbonate, magnesium oxide, or hydroxide (Coulton et al., 2003). This increases the pH, results in the oxidation of ferrous iron, and causes the precipitation of other metals in the form of hydroxides or carbonates (Johnson and Hallberg, 2005a). The addition of an oxidizing agent, either in the form of aeration or hydrogen peroxide, increases the rate of oxidation of ferrous iron.

Although this treatment is effective and proven, it is expensive due to the large chemical input, and constant monitoring is necessary. Moreover, it produces large quantities of toxic metallic sludge that may need further treatment. To reduce the volume of sludge, the high-density sludge (HDS) process has been developed (Coulton et al., 2004). This process produces a sludge with a higher density (<30%) through high levels of aeration and mixing, and the recirculation of a portion of the sludge to encourage precipitation (Kuyucak et al., 1999).

Various other active abiotic treatment technologies have also been investigated (Kefeni et al., 2017). These include ion exchange (Feng et al., 2000), adsorption (Mohan and Chander, 2006), membrane technology (Alkhudhiri et al., 2012; Ricci et al., 2015; Zhong et al., 2007), reverse osmosis (Zhong et al., 2007) and electrochemical reduction (Cardoso Buzzi et al., 2013; Chartrand and Bunce, 2003).

Examples of commercially available abiotic AMD remediation processes include:

- The Savmin process, Mintek, chemical neutralization and precipitation (https://www.mintek.co.za/);
- The Alkali-Barium-Calcium (ABC) process, Council for Scientific and Industrial Research (CSIR), chemical neutralization and precipitation, (https://www.csir.co.za/); and
- The HiPRO™ process, Nafasi Water, reverse osmosis, (https://nafasiwater.com/)

2.1.3.2 Biological acid mine drainage remediation

Different biological processes can be used for the removal of sulfate and metals from AMD including biosorption (Wan Ngah and Hanafiah, 2008); intracellular uptake and accumulation (Harris and Ramelow, 1990); complexation (McKnight and Morel, 1980); dissimilatory sulfate reduction (Johnson and Hallberg, 2005a); and extracellular precipitation (Skousen et al., 2017). There are also various bioprocesses that can generate alkalinity/consume acidity. These include photosynthesis (Van Hille et al., 1999); denitrification (Johnson, 1995; Kalin et al., 2006, 1991); ammonification; methanogenesis; reduction of iron; and dissimilatory sulfate reduction (Johnson, 1995; Johnson and Hallberg, 2005b; Kalin et al., 1991; Lu et al., 2011; White et al., 1997).

Sulfate reduction has the combined ability to remove metals and sulfur and produce alkalinity, making it a promising bioprocess for the remediation of AMD.

Dissimilatory sulfate reduction (DSR) is catalyzed by sulfate-reducing bacteria (SRB) according to the reaction:

$$SO_4^{2-} + 2H_2^+ + 2CH_2O \xrightarrow{SRB} H_2S + 2H_2O + 2CO_2 \quad (2.5)$$

By transforming a strong acid (H_2SO_4) into a weaker acid (H_2S), there will be an increase in pH, resulting in the precipitation of metals. In addition, dissolved metals will also react with sulfide to form highly insoluble metal sulfides:

$$M^{2+} + H_2S \rightarrow MS + 2H^+ \quad (2.6)$$

Where M^{2+} represents a metal ion. Recent interest in the application of sulfate reduction for the remediation of AMD has been growing both in passive and active systems (Kaksonen and Puhakka, 2007).

Passive sulfate-reducing reactors

There is a substantial body of literature which measured the effectiveness of SRB in remediating AMD using organic carbon sources as an electron donor (Béchard et al., 1994; Chang et al., 2000; Chockalingam and Subramanian, 2006; Greben et al., 2009; Lefticariu et al., 2015; Magowo et al., 2015; Ramla and Sheridan, 2015; Zagury and Neculita, 2007)

One possible method of passive biological sulfate reduction for the remediation of AMD is through constructed anaerobic wetlands, which are constructed with an organic substrate

layer and/or limestone aggregate. Sulfate-reducing bacteria living in the anaerobic zones of wetlands generate alkalinity through dissimilatory sulfate reduction, using the organic substrate as an electron donor. Acid soluble metals also undergo oxidation to metal sulfides, removing metals from solution and depositing them in the substrate. The dissolution of limestone contributes further alkalinity to the system (Johnson and Hallberg, 2005a). Constructed wetlands can be designed to have different types of water flow including surface, subsurface horizontal, and vertical flow (Figure 1.6).

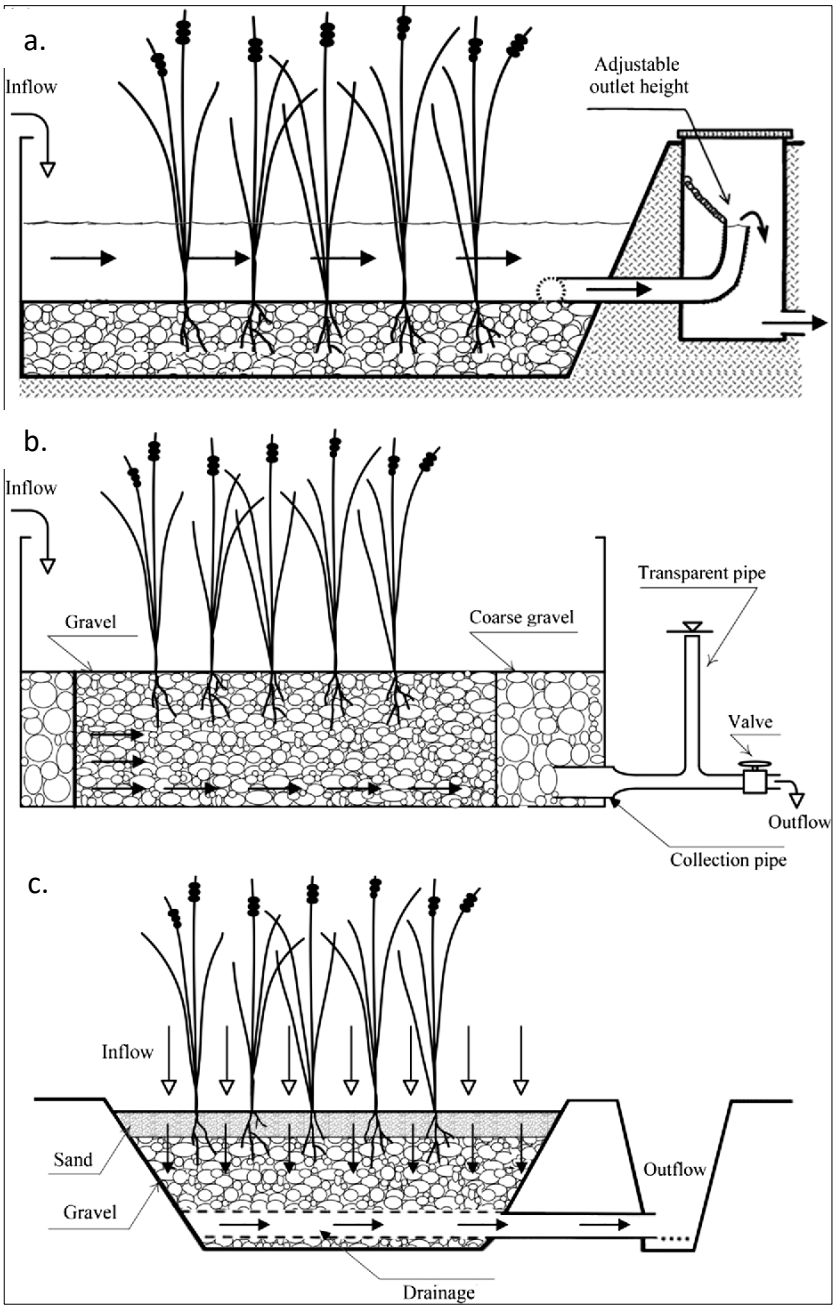

Figure 2.6: Summary of different directions in constructed wetlands. a. surface flow b. subsurface horizontal flow c. vertical flow (Wang et al., 2018).

Although the inclusion of macrophytes in constructed wetlands aids in reducing channeling, it is not necessarily required and can be potentially detrimental to sulfate reduction processes due to translocation of oxygen by plant roots (Zipper et al., 2011). Various other passive bioreactors that employ the same concept as anaerobic wetlands, and have an organic substrate and limestone aggregate, were proven effective at remediating AMD. These include composting or passive flow bioreactors which are completely sealed underground (Johnson and Halberg 2005b); vertical flow systems in which AMD flows through the system vertically; successive alkalinity producing systems (SAPS) which have successive bioreactors in series (Kepler and McCleary, 1994); and permeable reactor barriers (PRB) which are installed to intercept an underground AMD flow (Johnson and Hallberg, 2005a).

Active sulfate-reducing methods of treating AMD

There are various types of active sulfate-reducing bioreactors, with differing reactor configuration, substrate, source of inoculum, and operating conditions. However, all active sulfate-reducing bioreactors are constructed to mimic the natural processes occurring within anaerobic wetlands. The generation of alkalinity and precipitation of metals occurs in the same manner as in an anaerobic wetland.

One of the biggest differentiating factors is the choice of substrate, as this influences the design and operation of the reactor. There are two main types of substrates; either liquid organic substrates (ethanol, methanol, acetate, lactate, glycerol) or solid lignocellulosic biomass (agricultural waste, forestry residue). As sulfate-reducing bacteria cannot use lignocellulosic biomass directly, the inoculum of this type of reactor needs to contain a community of micro-organisms that will be able to break down the lignocellulosic biomass into a substrate that can be utilized by the SRB. This happens through the natural processes of hydrolysis, fermentation, acidogenesis, acetogenesis. Lignocellulosic bioreactors are therefore inoculated with a mixed community of anaerobic bacteria that contain micro-organisms that will catalyze these reactions (Greenway, 2019).

A critical design factor for the lignocellulosic bioreactor is the composition of the organic carbon source, as this has a strong influence on SRB activity (Zagury and Neculita, 2007). Previous studies investigated the effectiveness of various lignocellulosic materials as a substrate for SRB including, corn stover (Hiibel et al., 2011), timothy hay (Béchard et al., 1994), sugarcane bagasse (Magowo et al., 2015), switchgrass (Magowo et al., 2015; Ramla

and Sheridan, 2015) and woody biomass (Hiibel et al., 2011; Neculita et al., 2008). Co-treatment of AMD and municipal wastewater (MWW), which often contains cellulose and SRB, was also shown to be effective in reducing the chemical oxygen demand (COD) of the MWW while lowering sulfates and iron concentrations, and raising the pH of the AMD (Deng et al., 2016).

Greben and *et al.* (2009) performed benchtop studies to determine the ability of grass combined with rumen fluid micro-organisms to remediate AMD. They achieved a maximum sulfate removal efficiency of 78% with regular additions of grass cuttings to the system (Greben et al. 2009). A study by Lefticariu and co-workers (2015) showed that bioreactors with a limestone substrate were highly dependent on organic matter for the stimulation of sulfate-reducing micro-organisms and remediation of AMD. Furthermore, they found that the best type of organic matter for SRB had a high herbaceous content (Lefticariu et al., 2015). Ramla and Sheridan (2015) performed laboratory experiments on synthetic AMD using two indigenous South African grass species. All experiments showed some level of remediation, however, the best results obtained by Ramla and Sheridan (2015) was when soil was added as a microbial inoculum. Experiments conducted over a period of 70 days achieved a maximum of 99% iron removal, 80% sulfate removal and a final pH of 8.5 from a solution containing 2 000 mg/L iron, 6 000 mg/L sulfate and a pH of 3.0 (Ramla and Sheridan, 2015).

Magowo *et al*. (2014) performed similar benchtop experiments where switchgrass and sugarcane bagasse were tested for their ability to increase the pH (from an initial pH of 2.1), and remove iron (from an initial concentration of 500 mg/L) from a synthetic AMD solution. Both substrates were effective in reducing dissolved iron concentration, however, only switchgrass increased the pH substantially. The best result was observed with milled switchgrass, which increased the pH of the AMD to 5.0 and removed 64% of iron.

Sulfate-reducing bioreactors that utilize liquid organic substrate, can be configured in various ways including batch reactors, continuously stirred tank reactor (CSTR) fluidized bed reactors (FBR), gas-lift reactor (GLR), up-flow anaerobic sludge blanket reactors (UASB), anaerobic baffled reactors (ABR), membrane bioreactors (MB), as well as variations of all of these reactors. The reader is referred to Kaksonen & Puhakka (2007) for a full review of the various reactor types, their advantages and disadvantages, and possible configurations.

Liquid substrates that have been proven suitable include, ethanol, methanol, acetate, lactate, glycerol, and formate (Sánchez-Andrea et al., 2014). The bacteria are generally mesophilic (35°C), however, some thermophilic sulfate-reducing bacteria have successfully been used to perform sulfate reduction at 65°C (Weijma et al., 2000).

Various studies have investigated the rate of sulfate reduction in active sulfate-reducing bioreactors, with different substrates, source of inoculum, and reactor type. There is a large variation in the rate of sulfate reduction determined, ranging from 0.03 – 29 g/L.day. A summary of these studies is presented in Table 2.1

Table 2.1: Summary of the different sulfate-reducing bioreactors investigated adapted from (Sánchez-Andrea et al., 2014).

Reference	pH	Source	Carbon Source	HRT* hr	Reactor Type	Rate of SO_4 reduction g/L.day
(Moosa et al., 2002)	8	Wastewater treatment plant	Acetate and peptone	90-48	CSTR	0.17-0.40
(Weijma et al., 2000)	7.5	sludge from a sulfate-reducing reactor	Methanol	3.5	EGSB	15
(Houten et al., 2006)	7.3	THIOPAQ granular sludge	Synthesis gas-fed		GLB	15
(Nagpal et al., 2000)	7	Mixed SRB	Ethanol	5.1	FBR	6.336
(Lin and Lee, 2001)	7	Digested Sludge	Acetate and peptone	60	Packed Bed	0.312
(Chang et al., 2000)	6.8	Anaerobic Digester fluid	Waste material	480	Packed Bed	0.12
(Wybrant et al., 2002)	6.5	Water from the anaerobic zone of a creek	Reactive mixture		Packed Bed	0.12
(Hiibel et al., 2011)	6.2	Acidic enrichment culture	Ethanol or wood chips and corn stover	72-216		0.03
(Bijmans et al., 2008b)	6	Neutrophilic granular sludge	Formate	24	MB	29
(Bijmans et al., 2008a)	5	Neutrophilic granular sludge	H_2/CO_2	18	MB	5
(Bijmans et al., 2009a)	5	Neutrophilic granular sludge	Formate	12	MB	18
(Sánchez-Andrea et al., 2012)	5	Acidic sediment	Domestic water	24-48	UASB	0.34
(Jong and Parry, 2003)	4.5	Water from wetland filter of a mine site	Lactate	16.2	Packed bed	0.48
(Bijmans et al., 2010)	4.5	Neutrophilic granular sludge	H_2/CO_2		MBR	7.5
(Tsukamoto and Miller, 1999)	4.2	Spent Manure	Methanol	6.6	Packed bed	1.608
(Kolmert and Johnson, 2001)	4	Derelict mine site	Ethanol, lactate, and glycerol	49.3	Packed bed	0.5
(Bijmans et al., 2010)	4	Acclimated granular sludge	Formate	12	MB	6.1
(Bijmans et al., 2010)	4	Acclimated granular sludge	H_2/CO_2	12	MB	8
(Jong and Parry, 2006)	4	SRB enriched from a wetland	Lactate	3.5, 16, 10	UASB	1.28
(Montoya et al., 2013)	4	Disintegrated granular sludge	Acetate, lactate (9:1)	24	Downflow FBR	0.89
(Kaksonen et al., 2004)	3	methanogenic sludge and mine sediment	Ethanol	21-6.1	FBR	4.3
(Glombitza, 2001)	3	Water from a lignite mine	Methanol	12, 4.2	Packed bed	3.12
(Foucher et al., 2001)	2.5	–	Acetate and H_2/CO_2	21.6	Packed bed	4.8
(Kaksonen et al., 2003)	2.5-3	Methanogenic sludge and mine sediment	Lactate	16	UASB and FBR	1.9
(Nancucheo and Johnson, 2012)	2.3	Acidophilic microbial community	Glycerol	47	CSTR	0.12

*HRT – Hydraulic retention time

2.2. Lignocellulosic Biotechnology

The world's economy is highly dependent on fossil fuels such as natural gas, coal, and oil for the production of fuel, electricity, and various petrochemicals and petrochemical-based products (Uihlein and Schebek, 2009). Unfortunately, the burning of fossil fuels is the cause of recently observed atmospheric and oceanic warming, and associated climate change (IPCC, 2014a). To limit the global temperature rise to 1.5°C the world will need to reduce its carbon emissions, compared to 2010, by 45% by 2030 and have a net-zero carbon emission by 2050 (IPCC, 2018). To do this, the world needs to find renewable alternatives to fossil fuels for the production of energy and chemicals. The production of renewable energy can be achieved through a variety of sources such as wind, water, sun, biomass, and geothermal heat. In contrast, the production of fuel and chemicals from renewable sources is limited to biomass (Lynd and Wang, 2003).

Biofuels and biochemicals are any fuels or chemicals that are produced from biomass. Sources of biomass include starch or sugary crops (sugar cane, maize), triglyceride feedstocks (waste oil, oil crops, algae), or lignocellulosic feedstocks (trees and forestry residues, agricultural residue, long grasses). These sources of biomass can undergo a range of processing routes such as the thermo-chemical (gasification, pyrolysis, combustion), biochemical (hydrolysis, fermentation), and physical (pre-treatment, mechanical fractionization, pulp production), to produce both biofuels (electricity and heat, FT biofuels, bioethanol, biomethane, biodiesel), and bioproducts (hydrogen, waxes, pulp and paper, biomaterials, organic acids, phenols) (Jungmeier et al., 2014).

To increase the economic feasibility of the production of biofuels and bioproducts from biomass the concept of the biorefinery has been developed. In a biorefinery, multiple processes are integrated to efficiently produce a range of marketable products.

2.2.1 Biorefineries

The International Energy Agency (IEA) Bioenergy Task 42 has defined biorefining as “The sustainable processing of biomass into a spectrum of marketable products and energy” (de Jong et al., 2012). A biorefinery is designed, analogous to a fossil fuel refinery, such that multiple processes are integrated to efficiently produce multiple products and co-generate heat and electricity. Ideally, the range of products will include a large volume of low-value

products (biodiesel, bioethanol), small volumes of high-value specialty chemicals (polyhydroxyalkanoates, 1,4,-Butnaediol), and heat or electricity which can be used on site or sold to local utility suppliers (Cherubini, 2010).

As there are multiple different feedstocks, processes and products that could be integrated into any given biorefinery, the classification of biorefineries has been confusing. The IEA Bioenergy Task 42 has come up with a classification scheme that defines each biorefinery in terms of feedstock, intermediary platforms, processes, and products (Figure 2.7) (Cherubini et al., 2009).

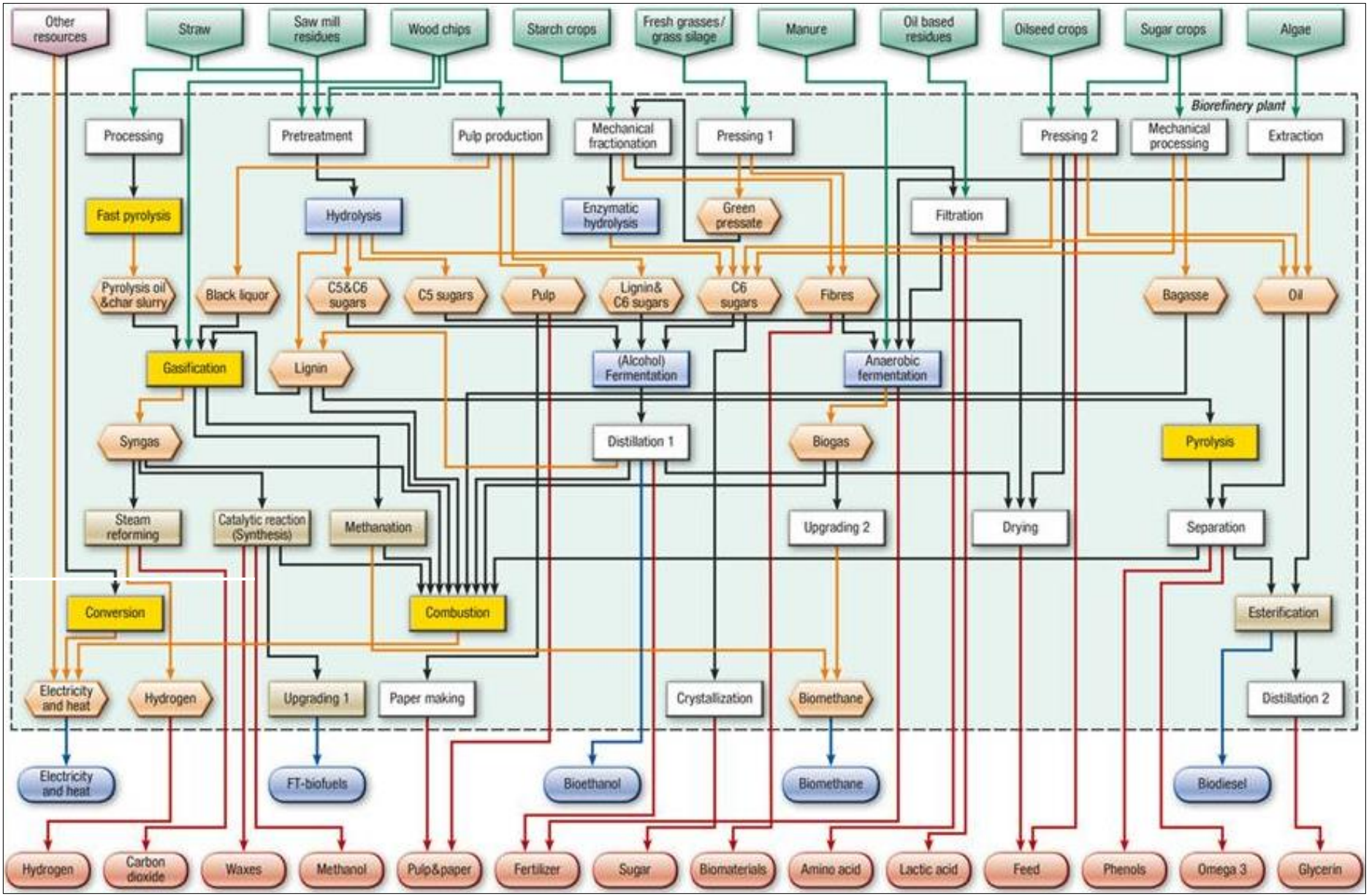

Figure 2.7: Biorefinery classification scheme according to the IEA Task 42 Biorefining (IEA Bioenergy, 2013)

To make the evaluation of different biorefinery options easier to decision makers, industry partners, and investors, the Biorefinery Complexity Index (BCI) has been developed. This is analogous to the Nelsons Complexity Index for petrochemical refineries (Jungmeier et al., 2014). In this, each feedstock, intermediary platform, process, and product is assigned a technological readiness score, from 1 (most ready) to 9 (least ready). The BCI is then calculated by the addition of the technological readiness scores of all features in that biorefinery. A low BCI indicates a biorefinery that is less complicated (lower capital cost) and has a higher level of technological readiness (shorter development time for required technology). A comparison of the BCIs of different options can be used for the identification of the most technically and economically feasible biorefinery options.

2.2.2 Lignocellulosic bioethanol

Currently, bioethanol is the most important product of biotechnology in terms of volume and market value (Taherzadeh and Karimi, 2007a), with 71 billion kilograms produced in 2015 (E4TECH 2015). Brazil and the USA are the main producers, accounting for 70% of the bioethanol produced in 2007 (Birur et al., 2008). The main feedstocks for bioethanol production are sugar and starch sourced from food crops such as sugarcane in Brazil and corn in the USA. The increased demand of these feedstocks for bioethanol production led to increases in the price of these food crops and impacted negatively on food security. Therefore, alternative feedstocks that do not affect food security, such as lignocellulose, have been evaluated. Apart from bioethanol, other useful products can be produced from lignocellulosic biomass, such as xylitol, lactic acid, 1,4-butanediol, isobutene, acrylic acid, and acetone (E4TECH 2015).

Lignocellulose is the most abundant biomass on earth, occurring naturally in woody and herbaceous plants. Important sources of lignocellulosic biomass include agricultural residue (sugarcane bagasse, corn stover), forestry residues (wood chips, sawdust), and energy crops (long stem grasses, hard and softwoods). Although lignocellulose is highly abundant and comparatively cheap lignocellulose based biotechnologies have not been widely implemented due to process inefficiencies.

2.2.3 Lignocellulosic biomass

Lignocellulose is the main constituent of the plant cell wall, providing strength and rigidity. It is comprised of three main fractions: cellulose, hemicellulose, and lignin. Cellulose is composed of chains of β 1-4 linearly linked D-glucose units, that are stacked together forming microfibrils. Hemicellulose is an amorphous, branched polymer consisting of both pentose, (xylose and arabinose), and hexose (glucose, galactose, mannose) sugars. Lignin is also an amorphous polymer made up of three main monomers, p-coumaryl alcohol, coniferyl alcohol, and sinapyl alcohol (Alonso et al., 2012). Lignin and hemicellulose form a ligno-hemicellulosic matrix that surrounds the cellulose fibrils (Figure 2.8).

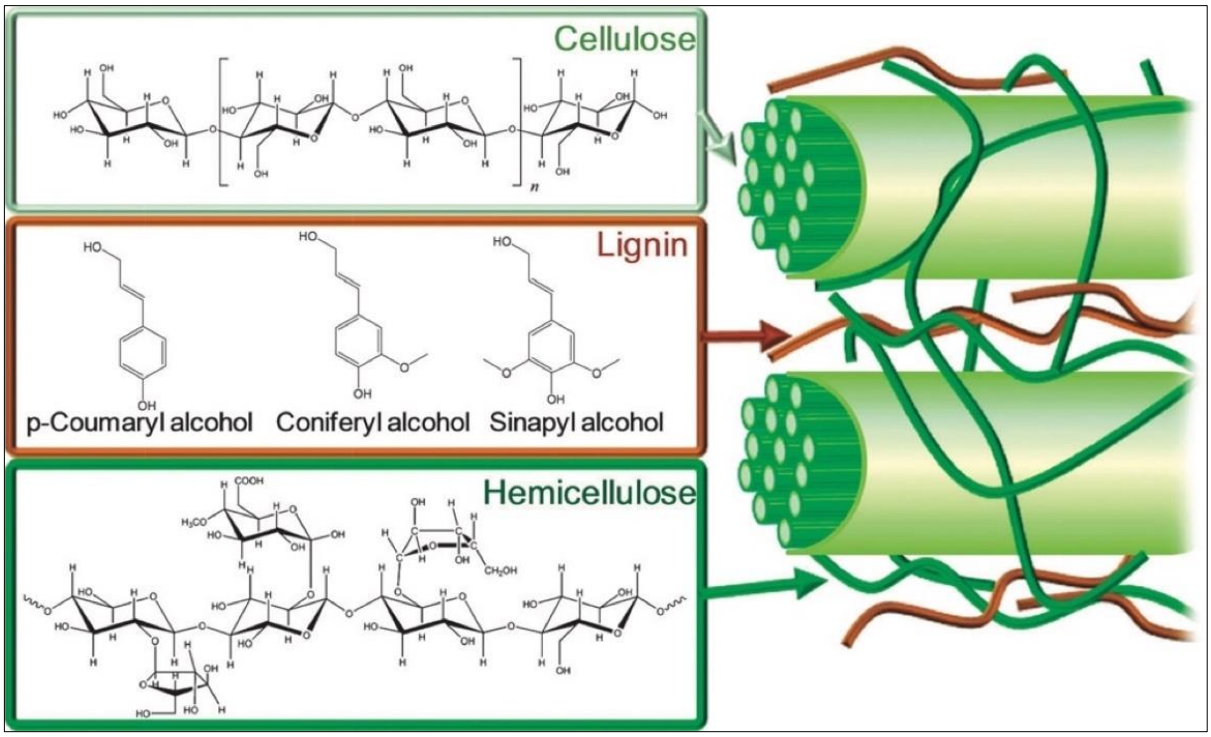

Figure 2.8: Structure of lignocellulosic biomass (Alonso et al., 2012)

Cellulose, hemicellulose, and lignin make up roughly 90% of the biomass composition, the remaining fraction is made up of extractives (proteins) and ash. A summary of the cellulose, hemicellulose and lignin composition of various lignocellulosic feedstocks is given in Table 2.2.

Table 2.2: Main structural composition of various common lignocellulosic feedstocks.

Reference	Feedstock	Cellulose %	Hemicellulose %	Lignin %
(Esteghlalian et al., 1997)	Switchgrass	32.2	24.4	23.2
	Poplar	39.8	18.4	29.1
	Corn stover	36.0	23.9	18.8
(Yat et al., 2008)	Aspen	52.4	25.9	26.7
	Balsam	47.1	28.7	36.0
	Basswood	44.0	25.1	28.4
	Red Maple	43.2	32.9	36.5
	Switchgrass	47.7	37.7	26.0
(Tizazu and Moholkar, 2017)	Sugarcane bagasse	40.3	30.1	27.1
(Torget et al., 1990)	Weeping lovegrass	36.7	21.9	21.2
(Lee et al., 2007)	Switchgrass	37.3	28.5	19.7
(Menegol et al., 2014)	Elephant grass	38.0	20.5	20.7
(Wongwatanapaiboon et al., 2012)	Dwarf Napier	35.6	34.2	3.7*

*The lignin composition reported in this study is thought to be significantly lower than in other studies as the acid insoluble lignin was not reported. An "other" category was, however, reported.

The biochemical production of biofuels and biochemicals from lignocellulosic biomass is achieved through the hydrolysis of poly-, oligo- and disaccharides into monomeric sugars. Monomeric sugars are then fermented to produce ethanol, xylitol, lactic acid, and other biochemicals. Further processing or separation of the fermentation product might be required to achieve the desired product, *i.e.* distillation of ethanol to obtain a higher ethanol concentration.

The general equation for the hydrolysis of cellulose ($C_6H_{10}O_5$) to glucose ($C_6H_{12}O_6$), and subsequent fermentation into ethanol (C_2H_5OH) and carbon dioxide (CO_2) is presented below.

$$C_6H_{10}O_5 + H_2O \rightarrow C_6H_{12}O_6 \rightarrow 2C_2H_5OH + 2CO_2 \quad (2.7)$$

Hydrolysis can be achieved either by acid catalyzed hydrolysis or enzymatic hydrolysis (E4TECH 2015).

2.2.4 Acid hydrolysis

Hydrolysis of lignocellulosic biomass can be performed through an acid catalyzed reaction. Acid penetrates the lignin and breaks down hemicellulose and cellulose into monomeric sugars (Taherzadeh and Karimi, 2007b). Several types of concentrated or dilute acids can be used such as formic, hydrochloric, hydrofluoric, nitric, phosphoric, sulfuric, and sulfurous acid

(Galbe and Zacchi, 2002). Sulfuric acid is the most commonly used acid (Alvira et al., 2010; Lenihan et al., 2010; Maurya et al., 2015; Mosier et al., 2005b; Taherzadeh and Karimi, 2008).

Concentrated acid hydrolysis is conducted at low temperatures and acid concentrations of 10 – 30% w/w. High glucose yields of ~90% of theoretical glucose have been reported using concentrated acid hydrolysis (Iranmahboob et al., 2002). The milder temperature of concentrated acid hydrolysis results in fewer thermal degradation products such as furfural and 5-hydroxymethyl-furfural (HMF), but the high acid concentration results in equipment corrosion (Verardi et al., 2012).

The main advantage of dilute acid hydrolysis is the low acid concentrations (2 – 5%) which has a lower chemical cost. To achieve reasonable reaction times, hydrolysis is carried out at higher temperatures (160 – 210°C) (Da Silva and Chandel, 2012). However, the high temperatures result in increased thermal degradation of sugars. Therefore, the fermentable sugar concentration is lower than that of the concentrated acid hydrolysis process. Additionally, certain degradation products, such as furfural and HMF, inhibit the yeast cells in the subsequent fermentation process (Kootstra et al., 2009; Larsson et al., 1999). High temperatures also increase equipment corrosion (Jones and Semrau, 1984). Various process configurations have been tested to maximize the recovery of monomeric sugars and minimize utility consumption using dilute acid hydrolysis. These include two-stage processes, percolation reactors, counter-current reactors, shrinking bed reactors, and rotating screw reactors. A more extensive discussion of different dilute acid reactor configurations can be found in Da Silva & Chandel (2012).

2.2.5 Enzymatic hydrolysis

Hydrolysis of lignocellulosic biomass can also be performed enzymatically. Enzymatic hydrolysis was first observed during WWII in the South Pacific. The fungi *Trichoderma reesei* was observed to break down cotton clothing and equipment. After further investigation, the fungi were found to produce cellulase enzymes. Various other micro-organisms have since been found capable of producing cellulase including, bacteria belonging to *Clostridium, Cellumonas, Bacillus, Thermomonospora, Ruminococus, Bacteroides, Erwinia, Acetovibrio, Streptococcus* (Sun and Cheng, 2002) and fungi such as species of *Aspergillus, Schizophylum, and Penicillium* (Zhou et al., 2008). *T. reesei* has been the favored micro-organism for cellulase

production due to the high quantities of enzyme it secretes (Wang and Cheng, 2011). Cellulases have been extensively researched during the past 60 years, and through genetic modification, have been optimized to increase the rate and yield of lignocellulosic hydrolysis (Zhang et al., 2006).

Cellulase enzymes are a class of enzymes that hydrolyze cellulose into glucose. This includes: enzymes that hydrolyses cellulose chains to cellobiose (endo-β-1,4-glucanase (EG) and exo-β-1,4-cellobiohydrolase (CBH); enzymes that hydrolyze cellobiose to glucose (β-glucosidase); and enzymes that hydrolyze cellulose directly to glucose (exo-β-1,4-cellobiohydrolase (CBH), and exo-β-1,4-glucanase) (Figure 2.9) (Zheng et al., 2009).

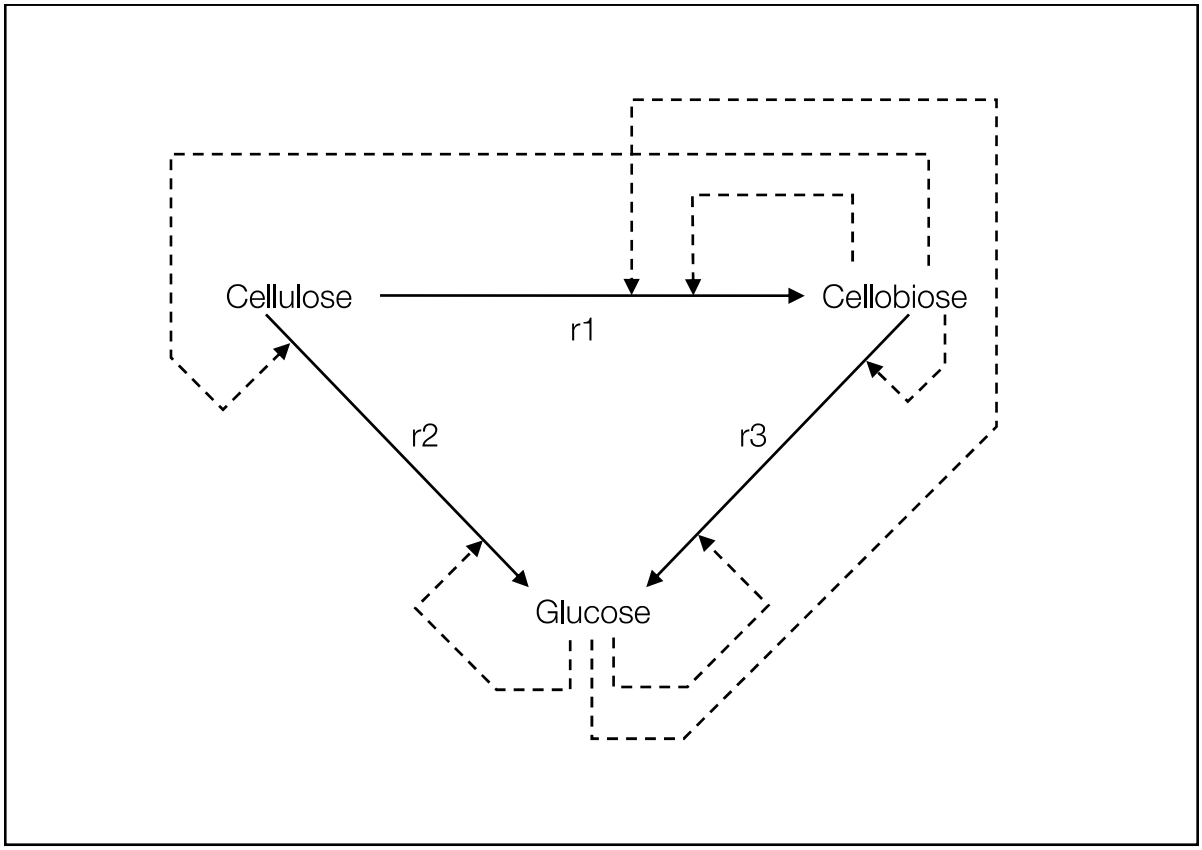

Figure 2.9: Reaction scheme for the enzymatic hydrolysis of cellulose to glucose. Enzymes included in each reaction are: **r1** – endo-β-1,4-glucanase (EG) and exo-β-1,4-cellobiohydrolase (CBH); **r2** – exo-b-1,4-cellobiohydrolase (CBH), and exo-β-1,4-glucanase; **r3** – β-glucosidase. Dashed lines indicate the inhibition of products on reactions (Zheng et al., 2009)

Enzymes secreted by *T. reesei* often lack sufficient β-glucosidase to hydrolyze cellobiose quickly enough to prevent cellobiose buildup and hence inhibition. Commercial cellulase enzymes are often mixtures that contain additional β-glucosidase (Viksø-Nielsen, 2008).

Commercially available enzymes include Celluclast 1.5L and Cellic® Ctec 1/2/3 (from Novozyme – www.novozymes.com) and ACCELLERASE® 1500 (from DuPont – http://biosciences.dupont.com/).

Since enzymes are protein-based, they have a very limited range of operating conditions in which they can function efficiently. Typically, cellulase enzymes require a pH in the range of 4.0 – 5.0, and temperature in the range of 40 – 50°C. Enzymatic hydrolysis is therefore carried out in temperature-controlled reactors, in the presence of a buffer which will maintain a constant pH throughout the course of the hydrolysis process (Balat, 2011).

Enzyme concentration (activity) is measured in Filter Paper Units (FPU) which is equal to the concentration of glucose that is released from the enzymatic hydrolysis of 1 g of Whatman Number 1 filter paper in one hour (NREL, 1996). Once the enzyme activity is known, the enzymes can be added to the hydrolysis mixture at a concentration between 7-33 FPU/gram substrate (Sun and Cheng, 2002).

Enzymatic hydrolysis offers the advantage of much milder process conditions but unlike acid, enzymes are not able to penetrate the lignin. For this enzymatic hydrolysis to proceed, the lignin-hemicellulose matrix first needs to be broken down, in a pre-treatment step, allowing enzymes access to cellulose and hemicellulose (Galbe and Zacchi, 2002). Different pre-treatment methods are discussed below (Section 2.2.5.1).

Another disadvantage of enzymatic hydrolysis is that the monomeric and dimeric sugars produced inhibit the enzymatic hydrolysis reactions (Figure 2.9) (Linde et al., 2007; Zheng et al., 2009). To overcome this negative feedback inhibition, various reactor configurations were designed in which fermentation of the sugars happens simultaneously to hydrolysis. Although this effectively overcomes the inhibitory effect of sugars on the rate of hydrolysis, the optimum conditions for fermentation and hydrolysis are often different, presenting new design challenges. Different reactor configurations are discussed below (Section 2.2.5.2).

2.2.5.1 Pre-treatment methods

The purpose of pre-treatment is to break the physical structure of the lignocellulose making it possible for hydrolysis enzymes to physically access the cellulose fibrils (Figure 2.10). This is achieved by a process step that can be physical, chemical, biological or a combination thereof (Alvira et al., 2010).

Physical methods

Physical pre-treatment methods aim to disrupt the lignocellulosic structure making cellulose and hemicellulose more accessible to enzymes. Comminution and milling are the two main physical pre-treatment methods, and effectively reduce particle size and disrupt polysaccharide crystallinity. This can be achieved with a variety of different mills, including ball, two roll, hammer, colloid, and vibrio-energy mills (Taherzadeh and Karimi, 2007a). High energy requirements and increasing electricity costs make it unlikely that these processes will be feasible in the future (Hendriks and Zeeman, 2009).

Physico-chemical Methods

Steam explosion is the most popular physico-chemical method. During this process, biomass is exposed to high-pressure steam at temperatures typically between 160 – 210 °C, for a period of between a few seconds to several minutes, before the pressure is reduced rapidly causing explosive decompression (Sun and Cheng, 2002). The chemical effects of acetic acid formed from auto-hydrolysis of acetyl groups in hemicellulose also contribute to the breakdown of hemicellulose. Steam explosion, is effective in treating various biomasses, such as poplar (Oliva et al., 2003), olive residues (Cara et al., 2006), corn stover (Varga et al., 2004), wheat straw (Ballesteros et al., 2006), as well as various hardwoods and herbaceous biomasses (Sun and Cheng, 2002). It is not effective on softwoods due to the low concentration of acetyl groups (Sun and Cheng, 2002).

The sugar recovery of steam explosion can be improved by using either a mixture of different chemicals and steam or different chemicals in isolation (Alvira et al., 2010). These processes include the steam-H_2SO_4 process (Tengborg et al., 1998), ammonia fiber explosion (AFEX) process (Charles E. Wyman et al., 2005a, 2005b), and the supercritical CO_2 explosion method (Schacht et al., 2008). The main drawback of these processes is the increased equipment and reagent costs.

Other physico-chemical methods, such as wet oxidation (Palonen et al., 2004), oxidative pre-treatment by air (Palonen et al., 2004), liquid hot water pre-treatment (Mosier et al. 2005; Alvira et al. 2010), and ultrasound pre-treatment (Sun and Tomkinson, 2002; Yachmenev et al., 2009), were also proven to be effective in pre-treating lignocellulosic biomass to make the biomass more susceptible to enzymatic hydrolysis.

Biological

Micro-organisms can also be used in pre-treatment. The most commonly used micro-organisms are species of white-rot fungi, which produce lignin-modifying enzymes, which are effective on various lignocellulosic biomasses (Kumar and Wyman, 2009; Shi et al., 2008). Although biological pre-treatment is favorable for its mild operating conditions, low energy input and chemical cost, the slow rate of reaction is a drawback for further development of this technology (Sun and Cheng, 2002).

Chemical methods

Various chemical pre-treatment methods have been proven effective. Chemical pre-treatment aims to solubilize a portion of the lignocellulosic structure, aiding enzyme access to cellulose and hemicellulose.

Solubilization of lignin can be achieved by pre-treatment with alkaline liquids such as sodium, potassium, calcium, and ammonia hydroxides (Alvira et al., 2010; Carvalheiro et al., 2008). This can be carried out at room temperature and was shown to be effective on various feedstocks (Chang et al., 2001; Kim and Holtzapple, 2006).

The strong oxidative effect of ozone can also be used to solubilize the lignin fraction (García-cubero Teresa et al., 2009). Ambient operating conditions result in fewer inhibitory products, but the high cost of ozone is a drawback (Sun and Cheng, 2002).

Organic Solvents (Organosolv) also effectively solubilize the lignin fraction increasing enzyme access to cellulose and hemicellulose (Papatheofanous et al., 1995). High lignin recovery is an advantage of the Organosolv process (X. Zhao et al., 2009) but the need to remove solvents before enzymatic hydrolysis increases operating costs (Sun and Cheng, 2002).

The use of Ionic liquids (ILs) with large organic cations and small inorganic anions is a promising novel pre-treatment method (Alvira et al., 2010). ILs effectively disrupt the intricate network of covalent bonds in the lignin-hemicellulose matrix. This simultaneously dissolves carbohydrates and lignin, while minimizing the production of degradation products (Lee et al., 2009; Li et al., 2009). Further research still needs to be done on effective methods of sugar recovery from ILs solution (Hayes, 2009) as well as the toxic effects of ILs on enzymes and fermentative micro-organisms (H. Zhao et al., 2009).

Acid catalyzed hydrolysis can also be used for the pre-treatment of lignocellulosic biomass. Like complete acid hydrolysis, this can be performed under both concentrated and dilute acid conditions. However, when used as pre-treatment, only the hemicellulose is hydrolyzed and the reaction is stopped before the hydrolysis of cellulose. The substrate then undergoes enzymatic hydrolysis of the cellulose portion. Similarly to complete acid hydrolysis the formation of inhibitory products from the use of concentrated acid make dilute acid pre-treatment preferable (Maurya et al., 2015).

Dilute acid is currently the most favorable pre-treatment method for industrial applications (Alvira et al., 2010; Maurya et al., 2015; Taherzadeh and Karimi, 2007a), with sulfuric acid being the most used type of acid, due to high hydrolysis yields (Mosier et al., 2005b).

Different dilute H_2SO_4 pre-treatment reactor configurations have been studied, such as percolation, plug flow, shrinking bed, batch, screw and counter current reactor (Taherzadeh and Karimi, 2008). Temperatures in the range of 120 – 210°C were used for a period of 30 seconds – 90 minutes. Although fewer degradation products are produced than would be for concentrated acid hydrolysis, furfural and HMF are still produced in certain quantities and are inhibitory to fermentative micro-organisms (Badal C. Saha et al., 2005).

The National Renewable Energy Laboratory (NREL) designed a two-stage pre-treatment process in which biomass is treated with sulfuric acid at a concentration of 18 mg/g dry mass, first at a temperature of 158°C for 5 minutes, and then at 130°C for 20-30 minutes with the addition of sulfuric acid (4.1 mg/g dry mass). This process effectively solubilized >95% of the xylose in hemicellulose with only 2.4% conversion to furfural (Humbird et al., 2011).

The acid hydrolysis of xylan is known to display bi-phasic kinetics in which biomass consists of both a fast and slow reacting fraction of xylan (Esteghlalian et al., 1997; Kobayashi and Sakai, 1956; Maloney et al., 1985). Xylose produced in both reactions can be converted further to form degradation products (Figure 2.10).

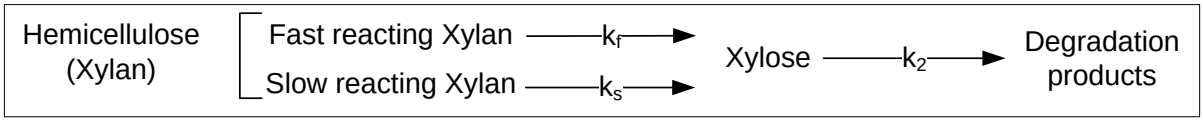

Figure 2.10: Schematic of xylan degradation mechanism (Esteghlalian et al., 1997)

Where k_f, k_s, and k_2 represent the rate of reaction of the fast reacting fraction; the slow reacting fraction and the xylose respectively (kmol/hr).

The rate of change of xylose can thus be expressed as (Esteghlalian et al., 1997):

$$\frac{dC_{C_5H_{10}O_5}}{dt} = k_f \cdot C_{C_5H_8O_4f} + k_s \cdot C_{C_5H_8O_4s} \quad (2.8)$$

Where kinetic constants k_f and k_s demonstrate modified Arrhenius type temperature dependence as according to (Esteghlalian et al., 1997):

$$k = A_0 \cdot C_a^n \cdot e^{\left(-\frac{Ea}{R \cdot T}\right)} \quad (2.9)$$

where A_0 is the pre-exponential factor (/hr); Ea activation energy (kJ/mol); R universal gas constant (8.31 x 10^{-3} kJ/mol.K); T temperature (K); C_a acid concentration (wt% H_2SO_4); and n is an exponential.

Various studies have used this kinetic mechanism to model acid hydrolysis (Aguilar et al., 2002; Esteghlalian et al., 1997; Kim et al., 2013; Kobayashi and Sakai, 1956; Lavarack et al., 2002; Maloney et al., 1985; Nee and Yee, 1976; Yat et al., 2008). These studies have been carried out for temperatures between 150 – 190°C and acid concentrations of 0.5 – 1.2% w/w. Although kinetic parameters determined by these studies can be useful in the design and optimization of similar processes, the validity of these kinetic parameters need to be verified before use at different operating conditions.

A summary of the different kinetics studies that have been conducted are presented in Table 2.3

Table 2.3: Summary of studies modeling xylose chemical hydrolysis according to first order Arrhenius type kinetics

Reference	Model type[1]	Substrate	Temperature °C	% acid w/w	Acid	Compounds modelled
(Saeman, 1945)	Mono	Hardwoods, Softwoods	170 - 190	0.40 - 1.6	Sulfuric	Glucose, Xylose, Galactose, Arabinose, Mannose
(Bhandari et al., 1984)	Mono	Corn Stover	160 - 240	0.49 - 1.5	Sulfuric	Glucose, Xylose
(Lavarack et al., 2002)	Mono	Sugarcane bagasse	80 - 200	0.25 - 8.0	Sulfuric, Hydrochloric	Xylose, Glucose, Arabinose, Furfural
(Yat et al., 2008)	Mono	Switchgrass, Hardwoods	160 - 190	0.25 - 1.0	Sulfuric	Xylose
(Jin et al., 2011)	Mono	Corn Stover	90 - 100	1.0 - 3.0	Sulfuric	Xylose
(Kim et al., 2013)	Mono	Xylo-Oligomers	140 - 180	0.30	Maleic, Oxilic, sulfuric acid	Xylose, Furfural
(Kobayashi and Sakai, 1956)	Bi	Hardwood	74 - 147	1.0 - 6.0	Sulfuric	Xylose
(Nee and Yee, 1976)	Bi	Sugarcane Bagasse	125 - 165	0.5 - 2	Sulfuric	Xylose
(Maloney et al., 1985)	Bi	Hardwood	100 - 170	0.4 - 1.7	Sulfuric	Xylose
(Esteghlalian et al., 1997)	Bi	Switchgrass, Hardwood Corn Stover	140 - 180	0.6 - 1.2	Sulfuric	Xylose
(Aguilar et al., 2002)	Bi	Sugarcane bagasse	100 - 128	2.0 - 6.0	Sulfuric	Xylose, Glucose, Acetic acid, Furfural
(Lavarack et al., 2002)	Bi	Sugarcane bagasse	80 - 200	0.25 - 8.0	Sulfuric, Hydrochloric	Xylose, Glucose, Arabinose, Furfural
(Schell et al., 2003)	Bi	Corn Stover	165 - 195	0.7 - 1.39	Sulfuric	Xylose, Furfural, oligomers,
(Rodriguez-Chong et al., 2004)	Bi	Sugarcane bagasse	100 - 128	2.0 - 6.0	Nitric, Sulfuric, Hydrochloric	Xylose, Glucose, Arabinose, Acetic Acid, Furfural,

[1]Mono = Mono-phasic, Bi = Bi-phasic.

2.2.5.2 Enzymatic hydrolysis reactor configurations

The inhibitory effect of monomeric sugars on enzymatic hydrolysis resulted in the development of various reactor configurations. All of these reactor configurations have advantages and disadvantages, and some are better suited than others for specific biomasses and products.

In separate hydrolysis and fermentation (SHF), pre-treated lignocellulosic biomass is first hydrolyzed to monomeric sugars in one reactor, which are then fermented in the following reactor. The advantage of this is that both hydrolysis and fermentation can be conducted in their optimum temperature ranges of 45 – 50°C and 30 – 37°C respectively (Olsson et al. 2006; Saha et al. 2005). The drawback of this process is that certain sugars have inhibitory effects

on enzyme activity, reducing the rate of hydrolysis. Another drawback is the inability of certain organisms to ferment both pentose and hexose sugars, requiring an additional process stream to process both groups of sugars (Taherzadeh and Karimi, 2007a).

To overcome the inhibitory effect of sugars on hydrolysis the simultaneous saccharification and fermentation (SSF) process was developed. Enzymatic hydrolysis of pre-treated biomass to monomeric sugars and the fermentation of these sugars happen in the same vessel. Fermentation of the sugars keeps the concentration low, limiting the inhibitory effect. SSF has been shown to yield higher ethanol concentrations using less enzyme than SHF (Eklund and Zacchi, 1995; Karimi et al., 2006; McMillan et al., 1999; Sun and Cheng, 2002). Unfortunately, certain fermentative micro-organisms become inactive above 40°C and the compromise in temperature results in hydrolysis becoming the rate-limiting step in SSF (Philippidis and Smith, 1995). Similarly to SHF, another drawback is the inability of certain organisms to ferment pentose and hexose sugars, requiring an additional process stream to process both groups of sugars (Taherzadeh and Karimi, 2007a).

To overcome the compromised activity of cellulase enzymes at lower temperatures a non-isothermal simultaneous saccharification and fermentation (NSSF) process was proposed. In this process, hydrolysis occurs in the first reactor which is maintained at an optimum hydrolysis temperature. Biomass is retained in this reactor while the effluent is recirculated through a second fermenter, which is maintained at optimum fermentation temperature. This reactor configuration was shown to reduce enzyme requirements by up to 40% and increased both ethanol yield and productivity (Wu and Lee, 1998).

The simultaneous saccharification and co-fermentation (SSCF) reactor was proposed to process both hexose and pentose sugars in the same SSF process. Specific micro-organisms with the ability to ferment both of these sugars need to be engineered to achieve this (Kim et al., 2012). The advantage of this process over conventional SSF configuration is the ability to process both pentose and hexose sugars and hence achieve a higher ethanol yield, with fewer product streams (McMillan, 1997). This process is especially well suited to biomasses with high pentose composition.

Ultrafiltration membranes can be used in membrane bioreactors (MBR) to reduce the inhibition of enzyme activity due to product formation, by continuously removing inhibitory products such as glucose, while retaining both substrate and enzyme. In addition to an

increased reaction rate, the retention of enzymes in the reactor results in prolonged enzyme life. Two drawbacks of membrane reactors are the relatively low glucose concentrations and the potential leaching of cellobiose. Various operating schemes have been investigated for both in-situ membranes located within the reactor and separate reactor and filtration units (Andric et al., 2010). Ultrafiltration membranes can also be applied to the separation of fermentation products both for product separation and prevention of inhibition of fermentative organisms. A recent review by Saha *et al.* (2017) provides an excellent summary of the different applications of membrane filtration in the production of lignocellulosic bioethanol.

Recently a consolidated bioprocessing reactor configuration (CBP), in which enzyme production, biomass hydrolysis, and fermentation happens in one reactor vessel, has shown promise (den Haan et al., 2015). The advantages of this are no enzyme procurement or production costs. Unfortunately, no suitable micro-organisms have been found that can achieve the required enzyme production and fermentation rates (Hamelinck et al., 2005). Research into engineering a micro-organism capable of simultaneous cellulase enzyme production and sugar fermentation is ongoing, through the manipulation of excellent cellulase producers to become excellent fermenters and vice versa (Lynd et al., 2005).

A summary of the different reactor configurations is presented in Figure 2.11.

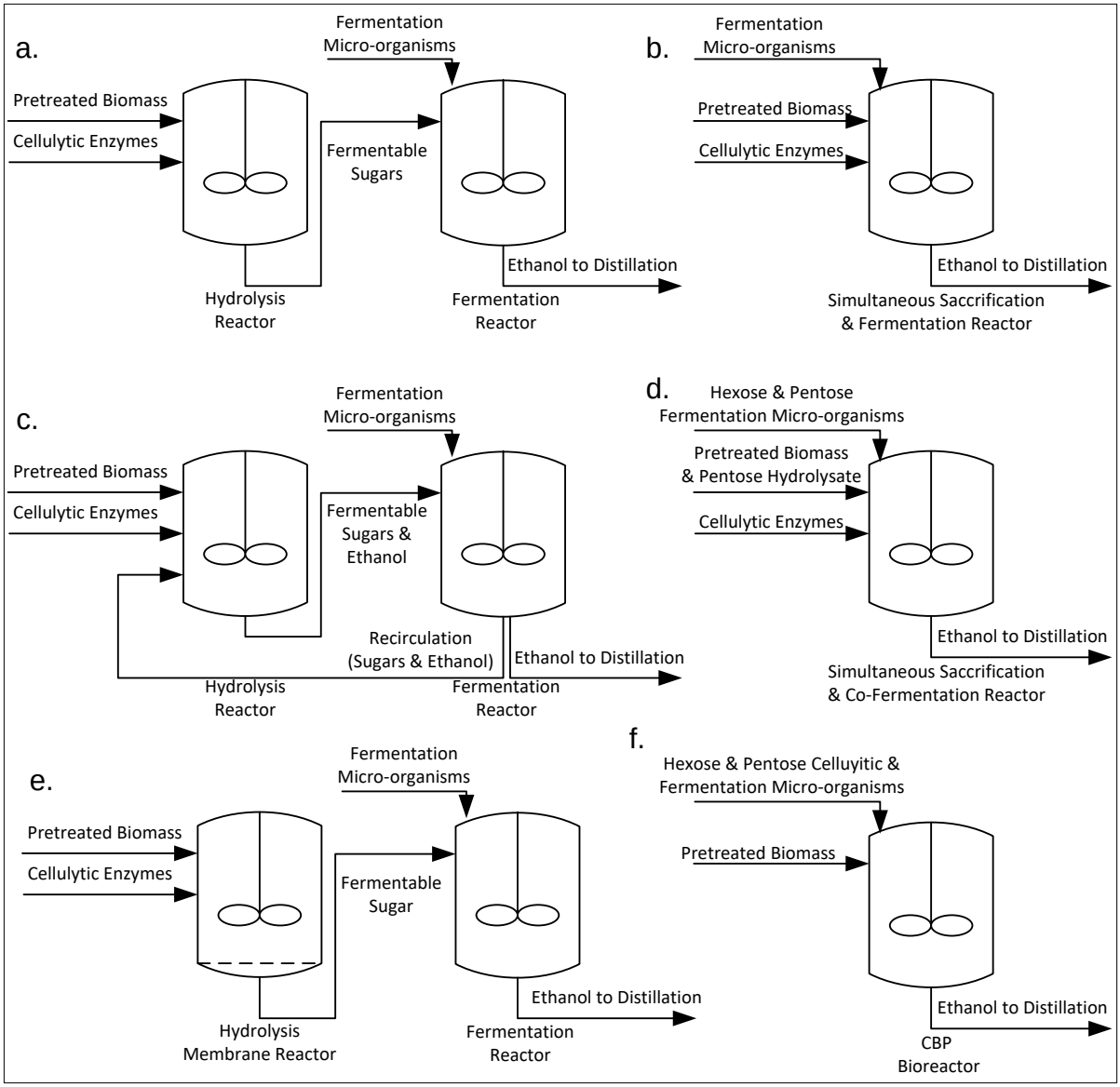

Figure 2.11: Summary of different hydrolysis reactor configurations. **a**. separate hydrolysis and fermentation (SHF) **b**. simultaneous saccharification and fermentation (SSF) **c.** non-isothermal simultaneous saccharification and hydrolysis (NSSF) **d.** simultaneous saccharification and co-fermentation (SSCF) **e.** membrane bioreactor (MBR) **f.** consolidated bioprocessing reactor (CBP)

The selection of a reactor configuration needs to consider various factors such as biomass composition, desired products, and biomass pre-treatment. The selected configuration then has to undergo optimization to achieve both a high rate of hydrolysis and fermentation.

2.2.5.3 Enzymatic hydrolysis kinetics

Various classes of models have been used for predicting the performance of enzymatic hydrolysis, including empirical models, Michaelis-Menten scheme based models accounting for adsorption of enzymes on the substrate, and models focused on hydrolysis of soluble substrates (Bansal et al., 2009).

Empirical models are used to predict hydrolysis variables such as conversion, reaction rate, and adsorbed enzyme based on system properties. Although effective at modeling specific variables for specific conditions these models cannot be used outside of the experimental conditions under which they were determined (Kim et al., 2008; Zhou et al., 2009). Michaelis-Menton models have been used to fit experimental data well, although, the assumptions of excess substrate loading and a well-mixed system do not necessarily apply to this system (Drissen et al., 2009; Shin et al., 2006). Adsorption models incorporate the adsorption of enzymes onto the substrate by utilizing the Langmuir adsorption isotherms. These models are often expanded to include enzyme inhibition caused by-product formation. (Kadam et al., 2004; Liao et al., 2008; Zheng et al., 2009). Various models focusing on the hydrolysis of soluble cello-oligosaccharides have been developed for polysaccharides with a degree of polymerization less than 10 (Harjunpaa et al., 1996; Nidetzky et al., 1994).

Recent kinetic models can be grouped into either enzyme-centric or substrate-models (Jeoh et al., 2017). Enzyme-centric models try to focus on the interaction between cellulose and cellulase to try to identify the rate-limiting enzyme-substrate reaction (Maurer et al., 2013; Shang et al., 2013). Substrate-centric models make a hypothesis into the physical structure and structural properties of the cellulose, at a molecular level, and the effect that this has on the rate of enzymatic hydrolysis (Huron et al., 2016; Lauterbacher et al., 2015).

Although lots of research has been conducted into the hydrolysis of enzymatic hydrolysis of cellulose, the exact mechanism has not been elucidated. Recent investigations have helped determine the effect of the various factors have on the process (Jeoh et al., 2017).

2.2.5.4 Fermentation

Sugars released in hydrolysis can include glucose, xylose, arabinose, galactose, and mannose, all of which can be fermented to ethanol and carbon dioxide using micro-organisms. The two most prominent micro-organisms that have been used for fermentation are the Fungi *Saccharomyces cerevisiae* (Azhar et al., 2017), and the bacteria *Zymomomas mobilis* (Aditiya et al., 2016). Although both of these micro-organisms have demonstrated the ability to rapidly ferment hexoses, they both lack the ability to ferment pentoses. Genetic engineering of S*accharomyces cerevisiae* DNA to include relevant xylose-fermenting DNA from *Pichia stipitis* has been performed to develop a recombinant strain of *S. cerevisiae* that can ferment xylose (Katahira et al., 2006). Similar genetic engineering has been performed on *Z. mobilis* using

DNA from *Escherichia coli* (Hahn-Hägerdal et al., 2006). *Z. Mobilis* has been found to achieve higher ethanol yields than *S. Cerevisiae* (Sáez-Miranda et al., 2006), which has been attributed to low biomass growth (Humbird et al., 2011). When not incorporated into a simultaneous saccharification and fermentation type reactor configuration fermenter operation can be batch, fed-batch or continuous mode (Balat, 2011).

Both *S. cerevisiae* and *Z. Mobilis* require the addition of nutrients both for cellular respiration and growth. These are normally supplied in small quantities to optimize the ethanol production rate (Aditiya et al., 2016). The pH range required for efficient fermentation using *S. Cerevisiae* is 3.5 – 5.0 (Balat et al., 2008) and 6.5 – 7.5 using *Z. mobilis* (Aminifarshidmehr, 1996).

2.2.6 Techno-economic evaluations

Various techno-economic evaluations have been performed evaluating the feasibility of the production of lignocellulosic bioethanol (Dao et al., 2018; Gnansounou and Dauriat, 2010). Although all of these processes utilize hydrolysis of lignocellulose to produces sugars, which are subsequently fermented to bioethanol, there have been various feedstocks and processes evaluated. Feedstocks evaluated included corn stover, switchgrass, hardwoods and softwoods, and paper sludge. There have been various pre-treatments evaluated including dilute acid pre-treatment, ammonia fiber explosion (AFEX), and hot water. Different reactor configurations for the enzymatic hydrolysis and fermentation process have been evaluated including SHF, SSF, CBP, and SSCF.

A summary of the main techno-economic evaluations that have been conducted is presented in Table 2.4.

Table 2.4: Summary of techno-economic evaluations of lignocellulosic bioethanol production processes

Source	MESP[1]		Feedstock	Scale	Feed price	Ethanol Yield		Reactor
	USD/Gal	USD/Ton		Ton_{DB}/day	USD/Ton_{DB}[2]	Gal/Ton_{DB}	L/Ton_{DB}	Config.
(A. Aden et al., 2002)	1.49	500	Corn stover	2200	51	90	341	SSCF
(Humbird et al., 2011)	2.15	721	Corn stover	2200	59	79	299	SHF
(Kazi et al., 2010)	3.40-4.44	1140-1489	Corn stover	2200	75	42-72	159-273	SSCF
(Huang et al., 2009)	1.42-1.87	476-627	Aspen, poplar, corn stover, Switchgrass	2200	58-100	83-111	315-420	SSCF
(Sendich et al., 2008)	1.03-1.41	345-472	Corn stover	2200	40	70	265	SSCF
(Sendich et al., 2008)	0.80-0.95	268-319	Corn stover	2200	40	78	295	CBP
(Laser et al., 2009)	0.63-0.83	211-278	Switchgrass	5000	44	97-105	367-397	CBP
(Bals et al., 2011)	1.86-2.20	623-738	Corn stover	850	45	78	295	SSCF
(Piccolo and Bezzo, 2009)	3.43-4.03	1150-1351	Hardwood	2200	65	75	284	SHF, SSCF
(Klein-marcuschamer et al., 2010)	3.53-4.58	1184-1535	Corn stover	1700	60	52-74	197-280	SHF
(National Academy of Sciences et al., 2009)	1.20-2.70	425-905	Poplar and high glucan	1000-1600	50-88	67-106	254-401	SHF
(Petersen et al., 2018)	1.97	660	Bagasse	2640	-	73	276	SSCF
(Sanchez et al., 2013)	2.95	990	Wheat Straw and Agro residue	2100	75	83	315	SHF
(Gubicza et al., 2016)	1.72	579	Bagasse	820	44	81	305	SSCF
(Boakye-boaten et al., 2017)	1.93	650	*Miscanthus x giganteus*	2000	80	87	330	SSCF

1 – Minimum ethanol selling price; 2 – USD/Ton dry biomass

Most of these techno-economic studies have been performed using a variety of process simulation, flowsheeting, and engineering software, *e.g.* Aspen Plus™, SuperPro Designer®, Microsoft® Excel, and Capcost. Typically, flowsheets and stream tables are first developed, after which they are used to provide estimates of operating and capital costs, which are used in a techno-economic evaluation of the process.

All of these studies use discounted cash flow methods to determine the minimum ethanol selling price (MESP) that is needed for the process to be financially sustainable. This can be compared to historical and forecasted bioethanol prices to determine the feasibility of the

process. The MESP is considered a fundamental variable in the economic feasibility of lignocellulosic bioethanol production (Dao et al., 2018).

Most of these studies make an "n^{th} plant" economic assumption. This means that various economic assumptions (plant uptime, yields, equipment costs, internal rate of return) are based on this plant not being a pioneer plant, but a plant of which several similar plants have already been built and are fully operational. Although this will most likely underestimate costs, it will help justify pioneer plants and encourage early technology adaptors (Humbird et al., 2011).

2.3. Simultaneous Pre-treatment of Grass and AMD Remediation

Taking the above information into consideration, it is evident that there is the possibility to combine the remediation of acid mine drainage with the pre-treatment of biomass. Pre-treated biomass can thereafter undergo further enzymatic hydrolysis, to produce fermentable sugars, and fermentation to produce bioethanol or other biochemicals. It is clear that both the topics of AMD remediation using SRB with lignocellulose as a feedstock and the pre-treatment of lignocellulose with dilute sulfuric acid (similar acid composition to AMD) have been extensively researched. On top of that, the demonstration of both technologies proves that they can be made economically feasible. The integration of the two processes will, however, be the challenge.

One study has recently experimentally investigated the potential of simultaneous AMD remediation, and production of fermentable sugars using sugarcane bagasse and switchgrass (Magowo et al., 2015). A synthetic AMD solution, with 3 000 mg/L sulfate and 500 mg/L iron was treated with biomass for 90 days, after which biomass underwent enzymatic hydrolysis using cellulase enzymes.

In the study by Magowo *et al.* (2015), both grass and sugarcane bagasse were effective in reducing dissolved iron concentration, however, only switchgrass increased the pH substantially. The best result was observed with milled switchgrass, which increased the pH of the AMD to 5.0 and removed 64% of iron. The maximum glucose and xylose production was found to be 3.7 g/L and 3.4 g/L respectively, however, the conversion of the carbohydrates to sugars was not calculated. The glucose concentration during pre-treatment was found to be as high as 8.2 g/L indicating effective breakdown of the polysaccharides by

the AMD solution. The potential for further biochemical transformation of glucose into biofuels or biochemicals was not investigated.

Another recent study that calculated the potential quantities of various biochemicals that could be produced in a process to simultaneously remediate acid mine drainage and produce biochemicals from indigenous South African grass (Westensee et al., 2018). It was found that 1 ha of grass (7 ton dry biomass) could produce, 1 400 kg of glucose. This could undergo further biochemical transformation to produce 205 kg cellulase, or 438 kg poly-β-hydroxybutyric acid (PHB) or 270 kg penicillin V. The potential revenue from these products was found to be 2 050, 569, and 270 USD for cellulase, PHB and penicillin V respectively.

These studies provided evidence for the possibility of simultaneously remediating AMD and producing biochemicals using a combination of lignocellulosic biomass and sulfate-reducing bacteria. However, the level of detail that these studies have gone to is very limited and there is still a large amount of research that is required to design, optimize, and determine the feasibility of such a process.

2.4. References

Aden, A., Ruth, M., Ibsen, K., Jechura, J., Neeves, K., Sheehan, J., Wallace, B., Montague, L., Slayton, A., Lukas, J., 2002. Lignocellulosic Biomass to Ethanol Process Design and Economics Utilizing Co-Current Dilute Acid Prehydrolysis and Enzymatic Hydrolysis for Corn Stover Lignocellulosic Biomass to Ethanol Process Design and Economics Utilizing Co-Current Dilute Acid Prehyd. Golden , Co.

Aditiya, H.B., Mahlia, T.M.I., Chong, W.T., Nur, H., Sebayang, A.H., 2016. Second generation bioethanol production: A critical review. Renew. Sustain. Energy Rev. 66, 631–653. doi:10.1016/j.rser.2016.07.015

Aguilar, R., Ramirez, J.A., Garrote, G., Vazquez, M., 2002. Kinetic study of the acid hydrolysis of sugar cane bagasse. J. Food Eng. 55, 309–318.

Akcil, A., Koldas, S., 2006. Acid Mine Drainage (AMD): causes, treatment and case studies. J. Clean. Prod. 14, 1139–1145. doi:10.1016/j.jclepro.2004.09.006

Alkhudhiri, A., Darwish, N., Hilal, N., 2012. Membrane distillation: A comprehensive review. Desalination 287, 2–18. doi:10.1016/j.desal.2011.08.027

Alonso, D.M., Wettstein, S.G., Dumesic, J.A., Alonso, D.M., Wettstein, G., Dumesic, J.A., 2012. Bimetallic catalysts for upgrading of biomass to fuels and chemicals w. Chem. Soc. Rev. 41. doi:10.1039/c2cs35188a

Alvira, P., Tomas-Pejo, E., Ballesteros, M., Negro, M.J., 2010. Pretreatment technologies for an efficient bioethanol production process based on enzymatic hydrolysis: A review. Bioresour. Technol. 101, 4851–4861. doi:10.1016/j.biortech.2009.11.093

Aminifarshidmehr, N., 1996. The Management of Chronice Suppurative Otitis Media with Accid Media Solution. Am. J. Otol. 17, 24–25.

Andric, P., Meyer, A.S., Jensen, P.A., Dam-johansen, K., 2010. Reactor design for minimizing product inhibition during enzymatic lignocellulose hydrolysis II . Quanti fi cation of inhibition and suitability of membrane reactors. Biotechnol. Adv. 28, 407–425. doi:10.1016/j.biotechadv.2010.02.005

ATSDR, 2011. Uranium [WWW Document]. Toxic Subst. Portal. URL https://www.atsdr.cdc.gov/substances/toxsubstance.asp?toxid=77 (accessed 9.26.19).

Azhar, S.H.M., Abdulla, R., Jambo, S.A., Marbawi, H., Gansau, J.A., Faik, A.A.M., Rodrigues, K.F., 2017. Yeasts in sustainable bioethanol production: A review. Biochem. Biophys. Reports 10, 52–61. doi:10.1016/j.bbrep.2017.03.003

Balat, M., 2011. Production of bioethanol from lignocellulosic materials via the biochemical pathway : A review. Energy Convers. Manag. 52, 858–875. doi:10.1016/j.enconman.2010.08.013

Balat, M., Balat, H., Öz, C., 2008. Progress in bioethanol processing 34, 551–573. doi:10.1016/j.pecs.2007.11.001

Ballesteros, I., Negro, M.J., Oliva, J.M., Cabañas, A., Manzanares, P., Ballesteros, M., 2006. Twenty-Seventh Symposium on Biotechnology for Fuels and Chemicals, in: McMillan, J.D., Adney, W.S., Mielenz, J.R., Klasson, K.T. (Eds.), . Humana Press, Totowa, NJ, pp. 496–508. doi:10.1007/978-1-59745-268-7_41

Bals, B., Wedding, C., Balan, V., Sendich, E., Dale, B., 2011. Evaluating the impact of ammonia fiber expansion (AFEX) pretreatment conditions on the cost of ethanol production. Bioresour. Technol. 102, 1277–1283. doi:10.1016/j.biortech.2010.08.058

Bansal, P., Hall, M., Realff, M.J., Lee, J.H., Bommarius, A.S., 2009. Modeling cellulase kinetics on

lignocellulosic substrates. Biotechnol. Adv. 27, 833–848. doi:10.1016/j.biotechadv.2009.06.005

Béchard, G., Yamazaki, H., Gould, W.D., Bédard, P., 1994. Use of Cellulosic Substrates for the Microbial Treatment of Acid Mine Drainage. J. Environ. Qual. 23, 111–116. doi:10.2134/jeq1994.00472425002300010017x

Bhandari, N., Macdonald, D.G., Bakhshi, N.N., 1984. Kinetic Studies of Corn Stover Saccharification using Sulphuric Acid. Biotechnol. Bioeng. 26, 320–327. doi:10.1002/bit.260260405

Bijmans, M.F.M., Dopson, M., Ennin, F., Lens, P.N.L., Buisman, C.J.N., 2008a. Effect of sulfide removal on sulfate reduction at pH 5 in a hydrogen fed gas-lift bioreactor. J. Microbiol. Biotechnol. 18, 1809—1818.

Bijmans, M.F.M., Dopson, M., Peeters, T.W.T., Lens, P.N.L., Buisman, C.J.N., 2009a. Sulfate Reduction at pH 5 in a High-Rate Membrane Bioreactor : Reactor Performance and Microbial Community Analyses. J. Microbiol. Biotechnol. 19, 698–708. doi:10.4014/jmb.0809.502

Bijmans, M.F.M., Peeters, T.W.T., Lens, P.N.L., Buisman, C.J.N., 2008b. High rate sulfate reduction at pH 6 in a pH-auxostat submerged membrane bioreactor fed with formate. Water Res. 42, 2439–2448. doi:10.1016/j.watres.2008.01.025

Bijmans, M.F.M., Vries, E. De, Yang, C.-H., Buisman, C.J.N., Lens, P.N.L., Dopson, M., 2010. Sulfate Reduction at pH 4 . 0 for Treatment of Process and Wastewaters. Biotechnol. Prog. 26, 1029–1037. doi:10.1002/btpr.400

Birur, D.K., Hertel, T.W., Tyner, W.E., 2008. Impact of Biofuel Production on World Agricultural Markets: A Computable General Equilibrium Analysis, in: Tenth Annual Conference on Global Economic Analysis. West Lafayette, p. 59.

Boakye-boaten, N.A., Kurkalova, L., Xiu, S., 2017. Techno-economic analysis for the biochemical conversion of Miscanthus x giganteus into bioethanol. Biomass and Bioenergy 98, 85–94. doi:10.1016/j.biombioe.2017.01.017

Cara, C., Ruiz, E., Ballesteros, I., Negro, M.J., Castro, E., 2006. Enhanced enzymatic hydrolysis of olive tree wood by steam explosion and alkaline peroxide delignification. Process Biochem. 41, 423–429. doi:10.1016/j.procbio.2005.07.007

Cardoso Buzzi, D., Stéphano Viegas, L., Antônio Siqueira Rodrigues, M., Moura Bernades, A., Alberto Soares Tenório, J., 2013. Water recovery from acid mine drainage by electrodialysis. Miner. Eng. 40, 82–89. doi:10.1016/j.mineng.2012.08.005

Carvalheiro, F., Duarte, L.C., Girio, F.M., 2008. Hemicellulose biorefineries: A review on biomass pretreatments. J. Sci. Ind. Res. (India). 67, 849–864.

Chang, I.S., Shin, P.K., Kim, B.H., 2000. Biological treatment of acid mine drainage under sulphate-reducing conditions with solid waste materials as substrate. Water Res. 34, 1269–1277. doi:10.1016/s0043-1354(99)00268-7

Chang, V.S., Nagwani, M., Kim, C.H., Holtzapple, M.T., 2001. Oxidative lime pretreatment of high-lignin biomass: poplar wood and newspaper. Appl. Biochem. Biotechnol. 94, 1–28. doi:10.1385/ABAB:94:1:01

Chartrand, M.M.G., Bunce, N.J., 2003. Electrochemical remediation of acid mine drainage. J. Appl. Electrochem. 33, 259–264.

Cherubini, F., 2010. The biorefinery concept : Using biomass instead of oil for producing energy and chemicals. Energy Convers. Manag. 51, 1412–1421. doi:10.1016/j.enconman.2010.01.015

Cherubini, F., Jungmeier, G., Wellisch, M., Willke, T., Skiadas, I., Ree Van, R., de Jong, E., 2009. Toward a common classification approach for biorefinery systems. Biofuels, Bioprod. Biorefining 3, 534–

546. doi:10.1002/bbb

Chockalingam, E., Subramanian, S., 2006. Studies on removal of metal ions and sulphate reduction using rice husk and Desulfotomaculum nigrificans with reference to remediation of acid mine drainage. Chemosphere 62, 699–708. doi:10.1016/j.chemosphere.2005.05.013

Coulton, R., Bullen, C., Hallet, C., 2003. The design and optimisation of active mine water treatment plants. L. Contam. Reclam. 11, 273–279. doi:DOI: 10.2462/09670513.825

Coulton, R., Bullen, C., Williams, C., Williams, K., 2004. The formation of high density sludge from mine-water with low iron concentrations, in: Mine Water 2004 - Proceedings International Mine Water Association Symposium. Newcastle upon Tyne (University of Newcastle), pp. 24–30.

Da Silva, S.S., Chandel, A.K., 2012. D-Xylitol: Fermentative production, application and commercialization, in: Da Silva, S.S., Chandel, A.K. (Eds.), D-Xylitol: Fermentative Production, Application and Commercialization. Springer-Verlang, Berlin Heildelberg, pp. 39–61. doi:10.1007/978-3-642-31887-0

Dao, C.N., Mupondwa, E., Tabil, L., Li, X., Castellanos Lopez, E.C., 2018. A Review on Techno-Economic Analysis and Life-Cycle Assessment of Second Generation Bioethanol Production via Biochemical Processes, in: The Canadian Society for Bioengineering 2018 Annual Conference. Guelph, On.

de Jong, E., Higson, A., Walsh, P., Wellisch, M., 2012. Bio-based Chemicals: Value Added Products from Biorefineries. Waginingen.

den Haan, R., van Rensburg, E., Rose, S.H., Gorgens, J.F., van Zyl, W.H., 2015. Progress and challenges in the engineering of non-cellulolytic microorganisms for consolidated bioprocessing. Curr. Opin. Bioechnology 33, 32–38. doi:10.1016/j.copbio.2014.10.003

Deng, D., Weidhaas, J.L., Lin, L.S., 2016. Kinetics and microbial ecology of batch sulfidogenic bioreactors for co-treatment of municipal wastewater and acid mine drainage. J. Hazard. Mater. 305, 200–208. doi:10.1016/j.jhazmat.2015.11.041

Department of Water and Sanitation, 2013. WITWATERSRAND, GAUTENG: ACID MINE DRAINAGE: LONG TERM SOLUTION.

Drissen, R.E.T., Maas, R.H.., Van Der Maarel, M.J.E.C., Kabel, M.., Schols, H.A. Tramper, J., Beeftink, H.H., 2009. A generic model for glucose production from various cellulose sources by a commercial cellulase complex. Biocatals and Biotransformation 25, 419–429. doi:10.1080/10242420701510668

Durand, J.F., 2012. The impact of gold mining on the Witwatersrand on the rivers and karst system of Gauteng and North West Province, South Africa. J. African Earth Sci. 68, 24–43. doi:10.1016/j.jafrearsci.2012.03.013

E4TECH, RE-CORD, WUR, 2015. From the Sugar Platform to biofuels and biochemicals, Final report for the European Commission Directorate-General Energy. doi:contract No. ENER/C2/423-2012/SI2.673791

Eklund, R., Zacchi, G., 1995. Simultaneous saccharification and fermentation of steam-pretreated willow. Enzyme Microb. Technol. 17, 255–259.

Esteghlalian, A., Hashimoto, A.G., Fenske, J.J., Penner, M.H., 1997. Modeling and optimization of the dilute-sulfuric-acid pretreatment of corn stover, poplar and switchgrass. Bioresour. Technol. 59, 129–136. doi:10.1016/S0960-8524(97)81606-9

Feng, D., Aldrich, C., Tan, H., 2000. Treatment of Acid Mine Water by Use of Heavey Metal Precipitation and Ion Exchange. Miner. Eng. 13, 623–642.

Foucher, S., Battaglia-Brunet, F., Ignatiadis, I., Morin, D., 2001. Treatment by sulfate-reducing bacteria

of Chessy acid-mine drainage and metals recovery. Chem. Eng. Sci. 56, 1639–1645. doi:10.1016/S0009-2509(00)00392-4

Galbe, M., Zacchi, G., 2002. A review of the production of ethanol from softwood. Appl. Microbiol. Biotechnol. 59, 618–628. doi:10.1007/s00253-002-1058-9

García-cubero Teresa, M., González-benito, G., Indacoechea, I., Coca, M., Bolado, S., 2009. Bioresource Technology Effect of ozonolysis pretreatment on enzymatic digestibility of wheat and rye straw. Bioresour. Technol. 100, 1608–1613. doi:10.1016/j.biortech.2008.09.012

Glombitza, F., 2001. Treatment of acid lignite mine ¯ ooding water by means of microbial sulfate reduction. Waste Manag. 21, 197–203. doi:10.1016/S0956-053X(00)00061-1

Gnansounou, E., Dauriat, A., 2010. Bioresource Technology Techno-economic analysis of lignocellulosic ethanol : A review. Bioresour. Technol. 101, 4980–4991. doi:10.1016/j.biortech.2010.02.009

Greben, H.A., Baloyi, J., Sigama, J., Venter, S.N., 2009a. Bioremediation of sulphate rich mine effluents using grass cuttings and rumen fluid microorganisms. J. Geochemical Explor. 100, 163–168. doi:10.1016/j.gexplo.2008.01.004

Greenway, N., 2019. The Bioremediation of Acid Mine Drainage Utilising Indigenous South African Grass as the Organic Carbon Source for Dissimilatory Sulfate Reduction. University of the Witwatersrand, Johannesburg.

Gubicza, K., Nieves, I.U., Sagues, W.J., Barta, Z., Shanmugam, K.T., Ingram, L.O., 2016. Techno-economic analysis of ethanol production from sugarcane bagasse using a Liquefaction plus Simultaneous Saccharification and co-Fermentation process. Bioresour. Technol. 208, 42–48. doi:10.1016/j.biortech.2016.01.093

Hahn-Hägerdal, B., Galbe, M., Gorwa-Grauslund, M.F., Lindén, G., Zacchi, G., 2006. Bio-ethanol – the fuel of tomorrow from the residues of today. Trends Biotechnol. 24. doi:10.1016/j.tibtech.2006.10.004

Hamelinck, C.N., van Hooijdonk, G., Faaij, A.P., 2005. Ethanol from lignocellulosic biomass : techno-economic performance in short- , middle- and long-term. Biomass and Bioenergy 28, 384–410. doi:10.1016/j.biombioe.2004.09.002

Harjunpaa, V., Tcleman, A., Koivula, A., Ruohonen, L., Teerp, T.T., 1996. Cello-oligosaccharide hydrolysis by cellobiohydrolase II from Trichoderma reesei Association and rate constants derived from an analysis of progress curves. Eur. J. Biochem. 240, 584–591.

Harris, P.O., Ramelow, G.J., 1990. Binding of Metal Ions by Particulate Biomass Derived from Chlorella Vulgaris and Scenedesmus Quadricauda. Environ. Sci. Technol. 24, 220–228. doi:10.1021/es00072a011

Hayes, D.J., 2009. An examination of biorefining processes, catalysts and challenges. Catal. Today 145, 138–151. doi:10.1016/j.cattod.2008.04.017

Hendriks, A.T.W.M., Zeeman, G., 2009. Pretreatments to enhance the digestibility of lignocellulosic biomass. Bioresour. Technol. 100, 10–18. doi:10.1016/j.biortech.2008.05.027

Hiibel, S.R., Pereyra, L.P., Breazeal, M.V.R., Reisman, D.J., Reardon, K.F., Pruden, A., 2011. Effect of Organic Substrate on the Microbial Community Structure in Pilot-Scale Sulfate-Reducing Biochemical Reactors Treating Mine Drainage 1. Enviromental Eng. Sci. 28, 563–572. doi:10.1089/ees.2010.0237

Houten, B.H.G.W. Van, Roest, K., Tzeneva, V.A., Dijkman, H., Smidt, H., Stams, A.J.M., 2006. Occurrence of methanogenesis during start-up of a full-scale synthesis gas-fed reactor treating sulfate and metal-rich wastewater. Water Res. 40, 553–560. doi:10.1016/j.watres.2005.12.004

Huang, H., Ramaswamy, S., Al-dajani, W., Tschirner, U., Cairncross, R.A., 2009. Effect of biomass species and plant size on cellulosic ethanol : A comparative process and economic analysis. Biomass and Bioenergy 33, 234–246. doi:10.1016/j.biombioe.2008.05.007

Humbird, D., Davis, R., Tao, L., Kinchin, C., Hsu, D., Aden, A., Schoen, P., Lukas, J., Olthof, B., Worley, M., Sexton, D., Dudgeon, D., 2011. Process Design and Economics for Biochemical Conversion of Lignocellulosic Biomass to Ethanol. Golden, Co.

Huron, M., Hudebine, D., Ferreira, N.L., Lachenal, D., 2016. Mechanistic Modeling of Enzymatic Hydrolysis of Cellulose Integrating Substrate Morphology and Cocktail Composition. Biotechnol. Bioeng. 113, 1011–1023. doi:10.1002/bit.25873

IEA Bioenergy, 2013. Factsheets Biorefineries [WWW Document]. URL http://www.iea-bioenergy.task42-biorefineries.com/en/ieabiorefinery/Factsheets.htm (accessed 7.21.17).

IPCC, 2018. Summary for Policy Makers, Summary for Policymakers. In: Global Warming of 1.5°C. An IPCC Special Report on the impacts of global warming of 1.5°C above pre-industrial levels and related global greenhouse gas emission pathways, in the context of strengthening the global response to. Geneva, Switzerland.

IPCC, 2014a. Climate Change 2014: Contribution of Working Groups I, II and III to the Fifth Assessment Report of the Intergovernmental Panel on Climate Change, in: Core Writing Team, Pachauri, R.K., Meyer, L.A. (Eds.), . IPCC, Geneva, Switzerland, p. 151.

Iranmahboob, J., Nadim, F., Monemi, S., 2002. Optimizing acid-hydrolysis: A critical step for production of ethanol from mixed wood chips. Biomass and Bioenergy 22, 401–404. doi:10.1016/S0961-9534(02)00016-8

Jeoh, T., Cardona, M.J., Karuna, N., Mudinoor, A.R., Nill, J., 2017. Mechanistic Kinetic Models of Enzymatic Cellulose Hydrolysis — A Review. Biotechnol. Bioeng. 114, 1369–1385. doi:10.1002/bit.26277

Jin, Q., Zhang, H., Yan, L., Qu, L., Huang, H., 2011. Kinetic characterization for hemicellulose hydrolysis of corn stover in a dilute acid cycle spray flow-through reactor at moderate conditions. Biomass and Bioenergy 35, 4158–4164. doi:10.1016/j.biombioe.2011.06.050

Johnson, D.B., 1995. Acidophilic microbial communities: Candidates for bioremediation of acidic mine effluents. Int. Biodeterior. Biodegrad. 35, 41–58. doi:10.1016/0964-8305(95)00065-D

Johnson, D.B., Hallberg, K.B., 2005a. Acid mine drainage remediation options: A review. Sci. Total Environ. 338, 3–14. doi:10.1016/j.scitotenv.2004.09.002

Johnson, D.B., Hallberg, K.B., 2005b. Biogeochemistry of the compost bioreactor components of a composite acid mine drainage passive remediation system. Sci. Total Environ. 338, 81–93. doi:10.1016/j.scitotenv.2004.09.008

Jones, J.L., Semrau, K.T., 1984. Wood hydrolysis for ethanol production - previous experience and the economics of selected processes. Biomass 5, 109–135. doi:10.1016/0144-4565(84)90052-0

Jong, T., Parry, D.L., 2006. Microbial sulfate reduction under sequentially acidic conditions in an upflow anaerobic packed bed bioreactor. Water Res. 40, 2561–2571. doi:10.1016/j.watres.2006.05.001

Jong, T., Parry, D.L., 2003. Removal of sulfate and heavy metals by sulfate reducing bacteria in short-term bench scale upflow anaerobic packed bed reactor runs. Water Res. 37, 3379–3389. doi:10.1016/S0043-1354(03)00165-9

Jungmeier, G., van Ree, R., Jørgensen, H., De Jong, E., Stichnothe, H., Wellisch, M., 2014. The Biorefinery Complexity Index. doi:???

Kadam, K.L., Rydholm, E.C., Mcmillan, J.D., 2004. Development and Validation of a Kinetic Model for

Enzymatic Saccharification of Lignocellulosic Biomass 698–705.

Kaksonen, A.H., Franzmann, P.D., Puhakka, J.A., 2004. Effects of Hydraulic Retention Time and Sulfide Toxicity on Ethanol and Acetate Oxidation in Sulfate-Reducing Metal- Precipitating Fluidized-Bed Reactor. Biotechnol. Bioeng. 86, 332–343. doi:10.1002/bit.20061

Kaksonen, A.H., Puhakka, J.A., 2007. Sulfate reduction based bioprocesses for the treatment of acid mine drainage and the recovery of metals. Eng. Life Sci. 7, 541–564. doi:10.1002/elsc.200720216

Kaksonen, A.H., Riekkola-vanhanen, M., Puhakka, J.A., 2003. Optimization of metal sulphide precipitation in fluidized-bed treatment of acidic wastewater. Water Res. 37, 255–266. doi:10.1016/S0043-1354(02)00267-1

Kalin, M., Cairns, J., McCready, R., 1991. Ecological engineering methods for acid mine drainage treatment of coal wastes. Resour. Conserv. Recycl. 5, 265–275. doi:10.1016/0921-3449(91)90030-R

Kalin, M., Fyson, A., Wheeler, W.N., 2006. The chemistry of conventional and alternative treatment systems for the neutralization of acid mine drainage. Sci. Total Environ. 366, 395–408. doi:10.1016/j.scitotenv.2005.11.015

Karimi, K., Emtiazi, G., Taherzadeh, M.J., 2006. Ethanol production from dilute-acid pretreated rice straw by simultaneous saccharification and fermentation with Mucor indicus , Rhizopus oryzae , and Saccharomyces cerevisiae. Enzyme Microb. Technol. 40, 138–144. doi:10.1016/j.enzmictec.2005.10.046

Katahira, S., Mizuike, A., Fukuda, H., Kondo, A., 2006. Ethanol fermentation from lignocellulosic hydrolysate by a recombinant xylose- and cellooligosaccharide-assimilating yeast strain. Appl. Microbiol. Biotechnol. 72, 1136–1143. doi:10.1007/s00253-006-0402-x

Kazi, F.K., Fortman, J.A., Anex, R.P., Hsu, D.D., Aden, A., Dutta, A., Kothandaraman, G., 2010. Techno-economic comparison of process technologies for biochemical ethanol production from corn stover q. Fuel 89, S20–S28. doi:10.1016/j.fuel.2010.01.001

Kefeni, K.K., Msagati, T.A.M., Mamba, B.B., 2017. Acid mine drainage : Prevention , treatment options , and resource recovery : A review. J. Clean. Prod. 151, 475–493. doi:10.1016/j.jclepro.2017.03.082

Kepler, D., McCleary, E., 1994. SuccessiveAlkalinity Producing Systems (SAPS) for theTreatment of Acidic Mine Drainage, in: International Land Reclamation and Mine Drainage Confrence and 3rd International Confrence on the Abatement of Acidic Drainage. Pittsburg, PA, pp. 195–204.

Khayatzadeh, J., Abbasi, E., 2010. The Effects of Heavy Metals on Aquatic Animals, in: The 1st International Applied Geological Congress. Mashad, Iran, pp. 26–28.

Kim, J.K., Oh, B.R., Shin, H., Eom, C., Kim, S.W., 2008. Statistical optimization of enzymatic saccharification and ethanol fermentation using food waste. Process Biochem. 43, 1308–1312. doi:10.1016/j.procbio.2008.07.007

Kim, S., Holtzapple, M.T., 2006. Delignification kinetics of corn stover in lime pretreatment. Bioresour. Technol. 97, 778–785. doi:10.1016/j.biortech.2005.04.002

Kim, S.R., Ha, S., Wei, N., Oh, E.J., Jin, Y., 2012. Simultaneous co-fermentation of mixed sugars : a promising strategy for producing cellulosic ethanol. Trends Biotechnol. 30, 274–282. doi:10.1016/j.tibtech.2012.01.005

Kim, Y., Kreke, T., Ladisch, M.R., 2013. Reaction Mechanisms and Kinetics of Xylo-Oligosaccharide Hydrolysis by Dicarboxylic Acids. Am. Inst. Chem. Eng. J. 59. doi:10.1002/aic

Klein-marcuschamer, D., Oleskowicz-popiel, P., Simmons, B.A., Blanch, H.W., 2010. Technoeconomic

analysis of biofuels : A wiki-based platform for lignocellulosic biorefineries. Biomass and Bioenergy 34, 1914–1921. doi:10.1016/j.biombioe.2010.07.033

Kobayashi, T., Sakai, Y., 1956. Bulletin of the Agricultural Chemical Society of Japan Hydrolysis Rate of Pentosan of Hardwood in Dilute Sulfuric Acid in Dilute Sulfuric Acid. Bull. Agric. Soc. Japan 20, 1–7. doi:10.1080/03758397.1956.10857296

Kolmert, A., Johnson, D.B., 2001. Remediation of acidic waste waters using immobilised , acidophilic sulfate-reducing bacteria. J. Chem. Technol. Biotechnol. 76, 836–843. doi:10.1002/jctb.453

Kootstra, A.M.J., Beeftink, H.H., Scott, E.L., Sanders, J.P.M., 2009. Comparison of dilute mineral and organic acid pretreatment for enzymatic hydrolysis of wheat straw. Biochem. Eng. J. 46, 126–131. doi:10.1016/j.bej.2009.04.020

Kumar, R., Wyman, C.E., 2009. Effects of cellulase and xylanase enzymes on the deconstruction of solids from pretreatment of poplar by leading technologies. Biotechnol. Prog. 25, 302–314. doi:10.1002/btpr.102

Kunz, R., Jewitt, G., 2013. Mapping the potential water use of biofuel feedstock production in South Africa, in: Dallemand, J.F. (Ed.), JRC Technical Reports - Bioenergy and Water. International Energy Agency, pp. 171–190. doi:10.2790/94402

Kuyucak, N., Lindvalf, M., Serrano, J.A.R., Oliva, A.F., 1999. IMPLEMENTATION OF A HIGH DENSITY SLUDGE " HDS " TREATMENT PROCESS AT THE BOLIDEN APIRSA MINE SITE, in: Mine, Water, & Enviroment. IMWA Congress,. Sevilla, Spain, pp. 473–479.

Larsson, S., Palmqvist, E., Hahn-Hagerdal, B., Tengborg, C., Stenberg, K., Zacchi, G., Nilvebrant, N.O., 1999. The generation of fermentation inhibitors during dilute acid hydrolysis of softwood. Enzyme Microb. Technol. 24, 151–159. doi:10.1016/S0141-0229(98)00101-X

Laser, M., Larson, E., Dale, B.E., Wang, M., Greene, N., Lynd, L.R., 2009. Comparative analysis of efficiency , environmental impact , and process economics for mature biomass refi ning scenarios. Biofuels, Bioprod. Biorefining 3, 247–270. doi:10.1002/bbb

Lauterbacher, J.S., Moran-mirabal, J.M., Burkholder, E.W., Walker, L.P., 2015. Modeling Enzymatic Hydrolysis of Lignocellulosic Substrates Using Confocal Fluorescence Microscopy I : Filter Paper Cellulose. Biotechnol. Bioeng. 112, 21–31. doi:10.1002/bit.25329

Lavarack, B.P., Gri, G.J., Rodman, D., 2002. The acid hydrolysis of sugarcane bagasse hemicellulose to produce xylose , arabinose , glucose and other products. Biomass and Bioenergy 23, 367–380.

Lee, D., Ownes, V.N., Boe, A., Jeramyama, P., 2007. Composition of Herbaceous Biomass Feedstocks. Brookings, SD.

Lee, S.H., Doherty, T. V, Linhardt, R.J., Dordick, J.S., 2009. Ionic Liquid-Mediated Selective Extraction of Lignin From Wood Leading to Enhanced Enzymatic Cellulose Hydrolysis. Biotechnol. Bioeng. 102, 1368–1376. doi:10.1002/bit.22179

Lefticariu, L., Walters, E.R., Pugh, C.W., Bender, K.S., 2015. Sulfate reducing bioreactor dependence on organic substrates for remediation of coal-generated acid mine drainage: Field experiments. Appl. Geochemistry 63, 70–82. doi:10.1016/j.apgeochem.2015.08.002

Lenihan, P., Orozco, A., O'Neill, E., Ahmad, M.N.M., Rooney, D.W., Walker, G.M., 2010. Dilute acid hydrolysis of lignocellulosic biomass. Chem. Eng. J. 156, 395–403. doi:10.1016/j.cej.2009.10.061

Li, Q., He, Y.C., Xian, M., Jun, G., Xu, X., Yang, J.M., Li, L.Z., 2009. Improving enzymatic hydrolysis of wheat straw using ionic liquid 1-ethyl-3-methyl imidazolium diethyl phosphate pretreatment. Bioresour. Technol. 100, 3570–3575. doi:10.1016/j.biortech.2009.02.040

Liao, W., Liu, Y., Wen, Z., Frear, C., Chen, S., 2008. Kinetic Modeling of Enzymatic Hydrolysis of Cellulose

in Differently Pretreated Fibers From Dairy Manure 101, 441–451. doi:10.1002/bit.21921

Lin, Y.H., Lee, K.K., 2001. Verification of Anarobic Biofilm Model for Phenol Degradation with Sulfate Reduction. J. Environ. Eng. 127, 119–125. doi:10.1061/(ASCE)0733-9372(2001)127:2(119)

Linde, M., Galbe, M., Zacchi, G., 2007. Simultaneous saccharification and fermentation of steam-pretreated barley straw at low enzyme loadings and low yeast concentration. Enzyme Microb. Technol. 40, 1100–1107. doi:10.1016/j.enzmictec.2006.08.014

Lu, J., Chen, T., Wu, J., Chris Wilson, P., Hao, X., Qian, J., 2011. Acid tolerance of an acid mine drainage bioremediation system based on biological sulfate reduction. Bioresour. Technol. 102, 10401–10406. doi:10.1016/j.biortech.2011.09.046

Lynd, L.R., Zyl, W.H. Van, Mcbride, J.E., Laser, M., 2005. Consolidated bioprocessing of cellulosic biomass : an update. Curr. Opin. Biotechnol. 16, 577–583. doi:10.1016/j.copbio.2005.08.009

Magowo, E., Rumbold, K., Sheridan, C., 2015. The Utilization of Cellulosic Biomass in treating AMD and the Subsequent Generation of Fermentable Sugars, in: 10th International Conference on Acid Rock Drainage and IMWA Anual Conference. pp. 1–12.

Maloney, M.T., Chapman, T.W., Baker, a J., 1985. Dilute acid hydrolysis of paper birch: kinetics studies of xylan and acetyl-group hydrolysis. Biotechnol. Bioeng. 27, 355–361. doi:10.1002/bit.260270321

Maurer, S.A., Brady, N.W., Fajardo, N.P., Radke, C.J., 2013. Journal of Colloid and Interface Science Surface kinetics for cooperative fungal cellulase digestion of cellulose from quartz crystal microgravimetry. J. Colloid Interface Sci. 394, 498–508. doi:10.1016/j.jcis.2012.12.022

Maurya, D.P., Singla, A., Negi, S., 2015. An overview of key pretreatment processes for biological conversion of lignocellulosic biomass to bioethanol. 3 Biotech 5, 597–609. doi:10.1007/s13205-015-0279-4

McCarthy, T.S., 2011. The impact of acid mine drainage in South Africa. S. Afr. J. Sci. 107, 1–7. doi:10.4102/sajs.v107i5/6.712

Mccarthy, T.S., Steyl, G., Maree, J., Zhao, H., 2010. MINE WATER MANAGEMENT IN THE WITWATERSRAND WITH SPECIAL EMPHASIS ON ACID MINE DRAINAGE: Report to the Inter-Ministerial Committee on Acid Mine Drainage 1–128.

McKnight, D.M., Morel, F.M.M., 1980. Copper complexation by siderophores from filamentous blue-green algae. Limnol. Oceanogr. 25, 62–71. doi:10.4319/lo.1980.25.1.0062

McMillan, J.D., 1997. Bioethanol Production: Status and Prospects. Renew. Energy 10, 295–302.

McMillan, J.D., Newman, M.M., Templeton, D.W., Mohagheghi, A., 1999. Simultaneous Saccharification and Cofermentation of Dilute-Acid Pretreated Yellow Poplar Hardwood to Ethanol Using Xylose-Fermenting Zymomonas mobilis. Appl. Biochem. Biotechnol. 77–79, 649–665.

Menegol, D., Scholl, A.L., Fontana, R.C., Dillon, A.J.P., Camassola, M., 2014. Increased release of fermentable sugars from elephant grass by enzymatic hydrolysis in the presence of surfactants. Energy Convers. Manag. 88, 1252–1256. doi:10.1016/j.enconman.2014.02.071

Mohan, D., Chander, S., 2006. Removal and recovery of metal ions from acid mine drainage using lignite — A low cost sorbent. J. Hazard. Mater. 137, 1545–1553. doi:10.1016/j.jhazmat.2006.04.053

Montoya, L., Celis, L.B., Gallegos-Garcia, M., Elias, R.-F., Alpuche-Solis, A., 2013. Consortium diversity of a sulfate-reducing biofilm developed at acidic pH influent conditions in a down-flow fluidized bed reactor. Eng. Life Sci. 13, 302–311. doi:10.1002/elsc.201200047

Moosa, S., Nemati, M., Harrison, S.T.L., 2002. A kinetic study on anaerobic reduction of sulphate , Part I : Effect of sulphate concentration. Chem. Eng. Sci. 57, 2773–2780. doi:10.1016/S0009-2509(02)00152-5

Mosier, N., Hendrickson, R., Ho, N., Sedlak, M., Ladisch, M.R., 2005a. Optimization of pH controlled liquid hot water pretreatment of corn stover. Bioresour. Technol. 96, 1986–1993. doi:10.1016/j.biortech.2005.01.013

Mosier, N., Wyman, C., Dale, B., Elander, R., Lee, Y.Y., Holtzapple, M., Ladisch, M., 2005b. Features of promising technologies for pretreatment of lignocellulosic biomass. Bioresour. Technol. 96, 673–686. doi:10.1016/j.biortech.2004.06.025

MPRDA, 2013. Mineral and Petroleum Resources Development Amendement Bill. Government Gazette No. 36523, South Africa.

Nagpal, S., Chuichulcherm, S., Peeva, L., 2000. Microbial Sulfate Reduction in a Liquid – Solid Fluidized Bed Reactor. Biotechnol. Bioeng. 70, 370–380. doi:10.1002/1097-0290(20001120)70:4<370::AID-BIT2>3.0.CO;2-7

Nancucheo, I., Johnson, D.B., 2012. Selective removal of transition metals from acidic mine waters by novel consortia of acidophilic sulfidogenic bacteria. Microb. Biotechnol. 5, 34–44. doi:10.1111/j.1751-7915.2011.00285.x

National Accademy of Sciences, National Academy of Engineering, National Research Council, 2009. The national academies press, 1st ed. The National Academies Press, Wachington, D.C. doi:10.17226/12620

Neculita, C.M., Zagury, G.J., Bussière, B., 2008. Effectiveness of sulfate-reducing passive bioreactors for treating highly contaminated acid mine drainage: II. Metal removal mechanisms and potential mobility. Appl. Geochemistry 23, 3545–3560. doi:10.1016/j.apgeochem.2008.08.014

Nee, C.I., Yee, W.F., 1976. Hydrolysis of Pentosans in Bagasse Pith. J. Appl. Chem. Biotechnol. 26, 283–287.

Nidetzky, B., Zachariae, W., Gercken, G., Hayn, M., 1994. Hydrolysis of ceilooligosaccharides by Trichoderma reesei cellobiohydrolases : Experimental data and kinetic modeling. Enzyme Microb. Technol. 16, 43–52.

NREL, 1996. Measurement of Cellulase Activities Laboratory Analytical Procedure NREL/TP-510-42628, Laboratory Analytical Procedure.

Oliva, J.M., Sáez, F., Ballesteros, I., González, A., Negro, M.J., Manzanares, P., Ballesteros, M., 2003. Effect of lignocellulosic degradation compounds from steam explosion pretreatment on ethanol fermentation by thermotolerant yeast Kluyveromyces marxianus. Appl. Biochem. Biotechnol. 105–108, 141–153. doi:10.1385/ABAB:105:1-3:141

Olsson, L., Soerensen, H.R., Christensen, H., Ktogh, K.M., Meyer, A.S., 2006. Separate and Simultaneous Enzymatic Hydrolysis and Fermentation of Wheat Hemicellulose With Recombinant Xylose Utilizing Saccharomyces cerevisiae. Appl. Biochem. Biotechnol. 129–132, 117–129.

Palonen, H., Thomsen, A.B., Tenkanen, M., Schmidt, A.S., Viikari, L., 2004. Evaluation of wet oxidation pretreatment for enzymatic hydrolysis of softwood. Appl. Biochem. Biotechnol. 117, 1–17. doi:10.1385/ABAB:117:1:01

Papatheofanous, M.G., Billa, E., Koullas, D.P., Monties, B., Koukios, E.G., 1995. Two-stage acid-catalyzed fractionation of lignocellulosic biomass in aqueous ethanol systems at low temperatures. Bioresour. Technol. 54, 305–310. doi:10.1016/0960-8524(95)00152-2

Petersen, A.M., Westhuizen, W.A. Van Der, Mandegari, M.A., Görgens, J.F., 2018. Economic analysis

of bioethanol and electricity production from sugarcane in South Africa. Biofuels, Bioprod. Biorefining 12, 224–238. doi:10.1002/bbb

Philippidis, G.P., Smith, T.K., 1995. Limiting factors in the simultaneous saccharification and fermentation process for conversion of cellulosic biomass to fuel ethanol. Appl. Biochem. Biotechnol. 51, 117–124. doi:10.1007/BF02933416

Piccolo, C., Bezzo, F., 2009. A techno-economic comparison between two technologies for bioethanol production from lignocellulose. Biomass and Bioenergy 33, 478–491. doi:10.1016/j.biombioe.2008.08.008

Ramla, B., Sheridan, C., 2015. The potential utilisation of indigenous South African grasses for acid mine drainage remediation. Water SA 41, 247–252. doi:10.4314/wsa.v41i2.10

Ricci, B.C., Ferreira, C.D., Aguiar, A.O., Amaral, M.C.S., 2015. Integration of nanofiltration and reverse osmosis for metal separation and sulfuric acid recovery from gold mining effluent. Seperation Purif. Technol. 154, 11–21. doi:10.1016/j.seppur.2015.08.040

Rodriguez-Chong, A., Ramirez, J.A., Garrote, G., Manuel, V., 2004. Hydrolysis of sugar cane bagasse using nitric acid : a kinetic assessment. J. Food Eng. 61, 143–152. doi:10.1016/S0260-8774(03)00080-3

Saeman, J.F., 1945. Kinetics of Wood Saccharfifications-Hydrolysis of Cellulose and Decomposition of Sugars in Dilute Acid at High Temperature. Ind. Eng. Chem. 37, 43–52. doi:10.1021/ie50421a009

Sáez-Miranda, J.C., Saliceti-piazza, L., McMillan, J.D., 2006. Measurement and Analysis of Intracellular ATP Levels in Metabolically Engineered Zymomonas mobilis Fermenting Glucose and Xylose Mixtures. Biotechnol. Prog. 22, 359–368. doi:doi.org/10.1021/bp050115c

Saha, Badal C., Iten, L.B., Cotta, M.A., Wu, Y.V., 2005. Dilute acid pretreatment, enzymatic saccharification and fermentation of wheat straw to ethanol. Process Biochem. 40, 3693–3700. doi:10.1016/j.procbio.2005.04.006

Sánchez-Andrea, I., Sanz, J.L., Bijmans, M.F.M., Stams, A.J.M., 2014. Sulfate reduction at low pH to remediate acid mine drainage. J. Hazard. Mater. 269, 98–109. doi:10.1016/j.jhazmat.2013.12.032

Sánchez-Andrea, I., Triana, D., Sanz, J.L., 2012. Bioremediation of acid mine drainage coupled with domestic wastewater treatment. Water Sci. Technol. 66, 2425–2431. doi:10.2166/wst.2012.477

Sanchez, A., Sevilla-Güitrón, V., Magaña, G., Gutierrez, L., 2013. Parametric analysis of total costs and energy efficiency of 2G enzymatic ethanol production. Fuel 113, 165–179. doi:10.1016/j.fuel.2013.05.034

Schacht, C., Zetzl, C., Brunner, G., 2008. From plant materials to ethanol by means of supercritical fluid technology. J. Supercrit. Fluids 46, 299–321. doi:10.1016/j.supflu.2008.01.018

Schell, D.J., Farmer, J., Newman, M., McMillan, J.D., 2003. Dilute – Sulfuric Acid Pretreatment of Corn Stover in Pilot-Scale Reactor. Appl. Biochem. Biotechnol. 105–108, 69–85.

Sendich, E., Laser, M., Kim, S., Alizadeh, H., Laureano-perez, L., Dale, B., Lynd, L., 2008. Recent process improvements for the ammonia fiber expansion (AFEX) process and resulting reductions in minimum ethanol selling price. Bioresour. Technol. 99, 8429–8435. doi:10.1016/j.biortech.2008.02.059

Shang, B.Z., Chang, R., Chu, J., 2013. Systems-level Modeling with Molecular Resolution Elucidates the Rate-limiting Mechanisms of Cellulose Decomposition by. J. Biol. Chem. 288, 29081–29089. doi:10.1074/jbc.M113.497412

Shi, J., Chinn, M.S., Sharma-shivappa, R.R., 2008. Microbial pretreatment of cotton stalks by solid state

cultivation of Phanerochaete chrysosporium. Bioresour. Technol. 99, 6556–6564. doi:10.1016/j.biortech.2007.11.069

Shin, D., Yoo, A., Kim, S.W., Yang, D.R., 2006. Cybernetic Modeling of Simultaneous Saccharification and Fermentation for Ethanol Production from Steam-Exploded Wood with Brettanomyces custersii. J. Microbiol. Biotechnol. 16, 1355–1361.

Simate, G.S., Ndlovu, S., 2014. Acid mine drainage: Challenges and opportunities. J. Environ. Chem. Eng. 2, 1785–1803. doi:10.1016/j.jece.2014.07.021

Singh, J., Kalamdhad, A.S., 2011. Effects of Heavy Metals on Soil , Plants , Human Health and Aquatic Life. Int. J. Res. Chem. Enviroment 1, 15–21.

Singh, R., Gautam, N., Mishra, A., Gupta, R., 2011. Heavy metals and living systems: An overview. Indian J. Pharmacol. 43, 246–253. doi:10.4103/0253-7613.81505

Skousen, J., Zipper, C.E., Rose, A., Ziemkiewicz, P.F., Nairn, R., McDonald, L.M., Kleinmann, R.L., 2017. Review of Passive Systems for Acid Mine Drainage Treatment. Mine Water Environ. 36, 133–153. doi:10.1007/s10230-016-0417-1

Soderstrom, J., Pilcher, L., Mats, G., Zacchi, G., 2003. Combined Use of H 2 SO 4 and SO 2 Impregnation for Steam Pretreatment of Spruce in Ethanol Production. Appl. Biochem. Biotechnol. 105–108, 127–140.

Sun, R.C., Tomkinson, J., 2002. Characterization of hemicelluloses obtained by classical and ultrasonically assisted extractions from wheat straw. Carbohydr. Polym. 50, 263–271. doi:10.1016/S0144-8617(02)00037-1

Sun, Y., Cheng, J., 2002. Hydrolysis of lignocellulosic materials for ethanol production: A review. Bioresour. Technol. 83, 1–11. doi:10.1016/S0960-8524(01)00212-7

Taherzadeh, M.J., Karimi, K., 2008. Pretreatment of lignocellulosic wastes to improve ethanol and biogas production: A review. Int. J. Mol. Sci. 9, 1621–1651. doi:10.3390/ijms9091621

Taherzadeh, M.J., Karimi, K., 2007a. Enzyme based hydrolysis processes for ethanol from lignocellulosic materials : a review. Bioresources 2, 707–738.

Taherzadeh, M.J., Karimi, K., 2007b. Acid-based hydrolysis processes for ethanol from lignocellulosic materials: a review. BioResources 2, 472–499.

Tengborg, C., Stenberg, K., Galbe, M., Zacchi, G., Larsson, S., Palmqvist, E., Hahn-Hägerdal, B., 1998. Comparison of SO2 and H2SO4 impregnation of softwood prior to steam pretreatment on ethanol production. Appl. Biochem. Biotechnol. 70, 3–15. doi:10.1007/BF02920119

Tizazu, B.Z., Moholkar, V.S., 2017. Kinetic and Thermodynamic Analysis of Dilute Acid Hydrolysis of Sugarcane bagasse Bioresource Technology Kinetic and thermodynamic analysis of dilute acid hydrolysis of sugarcane bagasse. Bioresour. Technol. 250, 197–203. doi:10.1016/j.biortech.2017.11.032

Torget, R., Werdene, P., Himmel, M., Grohmann, K., 1990. Dilute Acid Pretreatment of Short Rotation Woody and Herbaceous Crops. Appl. Biochem. Biotechnol. 24, 115–126. doi:10.1007/BF02920238

Tsukamoto, T.K., Miller, G.C., 1999. METHANOL AS A CARBON SOURCE FOR MICROBIOLOGICAL TREATMENT OF ACID MINE DRAINAGE. Water Res. 33, 1365–1370. doi:10.1016/S0043-1354(98)00342-X

Uihlein, A., Schebek, L., 2009. Environmental impacts of a lignocellulose feedstock biorefinery system: An assessment. Biomass Bioenergy 33, 793–802. doi:10.1016/j.biombioe.2008.12.001

Van Hille, R.., Boshoff, G.., Rose, P.., Duncan, J.., 1999. A continuous process for the biological

treatment of heavy metal contaminated acid mine water. Resour. Conserv. Recycl. 27, 157–167. doi:10.1016/S0921-3449(99)00010-5

Varga, E., Réczey, K., Zacchi, G., 2004. Optimization of steam pretreatment of corn stover to enhance enzymatic digestibility. Appl. Biochem. Biotechnol. 113–116, 509–523. doi:10.1385/ABAB:114:1-3:509

Verardi, A., Bari, I. De, Ricca, E., Calabrò, V., 2012. Bioethanol, in: Lima, P.Ma.A.P. (Ed.), Bioethanol. Rijeka, pp. 95–122. doi:10.5772/23987

Viksø-Nielsen, A., 2008. Recent development in enzymes for bio- mass hydrolysis Anders, in: Landscape, H.F. and (Ed.), First European Workshop on Biotechnology for Lignocellulose Biorefineries. University of Copenhagen, Copenhagen, p. 29.

Wan Ngah, W.S., Hanafiah, M.A.K.M., 2008. Removal of heavy metal ions from wastewater by chemically modified plant wastes as adsorbents: A review. Bioresour. Technol. 99, 3935–3948. doi:10.1016/j.biortech.2007.06.011

Wang, M., Zhang, D., Dong, J., Tan, S.K., 2018. Application of constructed wetlands for treating agricultural runoff and agro-industrial wastewater: a review. Hydrobiologia 805, 1–31. doi:10.1007/s10750-017-3315-z

Wang, Z., Cheng, J.J., 2011. Lime Pretreatment of Coastal Bermudagrass for Bioethanol Production. Energy & Feuls 25, 1830–1836. doi:10.1021/ef2000932

Water Research Commision, 2017. The South Africa Mine Water Atlas,WRC Report no. TT670/16. Pretoria.

Weijma, J., Stams, A.J.M., Pol, L.W.H., Lettinga, G., 2000. Thermophilic Sulfate Reduction and Methanogenesis with Methanol in a High Rate Anaerobic Reactor. Biotechnol. Bioeng. 67, 354–363. doi:10.1002/(SICI)1097-0290(20000205)67:3<354::AID-BIT12>3.0.CO;2-X

Westensee, D.K., Rumbold, K., Harding, K.G., Sheridan, C.M., van Dyk, L.D., Simate, G.S., Postma, F., 2018. The availability of second generation feedstocks for the treatment of acid mine drainage and to improve South Africa's bio-based economy. Sci. Total Environ. 637–638, 132–136. doi:10.1016/j.scitotenv.2018.04.410

White, C., Sayer, J.A., Gadd, G.M., 1997. Microbial solubilization and immobilization of toxic metals: Key biogeochemical processes for treatment of contamination. FEMS Microbiol. Rev. 20, 503–516. doi:10.1016/S0168-6445(97)00029-6

Wingren, A., Galbe, M., Zacchi, G., 2003. Techno-Economic Evaluation of Producing Ethanol from Softwood : Comparison of SSF and SHF and Identification of Bottlenecks. Biotechnol. Prog. 19, 1109–1117.

Wongwatanapaiboon, J., Kangvansaichol, K., Burapatana, V., Inochanon, R., Winayanuwattikun, P., Yongvanich, T., Chulalaksananukul, W., 2012. The Potential of Cellulosic Ethanol Production from Grasses in Thailand. J. Biomed. Biotechnol. doi:10.1155/2012/303748

Wu, Z., Lee, Y.Y., 1998. Biotechnology for Fuels and Chemicals: Proceedings of the Nineteenth Symposium on Biotechnology for Fuels and Chemicals Held May 4-8. 1997, at Colorado Springs, Colorado, in: Finkelstein, M., Davison, B.H. (Eds.), . Humana Press, Totowa, NJ, pp. 479–492. doi:10.1007/978-1-4612-1814-2_44

Wybrant, K.R., Ptacek, C.J., Blowes, D.W., 2002. Treatment of Mine Drainage Using Permeable Reactive Barriers : Column Experiments. Environ. Sci. Technol. 36, 1349–1356. doi:10.1021/es010751g

Wyman, Charles E., Dale, B.E., Elander, R.T., Holtzapple, M., Ladisch, M.R., Lee, Y.Y., 2005a. Coordinated development of leading biomass pretreatment technologies. Bioresour. Technol.

96, 1959–1966. doi:10.1016/j.biortech.2005.01.010

Wyman, Charles E., Dale, B.E., Elander, R.T., Holtzapple, M., Ladisch, M.R., Lee, Y.Y., 2005b. Comparative sugar recovery data from laboratory scale application of leading pretreatment technologies to corn stover. Bioresour. Technol. 96, 2026–2032. doi:10.1016/j.biortech.2005.01.018

Wyman, Charles E, Decker, S.R., Himmel, M.E., Brady, J.W., Skopec, C.E., 2005. Hydrolysis of Cellulose and Hemicellulose, in: Dumitriu, S. (Ed.), Polysaccharides: Structural Diversity and Functional Versitility. CRC Press, pp. 1023–1062. doi:10.1201/9781420030822.ch43

Yachmenev, V., Condon, B., Klasson, T., Lambert, A., 2009. Acceleration of the enzymatic hydrolysis of corn stover and sugar cane bagasse celluloses by low intensity uniform ultrasound. J. Biobased Mater. Bioenergy 3, 25–31. doi:10.1166/jbmb.2009.1002

Yadav, S.K., 2010. Heavy metals toxicity in plants : An overview on the role of glutathione and phytochelatins in heavy metal stress tolerance of plants. South African J. Bot. 76, 167–179. doi:10.1016/j.sajb.2009.10.007

Yat, S.C., Berger, A., Shonnard, D.R., 2008. Kinetic characterization for dilute sulfuric acid hydrolysis of timber varieties and switchgrass. Bioresour. Technol. 99, 3855–3863. doi:10.1016/j.biortech.2007.06.046

Zagury, G.J., Neculita, C., 2007. Passive Treatment of Acid Mine Drainage in Bioreactors : Short Review , Applications , and Research Needs, in: 60th Canadian Geotechnical Conference & 8th Joint CGS/IAH-CNC Groundwater Conference. Ottow, pp. 1439–1446.

Zhang, P.Y.-H., Himmel, M.E., Mielenz, J.R., 2006. Outlook for cellulase improvement: screening and selection strategies. Biotechnol. Adv. 24, 452–81. doi:10.1016/j.biotechadv.2006.03.003

Zhao, H., Jones, C.L., Baker, G.A., Xia, S., Olubajo, O., Person, V.N., 2009. Regenerating cellulose from ionic liquids for an accelerated enzymatic hydrolysis. J. Biotechnol. 139, 47–54. doi:10.1016/j.jbiotec.2008.08.009

Zhao, X., Cheng, K., Liu, D., 2009. Organosolv pretreatment of lignocellulosic biomass for enzymatic hydrolysis. Appl. Microbiol. Biotechnol. 82, 815–827. doi:10.1007/s00253-009-1883-1

Zheng, Y., Pan, Z., Zhang, R., Jenkins, B.M., 2009. Kinetic Modeling for Enzymatic Hydrolysis of Pretreated Creeping Wild Ryegrass 102, 1558–1569. doi:10.1002/bit.22197

Zhong, C.-M., Xu, Z.-L., Fang, X.-H., Cheng, L., 2007. Treatment of Acid Mine Drainage (AMD) by Ultra-Low-Pressure Reverse Osmosis and Nanofiltration. Enviromental Eng. Sci. 24, 1297–1306. doi:10.1089/ees.2006.0245

Zhou, J., Wang, Y., Chu, J., Luo, L., Zhuang, Y., Zhang, S., 2009. Optimization of cellulase mixture for efficient hydrolysis of steam-exploded corn stover by statistically designed experiments. Bioresour. Technol. 100, 819–825. doi:10.1016/j.biortech.2008.06.068

Zhou, J., Wang, Y., Chu, J., Zhuang, Y., Zhang, S., Yin, P., 2008. Identification and purification of the main components of cellulases from a mutant strain of Trichoderma viride T 100-14. Bioresour. Technol. 99, 6826–6833. doi:10.1016/j.biortech.2008.01.077

Zipper, C., Skousen, J., Jage, C., 2011. Passive Treatment of Acid-Mine Drainage, Reclamation guidelines for surface mined land

Chapter 3: Evaluation of a Combined Lignocellulosic/ Wastewater Biorefinery for the Simultaneous Production of Valuable Biochemical Products and the Remediation of Acid Mine Drainage

(Published in Biofuels, Bioproducts and Biorefineries, 2018) This chapter investigates a process for the remediation of acid mine drainage and simultaneous production of biochemicals. Different biorefinery options are evaluated based on the biorefinery complexity profile. The most feasible process configurations were determined and recommendations into further research requirements are made. This addresses all objectives pertaining to desktop studies, *i.e.* objectives a, d, and e.

Burman, N.W., Harding, K.G., Sheridan, C.M., Van Dyk, L., 2018b. Evaluation of a combined lignocellulosic / wastewater biorefinery for the simultaneous production of valuable biochemical products and the remediation of acid mine drainage. Biofuels, Bioproducts, and Biorefining. 12, 649–664. doi:10.1002/bbb.1880

Abstract: The additional costs required for the pre-treatment of lignocellulosic biomass, prior to enzymatic hydrolysis, has limited the commercial implementation of lignocellulosic biochemical production. Recently, the use of acidic mine drainage (AMD) water as an acid source for lignocellulosic pre-treatment has been investigated. Large quantities of AMD in South Africa suggest that AMD can be obtained cheaply, thus reducing the cost and increasing the potential of lignocellulosic biochemicals. AMD could undergo further remediation using sulfate-reducing bacteria (SRB) such that the water is suitable for release. The feasibility of such a system could be greatly improved if this process were to be incorporated within a biorefinery, such that all fractions of the biomass are utilized to produce multiple products. This paper investigates such a biorefinery system and evaluates the different options based on the biorefinery complexity profile (BCP). Due to the abundance of grass in the regions where AMD is generated, this was found to be the most suitable feedstock. The most feasible biorefinery option was found to produce ethanol through fermentation of C6 sugars, although it is recommended that further investigation into additional high-value biochemicals from the C6 sugar platform be conducted. C5 sugars released in pre-treatment could be used as a substrate by SRB for AMD remediation. Gasification and direct combustion of lignin had similar BCP's and thus further investigation is required to determine the preferred path. Similarly, further investigation is required for the best processing route for distillery silage.

Keywords: Biorefinery; Lignocellulosic; Wastewater; Remediation; Acid Mine Drainage.

3.1. Introduction

Although there are large fossil fuel reserves, it is anticipated that annual oil production will decline due to greenhouse gas emissions and anthropogenic climate change (Shafiee and Topal, 2009). Although renewable resources such as wind, water, solar and geothermal can provide alternative sources of energy, the only viable alternative for the production of chemicals and fuels is biomass (Lynd and Wang, 2003).

In order to produce chemicals from lignocellulosic biomass, the hydrolysis of carbohydrates is needed. Commercial implementation of this technology has been limited by the high processing costs, that are introduced through the necessary pre-treatment of biomass. The feasibility of producing bio-based chemicals can be increased by producing a range of different products in the same facility (known as a biorefinery), thus introducing additional profit streams. Recently, there has also been research into reducing the processing costs through using acid mine drainage (AMD) as an alternative to typical mineral acid pre-treatment (Magowo et al., 2015). The AMD can then undergo remediation using sulfate-reducing bacteria (SRB), to decrease sulfate concentration and acidity.

Although evidence has been provided for a process utilizing AMD as a pre-treatment for lignocellulosic biochemicals, while simultaneously remediating the AMD (Magowo et al., 2015; Ramla and Sheridan, 2015), these studies did not investigate the incorporation of this process into a full biorefinery system. This paper will identify the different biorefinery configurations possible, and evaluate their feasibility using the biorefinery complexity profile (BCP). Recommendations will be made on the most feasible biorefinery configuration, potential feedstocks that could be used, as well as provide risks and opportunities associated with the process.

3.2. Biochemicals and Biorefineries

Various biofuels and biochemicals can be produced from biomass including fuel alcohols, organic acids, biogases, polymers and platform chemicals. Currently, the main feedstocks for the production of these are food crops such as sugarcane and maize. Biochemicals produced from food crops are termed 1st generation biochemicals, and although this technology is proven, there are problems associated with it. These include increased overall carbon

emissions, net energy losses, lack of available land and increased food prices (Cherubini, 2010).

To overcome the problems associated with 1st generation biochemicals, the production of 2nd generation biofuels/chemicals from lignocellulosic biomass, such as energy crops (switchgrass, miscanthus), agricultural waste (corn stover, sugarcane bagasse) and forestry residue has been investigated (Dale and Wyman, 2015; Kumar et al., 2008; Sun and Cheng, 2002). Although these sources are highly abundant, and their use does not compete with food production, there has only been limited commercial implementation of lignocellulosic biochemical production.

All sources of lignocellulosic biomass consist of three fractions (lignin, hemicellulose, and cellulose), which form a ligno-hemicellulosic matrix (Mosier et al., 2005b). Hydrolysis of the cellulose and hemicellulose fractions produces hexose and pentose sugars respectively, which can undergo further processing to produce bioethanol and other biochemicals. Hydrolysis can be catalyzed either chemically (in the presence of an acid) or biologically (in the presence of hydrolase enzymes). Enzymatic hydrolysis (≈50°C) is favored over acid hydrolysis (≈150 – 180°C) due to lower operating temperatures and hence operating costs. Unfortunately, the ligno-hemicellulosic matrix impedes enzymes from accessing the cellulose, making hydrolysis inefficient. Pre-treatment to disrupt the matrix and increase enzyme access is thus necessary (Figure 3.1) (Mosier et al., 2005b).

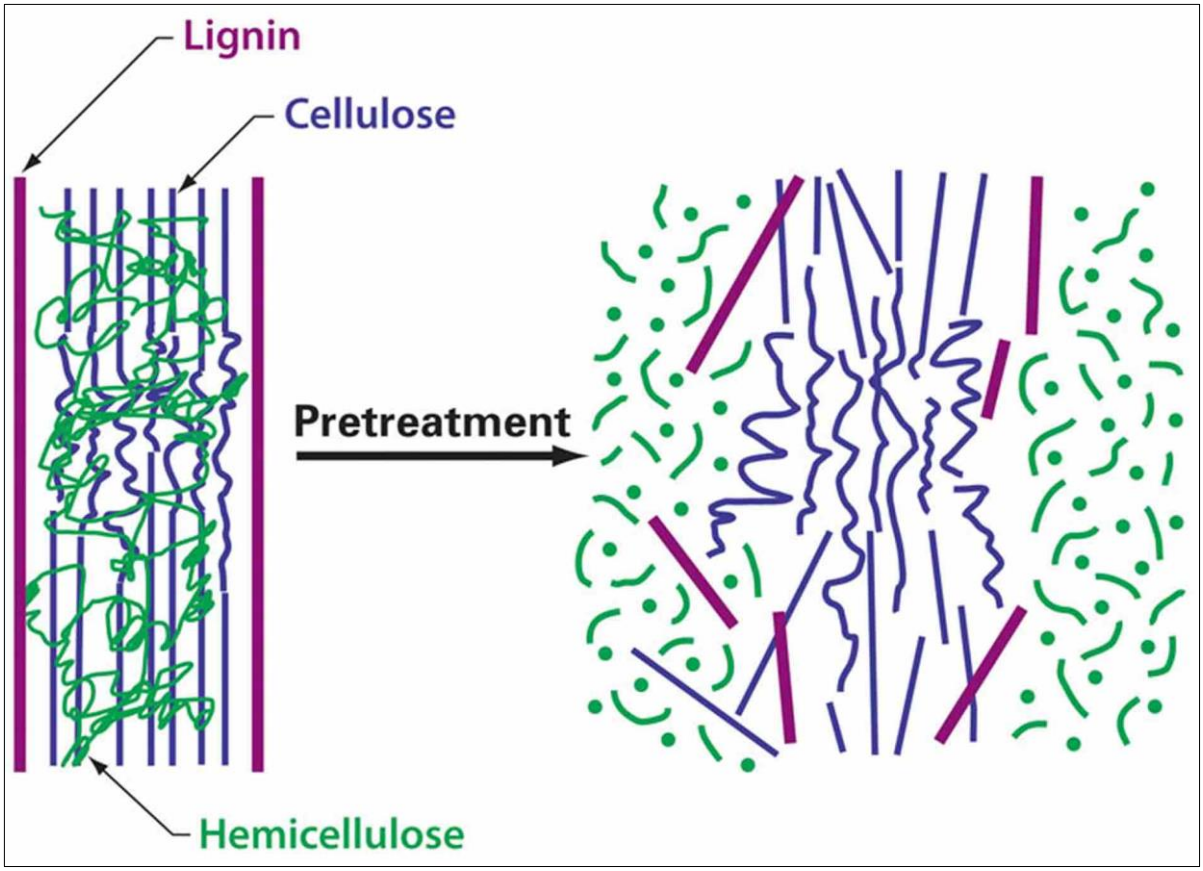

Figure 3.1: Lignocellulose structure and the disruptive effect of pre-treatment (Mosier et al., 2005b)

Various pre-treatment methods (physical, phyisco-chemical, biological and chemical) have been demonstrated to effectively disrupt the lignocellulosic structure and thereby increase the rate of enzymatic hydrolysis. Although effective, the inclusion of additional processing steps makes the production of 2nd generation biochemicals less favorable due to increased processing costs. The feasibility of producing of biochemicals from lignocellulosic biomass can be increased through the production of multiple products from all fractions of the lignocellulosic biomass through a biorefinery complex (Menon and Rao, 2012).

Biorefining is defined by the International Energy Agency (IEA) Bioenergy Task 42 as "The sustainable processing of biomass into a spectrum of marketable products and energy" (de Jong et al., 2012). A biorefinery is designed such that multiple processes are integrated to efficiently produce multiple products as well as co-generate electricity and heat. This is analogous to typical fossil fuel refineries. Ideally, the range of products produced will include both small volumes of several high-value chemical products, and a large volume of a low-value liquid fuel product (*e.g.* biodiesel or bioethanol) (Cherubini, 2010). The production of

heat and electricity can also be incorporated for use on-site or for sale to local utility providers.

Recently, there has been research into using AMD for the pre-treatment of lignocellulosic biomass (Magowo et al., 2015). This would be similar to dilute acid pre-treatment which aims to solubilize the hemicellulose fraction of the biomass increasing the accessibility of the cellulose to enzymes. Currently, dilute sulfuric acid pre-treatment is one of the preferred pre-treatment methods (Maurya et al., 2015). Current AMD levels in South Africa suggest that it could be obtained cheaply for the pre-treatment of lignocellulosic biomass. If utilized in a biorefinery, this could further improve the process economics and feasibility of 2nd generation biochemicals. It has also been found that lignocellulosic biomass can be utilized, in conjunction with sulfate-reducing-bacteria (SRB) to facilitate the remediation of AMD (Magowo et al., 2015; Ramla and Sheridan, 2015).

3.3. Acid Mine Drainage (AMD)

AMD is acidic water, with high concentrations of sulfate and metals, formed when sulfide rich minerals are exposed to oxygen and water. The acidity, sulfate, and metals present in the water have negative environmental effects on aquatic and riparian ecosystems (Simate and Ndlovu, 2014).

AMD is formed through the oxidation of pyrite (FeS_2) after exposure to air and water. This occurs through a series of geochemical reactions, as summarized in Equation (3.1) (Johnson and Hallberg, 2005a).

$$4FeS_2 + 15O_2 + 14H_2O \rightarrow 4Fe(OH)_3 + 8SO_4^{2-} + 16H^+ \qquad (3.1)$$

Further, the high levels of acidity lead to the dissolution and subsequent high concentrations of heavy metals in the water (Taylor et al., 2005).

Both open-pit and shaft-mining activity can lead to increased exposure of pyrite to oxygen and water, thereby generating AMD. Large scale mining in South Africa in the Witwatersrand area (Eastern, Central and Western basins), as well as the Mpumalanga and Kwazulu-Natal coalfields, caused the production of AMD in these areas. The adverse environmental effects of AMD on South African water systems (McCarthy, 2011) led to an amendment of legislature

enforcing the indefinite treatment of all mine effluent to acceptable standards after mine closure (MPRDA, 2013).

South Africa is meteorologically a water scare country as only 35% of the country receives sufficient annual rainfall for crop production (Kunz and Jewitt, 2013). The widespread generation of AMD exacerbates South Africa's water scarcity and threatens water security (McCarthy, 2011).

3.3.1 Remediation of AMD

Currently, the most widely used AMD remediation technology achieves an increase in alkalinity, and the subsequent precipitation of metals, through the addition of a neutralizing agent such as lime (Taylor et al., 2005).

The South African Department of Water and Sanitation (DWS) has set up three pumping and treatment plants in the Eastern, Western and Central Witwatersrand basins. These pump underground AMD such that the underground water level of AMD remains below the environmentally critical level (ECL) at which it would decant into surface water systems or contaminate other aquifers. The pH of the AMD found in the Central, Eastern and Western basins was 2.4, 5.9 and 3.5 respectively, while the sulfate concentrations were 3 000, 2 300 and 3 600 mg/L (Department Of Water Affairs (DWA), 2013). The estimated daily volume that is treated, through a process of neutralization and precipitation in a high-density sludge process, is approximately 181 ML/day (van Niekerk D, 2017, pers. comm.).

In the Mpumalanga coalfields, the eMalahleni water reclamation project uses a process of neutralization, precipitation and reverse osmosis to remediate 50 ML/day of AMD to produce potable water that is fed back to the municipality (http://xflow.pentair.com/en/case-studies/witbank). The pH of this AMD in the eMalahleni area has been found to be 2.4, with sulfate concentrations ranging between 8 300 and 20 000 mg/L (Naidu, T.S., unpublished).

Although these treatment facilities are effective, they are expensive due to the large chemical input requirements and the need for constant monitoring. Moreover, they produce large quantities of toxic metallic sludges that may need further treatment. Investigations into biological remediation techniques that require less input, produce less toxic by-products and are more affordable are currently underway (Johnson and Hallberg, 2005a).

Dissimilatory sulfate reduction (DSR) has been identified as a promising technique for the remediation of AMD due to its combined ability to reduce acidity and sulfate concentrations, with the increase in pH resulting in the precipitation of metals. SRB catalyze DSR, converting sulfates to sulfides, by using an organic carbon source as an electron donor. This reduces the acidity by transforming sulfuric acid to hydrogen sulfide (Equation 3.2) (Johnson and Hallberg, 2005a).

$$SO_4{}^{2-} + 2CH_2O + 2\,H^+ \xrightarrow{SRB} H_2S + 2H_2CO_3 \qquad (3.2)$$

In addition to the increase in pH, hydrogen sulfide plays an important role in the removal of toxic metals (*e.g.* iron, zinc, manganese) through the formation of metal mono-sulfides (Equation 3.3 using iron as an example) (Johnson and Hallberg, 2005a).

$$Fe^{2+} + H_2S \rightarrow FeS + 2H^+ \qquad (3.3)$$

Important considerations for designing reactors for sulfate reduction include reactor configuration, substrate and SRB inoculum (Sánchez-Andrea et al., 2014). Various reactor configurations have been investigated including batch reactors, continuously stirred tank reactors (CSTR), fluidized bed reactors (FBR), gas-lift reactors (GLR), up flow anaerobic sludge blanket reactors (UASB), anaerobic baffled reactors (ABR), membrane bioreactors (MB), as well as combinations of these (Kaksonen and Puhakka, 2007). The SRB inoculum consists of a community of anaerobic bacteria and archaea (Muyzer and Stams, 2008), sourced from various environmental aquatic locations, often where there is a prevalence of AMD or from an operational anaerobic water treatment facility. SRB can be classified as either acidophilic or neutrophilic with each performing better in their optimum pH range (Sánchez-Andrea et al., 2014).

Substrates that have been investigated, for the remediation of AMD, include organic acids, sugars, alcohols, waste sludge, biomass, and H_2/CO_2. Various biomass has been found to be an effective source of organic carbon with high levels of remediation achieved from grass (H. A. Greben et al., 2009b; Magowo et al., 2015; Ramla and Sheridan, 2015), sugarcane bagasse (Magowo et al., 2015), woody biomass (Neculita et al., 2008) as well as mixed lignocellulosic substrates (Zagury and Neculita, 2007). The performance of DSR bioreactors has been found to be highly dependent on the nature of organic matter used, with biomass containing a high

herbaceous content performing the best (Lefticariu et al., 2015). The composition of the microbial community has been found to change over time to include a greater proportion of micro-organisms that are adapted to survive at the reactor conditions (Bijmans et al., 2010).

By combining the remediation of AMD using lignocellulosic biomass together with the production of biochemicals from biomass pre-treated by AMD, the process economics of both processes could be improved. The two processes could be combined into a lignocellulosic/wastewater biorefinery which would utilize lignocellulosic biomass and AMD (both cheap and abundant) as inputs. The outputs from this biorefinery would be cleaned water and biochemicals, thus potentially contributing towards both water and energy security in South Africa. A conceptual representation of the combined lignocellulosic/wastewater biorefinery is presented in Figure 3.2. The first step towards realizing this biorefinery is the conceptualization and evaluation of the potential biorefineries, its products, feedstocks, and processes.

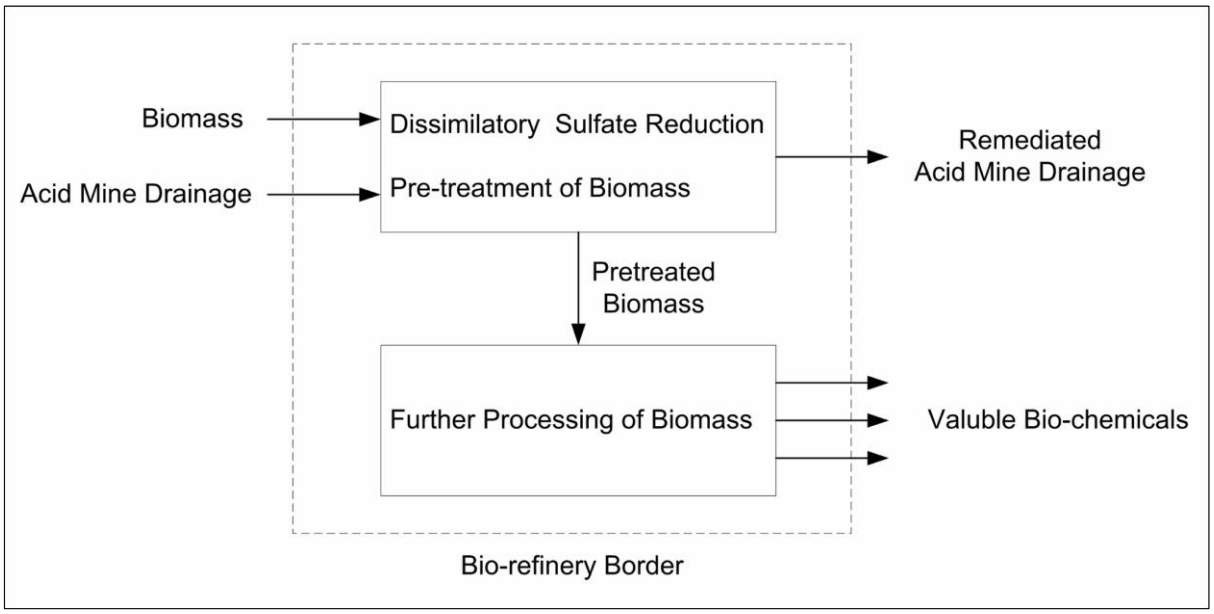

Figure 3.2: Conceptual representation of the combined lignocellulosic/wastewater biorefinery

3.4. Evaluation of Biorefineries

3.4.1 Classification of biorefineries

Biorefineries have been classified in various ways, including by feedstock type, processing route, intermediate products produced, and technological implementation status *i.e.* conventional *vs.* advanced biorefinery or 1st/2nd/3rd generation biorefinery. Since these classifications can often overlap, the IEA Bioenergy Task 42 has developed a comprehensive classification system for biorefineries (Cherubini et al., 2009). This considers platforms (process intermediates *e.g.* c5/c6 sugars, syngas), products (*e.g.* ethanol, lactic, electricity), feedstock groups (*e.g.* starch crops, lignocellulosic feedstock) and conversion process (*e.g.* gasification, fermentation) (Figure 3.3). Each biorefinery could be described by each of these features.

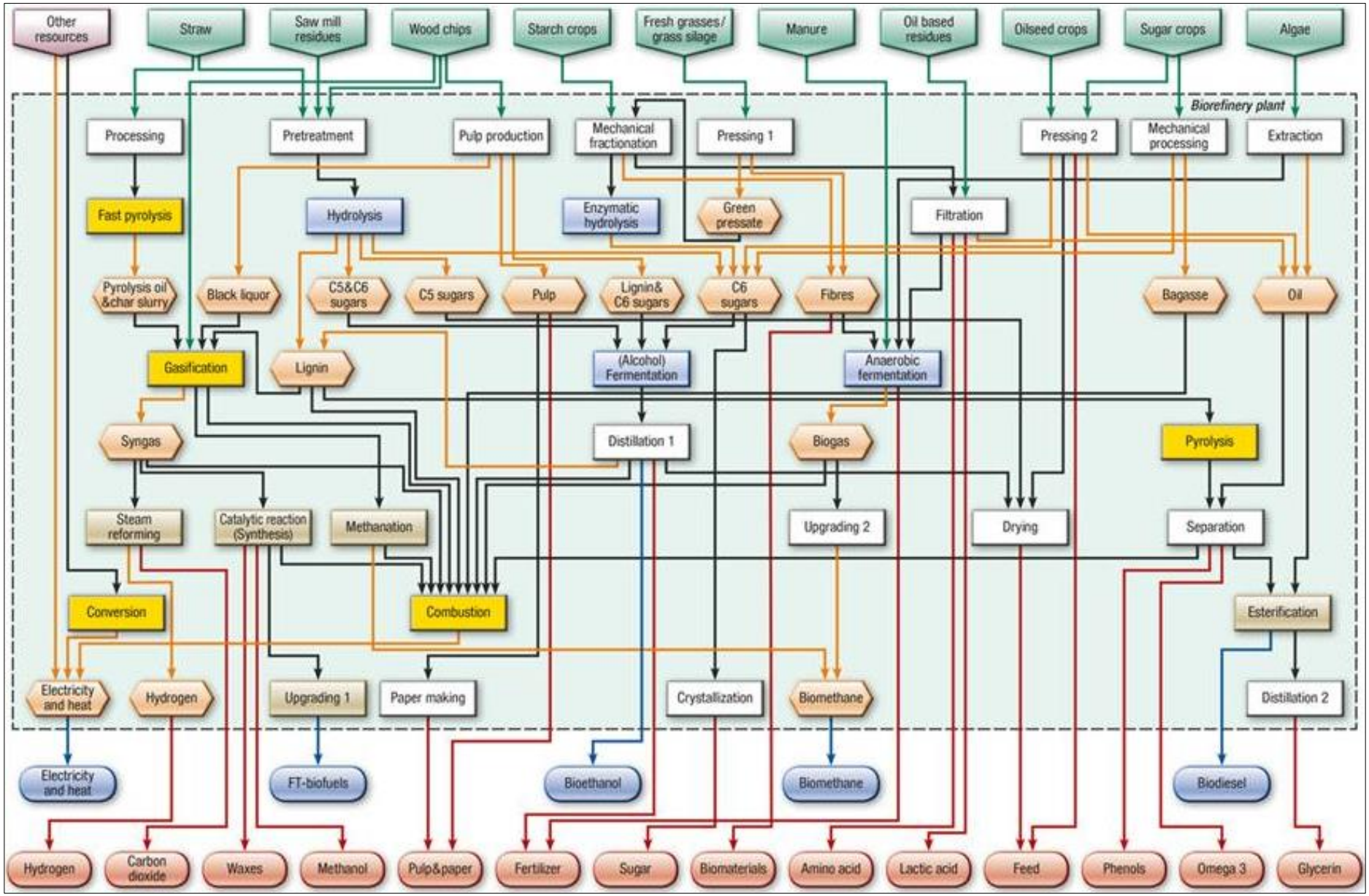

Figure 3.3: Overview of biorefinery classification scheme (IEA Bioenergy, 2013)

3.4.2 Feedstocks (green pentagon in Figure 3.3)

Various feedstocks have been incorporated into the classification scheme. These feedstocks can be grouped as follows:

- starch and sugary feedstocks: starch crops and sugar crops;
- triglyceride feedstocks: oil residues, oil crops and algae; and
- lignocellulosic feedstocks: straw, sawmill residue, wood chips, and fresh grasses/silage.

3.4.3 Processing routes (rectangle in Figure 3.3)

The different processing routes can be grouped into the following technologies:

- thermochemical (yellow rectangle): conversion, gasification, combustion, or pyrolysis;
- biochemical (blue rectangles): hydrolysis, enzymatic hydrolysis, fermentation, or anaerobic fermentation; and
- physical (white rectangle): pre-treatment, pulp production, mechanical fractionation, pressing, extraction, filtration, distillation, upgrading, drying, separation or paper making.

3.4.4 Platforms (orange hexagon in Figure 3.3)

The platform is the intermediate chemical that links the feedstock to a range of valuable products. Examples of platforms include syngas, lignin, C5/C6 sugar, and C6 sugars, green pressatte, biogas, fibers, oil, hydrogen, pulp, biomethane, electricity, and heat. Some of these platforms may also be final products (*e.g.* hydrogen, electricity, and heat), whereas others undergo further processing to produce products. For example, the platform “oil” can be a product or undergo esterification to produce biodiesel and glycerin.

3.4.5 Products (oval in Figure 3.3)

Products can be classified into two separate groups

- bioenergy (blue oval): electricity and heat, FT biofuels, bioethanol, biomethane or biodiesel; and
- bioproducts (red oval): hydrogen, carbon dioxide, waxes, pulp and paper, biomaterials, fertilizers, feed, amino acid, lactic acid, phenols, omega 3 or glycerin.

This classification scheme is useful for differentiating biorefinery types, as well as for the conceptualization of biorefinery schemes based on available feedstocks, potential processing routes, and desired products. For example, if an executive decision were to be made to rule out all starch, sugary and triglycerides feedstocks, and it was desired to produce phenols, lactic acid, and methanol, the potential platforms, and processing routes could easily be identified by using Figure 3.3. Once all processing routes/platforms have been identified, further evaluation of the different options could be conducted to identify the most feasible option.

3.5. Biorefinery Complexity Index (BCI)

Each biorefinery has a different level of complexity making the evaluation of each option difficult for decision-makers, investors, and industry partners. In order to evaluate different biorefinery complexes for the short-, medium- and long-term, the biorefinery complexity index (BCI) has been developed by stakeholders of the IEA Bioenergy Task 42 (Jungmeier et al., 2014). This method is analogous to the "Nelson's Complexity Index" for oil refineries and has been developed utilizing the IEA Bioenergy Task 42 biorefinery classification scheme. For a full explanation of the calculation of the BCI refer to Jungmeier *et al.* (2014) (Jungmeier et al., 2014).

The biorefinery complexity index evaluates the technological readiness of each individual platform, feedstock, product, and processing step by assigning it a feature complexity (FC) on a scale of 1 – 9, with 1 being the most and 9 being the least technologically ready (Table 3.1). The sum of individual scores is then presented either on its own (known as the biorefinery complexity index or BCI) or followed by the complexity index of each feature (platform, feedstock, product, processes), which is known as the biorefinery complexity profile (BCP).

Table 3.1: Description of the different feature complexity levels (Jungmeier et al., 2014)

Description	FC
Basic research	9
Applied research	8
Critical function or proof of concept established	7
Lab testing/validation of alpha prototype	6
Laboratory testing of integrated/semi-integrated system	5
Prototype system verified	4
Integrated pilot system demonstrated	3
System incorporated in commercial design	2
System proven and ready for full commercial deployment	1

For example, if a biorefinery has a feature complexity index of 5 for platform, 6 for processes, 4 for feedstock and 9 for products the BCI would be 24 and the BCP would be 24(5/6/4/9). A full example of the evaluation of a biorefineries BCI and BCP is given by Jungmeier *et al.* (2014).

The higher a biorefineries' BCP the more complicated this biorefinery is, with more processing steps. The BCP is also an indication of the readiness of technology required for the biorefinery. A biorefinery with a higher BCP is less feasible and more risky than a biorefinery with a lower BCP.

The feasibility and risk associated with different biorefineries can thus be evaluated by calculating and comparing the BCP's of the different options.

The evaluation and comparison of biorefineries using the BCP is useful for the identification of potentially feasible biorefinery configurations. Once potentially feasible configurations have been identified it is, however, still necessary to perform rigorous techno-economic evaluation comparing the different options. Although the techno-economic evaluation is much more thorough and can predict the feasibility of a biorefinery with greater accuracy, these require much more time and resources to perform. An evaluation by BCP can be used to quickly rule out infeasible options and reduce the amount of work required in the techno-economic evaluation.

3.6. Potential AMD Remediation Biorefinery

It has been shown that AMD can be used to pre-treat lignocellulosic biomass for further hydrolysis (Magowo et al., 2015). The availability of a free acid source could reduce the cost

associated with pre-treatment. All potential biorefineries were conceptualized using the biorefinery classification scheme (Figure 3.3). The following constraints were used:

- Processing routes: Pre-treatment and hydrolysis processing steps must be incorporated. Only processing steps that are required for the platforms produced through the pre-treatment and hydrolysis steps can be incorporated.
- Feedstocks: only lignocellulosic biomass feedstocks will be considered. No other feedstocks will be considered.

The biorefinery scheme (Figure 3.3) was redrawn (Figure 3.4) with all remaining biorefinery options once the above two criteria were applied. A summary of the potential options for feedstocks, platforms, processing routes and products is presented in Table 3.2.

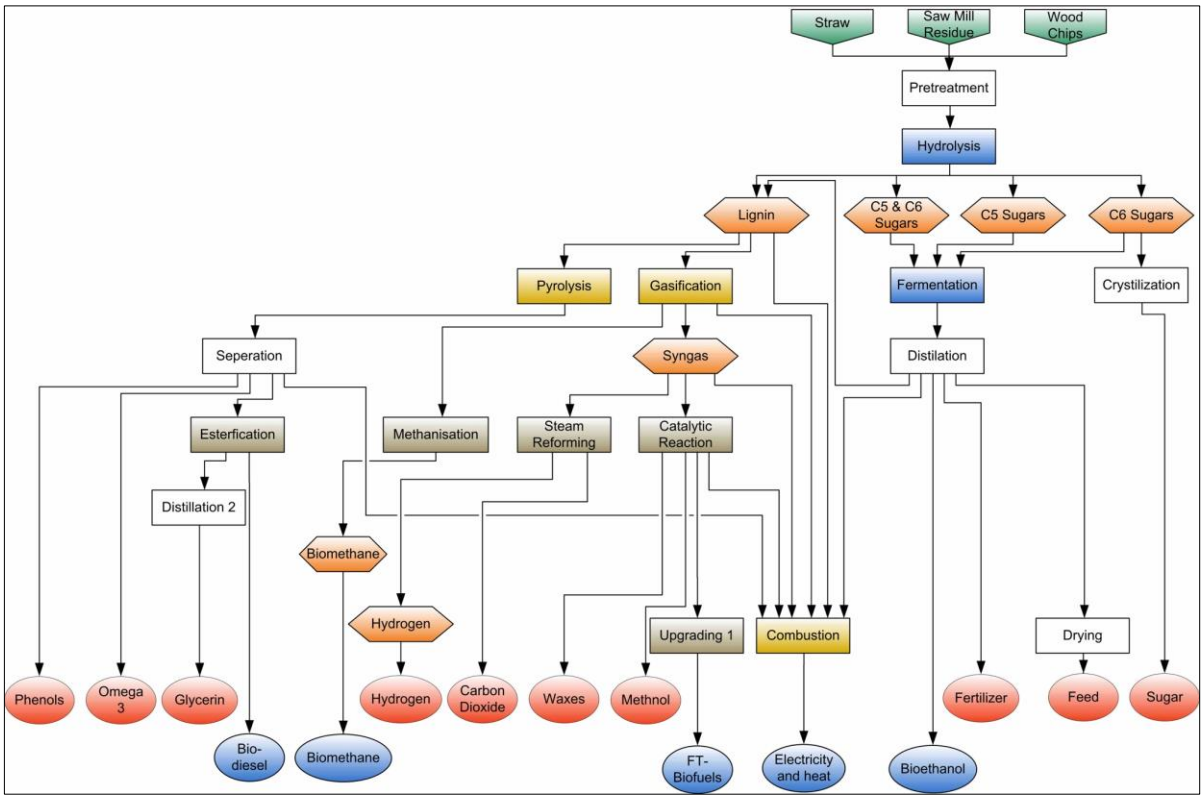

Figure 3.4: Potential biorefineries according to IEA Bioenergy Task 42 classification scheme

Table 3.2: Summary of biorefinery options (lignin specific options in italics)

Classification	Options
Feedstocks	Straw, Sawmill residues, woodchips
Platforms	*Lignin*, C5, and C6 sugars, C5 Sugars, C6 Sugars, syngas, Hydrogen
Processing routes	Pre-treatment, hydrolysis, Fermentation, Distillation, combustion, drying, *gasification, pyrolysis separation, esterification, distillation 2, steam reforming, catalytic reaction, upgrading.*
Products	*Phenols, Omega 3, glycerine, biodiesel, hydrogen, carbon dioxide, waxes, methanol, FT-Biofuels,* Heat and power, Bioethanol, Fertilizer, Feed, Sugar

As can be seen in Figure 3.4 there are a large number of options with regards to platforms, processing routes and products. This complexity is introduced through the processing of lignin.

3.6.1 Biorefinery options for the processing of lignin

The three main processing routes for lignin are combustion, gasification, and pyrolysis. The simplest processing route is through direct combustion of lignin to produce one product, electricity and heat. As this processing step is very simple the FC is 1, electricity and heat produced can be used on site for the running of other processes however excess electricity can be sold back into the local grid. Both pyrolysis and gasification are more complicated options requiring multiple processing steps and produce various products.

Gasification is the high temperature (>700 °C) combustion of organic material under limited oxygen to produce a mixture of CO and H_2 called syngas (Spath and Dayton, 2003). Syngas can either undergo steam reforming to produce H_2 and CO_2 or various catalytic reactions to produce methanol, waxes or crude biofuels. Crude biofuels can undergo Fischer-Tropsch synthesis to produce gasoline or diesel.

Pyrolysis is the decomposition of organic material at elevated temperatures (300 – 600 °C) in the absence of oxygen to produce liquid pyrolysis oil (bio-oil), biochar and light gases similar to syngas (Bridgwater and Peacocke, 2000). This pyrolysis oil undergoes separation to produce a range of products including phenols, omega 3, and esters. Further esterification of pyrolysis oil can produce biodiesel and glycerin.

The potential different biorefinery options for the processing of the lignin platform are presented in Figure 3.5.

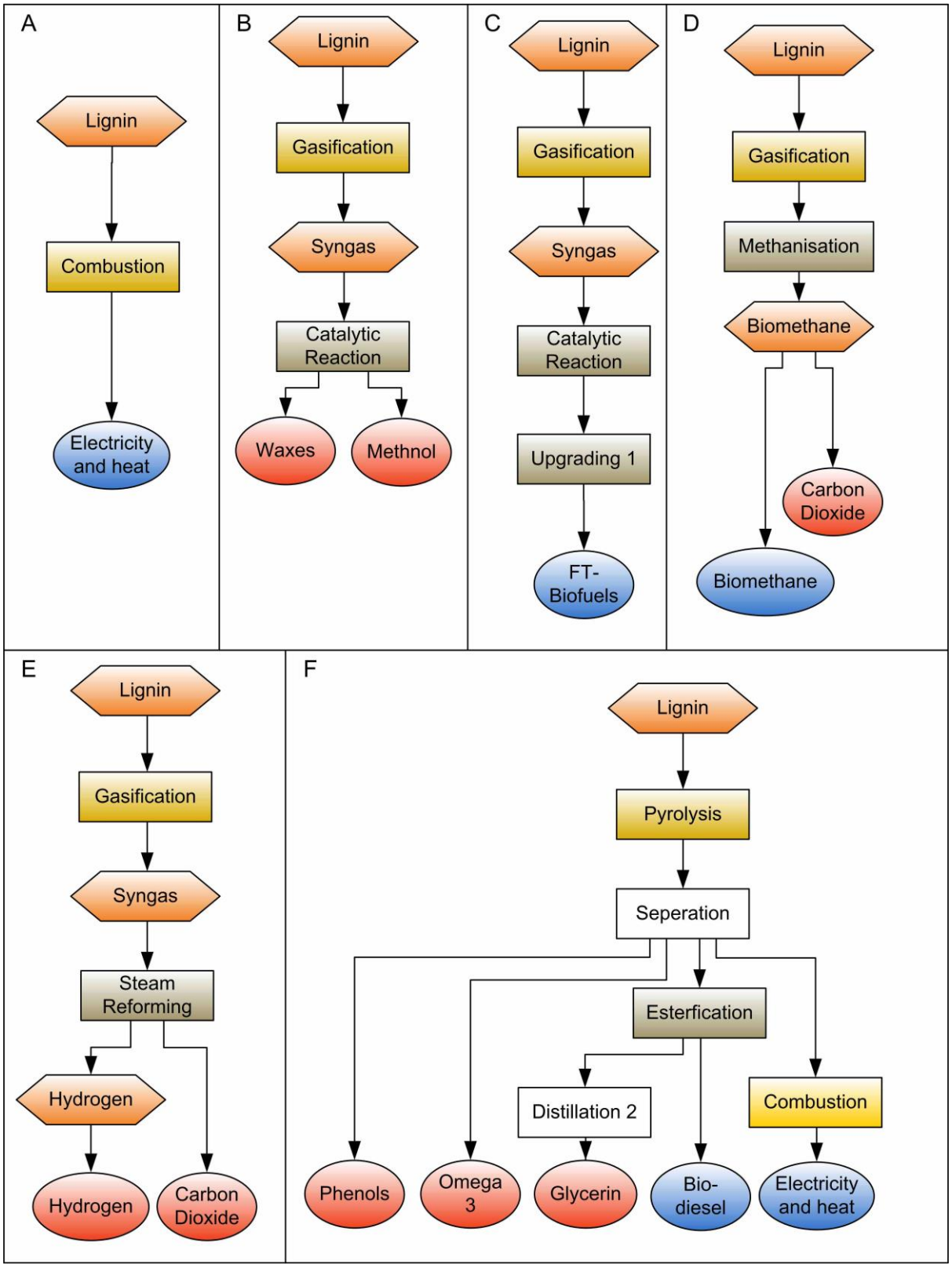

Figure 3.5: Potential biorefinery options for the processing of lignin. **A.** option L1: direct combustion. **B.** Option L2: gasification and catalytic reaction to produce methanol/waxes. **C.** Option L3: gasification, catalytic reaction, and upgrading to produce FT-biofuels. **D.** Option L4: gasification and methanation to produce biomethane. **E.** Option L5: gasification and steam reforming to produce hydrogen and carbon dioxide. **F.** Option L6: pyrolysis to produce a variety of products.

Although it is possible for certain platforms and products produced in gasification to undergo combustion, these processing routes are not considered as it is assumed that direct combustion of lignin would be more feasible due to the lack of additional processing steps. Processing route options subsequent to gasification will only be considered individually *i.e.* either steam reforming, catalytic reaction, catalytic reaction followed by upgrading or methanation, but no combination of these processes. The combustion of certain products from the pyrolysis process (*i.e.* biochar) will be considered as combustion is a logical use for biochar.

To evaluate the feasibility and risk associated with each different options the BCP was calculated. The BCP was calculated only for the lignin processing portion of the plant as this was the area under investigation. The feature complexity of the feedstocks was assumed to be 4 for all options (straw 2, sawmill residue 1, wood chips 1). A summary of the different platforms, processing route, potential products, and their BCP is presented in Table 3.3.

Table 3.3: Summary of different lignin processing options and BCP's

Option	Platform	Products	Processing route/sub-route		BCP
L1	Lignin (3) Electricity and heat (1)	Electricity and heat (1)	Combustion (2)		11(4/4/1/2)
L2	Lignin (3) Syngas (1)	Methanol (2)	Gasification (2)	Catalytic reaction (1)	13(4/4/2/3)
		Waxes (4)			15(4/4/4/3)
L3	Lignin (3) Syngas (1)	FT Biofuels (2)		Catalytic reaction (1) & Upgrading (3)	16(4/4/2/6)
L4	Lignin (3) Syngas (1) Hydrogen	Hydrogen (1) Carbon dioxide (1)		Steam reforming (1)	14(5/4/2/3)
L5	Lignin (3) Biomethane (2)	Biomethane (2)		Methanation (1)	13(5/4/2/2)
L6	Lignin (3) Electricity and heat (1)	Biodiesel (1), Glycerine (1) Omega 3 (4) Phenols (4) Electricity and heat (1)	Pyrolysis (4) Separation (1) Esterification (1) Distillation (1) Combustion (2)		28(4/4/11/9)

As can be seen in Table 3.3, the direct combustion of lignin (option L1) has the lowest BCP of 11(4/4/1/2). All gasification routes have similar BCI's ranging from 13 – 16. Pyrolysis (option L6) has a relatively high BCP of 28(4/4/11/9). Due to the high level of complexity and hence risk of pyrolysis, this option has been ruled out. As the option of direct combustion and all gasification options have similar BCP's an economic evaluation should be performed to determine which option would be more profitable/feasible.

The other platforms produced through enzymatic hydrolysis (*i.e.* C5 sugars, C5 and C6 sugars, C6 sugars) also introduce additional options into the biorefinery complex.

3.6.2 Biorefinery options for the processing platforms produced through enzymatic hydrolysis

Acid catalyzed pre-treatment preferentially attacks the hemicellulose portion of the lignocellulose. It is proposed that the pentose sugars released in this be utilized as a carbon source for the sulfate-reducing bacteria. This effectively rules out C5/C6 sugars and C5 sugars as a platform. The acid soluble lignin will also be removed in the pre-treatment section. This implies that the resulting platforms (after hydrolysis) will be C6 sugars and lignin.

The processing options for the C6 sugar platform, as per Figure 3.3, are either fermentation and subsequent distillation, to produce bioethanol, or crystallization to produce sugar for human consumption. The crystallization route has been ruled out as it is assumed that the production of sugar from lignocellulosic biomass would not be able to compete commercially with sugar produced from starch crops, such as sugar cane or sugar beet, due to the inclusion of additional pre-treatment processing steps required. The production of sugar from cane and beet is a well-established industry with a sufficient supply of raw materials. Demand for sugar in South Africa has recently declined with a further decline expected due to the introduction of a tax on sugar in 2018 (Donnelly, 2017). This has resulted in an oversupply of sugar, and as such, it is not envisioned that there will be any requirement for innovative technologies in this industry. The National Agricultural Marketing Commission has investigated alternative products from sugar that could be produced in addition to sugar so as to maintain the current economic output of the industry with a decreased demand for sugar (Conningarth Economists, 2013).

The main products of distillation are bioethanol and distillery silage. Bioethanol can be blended with gasoline (up to 15% *i.e.* E15) for use in normal gasoline vehicles or used on its own in specially designed vehicles. There are various uses for distillery silage such as combustion to produce electricity and heat, drying to produce animal feed or direct use as fertilizer. A summary of all the biorefinery processing routes for the processing of the different C6 platform products is presented in Figure 3.6.

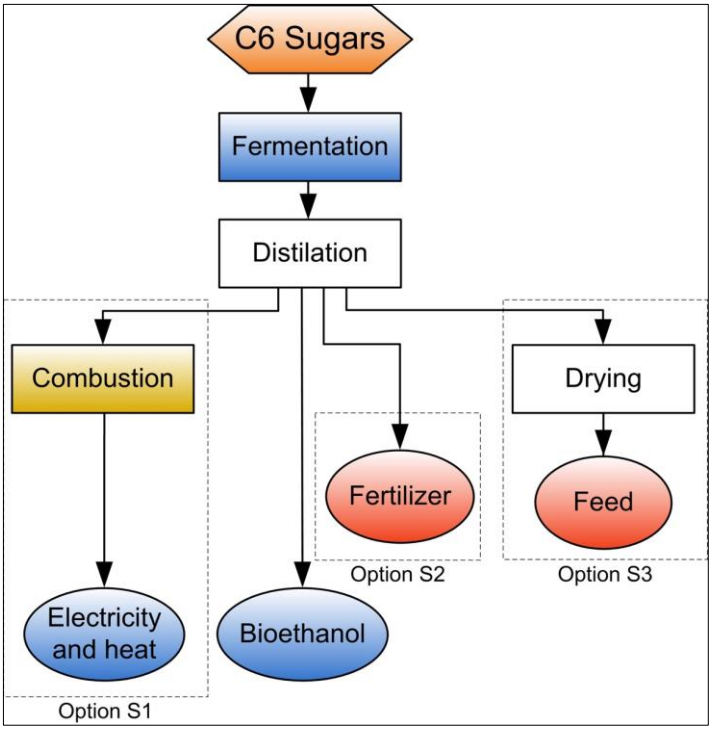

Figure 3.6: Potential biorefinery options for the processing of C6 sugars, with combustion of silage to produce electricity and heat (option S1), use of silage as fertilizer (option S2), drying of silage for the production of animal feed (option S3).

In order to evaluate the different options for the processing of the C6 sugar platform (including the processing of the silage), the BCP was calculated for each different processing route. The feature complexity of the feedstocks was assumed to be 4 for all options (straw 2, sawmill residue 1, wood chips 1). A summary of the BCP for each option is presented in Table 3.4.

Table 3.4: Summary of the different processing routes associated with distillery silage

Option	Platform	Product	Processing Route	BCP
S1	C6 Sugars (1)	Ethanol (1) Heat and power (1)	Fermentation (1) Distillation (1) Combustion (2)	11(1/4/2/4)
S2	C6 Sugars (1)	Ethanol (1) Fertilizer (1)	Fermentation (1) Distillation (1)	9(1/4/2/2)
S3	C6 Sugars (1)	Ethanol (1) Feed (1)	Fermentation (1) Distillation (1) Drying (1)	10(1/4/2/3)

As can be seen in Table 3.4, the production of either fertilizer or feed from distillery silage has a lower BCP than the production of electricity and heat through combustion. This suggests that combustion is less feasible, however, a techno-economic evaluation of the three options found combustion to be the most economically favorable (Sajbrt et al., 2010). Further

investigation into the most feasible processing route for distillery silage should, therefore, be conducted.

In addition to the potential processing routes of the C6 sugar platform presented in Figure 3.3, there are other processing routes to produce various high-value biochemical products. Products include alcohols, organic acids, biogases, and biopolymers which are produced through various processes including fermentation and various chemical reactions. A summary of potential bioproducts produced directly from the C6 sugar platform, their value, and the global market potential is presented in Table 3.5.

Table 3.5: Global market volume and price of potential biochemicals produced directly from the C6 sugar platform (E4TECH et al., 2015)

Product	Price USD/ton	Volume kton/yr
Ethanol	815	71 310
1,4-Butanediol	>3 000	3.0
Itaconic acid	1 900	41.0
n-Butanol	1 890	590
1,3-Propanediol	1 760	128
Lactic acid	1 450	472
Acetone	1 400	174
Sorbitol	650	164
Acetic acid	617	1 357
Iso-butanol	1 721	105
Succinic acid	2 940	38.0
Farnesene	5 581	12.0
Polyhydroxyalkanoates	6 500	17.0
Isoprene	>2 000	0.020
Hydroxymethylfurfural (HMF)	>2 655	0.020
Adipic acid	2 150	0.001
3-Hydroxypropionic acid	1 100	0.040
Iso-butene	>>1 850	0.010

As shown in Table 3.5, although bioethanol has the greatest market volume, it has the lowest economic value of all biochemicals. Typical biorefineries are designed to produce both a large quantity of low-value biofuels and a small quantity of high-value biochemicals (Cherubini, 2010). The advantage of producing multiple products, from one platform, is that the biorefinery generates additional profit through the sale of small volumes high-value chemicals, while still benefiting from economies-of-scale associated with large volume production. The production of large volumes of high-value chemicals is often limited by

market size. As the introduction of additional processing steps adds further complexity, which may negatively affect process economics, it is necessary to perform a techno-economic evaluation to determine if producing additional products is beneficial

If the production of additional products seems promising, it is suggested that bioethanol be produced as the low-value, high volume biofuel, and that small quantities of other high-value biochemicals should be produced. These could be produced either in parallel with bioethanol directly from the C6 platform (*e.g.* lactic acid, succinic acid), or subsequent to fermentation using a portion of the bioethanol product as a feedstock (*e.g.* acetic acid, hydroxymethylfurfural). The feature complexity of many of these products and associated processes are similar as they all are produced through fermentation or chemical reaction (FC=1) and are separated through established processes (distillation, membrane separation, ion exchange, *etc.*) with an FC of 1. It is thus necessary for a techno-economic evaluation to be carried out to identify the most feasible products.

The potential biorefinery options that would still be considered feasible based on their BCP's are presented in Figure 3.7. This classification diagram presents all the biorefinery options that meet the selection criteria of utilizing acid pre-treatment of lignocellulosic biomass, as well as not as having been ruled out due to having a high level of complexity. The production of sugar was ruled out as it was assumed that producing sugar from lignocellulosic biomass would not be able to complete with conventionally produced sugar. The amount of biorefinery options is greatly reduced by the application of selection criteria and elimination of highly complex processing routes. Although there are still multiple options that need to undergo techno-economic evaluation in order to determine the most feasible biorefinery option, the required amount of evaluations has been greatly reduced.

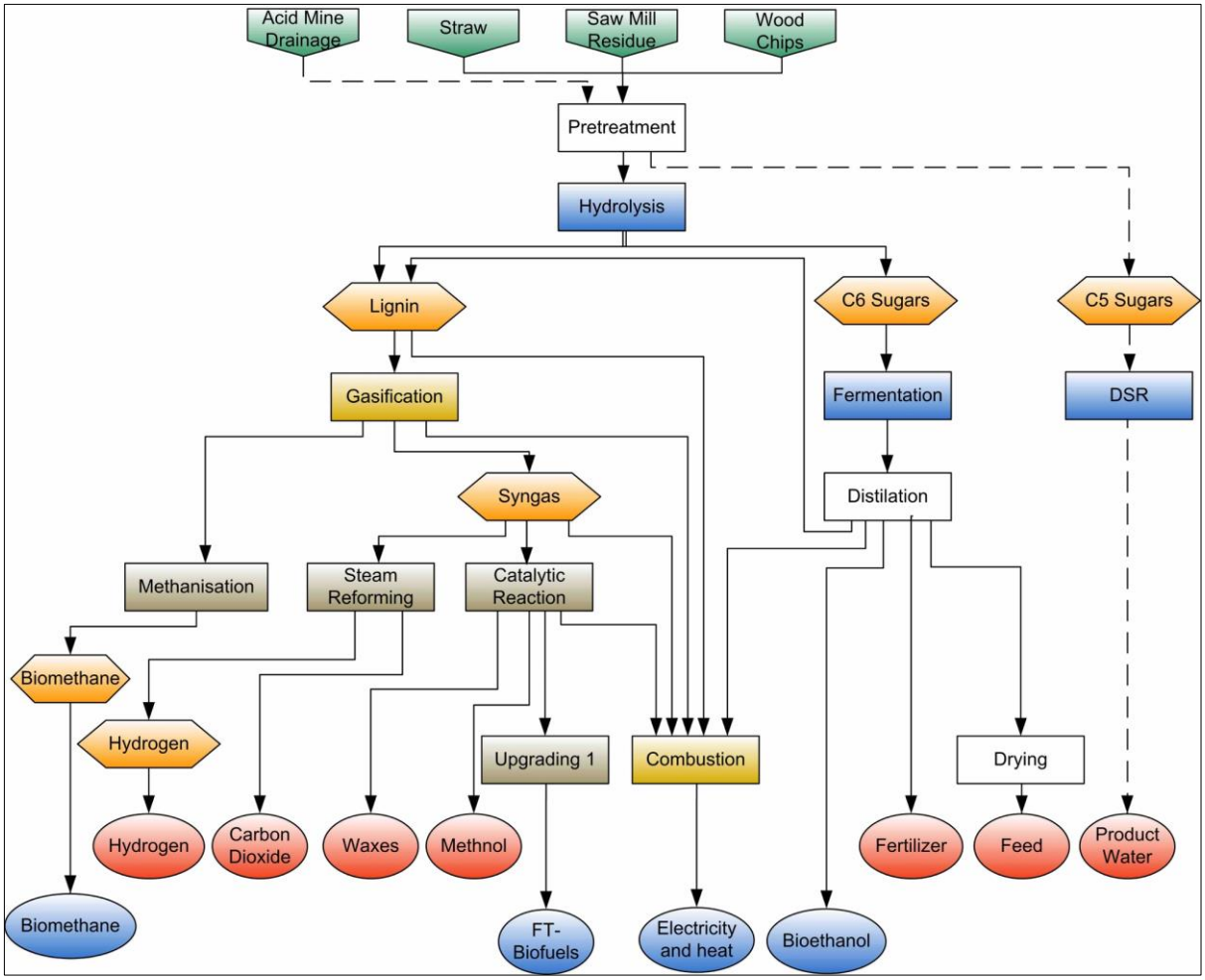

Figure 3.7: Potential biorefinery options, with the incorporation of AMD remediation, after all selection criteria have been applied and biorefineries with large BCP's have been ruled out.

3.6.3 Incorporation of AMD remediation into the biorefinery complex.

AMD will be utilized for pre-treatment of the biomass prior to hydrolysis. The acidity present in the AMD will hydrolyze the hemicellulose fraction of the biomass. The pentose sugars (C5 platform) released into the water will be utilized by SRB, in a subsequent reactor, as an energy source for DSR, as discussed in Section 3.2. The hydrolysis of hemicellulose and remediation of AMD will occur in a separate reactor so as to avoid limiting the temperature at which hydrolysis occurs due to the presence of SRB. The water after remediation will have a lower sulfate concentration and a higher pH and can either be utilized as process water or further treated to be suitable for human consumption, irrigation, or released into municipal or natural water systems (legislation permitting).

A pH of between 1.5 – 2.5 is typically required for acid pre-treatment (Negahdar et al., 2016). The pH of the AMD being treated at the DWS treatment plants in the Witwatersrand basin

range from 2.5 – 5.9 (Department Of Water Affairs (DWA), 2013). The pH of the AMD in the Mpumalanga coalfields has been found to be 2.4 (Naidu, T.S., unpublished). The more acidic sources of AMD in these areas could contain sufficient H_2SO_4 for efficient acid pre-treatment, however, the less acidic sources of AMD would not. It is, therefore, necessary to identify a source of AMD that is highly acidic for the successful implementation of such a biorefinery.

Further investigation into the design and operation of a DSR reactor needs to be conducted. This includes investigation into the following areas: optimal reactor configuration, inoculum, operating conditions, additional water treatment required, and disposal/sale of waste/by-products.

The incorporation of AMD remediation into the proposed biorefinery is presented in Figure 3.7.

3.6.4 Feasibility of various feedstocks

For this biorefinery to feasible, it is necessary that there is a cheap availability of both AMD and biomass feedstocks, in close proximity to the biorefinery complex. Due to a large amount of mining activity and a high concentration of sulfide-based minerals in the Witwatersrand basin and the Mpumalanga coalfields, there are large volumes of AMD being generated on an ongoing basis. The current cost of AMD remediation ranges from 42 USD/ML –697 USD/ML (Mccarthy et al., 2010), which can result in significant expenditure if there are large volumes of AMD. Institutions responsible for the remediation of this AMD are looking for cheaper and more sustainable treatment options and hence it should be assumed that there is sufficient AMD feedstock freely available in these areas.

The three biomass feedstocks that could be utilized by the proposed biorefinery are straw, sawmill residue, and wood chips. These have a feature complexity of 2, 1 and 1 respectively. The Witwatersrand basin and the Mpumalanga coalfields are primarily located on the South African Central Plateau, within the grassland biome (Mucina and Rutherford, 2006). A map of the mining activity, as well as the dominant biomes in the Witwatersrand basin and the Mpumalanga coalfields, is presented in Figure 3.8 (South African National Biodiversity Institute, 2012; Water Research Commission, 2017). Although there is agricultural activity in the area there are still large areas of uncultivated land, in which indigenous tall grass species are dominant. As these grasses are typically dry due to the climate, they are more like straw

than green crops such as alfalfa or clover. The low moisture content makes these grasses more suitable for a lignocellulosic biorefinery then a green biorefinery, which would typically process green grass with a high moisture content. The majority of this biomass is currently uncultivated, with wild-fires and controlled burning destroying large quantities of this biomass annually. There would, therefore, be sufficient supply of this biomass at favorable prices if the biorefinery could be located in these areas.

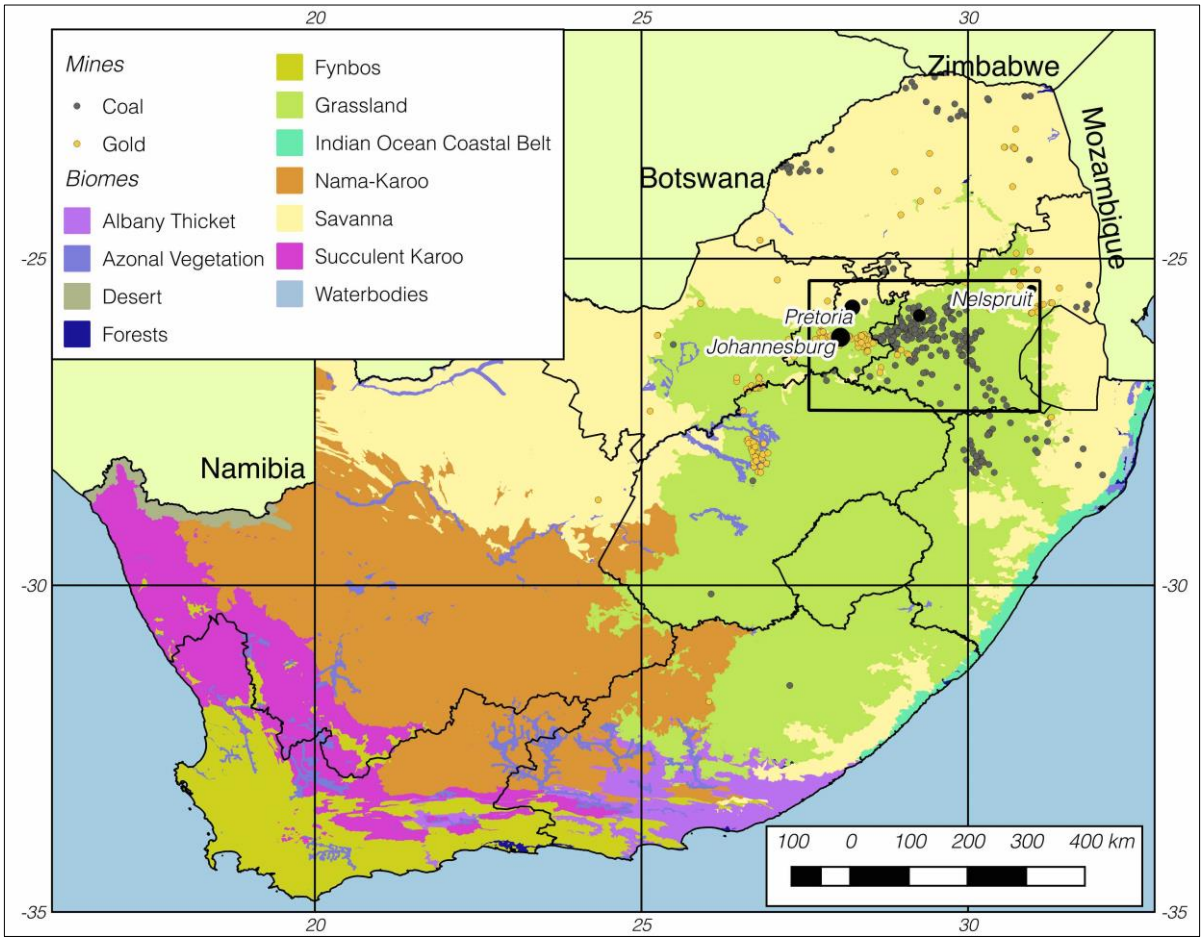

Figure 3.8: Map of the mining activity as well as the dominant biomes in South Africa with the Witwatersrand basin and the Mpumalanga coalfields demarcated (South African National Biodiversity Institute, 2012; Water Research Commission, 2017).

A study of grasses in South Africa found the yield of grass ranges from 4.0 – 20 ton/ha under various conditions of water limitation (Marais et al., 2017). There is an estimated 2 000 ton/day dry material available based on the assumption of 9 ton/ha yield and 10% land utilization within a 50 km radius. A plant size sensitivity analysis found that the cost reduction due to economies of scale were minimal in facilities bigger than 2 000 ton/day (a Aden et al., 2002).

3.7. Risks and Opportunities

Acid pre-treatment results in the production of various compounds that inhibit both enzymatic hydrolysis and fermentation. Non-productive binding of enzymes with unreactive constituents of the solid fraction (*e.g.* lignin) (Nakagame et al., 2011; Pareek et al., 2013; Rahikainen et al., 2013) decreases enzyme activity. Enzyme activity is further inhibited by by-products released during both pre-treatment and hydrolysis such as sugars (Berlin et al., 2006; Teugjas and Väljamäe, 2013) and solubilized aromatics (Ximenes et al., 2011). Both the rate and yield of fermentation can be inhibited by carboxylic acids (acetic acid, formic acid, luvinic acid)(Larsson et al., 1999) and furan aldehydes (furfural, hydroxymethylfurfural) (Banerjee et al., 1981; Du et al., 2010; Larsson et al., 1999) released during pre-treatment.

Strategies to counteract inhibitory effects include feedstock selection/engineering, detoxification, genetic engineering of micro-organisms, and reactor configurations that reduce concentrations of inhibitors (Jönsson and Martín, 2016). Although progress has been made in developing recombinant micro-organisms that have a higher tolerance to inhibition, detoxification of hydrolysate is still more effective at combating the inhibitory effects (Jönsson et al., 2013)

Differing biomass composition and process operating parameters result in the release of different inhibitory compounds (Jönsson and Martín, 2016). AMD contains high levels of sulfate and heavy metals. The effect that these components will have on the formation of inhibitory by-products is unknown. The precipitation of heavy metals onto the biomass surface could also block enzyme adsorption sites inhibiting hydrolysis. Since the degree to which this will occur is unknown, it introduces a high level of risk. It is thus necessary to perform further investigation into the specific inhibitory compounds that will be released, and the required measure to counteract their effect, before the feasibility of the biorefinery can be determined.

The production of high-value chemicals from the C6 platform should be strongly considered. Potential high-value chemicals include, polyhydroxyalkanoates (6 500 USD/ton), farmenese (5 581 USD/ton), 1,4-butanediol (>3 000 USD/ton) and succinic acid (2 940 USD/ton) (E4TECH et al., 2015). Although the production of these chemicals is not as well demonstrated as bioethanol (815 USD/ton) the market value is much greater and thus the production of a small

volume of these chemicals could provide great opportunity towards improving the economics of this biorefinery.

Recently there has been investigation into the use of brewer's yeast for the remediation of metallic wastewater (Andreea, 2013). Surplus yeast that is generated in the fermentation process can be used, at minimal cost, for the biosorption of the metals present in the AMD. If a biosorption step was incorporated prior to the hydrolysis step a portion of the metals present in the AMD could be removed. This could potentially help mitigate the potential effects of heavy metal precipitation on the process.

The reduction in operating cost associated with the availability of a free mineral acid source (*i.e.* AMD) provides an excellent opportunity for the development of a lignocellulosic biorefinery. The demand for cheap, sustainable remediation of AMD furthers this opportunity as remediation of AMD can be incorporated into the process. This will provide a potentially sustainable solution for AMD remediation at reduced cost.

3.8. Concluding Remarks

The exact configuration of a biorefinery to produce valuable biochemicals from lignocellulosic biomass, incorporating the pre-treatment of biomass utilizing AMD, and subsequent remediation of the AMD, has not been identified. However, it is evident that such a biorefinery would utilize the acid present in the AMD to pre-treat the biomass, releasing C5 sugars that will be consumed by SRB for the remediation of AMD. Pre-treated biomass will undergo further enzymatic hydrolysis to release C6 sugar. Most of the C6 sugars will undergo fermentation to produce bioethanol, with a fraction being processed to produce high-value biochemicals. Bioethanol will undergo distillation to produce high concentration alcohol. It is presently unclear what the best processing route for the distillery silage is, but it could either be used to produce electricity and heat, fertilizer or animal feed. It is also unclear on what the best lignin processing route is, however potential processes that have been identified include direct combustion and gasification.

To determine the most economically favorable biorefinery, it is recommended that the following techno-economic evaluations take place. These should include an evaluation of the capital cost, operating costs and market potential for each of the products:

- comparison of different lignin processing routes including direct combustion, and gasification;
- comparison of different distillery silage products including electricity and heat, fertilizer, and animal feed; and
- evaluation of the most feasible high-value biochemical produced from the C6 sugar platform.

Further investigation should be conducted so as to determine the effect of using acid mine drainage, as opposed to typical mineral acids, for the pre-treatment of lignocellulosic biomass and the subsequent effect that this will have on all processing routes. The potential for remediating AMD through the biosorption of heavy metals by surplus yeast (produced in fermentation) should also be investigated.

Another method that could be used to perform an exhaustive search for the optimal solution is a simultaneous supper structure approach. This approach is beyond the scope of this study but should be considered in future investigations.

Although there is still a lot of uncertainty associated with the proposed biorefinery, by linking pre-treatment of biomass and remediation of AMD the costs of both processes can potentially be reduced. The integration of these processes into a biorefinery which produces multiple products aids the economic feasibility of the process by introducing multiple revenue streams. This process shows great promise in the context of the Witwatersrand basin and the Mpumalanga coalfields due to the availability of AMD and unused lignocellulosic biomass in the area.

3.9. Acknowledgments

The support of the Global Change Institute (GCI); and the National Research Foundation (NRF) and the University of the Witwatersrand towards this research is hereby acknowledged. The authors would like to acknowledge Ms. Tamlyn Naidu for sharing data on the quality of AMD in the eMalahleni area.

3.10. References

Aden, a, Ruth, M., Ibsen, K., Jechura, J., Neeves, K., Sheehan, J., Wallace, B., Montague, L., Slayton, a, Lukas, J., 2002. Lignocellulosic Biomass to Ethanol Process Design and Economics Utilizing Co-Current Dilute Acid Prehydrolysis and Enzymatic Hydrolysis for Corn Stover. Other Inf. PBD 1 Jun 2002 Medium: ED; Size: 154 pages. doi:NREL/TP-510-32438

Andreea, S., 2013. Brewer's Yeast: an Alternative for Heavy Metal Biosorption from Waste Waters. ProEnviroment 6, 457–464.

Banerjee, N., Bhatnagar, R., Viswanathan, L., 1981. Inhibition of glycolysis by furfural in Saccharomyces cerevisiae. Eur. J. Appl. Microbiol. Biotechnol. 11, 226–228. doi:10.1007/BF00505872

Berlin, A., Maximenko, V., Cilkes, N., Saddler, J., 2006. Optimization of Enzyme Complexes for Lignocellulose Hydrolysis. Biotechnol. Bioeng. 97, 287–296. doi:10.1002/bit.21238

Bijmans, M.F.M., Vries, E. De, Yang, C.-H., Buisman, C.J.N., Lens, P.N.L., Dopson, M., 2010. Sulfate Reduction at pH 4 . 0 for Treatment of Process and Wastewaters. Biotechnol. Prog. 26, 1029–1037. doi:10.1002/btpr.400

Bridgwater, A. V, Peacocke, G.V.C., 2000. Fast pyrolysis processes for biomass. Renew. Sustain. Energy Rev. 4, 1–73. doi:10.1016/S1364-0321(99)00007-6

Cherubini, F., 2010. The biorefinery concept : Using biomass instead of oil for producing energy and chemicals. Energy Convers. Manag. 51, 1412–1421. doi:10.1016/j.enconman.2010.01.015

Cherubini, F., Jungmeier, G., Wellisch, M., Willke, T., Skiadas, I., Ree Van, R., de Jong, E., 2009. Toward a common classification approach for biorefinery systems. Biofuels, Bioprod. Biorefining 3, 534–546. doi:10.1002/bbb

Conningarth Economists, 2013. Growing the Sugar Industry in South Africa Document 5 : Investigation and Evaluation of Alternative Uses and Products from Sugarcane : A Cost Benefit and Macro-Economic Impact analysis. Pretoria.

Dale, B.E., Wyman, C.E., 2015. Producing Biofuels via the Sugar Platform. AICheME 45–57.

de Jong, E., Higson, A., Walsh, P., Wellisch, M., 2012. Bio-based Chemicals: Value Added Products from Biorefineries. Waginingen.

den Haan, R., van Rensburg, E., Rose, S.H., Gorgens, J.F., van Zyl, W.H., 2015. Progress and challenges

Department Of Water Affairs (DWA), 2013. Feasibility Study for a Long-Term Solution to address the Acid Mine Drainage associated with the East, Central and West Rand underground mining basins. Study Report No. 5.3: Options for Use or Discharge of Water. Pretoria.

Donnelly, L., 2017. SA's sugar industry under assault. Mail Gardian.

Du, B., Sharma, L.N., Becker, C., Chen, S.F., Mowery, R.A., van Walsum, G.P., Chambliss, C.K., 2010. Effect of varying feedstock-pretreatment chemistry combinations on the formation and accumulation of potentially inhibitory degradation products in biomass hydrolysates. Biotechnol. Bioeng. 107, 430–440. doi:10.1002/bit.22829

E4TECH, RE-CORD, WUR, 2015. From the Sugar Platform to biofuels and biochemicals, Final report for the European Commission Directorate-General Energy. doi:contract No. ENER/C2/423-2012/SI2.673791

Greben, H.A., Baloyi, J., Sigama, J., Venter, S.N., 2009a. Bioremediation of sulphate rich mine effluents using grass cuttings and rumen fluid microorganisms. J. Geochemical Explor. 100, 163–168. doi:10.1016/j.gexplo.2008.01.004

IEA Bioenergy, 2013. Factsheets Biorefineries [WWW Document]. URL http://www.iea-

bioenergy.task42-biorefineries.com/en/ieabiorefinery/Factsheets.htm (accessed 7.21.17).

Johnson, D.B., Hallberg, K.B., 2005a. Acid mine drainage remediation options: A review. Sci. Total Environ. 338, 3–14. doi:10.1016/j.scitotenv.2004.09.002

Jönsson, L.J., Alriksson, B., Nilvebrant, N.-O., 2013. Bioconversion of lignocellulose: inhibitors and detoxification. Biotechnol. Biofuels 6, 16. doi:10.1186/1754-6834-6-16

Jönsson, L.J., Martín, C., 2016. Pretreatment of lignocellulose: Formation of inhibitory by-products and strategies for minimizing their effects. Bioresour. Technol. 199, 103–112. doi:10.1016/j.biortech.2015.10.009

Jungmeier, G., van Ree, R., Jørgensen, H., De Jong, E., Stichnothe, H., Wellisch, M., 2014. The Biorefinery Complexity Index. doi:???

Kaksonen, A.H., Puhakka, J.A., 2007. Sulfate reduction based bioprocesses for the treatment of acid mine drainage and the recovery of metals. Eng. Life Sci. 7, 541–564. doi:10.1002/elsc.200720216

Kumar, R., Singh, S., Singh, O. V, 2008. Bioconversion of lignocellulosic biomass : biochemical and molecular perspectives. J. Ind. Microbiol. Biotechhnology 377–391. doi:10.1007/s10295-008-0327-8

Kunz, R., Jewitt, G., 2013. Mapping the potential water use of biofuel feedstock production in South Africa, in: Dallemand, J.F. (Ed.), JRC Technical Reports - Bioenergy and Water. International Energy Agency, pp. 171–190. doi:10.2790/94402

Larsson, S., Palmqvist, E., Hahn-Hagerdal, B., Tengborg, C., Stenberg, K., Zacchi, G., Nilvebrant, N.O., 1999. The generation of fermentation inhibitors during dilute acid hydrolysis of softwood. Enzyme Microb. Technol. 24, 151–159. doi:10.1016/S0141-0229(98)00101-X

Lefticariu, L., Walters, E.R., Pugh, C.W., Bender, K.S., 2015. Sulfate reducing bioreactor dependence on organic substrates for remediation of coal-generated acid mine drainage: Field experiments. Appl. Geochemistry 63, 70–82. doi:10.1016/j.apgeochem.2015.08.002

Lynd, L.R., Wang, M.Q., 2003. A Product-Nonspecific Framework for Evaluating the Potential of Biomass-Based Products to Displace Fossil Fuels. J. Ind. Ecol. 7, 17–32. doi:10.1162/108819803323059370

Magowo, E., Rumbold, K., Sheridan, C., 2015. The Utilization of Cellulosic Biomass in treating AMD and the Subsequent Generation of Fermentable Sugars, in: 10th International Conference on Acid Rock Drainage and IMWA Anual Conference. pp. 1–12.

Marais, D., Rethman, N., Annandale, J., 2017. Dry matter yield and water use efficiency of five perennial subtropical grasses at four levels of water availability. African J. Range Forage Sci. 23, 165–169. doi:10.2989/10220110609485900

Maurya, D.P., Singla, A., Negi, S., 2015. An overview of key pretreatment processes for biological conversion of lignocellulosic biomass to bioethanol. 3 Biotech 5, 597–609. doi:10.1007/s13205-015-0279-4

McCarthy, T.S., 2011. The impact of acid mine drainage in South Africa. S. Afr. J. Sci. 107, 1–7. doi:10.4102/sajs.v107i5/6.712

Mccarthy, T.S., Steyl, G., Maree, J., Zhao, H., 2010. MINE WATER MANAGEMENT IN THE WITWATERSRAND WITH SPECIAL EMPHASIS ON ACID MINE DRAINAGE: Report to the Inter-Ministerial Committee on Acid Mine Drainage 1–128.

Menon, V., Rao, M., 2012. Trends in bioconversion of lignocellulose : Biofuels , platform chemicals & biore fi nery concept. Prog. Energy Combust. Sci. 38, 522–550. doi:10.1016/j.pecs.2012.02.002

Mosier, N., Wyman, C., Dale, B., Elander, R., Lee, Y.Y., Holtzapple, M., Ladisch, M., 2005b. Features of

promising technologies for pretreatment of lignocellulosic biomass. Bioresour. Technol. 96, 673–686. doi:10.1016/j.biortech.2004.06.025

MPRDA, 2013. Mineral and Petroleum Resources Development Amendement Bill. Government Gazette No. 36523, South Africa.

Mucina, L., Rutherford, M.C., 2006. Vegitation of South Africa, Lesotho and Swaziland. Strelitzia, South African National Biodiversity Insitute, Pretoria.

Muyzer, G., Stams, A.J.M., 2008. The ecology and biotechnology of sulphate-reducing bacteria. Nat. Rev. Microbiol. 6, 441–454. doi:10.1038/nrmicro1892

Nakagame, S., Chandra, R.P., Kadla, J.F., Saddler, J.N., 2011. The isolation, characterization and effect of lignin isolated from steam pretreated Douglas-fir on the enzymatic hydrolysis of cellulose. Bioresour. Technol. 102, 4507–4517. doi:10.1016/j.biortech.2010.12.082

Neculita, C.M., Zagury, G.J., Bussière, B., 2008. Effectiveness of sulfate-reducing passive bioreactors for treating highly contaminated acid mine drainage: II. Metal removal mechanisms and potential mobility. Appl. Geochemistry 23, 3545–3560. doi:10.1016/j.apgeochem.2008.08.014

Negahdar, L., Delidovich, I., Palkovits, R., 2016. Aqueous-phase hydrolysis of cellulose and hemicelluloses over molecular acidic catalysts : Insights into the kinetics and reaction mechanism. Appl. Catal. B Environ. 184, 285–298. doi:doi:10.1016/j.apcatb.2015.11.039

Pareek, N., Gillgren, T., Jönsson, L.J., 2013. Adsorption of proteins involved in hydrolysis of lignocellulose on lignins and hemicelluloses. Bioresour. Technol. 148, 70–77. doi:10.1016/j.biortech.2013.08.121

Rahikainen, J.L., Martin-Sampedro, R., Heikkinen, H., Rovio, S., Marjamaa, K., Tamminen, T., Rojas, O.J., Kruus, K., 2013. Inhibitory effect of lignin during cellulose bioconversion: The effect of lignin chemistry on non-productive enzyme adsorption. Bioresour. Technol. 133, 270–278. doi:10.1016/j.biortech.2013.01.075

Ramla, B., Sheridan, C., 2015. The potential utilisation of indigenous South African grasses for acid mine drainage remediation. Water SA 41, 247–252. doi:10.4314/wsa.v41i2.10

Sajbrt, V., Rosol, M., Ditl, P., 2010. A Comparison of Distillery Stillage Disposal Methods production Stillage disposal methods. Acta Polytech. 50, 63–69.

Sánchez-Andrea, I., Sanz, J.L., Bijmans, M.F.M., Stams, A.J.M., 2014. Sulfate reduction at low pH to remediate acid mine drainage. J. Hazard. Mater. 269, 98–109. doi:10.1016/j.jhazmat.2013.12.032

Sanchez, A., Sevilla-Güitrón, V., Magaña, G., Gutierrez, L., 2013. Parametric analysis of total costs and energy efficiency of 2G enzymatic ethanol production. Fuel 113, 165–179.

Shafiee, S., Topal, E., 2009. When will fossil fuel reserves be diminished? Energy Policy 37, 181–189. doi:10.1016/j.enpol.2008.08.016

Simate, G.S., Ndlovu, S., 2014. Acid mine drainage: Challenges and opportunities. J. Environ. Chem. Eng. 2, 1785–1803. doi:10.1016/j.jece.2014.07.021

South African National Biodiversity Institute, 2012. 2012 Vegetation Map of South Africa, Lesotho and Swaziland [vector geospatial dataset] [WWW Document]. URL http://bgis.sanbi.org/SpatialDataset (accessed 11.20.17).

Spath, P.L., Dayton, D.C., 2003. Preliminary Screening — Technical and Economic Assessment of Synthesis Gas to Fuels and Chemicals with Emphasis on the Potential for Biomass-Derived Syngas , NREL task number BBB3.4210. Co. USA.

Sun, Y., Cheng, J., 2002. Hydrolysis of lignocellulosic materials for ethanol production: A review.

Bioresour. Technol. 83, 1–11. doi:10.1016/S0960-8524(01)00212-7

Taylor, J., Pape, S., Murphy, N., 2005. A Summary of Passive and Active Treatment Technologies for Acid and Metalliferous Drainage (AMD). Proc. 5th Aust. Work. Acid Drain.

Teugjas, H., Väljamäe, P., 2013. Product inhibition of cellulases studied with 14C-labeled cellulose substrates. Biotechnol. Biofuels 6, 104. doi:10.1186/1754-6834-6-104

Water Research Commision, 2017. The South Africa Mine Water Atlas,WRC Report no. TT670/16. Pretoria.

Zagury, G.J., Neculita, C., 2007. Passive Treatment of Acid Mine Drainage in Bioreactors : Short Review , Applications , and Research Needs, in: 60th Canadian Geotechnical Conference & 8th Joint CGS/IAH-CNC Groundwater Conference. Ottow, pp. 1439–1446.

Chapter 4: Flowsheet and Sensitivity Analyses for the Bioremediation of Acid Mine Drainage Using Sulfate-reducing Bacteria

(Presented at the 2nd International Conference on Environmental Engineering and Climate Change, Mauritius, 2017) This chapter developed process flowsheets for the remediation of AMD using SRB and simultaneous pre-treatment of lignocellulosic biomass. Three different reactor configurations were investigated, and the most suitable process configuration was determined based on estimates of the total reactor volumes. Knowledge gaps were identified and recommendations into further research were made. This chapter addresses objective a.

Burman, N.W., van Dyk, L., Postma, F., Sheridan, C., Simate, G.S., Harding, K.G., 2017. Flowsheet and Sensitivity Analyses for the Bioremediation of Acid Mine Drainage Using Sulfate Reducing Bacteria and South African Grasses, in: 2nd International Conference on Energy, Environment and Climate Change (ICEECC). Pointe Aux Piments, Mauritius.

Abstract: The potential for a process to treat acid mine drainage (AMD) using dissimilatory sulfate reduction (DSR) and biomass as a carbon source has been demonstrated previously. This study found that the acidity present in the water hydrolyzes the hemicellulose matrix releasing sugars that can be utilized by sulfate-reducing bacteria (SRB). It has been proposed that this process be used as an environmentally friendly alternative to traditional AMD remediation which uses costly chemical neutralization techniques that produce large volumes of toxic by-products. Although the potential for this process has been demonstrated, little attention has been given to the design of this process.

In this study, three different flow diagrams are proposed. Flowsheets for each of these reactor configurations were developed using desired overall reduction of sulfate concentration and extent of hydrolysis of grass. Design equations were then used so as to determine the approximate total reactor volume required for each process configuration.

It was found that the rate of hydrolysis of biomass is severely rate-limiting, and the only process which shows any promise for commercial implementation is one in which hydrolysis of biomass is operated at elevated temperatures (~100°C), in a stand-alone hydrolysis reactor separate from the DSR reactor. Sensitivity analyses were performed so as to determine what effect different kinetic data sources, as well as temperature, have on the total volume predicted. Some kinetic data sources predicted very similar total volumes, whereas other predicted volumes as much as 100 times larger than the smallest. The effect of decreasing the temperature from 100°C to 10°C was found to increase the volume between 10^2 – 10^5 times depending on the kinetic data source used. This highlights the need to determine the rate of hydrolysis at the specific operating conditions under which the process will operate for the accurate design of a commercial process.

Keywords: Acid Mine Drainage (AMD); Sulfate-reducing Bacteria (SRB); Dissimilatory Sulfate Reduction (DSR); Flowsheet Development

4.1. Introduction

The problem of acid mine drainage (AMD) has recently received much publicity in South Africa due to the negative impact that AMD decant had on aquatic environments both in the Witwatersrand basin and the Mpumalanga coalfields (McCarthy, 2011). This prompted research into strategies and technologies to treat AMD. Current AMD treatment methods typically use a chemical pH neutralizing agent, which concurrently results in the precipitation of heavy metals (Taylor et al., 2005). Although effective, this method is expensive and produces large volumes of toxic waste. Therefore, a sustainable, relatively low-cost environmentally conscious process is needed.

To this end, dissimilatory sulfate reduction (DSR) was identified to be an environmentally conscious and effective biological alternative to chemical AMD treatment methods. Various studies showed that DSR by sulfate-reducing bacteria (SRB) to be effective in reducing both the acidity and sulfate concentration of AMD (Béchard et al., 1994; Chang et al., 2000; Chockalingam and Subramanian, 2006; H. Greben et al., 2009; Lefticariu et al., 2015; Magowo et al., 2015; Ramla and Sheridan, 2015; Zagury and Neculita, 2007). Ramla and Sheridan (2015) and Magowo *et al.* (2015) found sulfate-reducing bacteria (SRB) effective in remediating AMD using South African grass, which is highly abundant and affordable, as a substrate (carbon source).

Although these two studies provided evidence that this process could be effective in remediating AMD there is still extensive design and research work required before this process can be implemented commercially. An efficient process configuration needs to be conceived, and this should then be optimized. Mathematical models can be used to estimate the performance and equipment sizing of proposed process configurations. Sensitivity analyses can then be performed on these mathematical models to determine optimum operating conditions.

A literature review of previous studies where mathematical models were developed to describe AMD remediation using SRB was conducted. Although the topic of AMD remediation using SRB is well studied, (Johnson and Hallberg, 2005a; Sánchez-Andrea et al., 2014; Zagury and Neculita, 2007) no studies were found investigating the development of mathematical models to describe the complete process.

Therefore, the aim of this study was to develop mathematical models of three different reactor configurations for the process of remediating AMD using SRB and South African grasses. The objectives were:

- to gain initial estimates on the total reactor volume required for each configuration to achieve a desired water quality;
- determine the sensitivity of the model to changes in operating temperature and kinetic data through sensitivity analyses;
- make a comparison between all three process configurations based on initial estimates of total volume and the results of the sensitivity analysis; and
- identify knowledge gaps that require further investigation, either experimental, theoretical, or a combination thereof, for the successful design of the proposed process.

4.2. Process Flow Diagrams

Three different reactor configurations were modeled to maximize the hydrolysis of the hemicellulose (xylan) in grass to xylose. The resulting sugars that are released subsequently serve as a carbon source for the SRB which removes sulfate from the AMD streams through DSR. The H_2S and bicarbonate react with Fe^{2+} to form FeS, a precipitate, and increase the pH respectively.

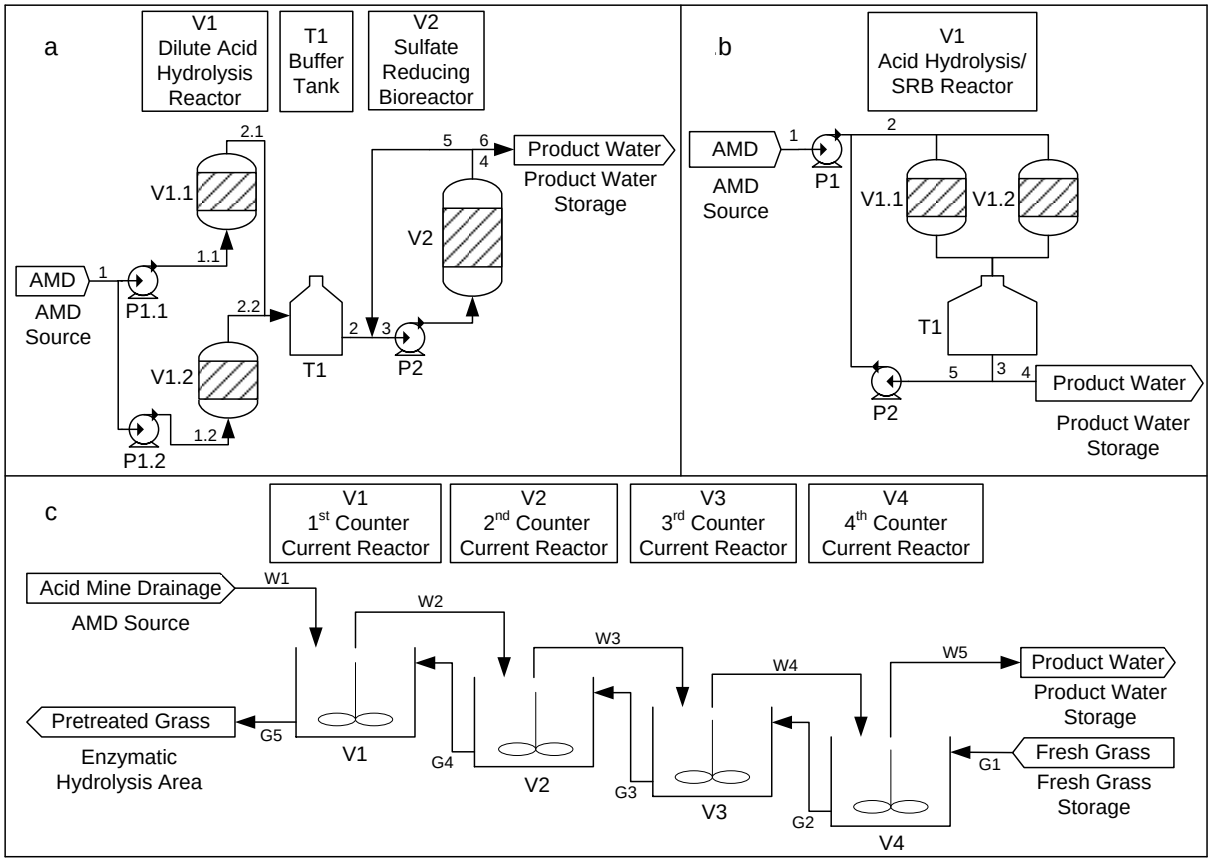

Figure 4.1: Process flow diagrams (PFD) for (a.) Process 1, (b.) Process 2, and (c.) Process 3

4.2.1 Process 1: Packed Bed Hydrolysis and SRB Recycle Reactor

Fresh AMD (stream 1) flows into the dilute acid hydrolysis reactor (V1), which is filled with grass, xylose released through hydrolysis enters the water stream (Figure 4.1.a). It is assumed that there is no change in the concentration of H^+, SO_4, and Fe^{2+}. A duplicate hydrolysis reactor is included for the changing of grass. To eliminate xylose concentration fluctuations further downstream, water exiting the hydrolysis reactor (stream 2) enters a buffer tank. Water from the buffer tank (stream 2.1) is mixed with a recycle stream (stream 5) to form stream 3, which flows into a sulfate-reducing bioreactor (V2) where DSR occurs.

A portion of the exit stream (stream 4) is recycled (stream 5), while the balance (stream 6) is product water which can either be released into natural or municipal water systems; used as process water; or further treated for alternative use, such as irrigation. The recycle stream ensures that the pH of stream 3 is not toxic to the SRB in the sulfate-reducing bioreactor.

Spent grass from the dilute hydrolysis reactor (V1) is transported to a storage facility from where it can either be used as a feedstock for another process or discarded as waste.

4.2.2 Process 2: Combined Hydrolysis and DSR Reactor

Grass is loaded into a reactor that retains the grass while allowing water to flow through. Fresh AMD (stream 1) is mixed with a recycle stream (stream 4) to form stream 2, which flows into the reactor in which both hydrolysis of xylan and DSR occur (Figure 4.1.b).

Water flows through the reactor and is collected in a buffer tank (stream 3). A portion of the water is recycled (stream 5) and mixed with the fresh AMD stream, while the remaining water (stream 4) is product water. After a period of time, the grass will be removed from the reaction vessel and transported to the spent grass storage. A duplicate reactor is included for the changing of grass.

4.2.3 Process 3: Counter Current Sequential CSTR's

In the third design (Figure 4.1.c), the grass and AMD move in a counter current flow pattern through a series of continuous stirred tank reactors (CSTR). Fresh AMD (stream W1) enters reactor 1 (V1) and solid grass cuttings from a downstream reactor (V2) are conveyed into this reactor. Both hydrolysis of xylan and DSR occur in each reactor.

The grass from this reactor is transported to the spent grass storage. Water exiting reactor V1 (stream W2) flows into reactor V2. Grass from a further downstream reactor (V3) is conveyed to reactor V2. The same biochemical reactions take place in this reactor as in reactor V1. Water from reactor V2 flow to a further downstream reactor (V3) while grass is conveyed upstream to reactor V1. Water leaving the last reactor is product water.

By replicating the reactor unit, a counter current flow is created between the grass and the AMD. AMD flows from reactor (Vi) to a downstream reactor (V(i+1)), while grass is transported to an upstream reactor (V(i-1)). The size and number of reactor units can be modified so as to optimize the efficiency and capital cost of the process. For the current model, 4 reactors were used.

4.3. Model Development

4.3.1 Reaction mechanism and mole balance

The reactions that occur are the hydrolysis of xylan to xylose (Equation 4.1) (Charles E Wyman et al., 2005), dissimilatory sulfate reduction (DSR), using xylose as a carbon source, producing H_2S and bi-carbonate (Equation 4.2) (Metcalf et al., 2013), and the reaction of ferrous iron and hydrogen sulfide to form FeS (Equation 4.3) (Johnson and Hallberg, 2005a).

$$C_5H_8O_4 + H_2O \xrightarrow{H^+} C_5H_{10}O_5 \quad (4.1)$$

$$SO_4^{2-} + {}^2/_5\, C_5H_{10}O_5 + 2H^+ \rightarrow H_2S + 2CH_2O_3 \quad (4.2)$$

$$Fe^{2+} + H_2S \rightarrow FeS + 2H^+ \quad (4.3)$$

For Process 1 and 2, grass is loaded/removed in batches, and thus the extent of the hydrolysis reaction (ϵ_1) is assigned to the batch reaction at the total time, t(hr), based on the total initial moles, $\left(n_{C_5H_8O_4,\mathrm{i}}\right)$, according to Equation (4.4).

$$\epsilon_1 = X_{C_5H_8O_4} \cdot n_{C_5H_8O_4,i} \quad (4.4)$$

The final number of moles of xylan remaining $\left(n_{C_5H_8O_4,\mathrm{f}}\right)$ after the total batch time (t) can thus be calculated from Equation (4.5)

$$n_{C_5H_8O_4,f} = n_{C_5H_8O_4,i} - \epsilon_1 \quad (4.5)$$

It was assumed that the release of xylose into the liquid stream exiting the reactor is constant over time. This assumption simplifies the model and can be justified by the inclusion of a buffer tank. It was thus assumed that the flow rate of xylose in exiting stream, $\dot{n}_{C_5H_{10}O_5,2.1}$, is constant over time and can be calculated according to Equation (4.6)

$$\dot{n}_{C_5H_{10}O_5,2.1} = \dot{n}_{C_5H_{10}O_5,1} + \frac{\epsilon_1}{t} \quad (4.6)$$

where t is the reaction batch time required for the reaction to proceed to the desired conversion (hr), $\dot{n}_{C_5H_8O_4,1}$ and $\dot{n}_{C_5H_8O_4,2.1}$ are the flow rate of xylose in stream 1 and 2.1 respectively (kmol/hr). An equivalent time-dependent extent of reaction ϵ_1^* (kmol/hr) can be expressed as

$$\epsilon_1^* = \frac{\epsilon_1}{t} \quad (4.7)$$

Equation (4.5) can thus be expressed as

$$\dot{n}_{C_5H_{10}O_5,2.1} = \dot{n}_{C_5H_{10}O_5,1} + \epsilon_1^* \quad (4.8)$$

For Process 3 the grass will move through the system continuously and the extent of the reaction is based on the molar flow rate entering each reactor, i, and the conversion in that reactor as according to Equation (4.9)

$$\epsilon_{2,1,i} = X_{C_5H_8O_4,i} \cdot \dot{n}_{C_5H_8O_4,f,G(5-i)} \tag{4.9}$$

The extent of reaction for Equation 4.2 and 4.3 can be expressed as below.

$$\epsilon_2 = X_{SO4,S} \cdot \dot{n}_{SO4,3} \tag{4.10}$$

$$\epsilon_3 = X_{Fe^{2+},S} \cdot \dot{n}_{Fe^{2+},3} \tag{4.11}$$

Where ϵ_2 and ϵ_3 are the extent of reaction 4.2 and 4.3 respectively (kmol/hr), $X_{SO4,S}$, and $X_{Fe^{2+},S}$ are the conversion of sulfate and iron respectively (% of moles reacted), and $\dot{n}_{SO4,3}$ & $\dot{n}_{Fe^{2+},3}$ are the inlet molar flow rate of sulfate and iron respectively (kmol/hr).

This model assumes that AMD has a sulfate concentration of 0.05M, an iron concentration of 0.01M and an H^+ concentration of 0.001M (pH = 3). This is based on an AMD sample taken from a coal mine situated within the Mpumalanga coalfields. With this assumption of water quality, there are insufficient H^+ ions available for the DSR reaction to proceed to any significant extent, since two moles of H^+ are required for the reduction of one mole of sulfate (Equation 4.2). This will limit the amount of alkalinity produced by means of DSR.

This suggests that the increase in pH happens by some unknown mechanism, and that the extent to which DSR reaction occurs is independent of the initial concentration of H^+ ions. The concentration of the H^+ ion is one of the crucial design parameters as it is required for water to be of a circumneutral pH before it can be returned to natural water systems. In order to incorporate the concentration of H^+ ions into the model, it was assumed that H^+ ions are consumed in some unknown reaction. Although this reaction is unknown it was assigned an extent of reaction ϵ_4 (kmol/hr) as according to:

$$\epsilon_4 = \mathrm{X}_{\mathrm{H}^+} \cdot \dot{\mathrm{n}}_{\mathrm{H}^+,3} \tag{4.12}$$

where X_{H^+} is the consumption of H^+ ions (%), and $\dot{n}_{H^+,3}$ is the inlet molar flow rate of H^+ ions (kmol/hr). The mechanism of pH increase in these processes was identified as an area that requires further investigation.

The extent of this reaction was set so as to result in a pH increase of 3 units across the whole process. This is similar to the pH increase that was observed by Magowo *et al.* (2015) and Ramla and Sheridan (2015).

In Process 2 and 3 the hydrolysis of xylan and DSR occur simultaneously. A literature review was performed to determine if either of these reactions are rate-limiting which could greatly simplify the process model. A review of experimentally determined rates of DSR was recently published by Sanchez-Andrea *et al.* (2014). A summary of the rate of DSR and the experimental conditions under which it was determined is presented in Table A1 in the supplementary notes (Appendix A).

The acid hydrolysis of xylan is known to display bi-phasic kinetics in which biomass consists of both a fast and a slow reacting fraction of xylan (Esteghlalian et al., 1997; Kobayashi and Sakai, 1956; Maloney et al., 1985). Xylose produced in both reactions can be converted further to form degradation products. This mechanism is shown in Figure 4.2. k_f, k_s, and k_2 represent the rate of reaction of the fast reacting fraction, the slow reacting fraction, and the xylose respectively (kmol/hr).

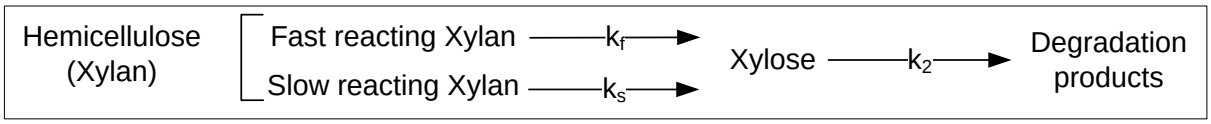

Figure 4.2: Schematic of xylan degradation mechanism (Esteghlalian et al., 1997)

The rate of change of xylose can thus be expressed as (Esteghlalian et al., 1997):

$$\frac{dC_{C_5H_{10}O_5}}{dt} = k_f \cdot C_{C_5H_8O_4f} + k_s \cdot C_{C_5H_8O_4s} \tag{4.13}$$

Where kinetic constants k_f and k_s demonstrate modified Arrhenius type temperature dependence as according to (Esteghlalian et al., 1997):

$$k = A_0 \cdot C_a^n \cdot e^{\left(-\frac{Ea}{R \cdot T}\right)} \tag{4.14}$$

where A_0 is the pre-exponential factor (/hr), Ea is activation energy (kJ/mol), R is the universal gas constant (8.31 x 10^{-3} kJ/mol.K), T is temperature (K), C_a is the acid concentration (wt% H_2SO_4), and n is an exponential.

A summary of the kinetic parameters determined by different researchers is presented in Table A2 (Appendix A).

The rate of hydrolysis under model test conditions was compared to the experimentally determined rate of DSR as summarized by Sanchez-Andrea *et al.* (2014). A summary of the rate of reactions is presented in Figure 4.3.

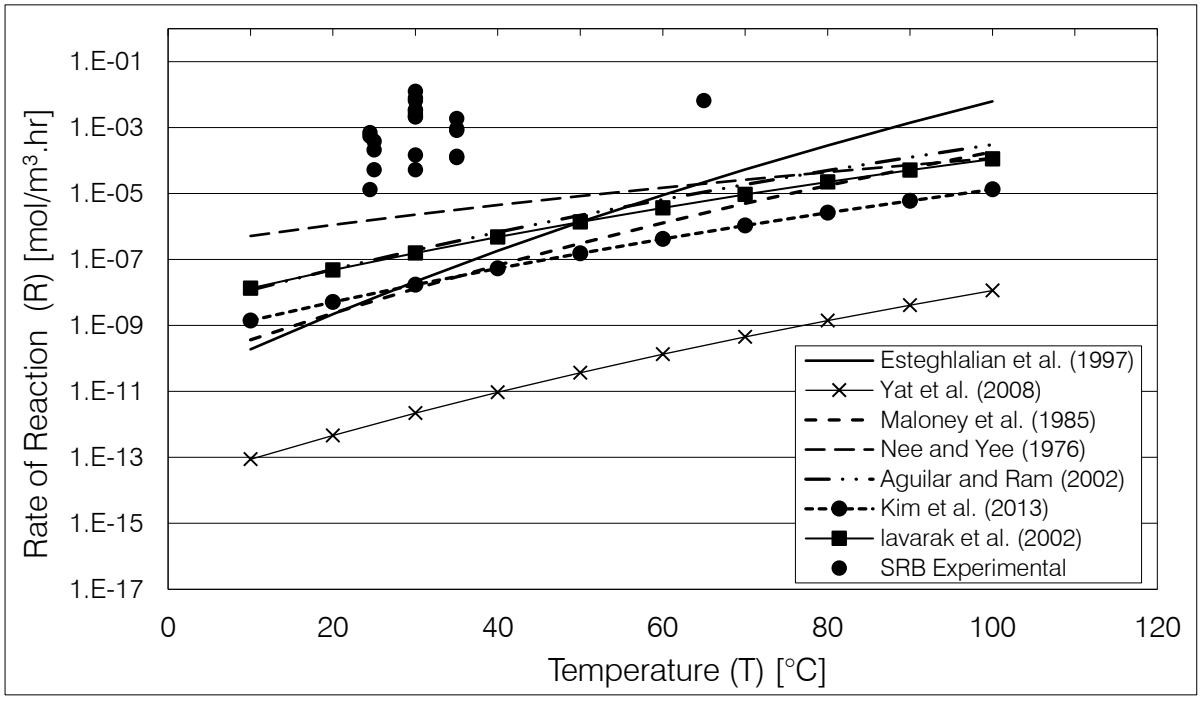

Figure 4.3: Kinetically predicted rate of acid hydrolysis (lines) and experimentally determined rate of sulfate reduction (points) *vs*. temperature

The rate of DSR was found to be orders of magnitude faster than the rate of xylan hydrolysis (Figure 4.3). This means that in Process 2 and 3, in which both the hydrolysis of xylan and DSR occur in the same reactor, the hydrolysis will be rate-limiting.

Using the reaction stoichiometry of Equation (4.1) and (4.2) the extent of DSR reaction was expressed as:

$$\epsilon_2 = \frac{5}{2} \times \epsilon_1 \tag{4.15}$$

Mole balances were written across both the hydrolysis and DSR reactor for Process 1, across the hydrolysis/DSR reactor in Process 2 and across each sequential reactor for Process 3. These mole balances have been expressed using the stoichiometric matrices and extent of reaction vectors. For simplification, mole balances were performed on both the fast and slow

reacting fractions in Process 3 with the fast reacting fraction assigned $\epsilon_{3,1f,i}$, and the slow fraction assigned $\epsilon_{3,1s,i}$.

A summary of the extent of reactions used can be found in Table 4.1 below. All extent of reactions have the units of kmol/hr except for $\epsilon_{1,1}$ and $\epsilon_{2,1}$ which have the units of kmol.

Table 4.1: Summary of the extent of reactions used in different processes

	Process 1	**Process 2**	**Process 3**
$\boldsymbol{\epsilon_1}$	$\epsilon_{1,1} = X_{C_5H_8O_4} \cdot n_{C_5H_8O_4,\mathrm{i}}$	$\epsilon_{2,1} = X_{C_5H_8O_4} \cdot n_{C_5H_8O_4,\mathrm{i}}$	$\epsilon_{3,1f,i} = X_{C_5H_8O_4,f,i} \cdot \dot{n}_{C_5H_8O_4,\mathrm{f},(5-1)}$
	$\epsilon^*_{1,1} = \frac{\epsilon_1}{t}$	$\epsilon^*_{2,1} = \frac{\epsilon_{2,1}}{t}$	$\epsilon_{3,1s,i} = X_{C_5H_8O_4,s,i} \cdot \dot{n}_{C_5H_8O_4,\mathrm{S},(5-1)}$
$\boldsymbol{\epsilon_2}$	$\epsilon_{1,2} = \mathrm{X_{SO4,S}} \cdot \dot{\mathrm{n}}_{\mathrm{SO4,3}}$	$\epsilon_{2,2} = \frac{5}{2} \times \epsilon_1$	$\epsilon_{3,2,i} = \frac{5}{2} \times (\epsilon_{1,f} + \epsilon_{1,s})$
$\boldsymbol{\epsilon_3}$	$\epsilon_{1,3} = \mathrm{X_{Fe^{2+},S}} \cdot \dot{\mathrm{n}}_{\mathrm{Fe^{2+},3}}$	$\epsilon_{2,3} = \mathrm{X_{Fe^{2+},S}} \cdot \dot{\mathrm{n}}_{\mathrm{Fe^{2+},3}}$	$\epsilon_{3,3,\mathrm{i}} = \mathrm{X_{Fe^{2+},S}} \cdot \dot{\mathrm{n}}_{\mathrm{Fe^{2+},3}}$
$\boldsymbol{\epsilon_4}$	$\epsilon_{1,4} = \mathrm{X_{H^+}} \cdot \dot{\mathrm{n}}_{\mathrm{H^+,3}}$	$\epsilon_{2,4} = \mathrm{X_{H^+}} \cdot \dot{\mathrm{n}}_{\mathrm{H^+,3}}$	$\epsilon_{3,4,\mathrm{i}} = \mathrm{X_{H^+}} \cdot \dot{\mathrm{n}}_{\mathrm{H^+,3}}$

Using these extents of reactions, mole balances were performed on each species across the various reactors. In all reactions below, $\dot{n}_{n,m}$ represents the molar flow rate of species n, in stream m (kmol/hr). Similarly, $\epsilon_{p,o}$, represents the extent of reaction o, in process p (kmol/hr) as described in Table 4.1.

In Process 1, the mole balances across the hydrolysis reactor was presented by Equation (4.8), and the mole balance across the sulfate-reducing bioreactor can be represented as:

$$\begin{bmatrix} \dot{n}_{H_2O,4} \\ \dot{n}_{SO_4,4} \\ \dot{n}_{Fe^{2+},4} \\ \dot{n}_{H^+,4} \\ \dot{n}_{C_5H_{10}O_5,4} \\ \dot{n}_{H_2S,4} \\ \dot{n}_{FeS,4} \\ \dot{n}_{CH_2O_3,4} \end{bmatrix} = \begin{bmatrix} \dot{n}_{H_2O,3} \\ \dot{n}_{SO_4,3} \\ \dot{n}_{Fe^{2+},3} \\ \dot{n}_{H^+,3} \\ \dot{n}_{C_5H_{10}O_5,3} \\ \dot{n}_{H_2S,3} \\ \dot{n}_{FeS,3} \\ \dot{n}_{CH_2O_3,3} \end{bmatrix} + \begin{bmatrix} 0 & 0 & 0 \\ -1 & 0 & 0 \\ 0 & -1 & 0 \\ 0 & 0 & -1 \\ -\frac{2}{5} & 0 & 0 \\ 1 & -1 & 0 \\ 0 & 1 & 0 \\ 2 & 0 & 0 \end{bmatrix} \times \begin{bmatrix} \epsilon_{1,2} \\ \epsilon_{1,3} \\ \epsilon_{1,4} \end{bmatrix} \tag{4.16}$$

In Process 2 the mole balance across the combined hydrolysis/DSR can be represented by Equation (4.17).

$$\begin{bmatrix} \dot{n}_{H_2O,3} \\ \dot{n}_{SO_4,3} \\ \dot{n}_{C_5H_{10}O_5,3} \\ \dot{n}_{H_2S,3} \\ \dot{n}_{CH_2O_3,3} \\ \dot{n}_{Fe^{2+},3} \\ \dot{n}_{FeS,3} \\ \dot{n}_{H^+,3} \end{bmatrix} = \begin{bmatrix} \dot{n}_{H_2O,2} \\ \dot{n}_{SO_4,2} \\ \dot{n}_{C_5H_{10}O_5,2} \\ \dot{n}_{H_2S,2} \\ \dot{n}_{CH_2O_3,2} \\ \dot{n}_{Fe^{2+},2} \\ \dot{n}_{FeS,2} \\ \dot{n}_{H^+,2} \end{bmatrix} + \begin{bmatrix} -1 & 0 & 0 & 0 \\ 0 & -1 & 0 & 0 \\ 1 & -2/5 & 0 & 0 \\ 0 & 1 & -1 & 0 \\ 0 & 2 & 0 & 0 \\ 0 & 0 & -1 & 0 \\ 0 & 0 & 1 & 0 \\ 0 & 0 & 0 & -1 \end{bmatrix} \times \begin{bmatrix} \epsilon^*_{2,1} \\ \epsilon_{2,2} \\ \epsilon_{2,3} \\ \epsilon_{2,4} \end{bmatrix} \quad (4.17)$$

In Process 3, the mole balance across each sequential reactor (i) for the grass can be represented by Equation (4.18)

$$\begin{bmatrix} \dot{n}_{C_5H_8O_4,f,G(6-i)} \\ \dot{n}_{C_5H_8O_4,s,G(6-i)} \end{bmatrix} = \begin{bmatrix} \dot{n}_{C_5H_8O_4,f,G(5-i)} \\ \dot{n}_{C_5H_8O_4,s,G(5-i)} \end{bmatrix} + \begin{bmatrix} -1 & 0 \\ 0 & -1 \end{bmatrix} \times \begin{bmatrix} \epsilon_{1,f,(5-i)} \\ \epsilon_{1,s,(5-i)} \end{bmatrix} \quad (4.18)$$

Where $\dot{n}_{C_5H_8O_4,f,G(5-i)}$ and $\dot{n}_{C_5H_8O_4,f,G(6-i)}$ represent the molar flow rates of fast reacting xylan in the grass stream entering and exiting reactor i respectively (kmol/hr), and $\dot{n}_{C_5H_8O_4,s,G(5-i)}$ and $\dot{n}_{C_5H_8O_4,s,G(6-i)}$ represent the molar flow rates of slow reacting xylan in the grass stream entering and exiting reactor i respectively (kmol/hr).

The mole balance for the liquid species in Process 3 can be represented by Equation (4.19)

$$\begin{bmatrix} \dot{n}_{H_2O,W(i+1)} \\ \dot{n}_{SO_4,W(i+1)} \\ \dot{n}_{C_5H_{10}O_5,W(i+1)} \\ \dot{n}_{H_2S,W(i+1)} \\ \dot{n}_{CH_2O_3,W(i+1)} \\ \dot{n}_{Fe^{2+},W(i+1)} \\ \dot{n}_{FeS,W(i+1)} \\ \dot{n}_{H^+,W(i+1)} \end{bmatrix} = \begin{bmatrix} \dot{n}_{H_2O,Wi} \\ \dot{n}_{SO_4,Wi} \\ \dot{n}_{C_5H_{10}O_5,Wi} \\ \dot{n}_{H_2S,Wi} \\ \dot{n}_{CH_2O_3,Wi} \\ \dot{n}_{Fe^{2+},Wi} \\ \dot{n}_{FeS,Wi} \\ \dot{n}_{H^+,Wi} \end{bmatrix} + \begin{bmatrix} -1 & -1 & 0 & 0 & 0 \\ 0 & 0 & -1 & 0 & 0 \\ 1 & 1 & -2/5 & 0 & 0 \\ 0 & 0 & 1 & -1 & 0 \\ 0 & 0 & 2 & 0 & 0 \\ 0 & 0 & 0 & -1 & 0 \\ 0 & 0 & 0 & 1 & 0 \\ 0 & 0 & 0 & 0 & -1 \end{bmatrix} \times \begin{bmatrix} \epsilon_{3,1f,i} \\ \epsilon_{3,1s,i} \\ \epsilon_{3,2,i} \\ \epsilon_{3,3,i} \\ \epsilon_{3,4,i} \end{bmatrix} \quad (4.19)$$

Where $\dot{n}_{n,Wi}$ and $\dot{n}_{n,W(i+1)}$ represent the molar flow rate of liquid phase species n entering and exiting reactor i respectively (kmol/hr).

Although xylose is included in the balances above for Process 2 and 3, the extent of DSR is defined by the extent of hydrolysis (Equation 4.15) and DSR proceeds at a faster rate. The concentration of xylose will therefore always be zero.

4.3.2 Estimating reactor volumes

All reactor volumes were estimated using rates of reactions and reactor design equations. The rate of hydrolysis was used to determine the reactor volumes for Process 2 and 3 since this is the rate-limiting reaction. For Process 1 the rate of hydrolysis was used for estimating the volume of the hydrolysis reactor, while the rate of DSR was used to estimate the volume of the sulfate-reducing bioreactor.

The rate of DSR is zero-order at specific temperatures (Equation 4.20). Assuming that the DSR reactor behaves as a CSTR the volume could be estimated according to Equation (4.21) (Fogler, 2006)

$$r_{SO_4} = k \tag{4.20}$$

$$V = \frac{\dot{n}_{SO_4} X_{SO4}}{-r_{SO4}} \tag{4.21}$$

where r_{SO_4} is the rate of sulfate reduction (kmol/hr.m^3), and V is the volume of the sulfate reduction reactor in Process 1 (m^3). Initially, the rate of sulfate reduction was taken from (Moosa et al., 2005) to be 9.22 x 10^{-4} mol/m^3.hr.

The total batch time required for the desired hydrolysis of xylan in Process 1 and 2 were calculated through integration and manipulation of Equation (4.13). In order to find an analytical solution to this, it was assumed that the contribution of the slow reacting fraction to the rate of hydrolysis was negligible and could be ignored. This assumption was verified at the desired operating conditions. The final expression used to estimate the batch time for Process 1 and 2 are presented in Equation (4.22)

$$t = \frac{ln\left(\frac{X_{C_5H_8O_4} + C_{C_5H_8O_4 s,0} - 1}{C_{C_5H_8O_4 f,0}}\right)}{-k_f} \tag{4.22}$$

Where $C_{C_5H_8O_4 s,0}$ and $C_{C_5H_8O_4 f,0}$ are the initial concentration of fast reacting and slow reacting fractions of xylan (wt%). Kinetic parameter k_f has Arrhenius-type temperature dependence and can be determined by Equation (4.15). Kinetic parameters were taken from Esteghlalian *et al.* (1997) as summarized in Table A2 in the supplementary notes (Appendix A).

An overall grass mass balance was performed to determine the required mass of grass. This was based on the assumption that the rate of grass hydrolysis is constant over time and the stoichiometry of Equation (4.1) and (4.2) is valid. Although the grass is fed into the system in batches, the assumption that the rate of grass hydrolysis is constant over time can be used to calculate an equivalent flow rate of grass required ($\dot{M}_{grass}$). The conversion of xylan to xylose was taken to be 73% which is 95% of the fast reacting fraction of xylose, as determined by Estghlalian *et al.* (1997). The required equivalent flow rate of grass, $\dot{M}_{grass}$ (kg/hr) can thus be calculated according to:

$$\dot{M}_{grass} = \frac{\dot{n}_{SO_4,1} \times {}^{2}/_{5} \times MW_{C_5H_8O_4}}{wt\%\ xylan\ in\ grass} \times 0.73 \tag{4.23}$$

Where $MW_{C_5H_8O_4}$ is the molecular weight of xylan, ${}^{2}/_{5}$ represents the stoichiometrically required amount of xylan for each sulfate mole and the wt% of xylan was taken to be 28.5%.

Using the average flow rate of grass, the volume of the hydrolysis reactor required, $V_{hydrolysis}$ (m^3), can be calculated according to:

$$V_{hydrolysis} = \frac{\dot{M}_{grass} \times t}{\theta \times \rho_{sludge}} \tag{4.24}$$

Where θ is the solid loading of the grass in the hydrolysis reactor (% wt/wt) and ρ_{sludge} is the density of the sludge (kg/m^3).

The volume of Process 2 was also estimated using Equations (4.23) and (4.24).

All reactors in Process 3 were assumed to behave as CSTR's and thus the volume of reactor i (V_i) can be modeled using the CSTR design equation

$$V_i = \frac{\dot{n}_{C_5H_8O_4,f,G(5-i)} \cdot X_{C_5H_8O_4,f,(5-i)}}{-k_f \cdot C_{C_5H_8O_4,f,G(5-i)} \cdot (1 - X_{C_5H_8O_4,f,G(5-i)})} \tag{4.25}$$

Making $X_{C_5H_8O_4,f,G(5-i)}$ the subject of the formula yields

$$X_{C_5H_8O_4,f,i} = \frac{-k_f \cdot C_{C_5H_8O_4,f,G(5-i)} \cdot V_i}{\dot{n}_{SO_4,f,G(5-i)} - k \cdot C_{C_5H_8O_4,f,G(5-i)} \cdot V_i} \tag{4.26}$$

Similarly, for the slow fraction

$$X_{C_5H_8O_4,s,i} = \frac{-k_s \cdot C_{C_5H_8O_4,s,G(5-i)} \cdot V_i}{\dot{n}_{SO_4,s,G(5-i)} - i \cdot C_{C_5H_8O_4,s,G(5-i)} \cdot V_i} \quad (4.27)$$

Where kinetic parameters, k_f, and k_s can be calculated using Equation (4.15) using kinetic parameters taken from Esteghlalian *et al.* (1997) as summarized in Table A2 (Appendix A). The overall conversion of the xylan to xylose can be calculated according to

$$X_{C_5H_8O_4,tot} = \frac{\dot{n}_{SO_4,G1} - \dot{n}_{SO_4,G5}}{\dot{n}_{SO_4,G1}} \quad (4.28)$$

where $X_{C_5H_8O_4,tot}$ is the total conversion of xylan to xylose (%) across the entire process. The overall conversion of sulfate was set to a desired 80%, the volume of the reactor was solved iteratively so as to achieve this desired overall conversion.

4.3.3 General flowsheet calculations

General flowsheet calculations were necessary to solve the flowsheet mass balance. These include the introduction tear stream to calculate the flow rates of species in recycled streams in Process 1 and 2. Tear streams were solved by minimizing the sum of the squared difference between the teared stream and the actual stream.

In order to make a meaningful comparison between the different process configurations, the same operating conditions were used as far as possible. However, some conditions were not applicable to certain models. The operating temperature was taken to be 95°C in Process 1 and 35°C in Process 2 and 3. A summary of the main process parameters is presented in Table A3 in the supplementary notes (Appendix A).

4.4. Results

It is predicted that the total volume required will be 118, 615 000, and 728 000 m^3 for Process 1, 2 and 3 respectively. The total predicted volumes for Process 2 and 3 are orders of magnitude larger than Process 1 due to the slow rate of xylan hydrolysis at low temperatures. The large volumes estimated for Process 2 and 3 make them infeasible at the operating conditions investigated.

The concentration of SO_4, Fe^{2+}, and xylose in the final stream was also determined and are found to be 1.0 g/L and 0.06 g/L for SO_4 and Fe^{2+} respectively. The exit concentration of xylose

in Process 1 was found to be 0.3 g/L and 0.0 g/L for Process 2 and 3. There is a strong agreement between all these numbers as this was a design parameter.

Sensitivity analyses were performed in which different kinetic data sets were used, to determine their effect on the model. This was performed for both the rate of hydrolysis and DSR.

A sensitivity analysis was performed on the effect of operating temperature on the predicted volume of the hydrolysis reactor in Process 1. This was not done for Process 2 or 3 as the presence of SRB prevents operation at temperatures >35°C (Sánchez-Andrea et al., 2014).

4.4.1 Hydrolysis sensitivity analysis

The hydrolysis sensitivity analysis was conducted using different kinetic data sourced from the literature, to calculate the volume of the hydrolysis reactor. A summary of the kinetic parameters used, and its source is presented in Table A2 in the supplementary notes (Appendix A).

Some kinetic studies reported different fractions of fast and slow reacting xylan (Esteghlalian et al., 1997; Lavarack et al., 2002; Maloney et al., 1985; Nee and Yee, 1976) while others reported that all xylan reacts at the same rate (Aguilar et al., 2002; Kim et al., 2013; Yat et al., 2008). The conversion of the slow reacting fraction of xylan is severely rate-limiting, and as such, it is desired to only hydrolyze the fast reacting fraction. In order to account for this, there will be a different xylan conversion in each kinetic data set which is set to 95% conversion of the fast reacting fraction. The average flow rate of grass, $\dot{M}_{grass^*}$ (kg/hr) was recalculated to account for this.

For ease of comparison, the required volumes for each process have been normalized by dividing by the volume predicted by the model using kinetic data as determined by Nee and Yee (1976). These base volumes were chosen since the model predicted the smallest volumes for both Process 2 and 3. The results are presented in Table 4.2.

Table 4.2: Estimated relative total reactor volumes* of the three processes using hydrolysis rates reported by different studies.

Source	Process 1 m^3	Process 2 m^3	Process 3 m^3
(Esteghlalian et al., 1997)	0.70	2 936	716
(Yat et al., 2008)	106	3 034	17 296
(Maloney et al., 1985)	0.87	118	113
(Nee and Yee, 1976)	1.00	1.00	1.00
(Aguilar et al., 2002)	0.70	6.34	6.46
(Kim et al., 2013)	4.78	1 186	120
(Lavarack et al., 2002)	1.99	64	37

*Volumes are normalized relative to smallest volume predicted *i.e.* volumes predicted using data from Nee and Yee (1976)

As shown in Table 4.2 there is a large variation in the total volumes predicted using different kinetic data sets. Although there is agreement between certain kinetic models there are also large discrepancies between others. For example, the total volume predicted for Process 3 is ≈ 17 000 times larger using the kinetics determined by Yat *et al.* (2008) compared to the kinetics determined by Nee and Yee (1976). This large variation highlights the importance for kinetic parameters to be established experimentally for accurate modeling of the process. Kinetics of hydrolysis was identified as an area which needs to be investigated experimentally.

4.4.2 Sulfate-reducing kinetics sensitivity analysis

The sensitivity of the predicted volume of the SRB reactor in Process 1 (V1) to the rate of DSR was determined through a sensitivity analysis. The rate of DSR by SRB is known to vary between 1.03×10^{-5} and 1.26×10^{-2} mol/m^3.hr (Sánchez-Andrea et al., 2014). A sensitivity analysis was thus performed on the volume of the SRB reactor in Process 1 for DSR rates ranging between 1×10^{-5} and 1×10^{-2} mol/m^3.hr. A summary of the results is presented in Figure 4.4.

It was found that the model is highly sensitive to changes in the rate of sulfate reduction (Figure 4.4). The rate of DSR extends over three orders of magnitude, and similarly the predicted volume extending over three orders of magnitude. This highlights the necessity to determine the rate of DSR under the conditions under which the design will operate in order to accurately design the sulfate-reducing bioreactor.

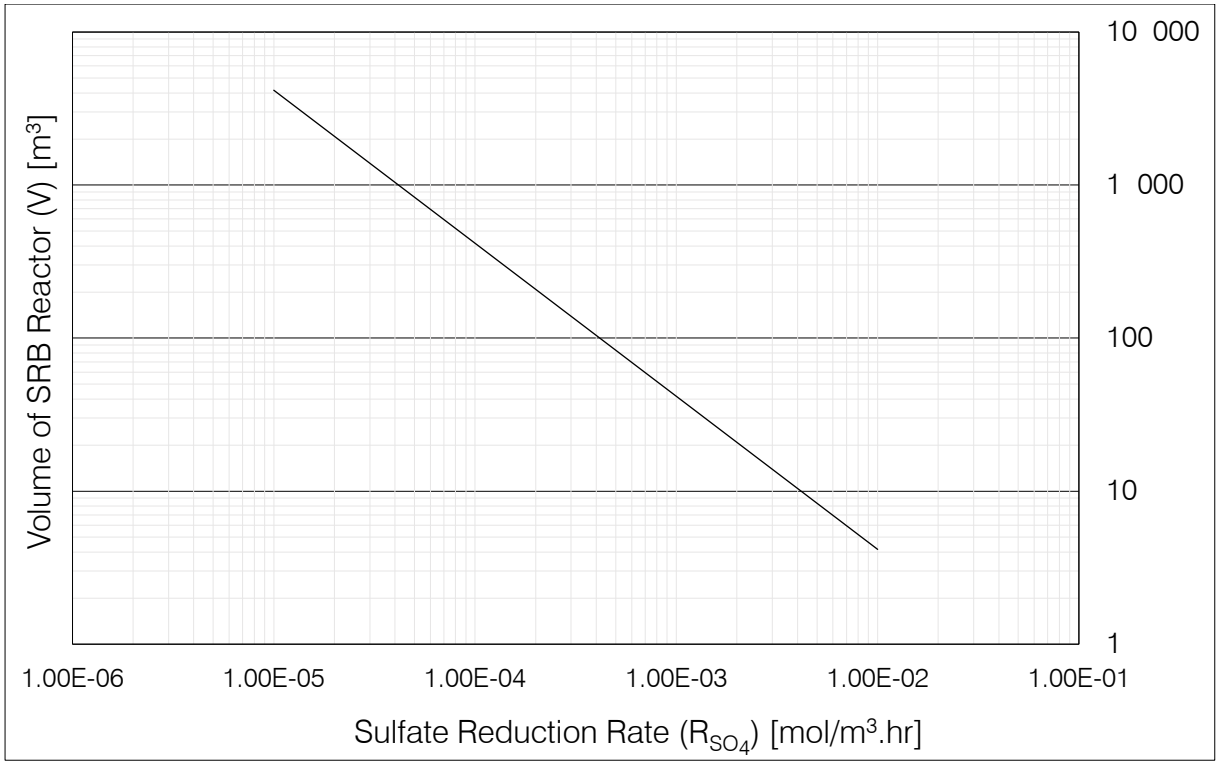

Figure 4.4: Results of sensitivity analysis of the effect of the rate of sulfate reduction on the volume of SRB reactor in Process 1

4.4.3 Operating temperature of hydrolysis reactor sensitivity analysis

A sensitivity analysis was performed on the effect of the operating temperature on the volume of the hydrolysis reactor in Process 1. Temperatures were varied between 10 – 100°C. This was done for all kinetic data sets that were investigated. The results are presented in Figure 4.5.

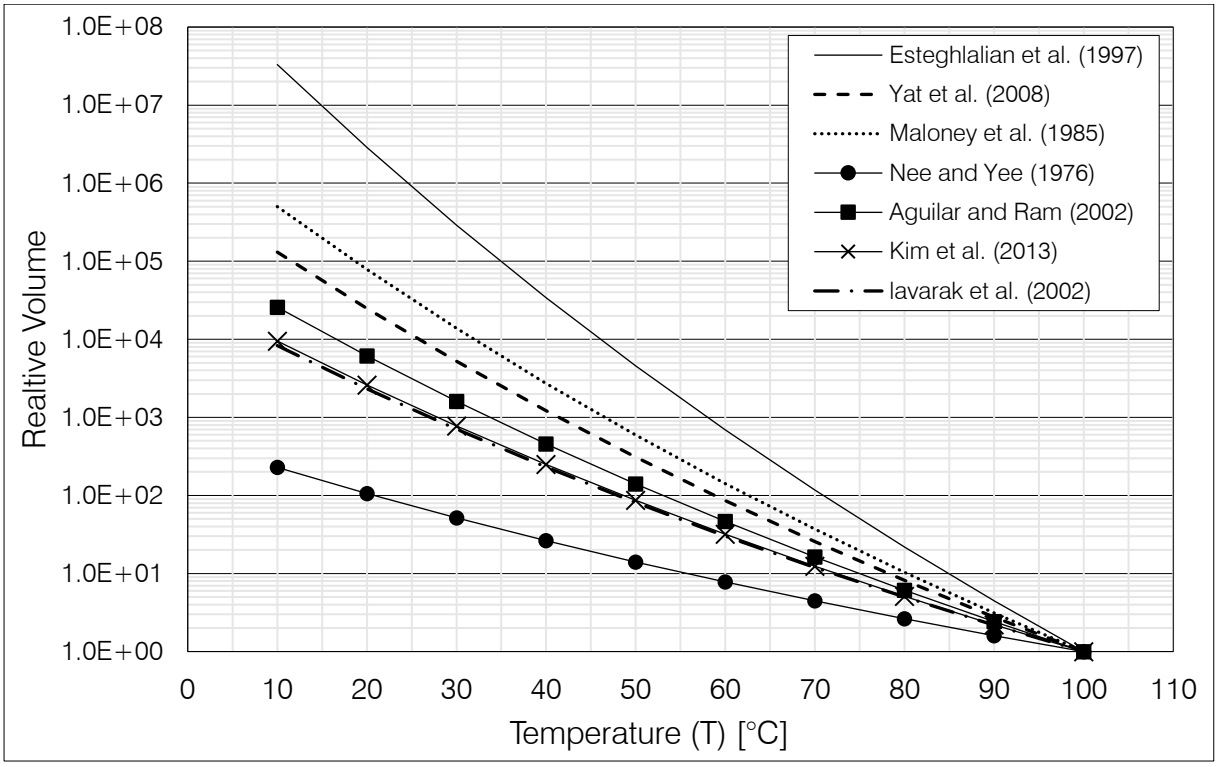

Figure 4.5: Temperature dependence of the predicted normalized volume of the hydrolysis reactor for different kinetic models

The volume of the hydrolysis reactor is highly dependent on the temperature (Figure 4.5). This motivates further investigation into the operation of the hydrolysis reactor at high temperatures. This investigation should include a techno-economic evaluation of different operating temperatures so as to determine the most economical operating temperature. A detailed energy balance and the possibility of heating the stream entering the reactor by means of a heat exchanger between the streams exiting and entering the reactor should be included.

It must be also noted that the calculated temperature dependence using different sets of kinetic data gave different behavior. When using the kinetic data determined by Esteghlalian *et al.* (1997) the volume of reactor at 10°C was calculated as 1×10^8 times larger than the volume at 100°C, whereas using kinetic data determined by Nee and Yee (1976) gave the volume of the reactor at 10°C as only 100 times larger than the volume of the reactor at 100°C. This once again highlights the importance of determining kinetic data for the rate of hydrolysis for the specific conditions at which the process might operate.

4.5. Conclusions

The results from the model show that process one is more feasible commercially as the predicted required volume is orders of magnitude smaller than that for Process 2 or 3. However, more detailed economic evaluations, in which the operating costs are included and other parameters are varied, should be performed to more accurately determine the feasibility of this process. This process entails two separate reactors, one for hydrolysis of xylan which is operated at elevated temperatures and the second reactor for the removal of sulfate through DSR. The model was found to be highly sensitive to different reaction kinetic parameters. This highlights the need to experimentally determine these parameters under the relevant operating conditions.

The volume of the hydrolysis reactor in Process 1 was found to be highly sensitive to the operating temperature with the predicted volume increasing by as much as 1×10^8 times when the temperature was decreased from 100°C to 10°C. This motivates the operation of this reactor at higher temperatures, although a full energy balance and techno-economic evaluation should be performed so as to evaluate the most economically viable operating temperature in terms of both capital and operating costs.

4.6. Acknowledgments

The support of the Global Change and Sustainability Research Institute (GCSRI), the National Research Foundation (NRF), and the University of Witwatersrand towards this research is hereby acknowledged. Opinions expressed and conclusions arrived at, are those of the author and are not necessarily to be attributed to the GCSRI, NRF or the University of the Witwatersrand.

4.7. References

Aguilar, R., Ramirez, J.A., Garrote, G., Vazquez, M., 2002. Kinetic study of the acid hydrolysis of sugar cane bagasse. J. Food Eng. 55, 309–318.

Béchard, G., Yamazaki, H., Gould, W.D., Bédard, P., 1994. Use of Cellulosic Substrates for the Microbial Treatment of Acid Mine Drainage. J. Environ. Qual. 23, 111–116. doi:10.2134/jeq1994.00472425002300010017x

Chang, V.S., Nagwani, M., Kim, C.H., Holtzapple, M.T., 2001. Oxidative lime pretreatment of high-lignin biomass: poplar wood and newspaper. Appl. Biochem. Biotechnol. 94, 1–28. doi:10.1385/ABAB:94:1:01

Chockalingam, E., Subramanian, S., 2006. Studies on removal of metal ions and sulphate reduction using rice husk and Desulfotomaculum nigrificans with reference to remediation of acid mine drainage. Chemosphere 62, 699–708. doi:10.1016/j.chemosphere.2005.05.013

Esteghlalian, A., Hashimoto, A.G., Fenske, J.J., Penner, M.H., 1997. Modeling and optimization of the dilute-sulfuric-acid pretreatment of corn stover, poplar and switchgrass. Bioresour. Technol. 59, 129–136. doi:10.1016/S0960-8524(97)81606-9

Greben, H., Sigama, J., Burke, L., 2009. Cellulose fermentation products as an energy source for biological sulphate reduction of acid mine drainage type wastewaters, Analysis.

Johnson, D.B., Hallberg, K.B., 2005a. Acid mine drainage remediation options: A review. Sci. Total Environ. 338, 3–14. doi:10.1016/j.scitotenv.2004.09.002

Kim, Y., Kreke, T., Ladisch, M.R., 2013. Reaction Mechanisms and Kinetics of Xylo-Oligosaccharide Hydrolysis by Dicarboxylic Acids. Am. Inst. Chem. Eng. J. 59. doi:10.1002/aic

Kobayashi, T., Sakai, Y., 1956. Bulletin of the Agricultural Chemical Society of Japan Hydrolysis Rate of Pentosan of Hardwood in Dilute Sulfuric Acid in Dilute Sulfuric Acid. Bull. Agric. Soc. Japan 20, 1–7. doi:10.1080/03758397.1956.10857296

Lavarack, B.P., Gri, G.J., Rodman, D., 2002. The acid hydrolysis of sugarcane bagasse hemicellulose to produce xylose , arabinose , glucose and other products. Biomass and Bioenergy 23, 367–380.

Lefticariu, L., Walters, E.R., Pugh, C.W., Bender, K.S., 2015. Sulfate reducing bioreactor dependence on organic substrates for remediation of coal-generated acid mine drainage: Field experiments. Appl. Geochemistry 63, 70–82. doi:10.1016/j.apgeochem.2015.08.002

Magowo, E., Rumbold, K., Sheridan, C., 2015. The Utilization of Cellulosic Biomass in treating AMD and the Subsequent Generation of Fermentable Sugars, in: 10th International Conference on Acid Rock Drainage and IMWA Anual Conference. pp. 1–12.

Maloney, M.T., Chapman, T.W., Baker, a J., 1985. Dilute acid hydrolysis of paper birch: kinetics studies of xylan and acetyl-group hydrolysis. Biotechnol. Bioeng. 27, 355–361. doi:10.1002/bit.260270321

McCarthy, T.S., 2011. The impact of acid mine drainage in South Africa. S. Afr. J. Sci. 107, 1–7. doi:10.4102/sajs.v107i5/6.712

Metcalf, E., Tchobanoglous, G., Stensel, H.D., Tsuchihashi, R., Franklin, L., 2013. Wastewater Engineering: Treatment and Resource Recovery, 5th ed. Mcgraw-Hill, New York, Ny, USA.

Moosa, S., Nemati, M., Harrison, S.T.L., 2005. A kinetic study on anaerobic reduction of sulphate , part II : incorporation of temperature effects in the kinetic model. Chem. Eng. Sci. 60, 3517–3524. doi:10.1016/j.ces.2004.11.036

Nee, C.I., Yee, W.F., 1976. Hydrolysis of Pentosans in Bagasse Pith. J. Appl. Chem. Biotechnol. 26, 283–

287.

Ramla, B., Sheridan, C., 2015. The potential utilisation of indigenous South African grasses for acid mine drainage remediation. Water SA 41, 247–252. doi:10.4314/wsa.v41i2.10

Sánchez-Andrea, I., Sanz, J.L., Bijmans, M.F.M., Stams, A.J.M., 2014. Sulfate reduction at low pH to remediate acid mine drainage. J. Hazard. Mater. 269, 98–109. doi:10.1016/j.jhazmat.2013.12.032

Taylor, J., Pape, S., Murphy, N., 2005. A Summary of Passive and Active Treatment Technologies for Acid and Metalliferous Drainage (AMD). Proc. 5th Aust. Work. Acid Drain.

Wyman, Charles E, Decker, S.R., Himmel, M.E., Brady, J.W., Skopec, C.E., 2005. Hydrolysis of Cellulose and Hemicellulose, in: Dumitriu, S. (Ed.), Polysaccharides: Structural Diversity and Functional Versitility. CRC Press, pp. 1023–1062. doi:10.1201/9781420030822.ch43

Yat, S.C., Berger, A., Shonnard, D.R., 2008. Kinetic characterization for dilute sulfuric acid hydrolysis of timber varieties and switchgrass. Bioresour. Technol. 99, 3855–3863. doi:10.1016/j.biortech.2007.06.046

Zagury, G.J., Neculita, C., 2007. Passive Treatment of Acid Mine Drainage in Bioreactors : Short Review , Applications , and Research Needs, in: 60th Canadian Geotechnical Conference & 8th Joint CGS/IAH-CNC Groundwater Conference. Ottow, pp. 1439–1446.

Chapter 5: Modeling of Low Temperature Dilute Sulfuric Acid Pre-treatment of South African Grass

(Published in Bioresource Technology Reports, 2018) This chapter experimentally investigated and determined the kinetics of dilute sulfuric acid hydrolysis of indigenous South African grass at low temperatures (<90°C). This addresses objective b.

Burman, N.W., Sheridan, C., van Dyk, L., Harding, K.G., 2018c. Modeling of low temperature dilute sulfuric acid pre-treatment of South African grass. Bioresource Technology Reports. 4, 21–28. doi:10.1016/j.biteb.2018.08.014

Abstract: Dilute acid hydrolysis is an effective method of pre-treatment of lignocellulosic biomass. Although there are many studies modeling this pre-treatment at high temperature (120 – 210°C), no studies were found modeling this reaction at low temperature. In this study, a long grass species was pre-treated with dilute sulfuric acid (pH 1, 2 & 3) at low temperatures (35°C, 65°C, 90°C). The hydrolysis of xylan was found to obey a bi-phasic model in which there are two fractions of xylan, with significantly different hydrolysis rates. The rate of hydrolysis of the fast reacting fraction was found to display Arrhenius type temperature dependence (Ea = 155.06 kJ/mol, A_0 = 1.65×10^{19}/min), which agrees with findings of similar studies at higher temperatures. A negligible rate of hydrolysis was determined for the slow fraction which differs from previous studies. The proportion of the slow reacting fraction was found to be 50%, which is lower than previously determined (55 – 100%).

Keywords: Dilute Acid Hydrolysis, Pre-treatment, Lignocellulose, Bioethanol, Kinetics

5.1. Introduction

Currently, there has been a drive to produce biofuel and other biochemicals from biomass as an alternative to fossil fuels, which has a finite supply and contributes to global warming (Uihlein and Schebek, 2009). Enzymatic hydrolysis of the cellulose contained in biomass produces monomeric glucose sugars, which can undergo a range of biochemical reactions (fermentation, dehydration, oxidation, *etc*.) to form various biochemicals such as bioethanol, succinic acid, hydroxymethylfurfural (HMF) and furfural (Menon and Rao, 2012). Food crops such as sugar cane and corn have successfully been used to produce bioethanol on an industrial scale, with 71 billion kilograms produced in 2015 (E4TECH 2015). Although effective, the use of food crops has been found to increase food prices and have a negative impact on food security. Other problems associated with the use of food crops include overall carbon emission, net energy loss, land degradation, and lack of available land (Lange, 2007).

Lignocellulosic biomass such as agricultural waste, forestry residue and energy cops are an abundant and cheap source of cellulosic biomass. A recent study has also identified *Salicornia bigelovii* (halophyte plant) as a suitable feedstock for bioethanol production (Bañuelos et al., 2018). Indigenous South African grass has been identified as a good feedstock for lignocellulosic biochemical production in the Highveld region of South Africa due to a large availability of unused feedstock (Burman et al., 2018a; Westensee et al., 2018).

Lignocellulosic biomass consists of a ligno-hemicellulosic matrix that surrounds cellulose fibrils. The presence of this ligno-hemicellulosic matrix prevents cellulase enzymes from accessing the cellulose fibril. To overcome this, biomass needs to undergo pre-treatment which disrupts the ligno-hemicellulosic matrix making the cellulose accessible to cellulase enzymes (Charles E. Wyman et al., 2005a).

Various pre-treatment methods have been investigated including physical (milling, comminution), physico-chemical (steam explosion, AFEX, wet oxidation), biological (white-rot hydrolysis), and chemical (dilute acid hydrolysis, alkaline, Ionic liquids, organic solvents, ozone) (Taherzadeh and Karimi, 2008). Dilute acid hydrolysis is currently the most favorable pre-treatment method for industrial applications (Alvira et al., 2010; Maurya et al., 2015; Taherzadeh and Karimi, 2007a), with sulfuric acid being the most used type of acid, due to high hydrolysis yields (Mosier et al., 2005b).

Pre-treatment using dilute sulfuric acid hydrolyzes the hemicellulose content of the biomass, leaving the cellulose content largely intact, and easily accessible for enzymatic hydrolysis. The rate of dilute sulfuric acid hydrolysis was found to display Arrhenius type reaction kinetics (Kobayashi and Sakai, 1956). This has been studied by either assuming that the hemicellulose reacts in a mono-phasic fashion in which all hemicellulose reacts at the same rate of reaction, or that the hemicellulose reacts in a bi-phasic fashion in which there are two different fractions of hemicellulose with very different rates of reactions. A summary of the conditions under which rates of reaction have been studied is presented in Table 5.1 for both mono-phasic and bi-phasic models.

Table 5.1: Summary of studies modeling xylose hydrolysis according to first order Arrhenius type kinetics.

Reference	Model type	Substrate	Temperature °C	% acid w/w	Acid	Compounds modelled
(Saeman, 1945)	Mono-phasic	Hardwoods, Softwoods	170 - 190	0.40 - 1.6	Sulfuric acid	Glucose, Xylose, Galactose, Arabinose, Mannose
(Bhandari et al., 1984)	Mono-phasic	Corn Stover	160 - 240	0.49 - 1.5	Sulfuric acid	Glucose, Xylose
(Lavarack et al., 2002)	Mono-phasic	Sugarcane bagasse	80 - 200	0.25 - 8.0	Sulfuric acid, Hydrochloric acid	Xylose, Glucose, Arabinose, Furfural
(Yat et al., 2008)	Mono-phasic	Switchgrass, Hardwoods	160 - 190	0.25 - 1.0	Sulfuric acid	Xylose
(Jin et al., 2011)	Mono-phasic	Corn Stover	90 - 100	1.0 - 3.0	Sulfuric acid	Xylose
(Kim et al., 2013)	Mono-phasic	Xylo-Oligomers	140 - 180	0.30	Maleic acid, Oxilic acid, sulfuric acid	Xylose, Furfural
(Kobayashi and Sakai, 1956)	Bi-phasic	Hardwood	74 - 147	1.0 - 6.0	Sulfuric acid	Xylose
(Nee and Yee, 1976)	Bi-phasic	Sugarcane Bagasse	125 - 165	0.5 - 2	Sulfuric acid	Xylose
(Maloney et al., 1985)	Bi-phasic	Hardwood	100 - 170	0.4 - 1.7	Sulfuric acid	Xylose
(Esteghlalian et al., 1997)	Bi-phasic	Switchgrass, Hardwood Corn Stover	140 - 180	0.6 - 1.2	Sulfuric acid	Xylose
(Aguilar et al., 2002)	Bi-phasic	Sugarcane bagasse	100 - 128	2.0 - 6.0	Sulfuric acid	Xylose, Glucose, Acetic acid, Furfural
(Lavarack et al., 2002)	Bi-phasic	Sugarcane bagasse	80 - 200	0.25 – 8.0	Sulfuric acid, Hydrochloric acid	Xylose, Glucose, Arabinose, Furfural
(Schell et al., 2003)	Bi-phasic	Corn Stover	165 - 195	0.7 - 1.39	Sulfuric acid	Xylose, Furfural, oligomers,
(Rodriguez-Chong et al., 2004)	Bi-phasic	Sugarcane bagasse	100 - 128	2.0 - 6.0	Nitric acid, Sulfuric acid, Hydrochloric acid	Xylose, Glucose, Arabinose, Acetic Acid, Furfural,

As can be seen in Table 5.1 the rate of hydrolysis has been well studied at high temperatures (120 – 210°C) with acid concentrations ranging from 0.25 to 6% wt/wt H_2SO_4 (Aguilar et al., 2002; Esteghlalian et al., 1997; Kim et al., 2013; Lavarack et al., 2002; Maloney et al., 1985; Nee and Yee, 1976; Yat et al., 2008). Typical reaction times are in the range of 0.5 – 90 minutes. Although the rate of reaction is well studied at high temperatures, only two studies have been found for low temperature (< 90°C) hydrolysis {Formatting Citation}.

The benefits of performing hydrolysis at lower temperatures include reduced heating requirements, reduced reactor operating pressures, increased potential for passive heating systems, cheaper material of construction for reactors and potential for implementation of passive heating processes. The benefits of lower operating temperatures could result in reduced operating and capital costs.

The aim of this study is to determine the compositional structure of a mixed sample of *Digitaria eriantha* and *Eragrostis* (indigenous South African Highveld grasses); model the rate of hemicellulose hydrolysis during dilute H_2SO_4 pre-treatment of this biomass; and determine the kinetic parameters for the rate of reaction of the hydrolysis, at temperatures between 35°C and 90°C and pH ranging from 1 – 3.

5.2. Methods and materials

In this work, the structural composition of the biomass was determined, before hydrolysis pre-treatment experiments were carried out. Liquid hydrolysis samples from hydrolysis experiments were analyzed for sugar concentration. A kinetic model was developed to model the hydrolysis of grass over time and predict the rate of hydrolysis over a range of temperatures and pH.

5.2.1 Structural determination of grass

Grass was sourced from a local roadside grass cutter in Gauteng, South Africa and was classified as a mixture of *Digitaria eriantha* and *Eragrostis*. The structural determination of this mixture was determined using the gravimetric method proposed by Li et al., (2004). In this method, the extractive content was determined gravimetrically through Soxhlet extraction using acetone as a solvent. Hemicellulose content was determined gravimetrically through hydrolysis of the hemicellulose portion in NaOH. The combined acid insoluble lignin

(AIL) and ash content was determined through hydrolysis of hemicellulose and cellulose portion in H_2SO_4. Acid soluble lignin (ASL) content was determined using spectrographic methods as described by Sluiter *et al.* (2008). Ash content was determined through proximate analysis on a thermogravimetric analyzer (Perkin Elmer STA 6000) using the method as described by Mani *et al.* (2010). Cellulose and AIL content was determined through closure of mass balance assuming the biomass consists of only extractives, hemicellulose, cellulose, ASL, AIL and ash

5.2.2 Hydrolysis pre-treatment

Pre-treatment experiments were carried out in 3 L constructed glass reaction vessels. These were constructed using glass jars fitted with an airtight lid. A sampling port was included, by fitting PVC tubes through the lid, to take samples and prevent the contamination of the reacting mixture. These reacting vessels were placed inside an orbital shaking incubator which was operated at 100 RPM. The solid loading of the reactor was 10 g/L with a liquid volume of 2.5 L. Duplicate factorial experiments were carried out at pH 1, pH 2 and pH 3 at temperatures of 35°C, 65°C and 90°C. For 65°C and 90°C samples were taken after the first day and then every second day for up to 19 days. For 35°C samples were taken every 4 days. A portion of the sample was used for measuring the pH with the balance stored frozen until the end of the experiment when they were analyzed.

5.2.3 Kinetic model development

The simplest kinetic models assume that hydrolysis occurs straight from polysaccharide substrate to monosaccharide product without the formation of any oligosaccharide intermediates. This is applied to cellulose and hemicellulose individually (Negahdar et al., 2016). The first kinetic model proposed assumed the hydrolysis of hemicellulose occurs via two consecutive pseudo-homogenous first order reactions, first forming xylose and then forming degradation products as presented in Equation (5.1).

$$Xylan \overset{k_1}{\rightarrow} Xylose \overset{k_2}{\rightarrow} Degradation\ products \tag{5.1}$$

where the concentration of hemicellulose, xylose and degradation products can be expressed as:

$$\frac{d[xylan]}{dt} = -k_1[xylan] \quad (5.2)$$

$$\frac{d[xylose]}{dt} = k_1[xylan] - k_2[xylose] \quad (5.3)$$

$$\frac{d[degradation\ products]}{dt} = k_2[xylose] \quad (5.4)$$

The rate constants were found to obey Arrhenius type temperature dependence, as described by Equation (5.5) (Saeman, 1945).

$$k_i = A_{0,i}.Ca^{n_i}.e^{\frac{Ea_i}{R.T}} \quad (5.5)$$

Where $A_{0,i}$ is the pre-exponential factor (/min), Ca is the concentration of acid (wt%), n_i is an empirical exponent, Ea_i is the activation energy (kJ/mol), R is the universal gas constant (8.314x10^{-3} kJ/mol.K), T is the temperature (K)

This model was expanded by Koboyashi and Sakai (1956) to include two different fractions of xylan, which have very different rates of reactions. Both the fast and slow reacting fractions undergo hydrolysis to form xylose in a bi-phasic fashion as shown in Equation (5.6).

$$\underset{(Xylan)}{Hemicellulose} \begin{cases} Fast\ reacting\ xylan \xrightarrow{k_f} \\ Slow\ reacting\ xylan \xrightarrow{k_s} \end{cases} Xylose \xrightarrow{k_2} Degradation\ prod. \quad (5.6)$$

The rate of change of xylan and xylose can now be expressed as

$$\frac{d[xylan]}{dt} = -k_f C_{xylan,f} - k_s C_{xylan,s} \quad (5.7)$$

$$\frac{d[xylose]}{dt} = k_f C_{xylan,f} + k_s C_{xylan,s} - k_2 C_{xylose} \quad (5.8)$$

Where subscripts f and s are used to denote the fast and slow reacting fractions of xylan.

The fraction of fast and slow reacting xylan is typically determined experimentally with the percent of the fast reacting fraction (α) ranging between 55% and 100%, although it is most frequently found to be between 70% – 80% (Negahdar et al., 2016).

The rate constant has been expanded in some studies to account for the neutralizing ability of the biomass. This neutralizing capacity is due to the ion exchange between the cations, associated with the bound and free anions contained in the biomass, and the hydronium ions in the acid solution. This can be represented by the simplified equation (Springer and Harris, 1985)

$$biomass \cdot COO^{-}M^{+} + H^{+} \rightarrow\ biomass \cdot COO^{-}H^{+} + M^{+} \qquad (5.9)$$

It was found that the most, but not all, inorganic cations were exchanged for hydronium ions, and the pH of the acid can be accurately predicted by determining the concentration of cations before and after hydrolysis (Springer and Harris, 1985).

Other studies have accounted for the neutralizing capacity of the biomass and calculated an actual acid concentration, C_a, from the original acid concentration, C, by the equation (Esteghlalian et al., 1997)

$$C_a = C - \%\ solid\ loading\ \times\ NC \qquad (5.10)$$

Where C is the original acid concentration (% wt/wt) and NC is the neutralizing capacity of the biomass (g H_2SO_4 neutralized/gram biomass). This neutralizing capacity is determined experimentally by the addition of biomass to an acid solution.

In the model to be used in this study, it was assumed that the hydrolysis of grass would obey the bi-phasic model as proposed by Kobayashi and Sakai (1956) (Equation 5.6). The concentration of potential xylose units remaining was evaluated by integrating Equation (5.3) to give Equation (5.11).

$$X_r = X_{f,0}e^{-k_f.t} + X_{s,0}e^{-k_s.t} \qquad (5.11)$$

Where X_r is the percentage of equivalent xylose units remaining in the solid residue relative to initial equivalent xylose units in the biomass, $X_{f,0}$, $X_{s,0}$ are the initial percentages of fast reacting and slow reacting fractions, t is the time (min), k_f, k_s are reaction rate constants for the fast and slow reacting fractions of the biomass assumed to have Arrhenius-type temperature dependence as according to Equation (5.5).

Xylan is expressed in terms of equivalent xylose units, so to account for the difference in molecular weights between xylan (132 g/mol) and xylose (150 g/mol). The initial equivalent xylose units (X_0) in the biomass can be calculated according to

$$X_0 = C_{xylan,total} \times solid\ loading \times \frac{150}{132} \quad (5.12)$$

Where $C_{xylan,total}$ is the concentration of xylan in biomass (% wt/wt), and $solid\ loading$ is the solid loading of biomass in the reaction liquid (g/L).

The equivalent xylose units remaining in the solid residue (X_i) can be calculated according to

$$X_i = X_0 - X_t \quad (5.13)$$

Where X_t is the measured xylose concentration (g/L) at time t (min).

The fraction of fast reacting xylose units is assigned a value α such that

$$X_{f,0} = \alpha \quad (5.14)$$

$$X_{s,0} = (1 - \alpha) \quad (5.15)$$

As the fraction of fast reacting and slow reacting xylan is considered to be a physical property of the biomass (Shen and Wyman, 2011), it is assumed that, for a specific biomass, there can only be one value for α for all operating conditions. The fraction of fast reacting biomass was determined through trial and error fitting of the equivalent xylose remaining (X_r) data over time.

The proposed kinetic model (Equation 5.11) was fitted to the data using Scilab's (https://www.scilab.org/) least-square non-linear error minimization function ("lsqnonlin") to optimize the values of k_f and k_s. The values of k_f and k_s were determined for each set of experimental conditions and are presented in the results section.

5.2.4 Determination of kinetic parameters

Once values for k_f and k_s were determined, kinetic parameters (A_0, Ea, n_i) were obtained by linearizing Equation (5.5)

$$ln(k_f) = -\frac{Ea}{R} \cdot \frac{1}{T} + ln(A_0) + n.ln(C_a) \quad (5.16)$$

$ln(k_f)$ can then be plotted against $1/T$ to give a straight line where the gradient is equal to Ea/R and the intercept is given by $ln(A_0) + n.ln(C_a)$. This can be plotted for each different acid concentration tested, each of which would have the same gradient but different intercepts.

This system of linear equations can be solved using the linear regression "\ operator" in Scilab, to give the gradient (Ea/R) and the intercept ($ln(A_0) + nln(C_a)$) of each different acid concentration tested. The intercepts determined can be plotted against $ln(C_a)$ to give another straight line, where the gradient is equal to the empirical exponent, n, and the intercept equal to $ln(A_0)$. Linear regression can once again be performed using Scilab's "\ operator" to determine the values for n and A_0. Values for Ea, A_0, and n are presented in the results section.

5.2.5 Analytical methods

Liquid hydrolysate samples from the hydrolysis pre-treatment experiment were filtered through 0.25 µm filters before being analyzed by high performance liquid chromatography (HPLC). The Agilent Zorbax Carbohydrate Column was used for quantification of xylose, glucose and cellobiose using 75% acetonitrile as the mobile phase at a flow rate of 1.4mL/min at 35°C and a sample injection volume of 20 µL. A Biorad Aminex Fermentation Monitoring column was used for quantification of hydroxymethylfurfural, furfural, glycerol and acetic acid using 0.05M H_2SO_4 at a flow rate of 0.8mL/min at 65°C and a sample injection volume of 20 µL.

As furfural is a degradation product of xylose the equivalent concentration of xylose that would yield the measured concentration of furfural was determined and added to the measured concentration of xylose (X) to give a total concentration of xylose (X_{tot}) according to

$$X_{tot} = X + F \times \frac{150}{96} \tag{5.17}$$

where X_{tot} is the total equivalent concentration of xylose(g/L), X is the measured concentration of xylose (g/L), F is the measured concentration of Furfural (g/L), $150/96$ is included so as to account for the difference in molecular weight between xylose (150 g/mol) and furfural (96 g/mol).

To account for the neutralizing ability of lignocellulosic biomass the pH was monitored throughout the process, and the wt% H_2SO_4 was calculated from the pH. After the effects of the neutralizing ability of the grass had subsided there was only minor variation in the pH. The pH was thus taken to be the average pH over the duration of the experiment.

5.3. Results and discussion

5.3.1 Structural composition of grass

The average composition of the grass (mixed sample of *Digitaria eriantha* and *Eragrostis)* is given in Table 5.2 and compared to the composition of switchgrass found in literature (Lee et al., 2007)

Table 5.2: Experimentally determined composition of a mixed sample of *Digitaria eriantha* and *Eragrostis* compared with switchgrass composition reported in the literature.

	Experimentally Determined		From Literature (Lee et al., 2007)	
	Mean	**SD**	**Mean**	**SD**
Hemicellulose	36.0%	19.7%	28.5%	3.5%
Cellulose	36.6%	18.6%	37.3%	4.4%
Acid Soluble Lignin	1.3%	0.05%	3.5%	0.3%
Acid Insoluble Lignin	24.5%	1.7%	16.2%	0.5
Ash	3.5%	0.59%	5.9%	1.0%
Extractives	1.7%	0.3%	3.1%	0.7%

The structural composition of the grass was found to be comparable to the mean of switchgrass compositions reported in literature (Lee et al., 2007). There was a discrepancy between the hemicellulose content (36.0% determined experimentally *vs*. 28.5% from literature) and acid soluble lignin (24.5% determined experimentally *vs*. 16.2% from literature). All other fractions were found to be within 3% of the values found in literature.

5.3.2 Kinetic model

The remaining xylose determined experimentally and predicted by the model at different temperatures is presented in Figures (5.1) – (5.3). These show the degradation of hemicellulose over time. The error bars represent the standard deviation between data calculated from duplicate experiments.

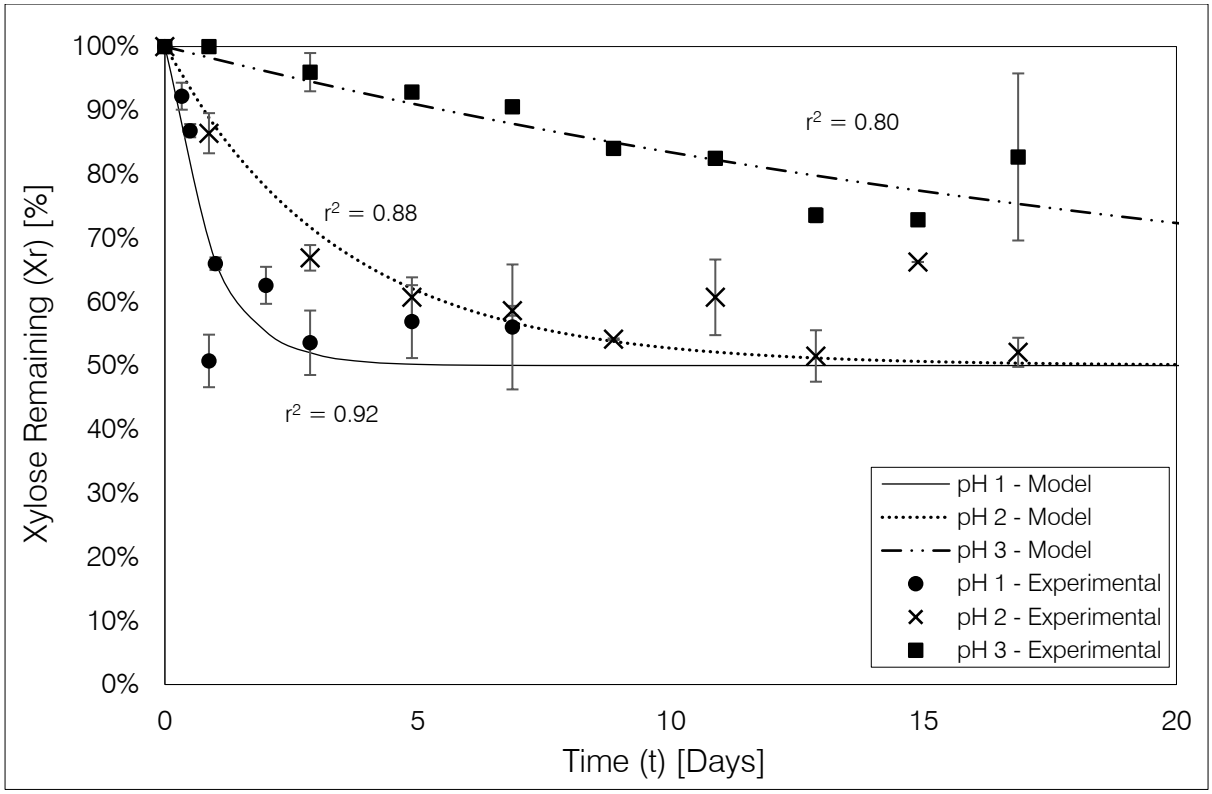

Figure 5.1: Hydrolysis of xylose over time determined experimentally and predicted by the model at T = 90°C

As can be seen in Figure 5.1, at 90°C and pH 1 and 2, the rate of hydrolysis of the xylan is relatively fast up until 50% of the xylan is remaining, after which point the rate of hydrolysis slows considerably. Therefore, it is assumed that the fraction of fast reacting xylan is 50%. Only approximately 30% of the xylan is hydrolyzed at 90°C and pH 3, by the time the experiment was stopped. The model predictions seem to fit experimental data well.

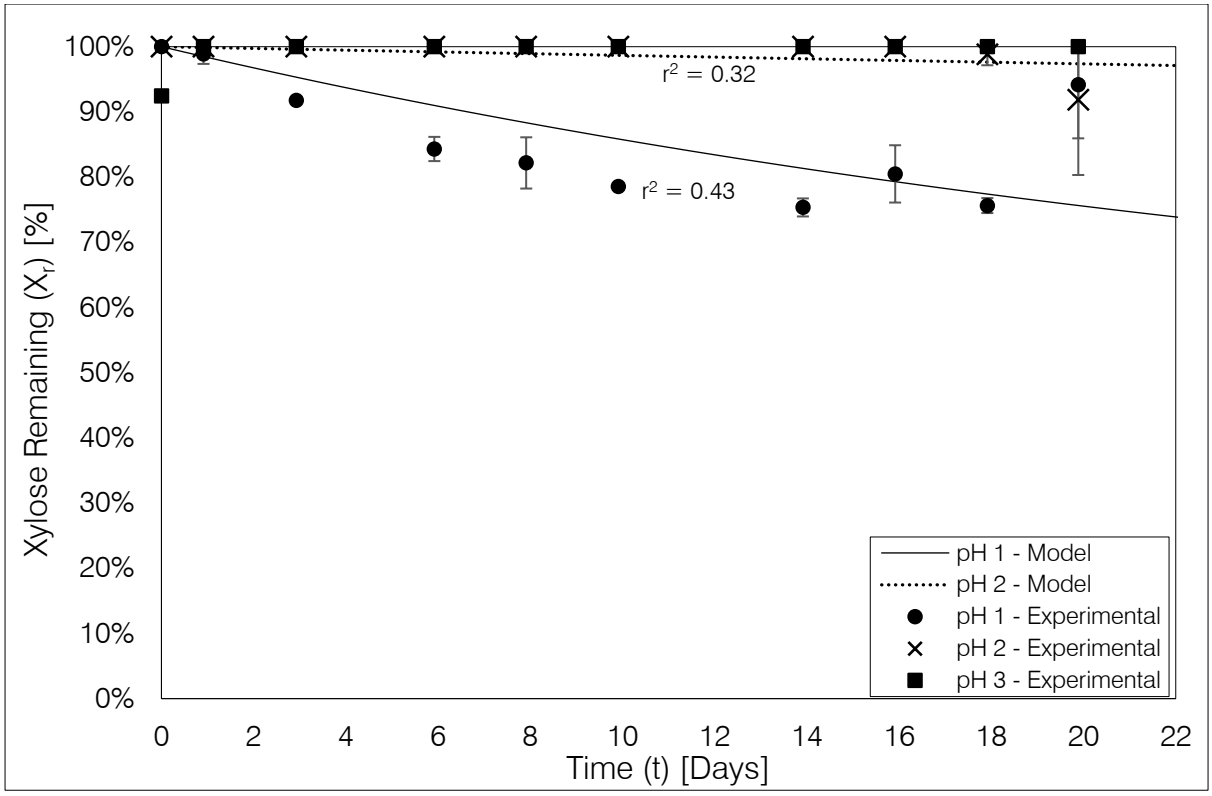

Figure 5.2: Hydrolysis of xylose over time determined experimentally and predicted by the model at T = 65°C

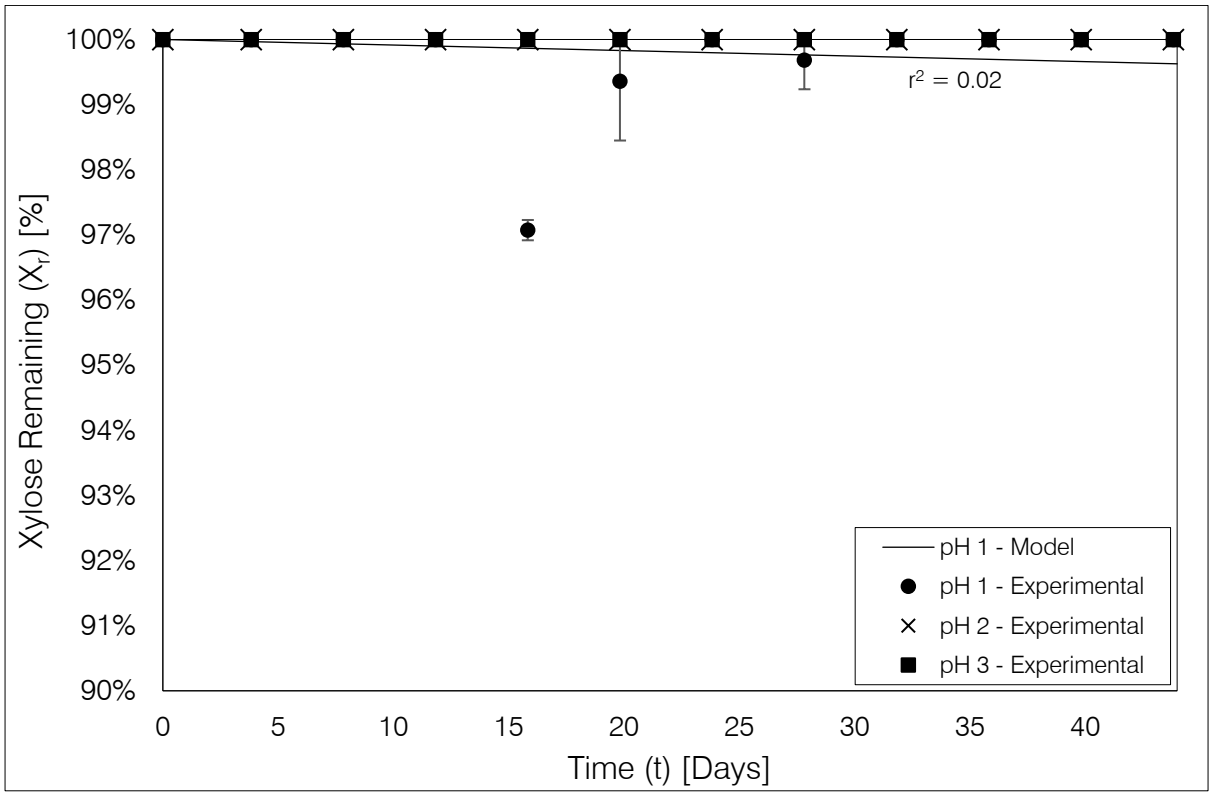

Figure 5.3: Hydrolysis of xylose over time determined experimentally and predicted by the model at T = 35°C

As can be seen in Figure 5.2, at 65°C and pH 1 there is limited hydrolysis of xylan with just less than 25% of the xylan undergoing hydrolysis. At 65°C and pH 2, there is only very limited hydrolysis (~10%). At 65°C and pH 3, there is a negligible amount of hydrolysis observed.

As can be seen in Figure 5.3, at 35°C and pH 1, there is limited hydrolysis of xylan (< 3%). At 35°C and pH 2 and 3 negligible hydrolysis was observed.

Although no hydrolysis was observed at some experimental conditions, there may have been low levels of hydrolysis occurring at these experimental conditions, but low concentrations of xylose (<0.1 g/L) were not detected by the HPLC method used.

The rate constants for k_f and k_s at each experimental condition are presented in Table 5.3.

Table 5.3: Reaction rate constant for the fast reacting and slow reacting fraction at various pH and temperatures (/min)

Temperature (°C)		35°C	65°C	90°C
pH 1	k_f	4.93×10^{-9}	9.72×10^{-7}	3.25×10^{-5}
	k_s	2.89×10^{-18}	nv	nv
pH 2	k_f	nv*	7.84×10^{-8}	8.42×10^{-6}
	k_s	nv	8.59×10^{-18}	nv
pH 3	k_f	nv	nv	1.17×10^{-6}
	k_s	nv	nv	nv

*nv – no value

For some experimental conditions (65°C at pH 2 and pH 3, 35°C at pH 1, pH 2 and pH 3) no rate of reaction was determined for the fast reacting fraction. These are milder experimental conditions, where a slower rate of reaction would be expected.

By comparing the values in for k_f and k_s in Table 5.4, the rate of reaction for the slow reacting fraction was found to be orders of magnitude smaller, and hence negligible, compared to the rate of reaction of the fast reacting fraction. No value was determined for all the rates of reaction of the slow fraction, except for 65°C at pH 2 and 35°C at pH 1. These results are counter-intuitive as it would be expected that a rate of reaction be determined for the following, more severe, experimental conditions of 90°C at pH1 and pH2, and 65°C at pH 1.

As the rate of reaction of the slow reacting fraction, was often found to be negligible, it was decided to evaluate the model assuming that the slow reacting fraction did not react *i.e.* $k_s = 0$ in all cases. The kinetic model was thus modified from Equation (5.11) to:

$$X_r = X_{f,0} e^{-k_f . t} + X_{s,0} \quad (5.18)$$

The values for k_F were once again determined through optimization in Scilab.

The remaining xylose predicted by the modified model was compared to the remaining xylose predicted by the original model. The difference between the two models was found to be negligible in all cases. The rate of reactions determined in the modified model were compared to the rate of reactions determined in the original model and were found to be identical. The rate of reaction of the slow reacting fraction can thus be assumed to be negligible. The hemicellulose can thus be considered to consists of a reactive and an unreactive fraction.

There is a large range of r^2 values found (presented on graphs). There was a good correlation between experimental data and model predictions for all acid concentrations at 90°C. The correlation was found to be 0.80 at pH 3, 0.88 at pH 2 and 0.92 at pH 1. This good correlation between the model and the data indicates an acceptable accuracy of the model.

At 65°C, r^2 values ranged between 0.32 at pH 2 and 0.4 at pH 1, indicating a low correlation between experimental data and model predictions. It must be noted that the correlation for pH 1 at 65°C would be higher (0.80 instead of 0.43) if the last point at 20 days was excluded. If it is assumed that this point is an outlier, then there is an acceptable level of accuracy in the model at pH 1 and 65°C. The level of model accuracy at pH 2 and 65°C is not acceptable. It should be noted that the peaks in the RID signal detected by the HPLC at low xylose concentrations using this HPLC method was very small, which allows for large inaccuracy. The inaccuracy in the model may be due to this lack of accuracy in concentrations of xylose determined by the HPLC method.

The correlation between experimental data and model prediction at 35°C and pH1 was poor (r^2 = 0.02), indicating a lack of accuracy of the model at these conditions. This inaccuracy may be due to a lack of accuracy of the HPLC method at low xylose concentrations, as discussed above.

5.3.3 Determination of kinetic parameters

The fitted kinetic parameters determined experimentally are of similar magnitude to those determined in previous studies (Table 5.4). Discrepancies in the kinetic parameters may be due to the different temperature ranges in which previous studies we conducted as well as different substrates considered in each study.

Table 5.4: Kinetic parameters determined experimentally compared to other studies

Source	A_f /min	Ea_f kJ/mol	n_f	A_s /min	Ea_s kJ/mol	n_s	X_f	Substrate
This Study	1.65×10^{19}	155.06	0.74	-	-		0.5	South African grass varieties
(Esteghlalian et al., 1997)	1.90×10^{21}	169	0.4	4.20×10^{23}	210.7	2	0.768	Switchgrass
(Yat et al., 2008)	2.48×10^{13}	115	1.75	-	-	-	1	Switchgrass
(Maloney et al., 1985)	2.67×10^{16}	128.1	1	1.63×10^{19}	156	1	0.684	Paper Birch
(Nee and Yee, 1976)	6.40×10^{5}	53	1.02	10.7×10^{0}	23.5	0.363	0.65	Bagasse
(Aguilar et al., 2002)	3.93×10^{12}	99.15	1	-	-	-	1	Bagasse
(Kim et al., 2013)	6.88×10^{12}	89.4	1.74	-	-	-	1	Xylo-oligomers
(Lavarack et al., 2002)	5.86×10^{9}	88.1	0.79	8.76×10^{7}	73.5	0.79	0.58	Bagasse

These kinetic parameters determined (presented in Table 5.4) were then used to predict the rate of hydrolysis of grass over a range of temperatures and acidity (Figure 5.4).

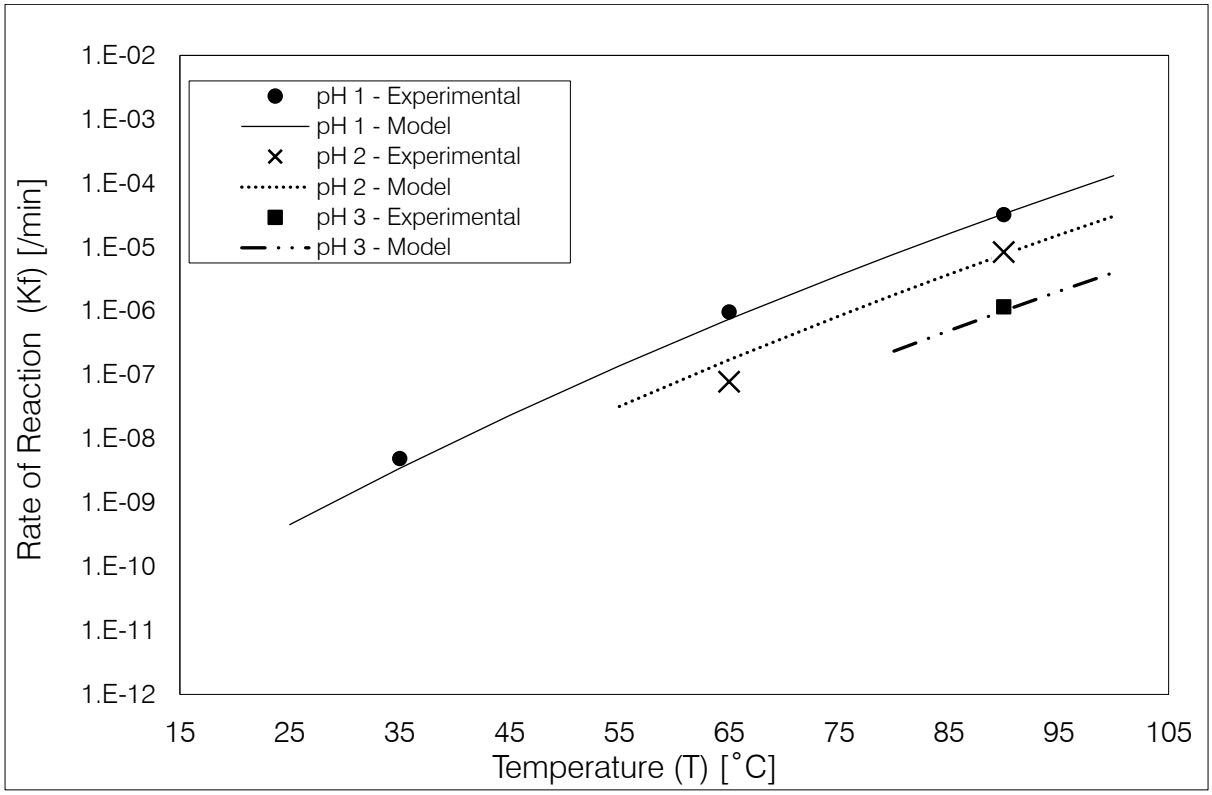

Figure 5.4: Predicted model reaction rate using determined kinetic parameters and experimentally observed reaction rates

The model has only been used to predict reaction rates 10°C above and below the range in which a rate was determined experimentally. Both temperature and pH can be seen to have a major effect on the rate of reaction, with the rate of reaction increasing with both the temperature and the pH.

A comparison between the predicted rate of reaction and rate of reaction found in literature was conducted. Esteghlalian *et al.* (1997) was chosen for comparison as their conditions are the most similar to this study (Figure 5.5).

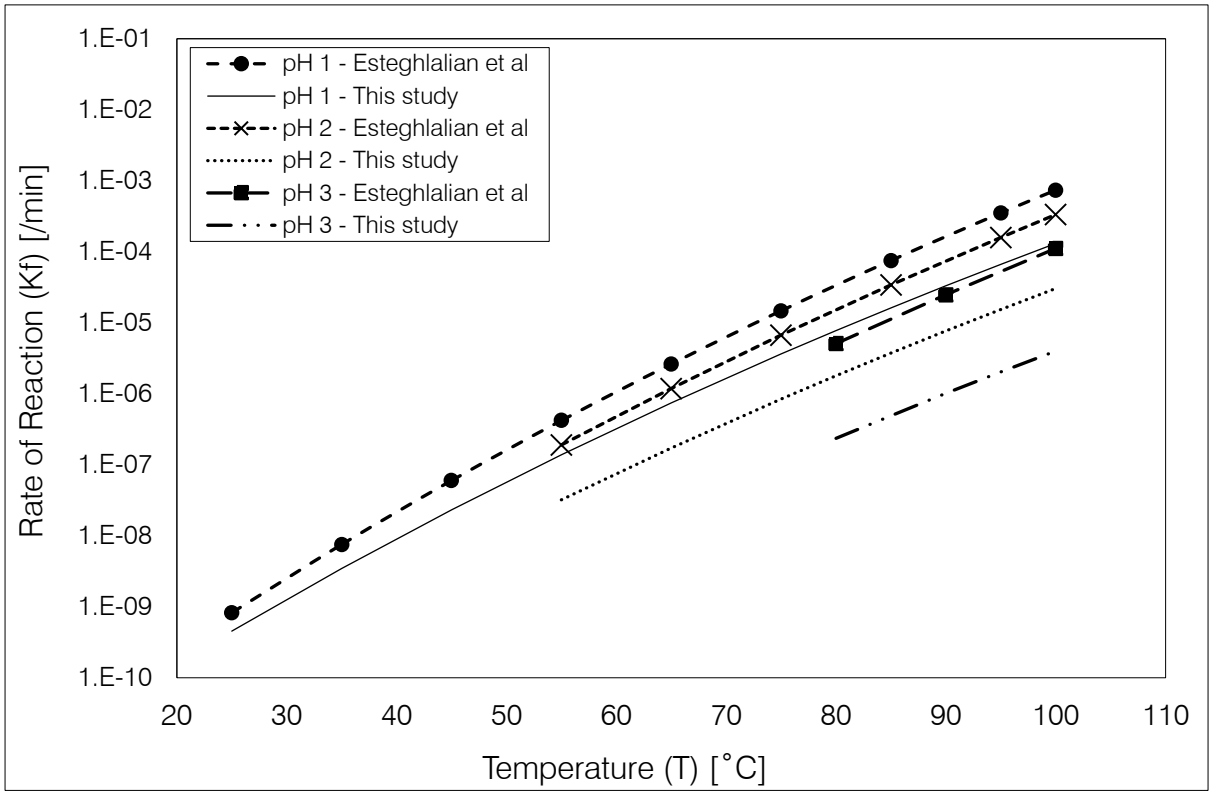

Figure 5.5: Rate of reaction at various pH and temperature conditions *vs.* literature (Esteghlalian et al., 1997)

The kinetic parameters determined in this study and Esteghlalian *et al.* (1997) predict rates of reaction for the fast reacting fraction of grass of the same order of magnitude. No comparison was made for the slow reacting fraction as it was assumed that it was non-reactive at these conditions. The values determined by Esteghlalian *et al.* (1997) predict faster rates under all temperatures and acid concentrations. Esteghlalian *et al.'s* (1997) values were between 1.8 and 26 times greater than the values determined in this study, with the largest discrepancy being at low acid concentration and high temperature, and the lowest discrepancy being at high acid concentration and low temperature.

5.4. Conclusion

The rate of hydrolysis was investigated at temperatures (35 – 90°C) far lower than previously investigated (>74°C). The hydrolysis of xylan at these temperatures was found to exhibit a reaction mechanism in which there were two portions of xylan, one which undergoes

hydrolysis, and another which undergoes hydrolysis at such a slow rate it can be assumed to be negligible. The rate of hydrolysis of the reacting fraction was found to obey Arrhenius type temperature dependence (Ea = 155.06 kJ/mol, A_0 = 1.65×10^{19}/min). The rate of hydrolysis of fast reacting fraction is similar to that determined in previous studies, however, the proportion of fast reacting fraction was found to be 50% which is lower than previously determined (55%-100%). It is recommended that the kinetic parameters determined in this study be utilized to perform a rigorous techno-economical evaluation of the feasibility of low temperature dilute H_2SO_4 pre-treatment.

5.5. Acknowledgments

The authors would like to acknowledge the University of the Witwatersrand, Johannesburg, The National Research Foundation (NRF), The Global Change Institute (GCI), The Centre in Water Research and Development (CiWARD) and the Industrial and Mining Water Research Unit (IMWaRU) for their support of this study.

5.6. References

Aguilar, R., Ramirez, J.A., Garrote, G., Vazquez, M., 2002. Kinetic study of the acid hydrolysis of sugar cane bagasse. J. Food Eng. 55, 309–318.

Alvira, P., Tomas-Pejo, E., Ballesteros, M., Negro, M.J., 2010. Pretreatment technologies for an efficient bioethanol production process based on enzymatic hydrolysis: A review. Bioresour. Technol. 101, 4851–4861. doi:10.1016/j.biortech.2009.11.093

Bañuelos, J.A., Velázquez-Hernández, I., Guerra-Balcázar, M., Arjona, N., 2018. Production, characterization and evaluation of the energetic capability of bioethanol from Salicornia Bigelovii as a renewable energy source. Renew. Energy 123, 125–134. doi:10.1016/j.renene.2018.02.031

Bhandari, N., Macdonald, D.G., Bakhshi, N.N., 1984. Kinetic Studies of Corn Stover Saccharification using Sulphuric Acid. Biotechnol. Bioeng. 26, 320–327. doi:10.1002/bit.260260405

Burman, N.W., Harding, K.G., Sheridan, C.M., Van Dyk, L., 2018a. Evaluation of a combined lignocellulosic / waste water bio-refinery for the simultaneous production of valuable biochemical products and the remediation of acid mine drainage. Biofuels, Bioprod. Biorefining 12, 649–664. doi:10.1002/bbb.1880

E4TECH, RE-CORD, WUR, 2015. From the Sugar Platform to biofuels and biochemicals, Final report for the European Commission Directorate-General Energy. doi:contract No. ENER/C2/423-2012/SI2.673791

Esteghlalian, A., Hashimoto, A.G., Fenske, J.J., Penner, M.H., 1997. Modeling and optimization of the dilute-sulfuric-acid pretreatment of corn stover, poplar and switchgrass. Bioresour. Technol. 59, 129–136. doi:10.1016/S0960-8524(97)81606-9

Jin, Q., Zhang, H., Yan, L., Qu, L., Huang, H., 2011. Kinetic characterization for hemicellulose hydrolysis of corn stover in a dilute acid cycle spray flow-through reactor at moderate conditions. Biomass and Bioenergy 35, 4158–4164. doi:10.1016/j.biombioe.2011.06.050

Kim, Y., Kreke, T., Ladisch, M.R., 2013. Reaction Mechanisms and Kinetics of Xylo-Oligosaccharide Hydrolysis by Dicarboxylic Acids. Am. Inst. Chem. Eng. J. 59. doi:10.1002/aic

Kobayashi, T., Sakai, Y., 1956. Bulletin of the Agricultural Chemical Society of Japan Hydrolysis Rate of Pentosan of Hardwood in Dilute Sulfuric Acid in Dilute Sulfuric Acid. Bull. Agric. Soc. Japan 20, 1–7. doi:10.1080/03758397.1956.10857296

Lange, J., 2007. Lignocellulose conversion : an introduction to chemistry ,. Biofuels, Bioprod. Biorefining 1, 39–48. doi:10.1002/bbb

Lavarack, B.P., Gri, G.J., Rodman, D., 2002. The acid hydrolysis of sugarcane bagasse hemicellulose to produce xylose , arabinose , glucose and other products. Biomass and Bioenergy 23, 367–380.

Lee, D., Ownes, V.N., Boe, A., Jeramyama, P., 2007. Composition of Herbaceous Biomass Feedstocks. Brookings, SD.

Li, S., Xu, S., Liu, S., Yang, C., Lu, Q., 2004. Fast pyrolysis of biomass in free-fall reactor for hydrogen-rich gas. Fuel Process. Technol. 85, 1201–1211. doi:10.1016/j.fuproc.2003.11.043

Maloney, M.T., Chapman, T.W., Baker, a J., 1985. Dilute acid hydrolysis of paper birch: kinetics studies of xylan and acetyl-group hydrolysis. Biotechnol. Bioeng. 27, 355–361. doi:10.1002/bit.260270321

Mani, T., Murugan, P., Abedi, J., Mahinpey, N., 2010. Pyrolysis of wheat straw in a thermogravimetric analyzer : Effect of particle size and heating rate on devolatilization and estimation of global kinetics. Chem. Eng. Res. Des. 88, 952–958. doi:10.1016/j.cherd.2010.02.008

Maurya, D.P., Singla, A., Negi, S., 2015. An overview of key pretreatment processes for biological conversion of lignocellulosic biomass to bioethanol. 3 Biotech 5, 597–609. doi:10.1007/s13205-015-0279-4

Menon, V., Rao, M., 2012. Trends in bioconversion of lignocellulose : Biofuels , platform chemicals & biore fi nery concept. Prog. Energy Combust. Sci. 38, 522–550. doi:10.1016/j.pecs.2012.02.002

Mosier, N., Wyman, C., Dale, B., Elander, R., Lee, Y.Y., Holtzapple, M., Ladisch, M., 2005b. Features of promising technologies for pretreatment of lignocellulosic biomass. Bioresour. Technol. 96, 673–686. doi:10.1016/j.biortech.2004.06.025

Nee, C.I., Yee, W.F., 1976. Hydrolysis of Pentosans in Bagasse Pith. J. Appl. Chem. Biotechnol. 26, 283–287.

Negahdar, L., Delidovich, I., Palkovits, R., 2016. Aqueous-phase hydrolysis of cellulose and hemicelluloses over molecular acidic catalysts : Insights into the kinetics and reaction mechanism. Appl. Catal. B Environ. 184, 285–298. doi:doi:10.1016/j.apcatb.2015.11.039

Rodriguez-Chong, A., Ramirez, J.A., Garrote, G., Manuel, V., 2004. Hydrolysis of sugar cane bagasse using nitric acid : a kinetic assessment. J. Food Eng. 61, 143–152. doi:10.1016/S0260-8774(03)00080-3

Saeman, J.F., 1945. Kinetics of Wood Saccharfifications-Hydrolysis of Cellulose and Decomposition of Sugars in Dilute Acid at High Temperature. Ind. Eng. Chem. 37, 43–52. doi:10.1021/ie50421a009

Schell, D.J., Farmer, J., Newman, M., McMillan, J.D., 2003. Dilute – Sulfuric Acid Pretreatment of Corn Stover in Pilot-Scale Reactor. Appl. Biochem. Biotechnol. 105–108, 69–85.

Shen, J., Wyman, C.E., 2011. Bioresource Technology A novel mechanism and kinetic model to explain enhanced xylose yields from dilute sulfuric acid compared to hydrothermal pretreatment of corn stover. Bioresour. Technol. 102, 9111–9120. doi:10.1016/j.biortech.2011.04.001

Sluiter, A., Hames, B., Ruiz, R., Scarlata, C., Sluiter, J., Templeton, D., Crocker, D., 2008b. Determination of Structural Carbohydrates and Lignin in Biomass.

Springer, E.L., Harris, J.F., 1985. Procedures for Determining the Neutralizing Capacity of Wood during Hydrolysis with Mineral Acid Solutions. Ind. Eng. Chem. Prod. Res. Dev. 24, 485–489. doi:10.1021/i300019a030

Taherzadeh, M.J., Karimi, K., 2008. Pretreatment of lignocellulosic wastes to improve ethanol and biogas production: A review. Int. J. Mol. Sci. 9, 1621–1651. doi:10.3390/ijms9091621

Taherzadeh, M.J., Karimi, K., 2007a. Enzyme based hydrolysis processes for ethanol from lignocellulosic materials : a review. Bioresources 2, 707–738.

Uihlein, A., Schebek, L., 2009. Environmental impacts of a lignocellulose feedstock biorefinery system: An assessment. Biomass Bioenergy 33, 793–802. doi:10.1016/j.biombioe.2008.12.001

Westensee, D.K., Rumbold, K., Harding, K.G., Sheridan, C.M., van Dyk, L.D., Simate, G.S., Postma, F., 2018. The availability of second generation feedstocks for the treatment of acid mine drainage and to improve South Africa's bio-based economy. Sci. Total Environ. 637–638, 132–136. doi:10.1016/j.scitotenv.2018.04.410

Wyman, Charles E., Dale, B.E., Elander, R.T., Holtzapple, M., Ladisch, M.R., Lee, Y.Y., 2005a. Coordinated development of leading biomass pretreatment technologies. Bioresour. Technol. 96, 1959–1966. doi:10.1016/j.biortech.2005.01.010

Yat, S.C., Berger, A., Shonnard, D.R., 2008. Kinetic characterization for dilute sulfuric acid hydrolysis of timber varieties and switchgrass. Bioresour. Technol. 99, 3855–3863. doi:10.1016/j.biortech.2007.06.046

Chapter 6: Lignocellulosic Bioethanol Production from Grasses Pre-treated with Acid Mine Drainage: Modeling and Comparison of SHF and SSF

(Published in Bioresource Technology Reports, 2019) This chapter experimentally determined the optimum level of pre-treatment and the rate of enzymatic hydrolysis and fermentation of biomass pre-treated with acid mine drainage. Both separate hydrolysis and fermentation (SHF) and simultaneous saccharification and fermentation (SSF) were investigated. This addresses objective c.

Burman, N.W., Harding, K.G., Sheridan, C.M., 2019b. Lignocellulosic Bioethanol Production from Grasses Pre-treated with Acid Mine Drainage. Modeling and Comparison of SHF and SSF. Bioresource Technology Reports. 7. doi:10.1016/j.biteb.2019.100299

Abstract: Acid mine drainage (AMD) was used for the pre-treatment of indigenous South African grass (*Eragrostis curvula*), and compared to H_2SO_4 (1 wt%) pre-treatment. The optimal pre-treatment durations were investigated and found to be 1 day for H_2SO_4 and 3 days for AMD pre-treatment. The optimal biomass solid loadings were investigated and found to be 20 wt% for both pre-treatment methods. Additionally, enzymatic hydrolysis and fermentation to produce ethanol was investigated for both separate hydrolysis and fermentation (SHF) and simultaneous saccharification and fermentation (SSF). In both SHF and SSF, the H_2SO_4 pre-treatment obtained higher concentrations of glucose/ethanol compared to AMD pre-treatment. The concentration of glucose/ethanol obtained using AMD pre-treatment was 70 – 80% of that achieved using H_2SO_4 pre-treatment. Empirical equations modeling the glucose/ethanol concentration in all processes were determined using a least-squares method. Concentrations predicted by the models were found to have a high correlation (r^2 = 0.87 – 0.99) to concentrations determined experimentally.

Keywords: Dilute Acid Pre-treatment, Lignocellulosic Bioethanol; Separate Hydrolysis and Fermentation (SHF); Simultaneous Saccharification and Fermentation (SSF)

6.1. Introduction

The burning of fossil fuels is the cause of recently observed atmospheric and oceanic warming, and associated climate change (IPCC, 2014a). Although the production of starch-based bioethanol as an environmentally friendly alternative to fossil fuels has been growing (71 billion kg produced in 2015 (E4TECH et al., 2015)), its use has various drawbacks. These include increases in food prices, not being entirely carbon neutral, net energy losses, a reduction of available land for food production, and land degradation (Lange, 2007).

To overcome these drawbacks, the production of bioethanol from lignocellulosic biomass (agricultural waste, forestry residue and energy crops) has been investigated (Sun and Cheng, 2002), and found to be more environmentally friendly (Searcy and Flynn, 2008). Lignocellulosic biomass consists of cellulose fibrils that are surrounded by a matrix of hemicellulose and lignin. The presence of the ligno-hemicellulose matrix hinders cellulase enzymes from accessing cellulose fibrils, preventing hydrolysis of cellulose to glucose. To overcome this, lignocellulosic biomass needs to undergo pre-treatment to fragment the ligno-hemicellulosic matrix, making the cellulose accessible to enzymes (Figure 6.1) (Mosier et al., 2005b). Glucose produced in hydrolysis can then be fermented to bioethanol by *Saccharomyces cerevisiae* or other micro-organisms (Yu and Zhang, 2003).

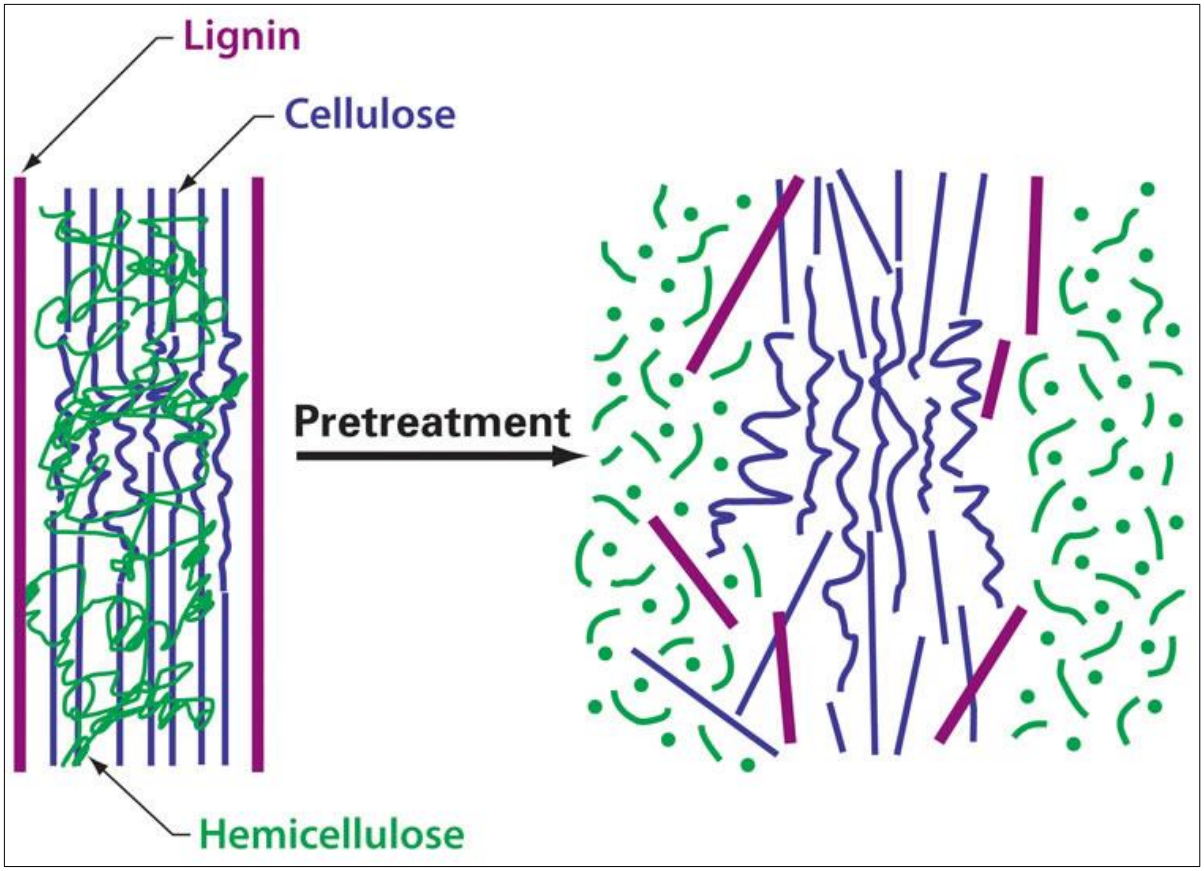

Figure 6.1: Effect of pre-treatment on the structure of lignocellulose (Mosier et al., 2005b)

Various pre-treatment methods have been shown to be effective, including physical, physico-chemical, chemical, and biological pre-treatment (Sindhu et al., 2016). Chemical pre-treatment using dilute sulfuric acid has been shown to be the most favorable method of pre-treatment for industrial applications (Alvira et al., 2010; Burman et al., 2018b; Maurya et al., 2015; Mosier et al., 2005b; Taherzadeh and Karimi, 2008). Recently, Magowo *et al.* (2015) demonstrated the suitability of acid mine drainage (AMD) as a source of dilute sulfuric acid for the pre-treatment of lignocellulosic biomass, producing glucose concentrations of up 4.8 g/L from subsequent enzymatic hydrolysis.

AMD is highly acidic (pH 1-3) water with high concentrations of sulfate (<20 g/L) and heavy metals (iron, aluminum <5 g/L) that is formed through a series of geochemical reactions when sulfite rich rocks are exposed to oxygen and water, often as a result of mining activities (Johnson and Hallberg, 2005b).

AMD has been found to have a negative effect on aquatic and riparian ecosystems due to the toxicity effects of increased chemical concentration. As the pH increases naturally dissolved heavy metals deposit on the ecosystem floor (Simate and Ndlovu, 2014). There is a high

prevalence of AMD in the Witwatersrand area and Mpumalanga and KwaZulu-Natal coalfields of South Africa due to mining of gold and coal respectively (Mccarthy et al., 2010).

In addition to the suitability of AMD for pre-treatment of biomass, it has also been shown that this could be combined with a process to remediate the AMD using sulfate-reducing bacteria (SRB) (Magowo et al., 2015; Ramla and Sheridan, 2015). Long stem grasses have been identified as a good source of lignocellulosic biomass due to their prevalence in the Grassland and Savanah biomes in which both the Witwatersrand area and KwaZulu-Natal mines are located (Burman et al., 2018a, 2017; Westensee et al., 2018). However, previous studies have yet to determine the optimum conditions of pre-treatment with AMD, or the final ethanol/glucose concentration achievable. There is also a need for modeling of the reactions in order to perform a full process design and techno-economic evaluation.

Enzymatic hydrolysis and fermentation has been investigated in different reactor configurations including separate hydrolysis and fermentation (SHF), in which hydrolysis and fermentation occur in separate reactors, and simultaneous saccharification and fermentation (SSF), in which hydrolysis and fermentation occur in the same reactor. Although SSF reduces the product inhibition of glucose on the hydrolysis reaction by keeping glucose concentration low, the compromise of reactor temperature of SSF (38°C) between optimal temperature for hydrolysis (45 – 50°C) and fermentation (30 – 37°C) (Olsson et al., 2006; Badal C Saha et al., 2005), results in a decrease in the rate of both reactions. It is therefore not always clear which reactor configuration is more environmentally and economically favorable (Philippidis and Smith, 1995). Ethanol concentrations ranging from 4.72 – 16.0 g/L for SHF and 1.8 – 28.1 g/L for SSF have been achieved using various species of grass biomass (Mohapatra et al., 2017).

Previous studies have shown that glucose and ethanol concentrations from hydrolysis and fermentation can be predicted using kinetic models (Bansal et al., 2009; Liao et al., 2008; Ye and Berson, 2011; Zheng et al., 2009). Various different types of kinetic models have been developed including, Michaelis-Menton based models, adsorption-based models, and soluble substrate-based models. Although these models predict concentrations over time well, the experimental work required to develop them is time and resource intensive. The use of these models outside of the conditions at which they were developed (biomass, pre-treatment, operating conditions) is also not applicable. It is thus proposed that an empirical model be

developed to predict the concentration of glucose and ethanol over time during both SHF and SSF, for biomass pre-treated with AMD.

This paper presents the optimum conditions for pre-treatment of long-stem grass using AMD and H_2SO_4, determines the concentration of glucose and ethanol in SHF and SSF reactor configurations for biomass pre-treated with AMD and H_2SO_4, and develops an empirical mathematical model for the processes of SHF and SSF.

6.2. Materials and methods

The materials and methods are presented in five main sub-sections: materials (characterization of AMD and grass); optimization of biomass pre-treatment (determination of optimal pre-treatment for maximized enzymatic hydrolysis sugar recovery); enzymatic hydrolysis and fermentation (performance of SHF and SSF using optimally pre-treated biomass); analytical methods; and empirical model development.

6.2.1 Materials

AMD was sourced from a coal mine in the eMalahleni district in South Africa. The pH was determined using an Ohaus ST2100-F Benchtop pH meter. Sulfate concentrations were determined using a Merck Sulfate Test Kit #114548 (www.sigmaaldrich.com). Dissolved metal concentrations were determined by ICP-OES by UIS Analytical Services (www.uis-as.co.za) using method UIS-AC-T007. A summary of the results is presented in the results section.

An indigenous South African grass classified as *Eragrostis curvula* (Weeping lovegrass or Oulandsgrass) was sourced from an agricultural supplier in Gauteng Province, South Africa. The structural composition of this grass was determined using the National Renewable Energy Laboratory (NREL) method (Sluiter et al., 2008b). This method first determines the extractives through Soxhlet extraction, then determines the monosaccharide composition by hydrolyzing the grass using a two-stage concentrated/dilute sulfuric acid, and then analyzes the hydrolysate for monosaccharides by high performance liquid chromatography (HPLC). The only deviation from this method was the use of a single-stage Soxhlet extraction using acetone as opposed to a two-stage ethanol/water extraction. The structural composition is presented in the results section.

Celluclast 1.5L cellulase enzyme (Novozyme), with an activity of 80 FPU/mL, was used for enzymatic hydrolysis at a dosage of 16.5 FPU/g substrate. This was mixed with 0.05M sodium citrate buffer (pH 4.8).

6.2.2 Optimization of biomass pre-treatment

The effect of pre-treatment time on the yield of enzymatic hydrolysis was evaluated. 20 g of grass was loaded in 250 mL Erlenmeyer flasks with 200 mL of either 100 wt% AMD or 1 wt% H_2SO_4, incubated at 90°C and 100 RPM (Burman et al., 2018b). Flasks were removed from the incubator at 0, 24, 48, 96, 192 and 288 hrs for the AMD pre-treatment, and 0, 3, 6, 12, 24, 48, and 72 hrs for H_2SO_4 pre-treatment. Pre-treated biomass was washed with de-ionized water filtered and dried.

The effect of biomass solid loading during pre-treatment on the yield of enzymatic hydrolysis was evaluated. 250 mL Erlenmeyer flasks were loaded with 200 mL of either 1 wt% H_2SO_4 or AMD and 5, 10, 15 and 20 wt% grass. These were placed in a shaking incubator at 100 RPM and 90°C. After the optimum pre-treatment time, flasks were removed from the incubator and biomass was washed, filtered and dried.

Enzymatic hydrolysis of pre-treated biomass was then carried out by loading pre-treated biomass (20 wt%) into 250 mL Erlenmeyer flasks containing buffer/cellulase mixture. These were placed in the shaking incubator at 50°C and 100RPM. Samples were taken after 24 and 48 hours and analyzed for glucose.

The optimum pre-treatment time was taken as the time after which there was no longer a rapid increase in glucose produced in enzymatic hydrolysis. This was determined to be 24 hrs for H_2SO_4 pre-treatment and 72 hrs for AMD pre-treatment. The optimal solid loading was taken to be 20 wt%.

All further SHF and SSF experiments were conducted with the optimal pre-treatment conditions determined.

6.2.3 Enzymatic hydrolysis and fermentation

Many of the methods used in the evaluation of the performance of SHF and SSF were based the NREL LAP "SSF Experimental Protocols — Lignocellulosic Biomass Hydrolysis and Fermentation" (Dowe and Mcmillan, 2008), however as significant modifications to this method were required, the method used has been described in full.

6.2.3.1 Yeast identification

Yeast for fermentation in both SHF and SSF was isolated from a commercially available home distillers' yeast that has been identified for its fast rate of fermentation and high ethanol tolerance (Alcotech Turbo-yeast 48).

The yeast was isolated by inoculating the yeast from packaging into a glucose solution, which was grown at room temperatures for 24 hrs. YPD agar slants (screw-topped culture tubes with YPD agar set at an angle) were then produced from the fermentation broth. Identification of the yeast strain was done using Multi-Locus Sequence Typing (MLST) of the following loci ATF1, RPN2, NUP116, STE50, and YBL081W. The extraction of DNA and sequencing of loci was performed by Inqaba Biotech laboratories (http://www.inqababiotec.co.za/) according to the method described by Ayoub *et al.* (2006). Sequences were then analyzed using BLAST analysis on the NCBI website (https://blast.ncbi.nlm.nih.gov/Blast.cgi). As there was a lack of allele sequenced for these loci it was not possible to identify the specific strain, however, it was confirmed that the micro-organism responsible for fermentation was *Saccharomyces cerevisiae*.

6.2.3.2 Yeast inoculation preparation

A loopful (10 µL) of *Saccharomyces cerevisiae* was added to a 250 mL Erlenmeyer flask, which contained 100 mL sterile medium (5g/L glucose, 20 g/L peptone, and 10 g/L yeast extract). The culture was incubated at 30°C and grown until the OD_{600} was between 0.5 and 0.6 (Dowe and Mcmillan, 2008).

6.2.3.3 Pre-treatment of biomass

To evaluate the performance of SHF and SSF a standard pre-treated biomass was produced as follows. 500 g of grass underwent pre-treatment at 90°C with either sulfuric acid or AMD at a solid loading ratio of 20 wt%. Sulfuric acid pre-treatment was carried out at 1 wt% H_2SO_4 for 24 hrs. AMD pre-treatment was carried out using AMD for 72 hrs. All biomass was pre-treated in the same vessel to ensure the consistent pre-treatment of biomass for all enzymatic

hydrolysis and fermentation experiments. Pre-treated biomass was washed, filtered and dried.

6.2.3.4 Separate hydrolysis and fermentation (SHF)

Pre-treated biomass was loaded into 250 mL Erlenmeyer flasks with 200 mL of buffer/ cellulase mixture at the following solid loading fractions 5, 10, 15 and 20 wt%. Experiments were carried out in duplicate. Flasks were placed in the shaking incubator operating at 50°C and 100 RPM. Samples were taken after 0, 3, 6, 12, 24, 48, 72, and 168 hrs and analyzed. At 168 hrs the slurry was filtered using Whatman 54 filter paper. The biomass was washed and dried.

The filtrate from the hydrolysis experiments was added to 250 mL Erlenmeyer flasks and inoculated with 10% v/v *Saccharomyces cerevisiae* inoculum, substituted with yeast extract (10 g/L) and peptone (20 g/L). Flasks were placed in the shaking incubator at 35°C and 100 RPM. Samples were taken at 0, 6, 12, 24, 48, 72 and 96 hrs and analyzed.

6.2.3.5 Simultaneous saccharification and fermentation (SSF)

Pre-treated biomass was loaded into 250 mL Erlenmeyer flasks with 200 mL of buffer/ cellulase mixture at solid loading fractions of 5, 10, 15 and 20 wt%. Experiments were carried out in duplicate. The flasks were inoculated with 10% v/v *Saccharomyces cerevisiae* inoculum substituted with the following nutrients yeast extract (10 g/L), peptone (20g/L). Flasks were placed in the shaking incubator operating at 37°C and 100 RPM. Liquid samples were taken at 0, 8, 24, 48, 72, 96, 120, 144 and 168 hrs and analyzed.

6.2.4 Analytical methods

All liquid samples were centrifuged at 2348g for 10 minutes, then filtered through 0.45 µm syringe filters and stored for analysis. All samples were analyzed by HPLC for xylose, glucose, cellobiose, and ethanol using the Biorad-Aminex HPX-87H Column operating at 65°C using 0.05M H_2SO_4 as the mobile phase at a flow rate of 0.8 mL/min and 20 µL injection volume. The run time was set to 10 min. (Sluiter et al., 2008a)

The results from the SHF/SSF experiments were then used to develop an empirical model of the reactions taking place.

6.2.5 SHF empirical model development

Empirical equations were determined using a least-squares method for fitting empirical equations. Different forms of equations were used for hydrolysis in SHF, fermentation in SHF, and SSF due to the different nature of the data received.

6.2.5.1 Separate hydrolysis and fermentation (SHF)

The glucose concentration during hydrolysis in SHF was found to follow a logarithmic equation of the form

$$G = M_1 ln(t_e) + C_1 \quad (6.1)$$

where G is the glucose concentration (g/L), t_e is the time of enzymatic hydrolysis (days), and M_1 and C_1 are constants.

Values for M_1 and C_1 were determined using a least-square fitting function in Microsoft® Excel (LINEST). Values for M_1 and C_1 were determined for each wt% investigated. These were then plotted against the wt%. Both M_1 and C_1 were found to increase linearly with the increasing wt%. Equations for M_1 and C_1 as a function of wt% were determined, using the least-squares function (LINEST) as shown below for M_1

$$M_1 = m_{1,M} \times W + c_{1,M} \quad (6.2)$$

where W is the biomass solid loading hydrolysis (wt%) and $m_{1,M}$ and $c_{1,M}$ are empirical constants.

Substituting the equations for M_1 and C_1 into Equation (6.1) we get an empirical equation that can predict the concentration of glucose during hydrolysis under the conditions mentioned above for a range of different solid loadings (5 – 20 wt%). The final form of the equation is presented in Table 6.2.

The rate of fermentation was found to have two distinct phases during fermentation *i.e.* a growth phase and a stationary phase. The rate of fermentation was found to be very different during the different phases, with the rate of reaction in the growth phase (r_g) being much slower than the rate of reaction in the stationary phase (r_s). Both phases were found to last six hours. After 12 hours all glucose had been consumed, and thus no more ethanol was produced.

The concentration of glucose was thus equal to

$$G = G_0 - r_g \times t_f \qquad for\ t_f \in 0{:}\ 6\ hr \tag{6.3}$$

$$G = G_0 - r_g \times 6 - r_s \times (t_f - 6) \qquad for\ t_f \in 6{:}\ 12\ hr \tag{6.4}$$

Where G_0 is the initial glucose concentration (g/L) and t_f is the fermentation time (hrs).

The ethanol concentration, E (g/L) was determined based on the yield of ethanol produced from glucose consumed, $Y_{\frac{A}{P}}$, (g/g). Note the stoichiometric maximum for this is 0.5111 g/g.

6.2.5.2 Simultaneous saccharification and fermentation (SSF)

The concentration of ethanol during SSF was found to follow a logarithmic equation of the form

$$E = M_2 ln(t_s) + C_2 \tag{6.5}$$

where E is the ethanol concentration; t_s is the time of SSF; and M_2 and C_2 are constants.

Values for M_2 and C_2 were determined using a least-square fitting function in Microsoft® Excel (LINEST). Values for M_2 and C_2 were determined for each wt% investigated. With increasing solid loading, M_2 was found to increase linearly (similar to equation (6.2)), whereas C_2 was found to increase logarithmically according to

$$C_2 = m_{2,C} ln(W) + c_{2,C} \tag{6.6}$$

where W is the biomass solid loading in SSF (wt%) and $m_{2,M}$, $c_{2,M}$, $m_{2,c}$, and $c_{2,c}$ are empirical constants. The final form of the equation is presented in Table 6.2 in the results section. All empirical constants determined are presented in Table 6.3 in the results section.

The correlation between the experimentally determined data and the results that the model predicts was determined using Microsoft® Excel's CORREL function that determines the coefficient of determination (r^2).

6.3. Results and discussion

6.3.1 Grass composition

The composition of the biomass is presented in Table 6.1 along with the standard deviation (SD). Results from previous studies are also presented for Weeping lovegrass (Torget et al., 1990); switchgrass (Lee et al., 2007); Elephant grass (Menegol et al., 2014); and Dwarf Napier grass (Wongwatanapaiboon et al., 2012). Switchgrass, Dwarf Napier grass, and Elephant grass

were chosen for comparison as they are grasses that have been found suitable feedstocks for bioethanol production.

Table 6.1: Experimentally determined the structural composition of Weeping lovegrass, compared to results presented in literature for Weeping lovegrass and switchgrass.

	This study		(Torget et al., 1990)	(Lee et al., 2007)		(Menegol et al., 2014)		(Wongwatanapaiboon et al., 2012)	
Biomass Type	**Weeping lovegrass**		**Weeping lovegrass**	**Switchgrass**		**Elephant grass**		**Dwarf Napier[3]**	
Structural Composition	**Mean %**	**SD %**	**Mean %[1]**	**Mean %**	**SD %**	**Mean %**	**SD %**	**Mean %**	**SD %**
Hemicellulose	20.6	3.0	21.9%	28.5	3.5	20.51	0.023	34.19	1.24
Cellulose	35.3	3.0	36.7%	37.3	4.4	37.95	1.06	35.64	0.21
Acid Soluble Lignin	2.46	0.15	21.8%[2]	3.5	0.3	1.12	0.02	3.66	0.20
Acid Insoluble Lignin	26.1	5.19		16.2	0.5	19.65	0.78		
Ash	3.08	0.34	5.6%	5.9	1.0	8.53	0.23	0.13	0.12
Extractives	2.33	0.99	6.3%	3.1	0.7	8.84	0.83		
Other								26.38	1.38

[1]The standard deviation was not reported by this study.
[2]The lignin was not reported as acid soluble and acid insoluble lignin just as Klason lignin which was taken to be the total lignin content.
[3]The acid-insoluble lignin and extractives were not reported in this study, however, an "other" category was reported

The composition of Weeping lovegrass determined in this study is similar to that reported by Torget *et al.* (1990). The cellulose content was found to be similar for all different grasses presented (35.3 – 38.0%). The comparable cellulose content of Weeping lovegrass to other grass species indicates that it would be a suitable feedstock for the production of bioethanol from the C6 sugar platform. There was, however, significant variation in the hemicellulose content in the grasses presented. The hemicellulose content was much higher in switchgrass (28.5%) and Dwarf Napier grass (34.2%) than in Weeping lovegrass (20.6 – 21.9%) and Elephant grass (20.5%). The comparatively low hemicellulose content of Weeping lovegrass indicates it would not be a good feedstock for the production of bioethanol through co-fermentation of both C5 and C6 sugars.

6.3.2 AMD composition

The AMD was found to be highly acidic (pH 2.4) with a high concentration of sulfate (12.5 g/L). There was also a high concentration of dissolved iron (4.29 g/L) and low concentrations of dissolved magnesium (0.474 g/L) and aluminum (0.396 g/L). There were trace concentrations (<0.1 g/L) of various other metal such as manganese, silicon, sodium, and zinc. Trace

concentrations of other elements were found, however, elements with a concentration of less than 10 mg/L were not listed.

The quality of the AMD used in this investigation was relatively strong, with previous studies reporting AMD pH of 2 – 3, and sulfate concentrations of 3.5 g/L (McCarthy, 2011). The low pH of AMD should enable effective pre-treatment of biomass.

6.3.3 Optimum pre-treatment of grass

The results for the experiment to determine the optimum pre-treatment time (t) is presented in Figure 6.2 for both H_2SO_4 (a.) and AMD (b.). The results of the optimum pre-treatment solid loading ratio is presented in Figure 6.3 for both H_2SO_4 (a.) and AMD (b.).

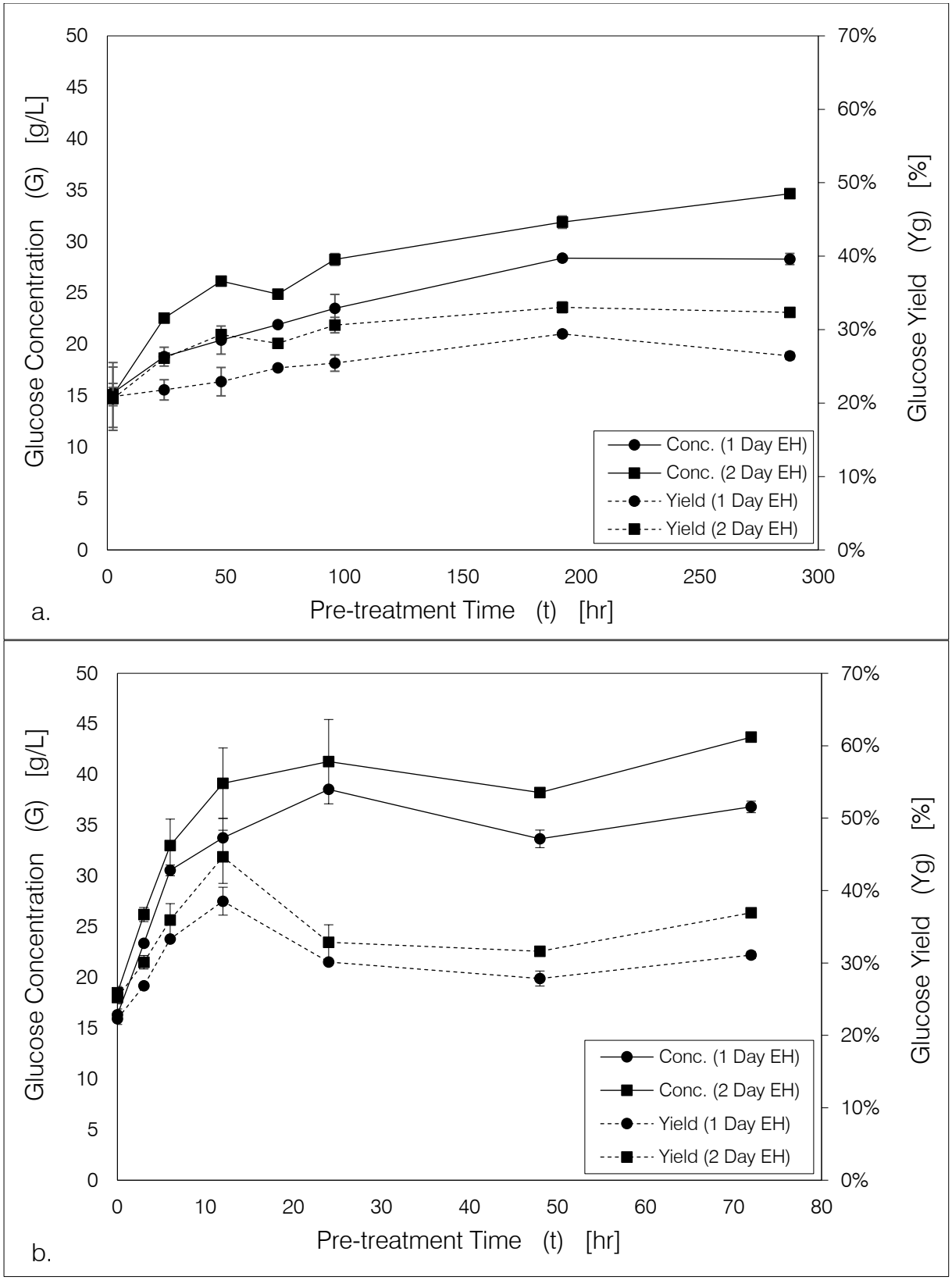

Figure 6.2: Concentration of glucose and glucose yield in enzymatic hydrolysis, after pre-treatment of different times for both H_2SO_4 pre-treatment (a.) and AMD pre-treatment (b.). Results are shown for both 1 day of enzymatic hydrolysis (1 Day EH) and 2 days of enzymatic hydrolysis (2 Day EH).

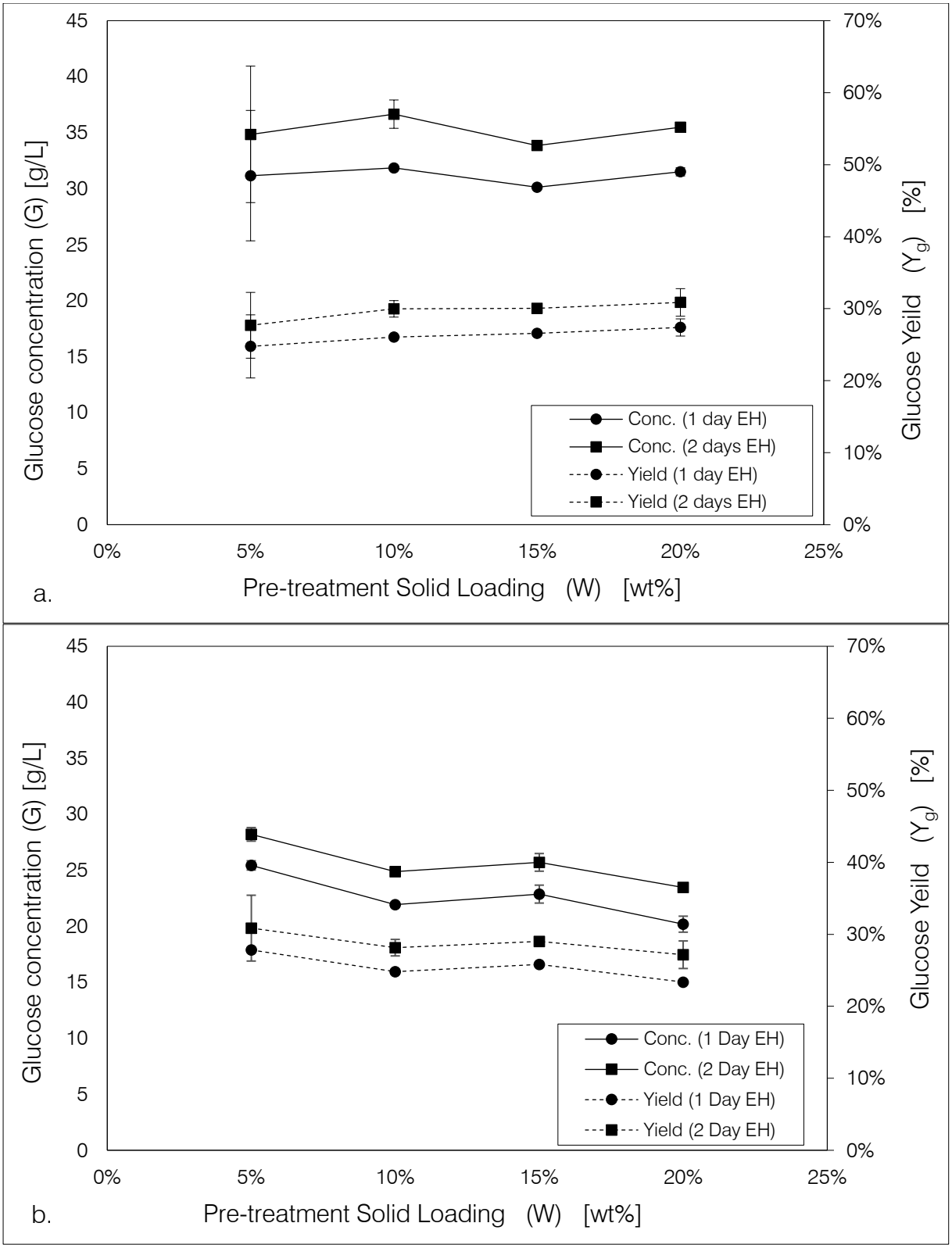

Figure 6.3: Concentration of glucose and glucose yield in enzymatic hydrolysis after pre-treatment at different biomass solid loading ratios, for both H_2SO_4 pre-treatment (a.) and AMD pre-treatment (b.). Results are shown for both 1 day of enzymatic hydrolysis (1 Day EH) and 2 days of enzymatic hydrolysis (2 Day EH).

The concentration of glucose initially increases rapidly with increasing pre-treatment time, followed by a steady increase (Figure 6.2). For H_2SO_4 pre-treatment, the glucose increases rapidly up to 1 day of pre-treatment (~42 g/L) after which the concentration does not increase significantly. For AMD pre-treatment the glucose concentration increases rapidly up to 3 days of pre-treatment (~25 g/L) after which it increases steadily until the 12^{th} day of pre-treatment (~35 g/L). The glucose yield was found to range between 30% – 45% for H_2SO_4 pre-treatment, although there was no obvious correlation between it and pre-treatment time. The yield for AMD pre-treatment was seen to increase from 25% with no pre-treatment to 35% for 3 days of pre-treatment after which it does not increase significantly. For all following experiments, the optimal pre-treatment time was taken to be 1 day for H_2SO_4 pre-treatment and 3 days for AMD pre-treatment, although further investigations should be carried out so as to more accurately determine the optimal pre-treatment time.

There is no correlation between the biomass solid loading in H_2SO_4 pre-treatment and the enzymatic hydrolysis glucose concentration, however, the glucose yield was found to increase slightly with increasing biomass solid loading (Figure 6.3(a.)). With AMD pre-treatment both glucose yield and concentration in enzymatic hydrolysis are seen to decrease slightly with increasing pre-treatment solid loading (Figure 6.3(b.)). The low correlation between pre-treatment solid loading and enzymatic hydrolysis sugar concentration is similar to what was reported previously (Lu et al., 2009). Operating pre-treatment at high solid loadings is economically favorable due to the reduced reactor volume and chemical costs, however, biomass was found to not be fully wetted at solid loading ratios above 20 wt%. The optimal pre-treatment solid loading was thus taken to be 20 wt% for both AMD and H_2SO_4 pre-treatment.

As can be seen in Figure 6.2 and Figure 6.3 there is only a slight increase in the glucose concentration and yield from 1 day of enzymatic hydrolysis to 2 days of enzymatic hydrolysis.

6.3.4 SHF & SSF experiments

The concentration of glucose during hydrolysis in SHF is presented in Figure 6.4

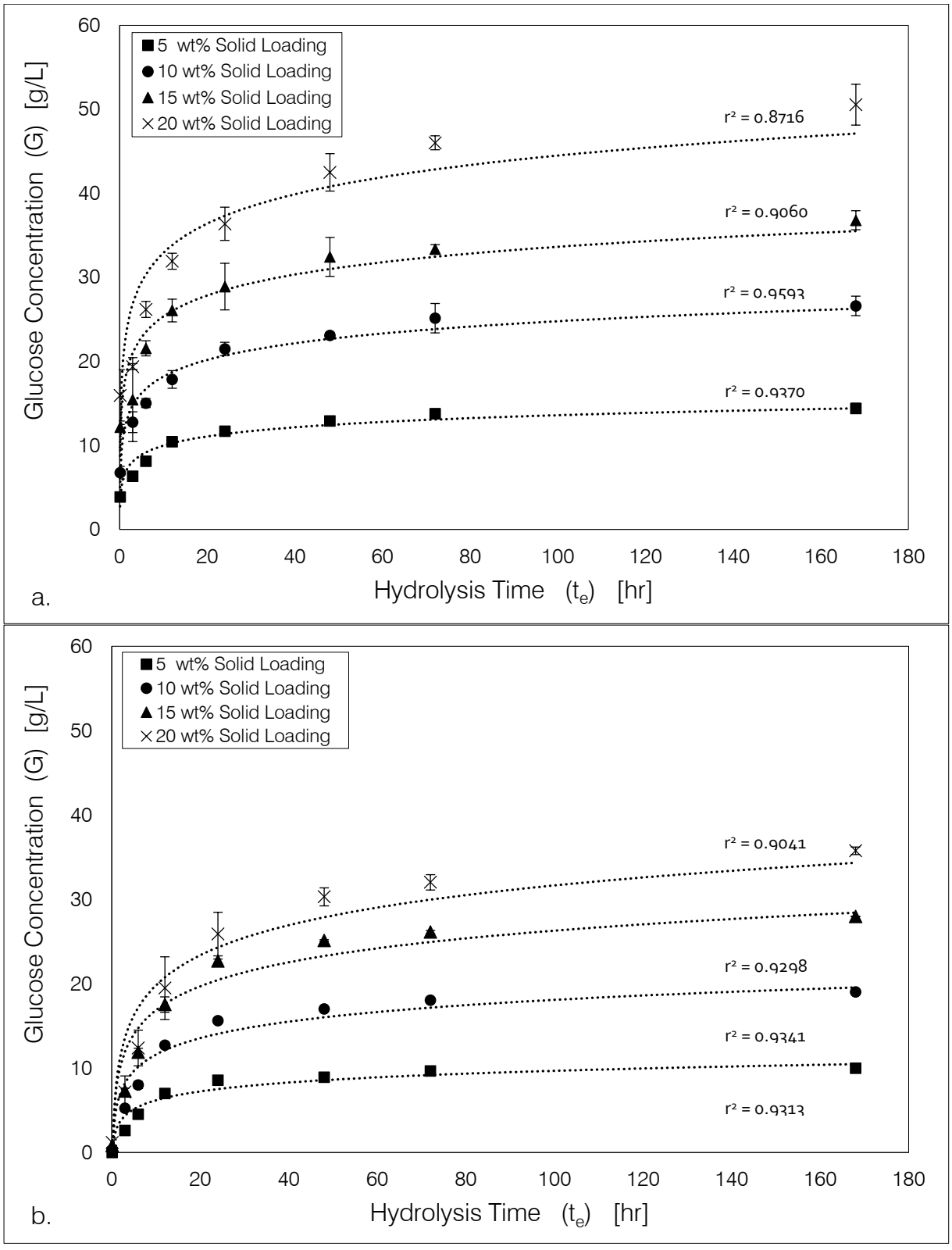

Figure 6.4: Concentration of glucose during hydrolysis for different solid loadings for biomass pre-treated with H_2SO_4 (a.) and AMD (b.)

Increasing the solid loading results in an increase in final glucose concentration. This was found for both H_2SO_4 pre-treatment (Figure 6.4(a.)), ranging from 14.41 g/L at 5 wt% to 50.56 g/L at 20 wt%, and AMD pre-treatment (Figure 6.4 (b)), ranging from 9.89 g/L at 5 wt% to 35.76 g/L at 20 wt%. An increase in glucose inhibition at higher solid loadings was not apparent.

A previous study that investigated the production of glucose from grass pre-treated with AMD achieved a maximum glucose concentration of 4.8 g/L (Magowo et al., 2015). The final glucose concentrations achieved in this study are significantly better than this at all biomass solid loading ratios.

It was found that in hydrolysis the final concentration of glucose produced from biomass pre-treated with AMD was 71.9 ± 2.9% of that achieved in biomass pre-treated with H_2SO_4.

As can be seen in Figure 6.4, the proposed equations (Equations 6.1 – 6.2) fit the experimentally determined glucose concentration. The correlation between the measured and predicted glucose concentration ranges between 0.87 and 0.93 for H_2SO_4 pre-treatment, and 0.90 to 0.93 for AMD pre-treatment of the biomass. The predicted concentration is generally within the standard deviation of the measured concentrations. Notwithstanding this, the model appears to overpredict the glucose concentration initially (before 1 day) and thereafter predicts slightly less than that measured.

The concentration of ethanol and glucose during fermentation is presented in Figure 6.5, along with the model.

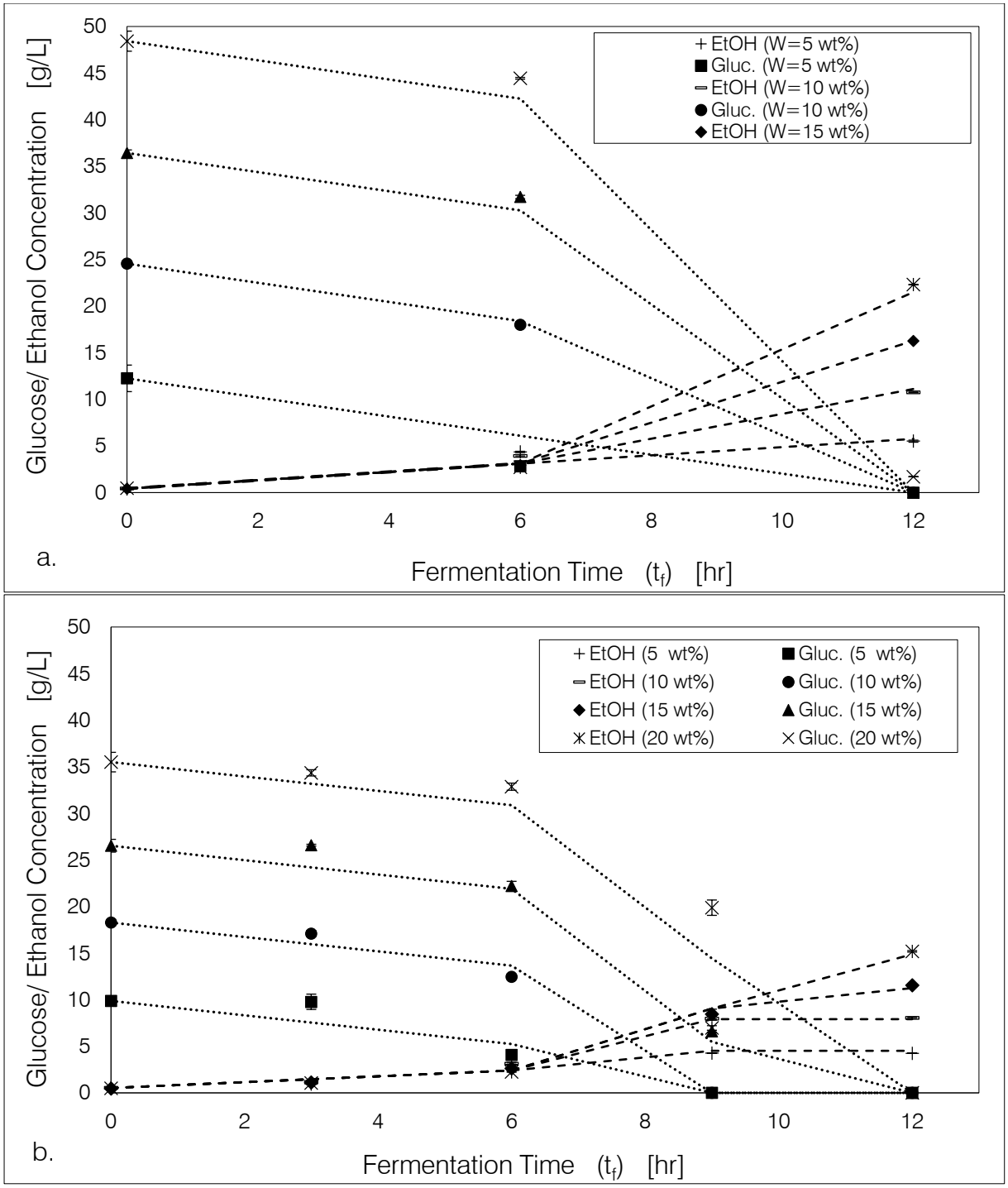

Figure 6.5: Concentration of glucose (Gluc.) and ethanol (EtOH) during fermentation for different enzymatic hydrolysis solid loadings (wt%) for biomass pre-treated with H_2SO_4 (a.) and AMD (b.).

As can be seen in Figure 6.5, the proposed equations (Equations 6.3 – 6.4) fit the experimentally determined glucose and ethanol concentrations. The correlation between the measured and predicted glucose concentration ranges between 0.96 and 0.99 for H_2SO_4 pre-treatment, and 0.87 to 0.99 for AMD pre-treatment of the biomass.

Likewise, the correlation between measured and predicted ethanol concentration ranges between 0.95 and 0.99 for H_2SO_4 pre-treatment, and 0.93 to 0.99 for AMD pre-treatment of the biomass. This correlation indicates that these equations can be used to accurately model the glucose and ethanol concentrations in this process.

Ethanol produced from hydrolysates with a higher initial glucose concentration produced a higher final ethanol concentration. This was found for both hydrolysates produced from H_2SO_4 pre-treated biomass (Figure 6.5(a.)), ranging from 5.29 g/L to 22.25 g/L, and AMD pre-treated biomass (Figure 6.5(b.)), ranging from 4.11 g/L to 14.83 g/L. As the ethanol concentration was relatively low in all experiments the effects of ethanol toxicity were not apparent. As increasing the solid loading did not result in an increase of either glucose inhibition or ethanol toxicity it is recommended that SHF be conducted at 20 wt% solid loading.

It was found that in fermentation the final concentration of ethanol produced from biomass pre-treated with AMD was 73.5 ± 5.7% of that achieved in biomass pre-treated with H_2SO_4.

A review of bioethanol production from grass reported a final ethanol concentrations ranging between 4.72 – 16.0 g/L using SHF (Mohapatra et al., 2017). The final ethanol concentration achieved at 20 wt% in this study are towards the higher end of this range for AMD pre-treatment (14.83 g/L), and better than previously reported for H_2SO_4 pre-treatment (22.25 g/L). Although the final ethanol concentration achieved in this study was relatively good, the enzymatic hydrolysis used in this study was longer than in previous studies.

The concentration of ethanol produced during SSF is presented in Figure 6.6. The glucose concertation measured during SSF was found to be negligible at all times.

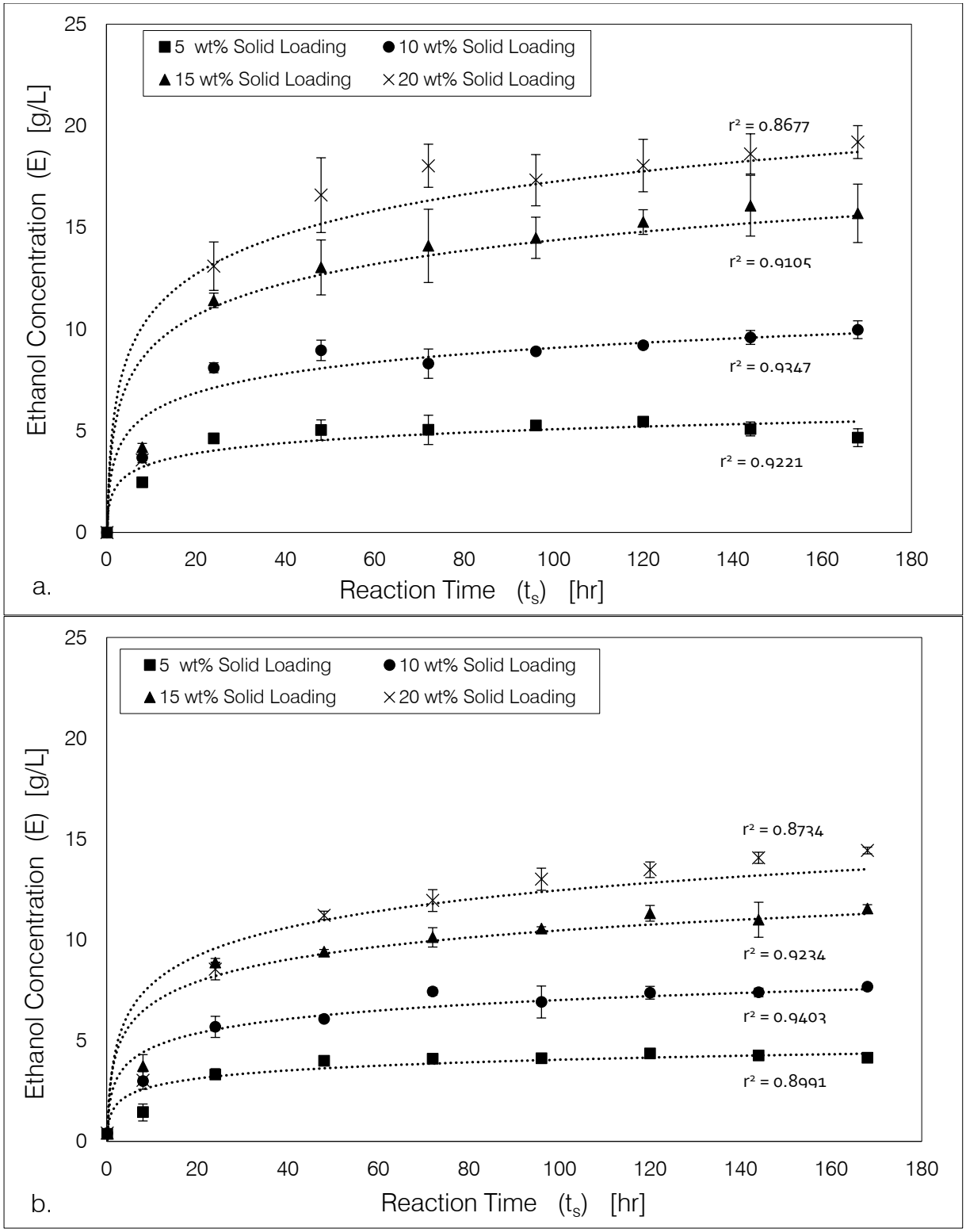

Figure 6.6: Concentration of ethanol during SSF at different biomass solid loadings (wt%) for biomass pre-treated with H_2SO_4 (a.) and AMD (b.).

As can be seen in Figure 6.6, the proposed equations (Equations 6.5 – 6.6) fit the experimentally determined ethanol concentrations. The correlation between the measured and predicted ethanol concentration ranges between 0.87 and 0.93 for H_2SO_4 pre-treatment,

and 0.87 to 0.94 for AMD pre-treatment of the biomass. This indicates these equations can be used to accurately model the ethanol concentration.

Increasing the solid loading results in an increase in final ethanol concentration for both H_2SO_4 pre-treatment (Figure 6.6(a.)), ranging from 4.65 g/L at 5 wt% to 19.20 g/L at 20 wt%, and AMD pre-treatment (Figure 6.6(b.)), ranging from 4.14 g/L at 5 wt% to 14.43 g/L at 20 wt%. As the ethanol concentration was relatively low in all experiments no ethanol toxicity was experienced, it is hence recommended that SSF be conducted at 20 wt% solid loading.

It was found that in SSF the final ethanol concentration produced from biomass pre-treated with AMD was 78.6 ± 6.9% of that achieved with biomass pre-treated with H_2SO_4.

A review of bioethanol production from grass reported a final ethanol concentration ranging between 1.8 – 28.1 g/L using SSF (Mohapatra et al., 2017). The final ethanol concentrations achieved at 20 wt% in this study are in the middle of this range for both AMD pre-treatment (14.43 g/L), and H_2SO_4 pre-treatment (19.20 g/L). Although the use of different operating conditions in different studies makes a direct comparison between studies less meaning full, the final ethanol concentration is a good indicator as operating conditions are often optimized to achieve a higher final ethanol concentration so as to reduce product separation cost.

Although the final ethanol concentrations achieved in this study are comparable to previous studies for SSF and SHF using grasses, the final concentration of ethanol is still significantly lower than what is assumed to be achievable (53 g/L) using the most advanced technology and suitable feedstocks (Humbird et al., 2011).

A summary of the empirical equations used is presented in Table 6.2, and the values for the different empirical constants are presented in Table 6.3.

Table 6.2: Summary of empirical equations

Reaction	Equation	
SHF Hydrolysis	$G = (m_{1,M}W + c_{1,M})ln(t) + (m_{1,C}W + C_{1,C})$	
SHF Fermentation	$G = G_0 - r_g \times t_f$	$for\ t_f \in 0{:}6\ hr$
	$G = G_0 - r_{lg} \times 6 - r_s \times (t_f - 6)$	$for\ t_f \in 6{:}12\ hr$
SSF	$E = (m_{2,M}W + c_{2,M})ln(t) + (m_{2,C}ln(W) + c_{2,C})$	

Table 6.3: Empirically determined constants for equations modeling concentration of glucose and ethanol over time in SHF and SSF.

	Constant	Value for biomass pre-treated with H_2SO_4	Value for biomass pre-treated with AMD
Hydrolysis	$m_{1,M}$	0.2224	0.2432
	$c_{1,M}$	0.4858	0.3535
	$m_{1,C}$	1.0071	0.3625
	$C_{1,C}$	1.4986	1.2735
Fermentation	r_g	1.0282	0.7723
	r_s	7.1231	5.4772
	$Y_{\frac{P}{S}}$	0.4352	0.4043
	Yield (%)	85.15	79.10
SSF	$m_{2,M}$	0.1437	0.0973
	$c_{2,M}$	0.0135	0.0865
	$m_{2,C}$	1.8872	1.3983
	$c_{2,C}$	-1.4286	-0.8637

The concentration of glucose and ethanol achieved from biomass pre-treated with AMD ranged between 67 – 89% of that produced from biomass pre-treated with H_2SO_4. The average was 74.8 ± 5.2%. The lower concentrations of glucose/ethanol obtained from AMD pre-treatment indicates that it is a less effective pre-treatment. This may be due to a lower concentration of H^+ ions in the AMD compared to the 1% H_2SO_4 solution. The deposition of metals onto the grass surface during AMD pre-treatment may also hinder enzymatic hydrolysis.

Although lower final ethanol concentrations require more energy for product separation (distillation), the possible benefit of partial remediation of AMD or incorporation of the two processes into one may make pre-treatment with AMD advantageous. The potential for cheap/free AMD may also provide added economic incentive for its use. It is recommended that further research be carried out so as to try to achieve higher glucose/ethanol concentrations from biomass pre-treated with AMD that are comparable to that of biomass pre-treated with H_2SO_4.

The high correlation between the experimentally determined and model-predicted concentrations (both glucose and ethanol) indicates that the proposed equations accurately model the glucose and ethanol concentration over time. The proposed equations are well suited to initial process design as determining the equation coefficients is less demanding of time and resources than more complicated models.

6.4. Conclusion

It was found that the optimum conditions for pre-treatment at low temperature (90°C) were 20 wt% solid loading for both AMD and H_2SO_4, with a pre-treatment time of 3 days for AMD pre-treatment and 1 day for H_2SO_4 pre-treatment. The AMD pre-treatment was found to achieve glucose and ethanol concentrations of 70 – 80% of the glucose and ethanol concentrations achieved with H_2SO_4 pre-treatment. Simple equations were proposed that were able to model the glucose and ethanol concentration in SHF and SSF based only on the solid loading of biomass and empirically determined coefficients. The empirical equations and optimal parameters determined in this chapter can be used for modeling of bioethanol production under the conditions tested. This can be integrated into a techno-economic evaluation of a process to produce lignocellulosic bioethanol from indigenous South African grasses using either AMD or dilute H_2SO_4 pre-treatment.

6.5. Acknowledgments

This work is based on research supported in part by the National Research Foundation of South Africa (Grant Numbers: 111864). The support of the University of the Witwatersrand, Johannesburg is also acknowledged.

6.6. References

Alvira, P., Tomas-Pejo, E., Ballesteros, M., Negro, M.J., 2010. Pretreatment technologies for an efficient bioethanol production process based on enzymatic hydrolysis: A review. Bioresour. Technol. 101, 4851–4861. doi:10.1016/j.biortech.2009.11.093

Ayoub, M.-J., Legras, J.-L., Saliba, R., Gaillardin, C., 2006. Application of Multi Locus Sequence Typing to the analysis of the biodiversity of indigenous Saccharomyces cerevisiae wine yeasts from Lebanon. J. Appl. Microbiol. 100, 699–711. doi:10.1111/j.1365-2672.2006.02817.x

Bansal, P., Hall, M., Realff, M.J., Lee, J.H., Bommarius, A.S., 2009. Modeling cellulase kinetics on lignocellulosic substrates. Biotechnol. Adv. 27, 833–848. doi:10.1016/j.biotechadv.2009.06.005

Burman, N.W., Harding, K.G., Sheridan, C.M., Van Dyk, L., 2018a. Evaluation of a combined lignocellulosic / waste water bio-refinery for the simultaneous production of valuable biochemical products and the remediation of acid mine drainage. Biofuels, Bioprod. Biorefining 12, 649–664. doi:10.1002/bbb.1880

Burman, N.W., Sheridan, C., van Dyk, L., Harding, K.G., 2018b. Modelling of low temperature dilute sulfuric acid pre-treatment of South African grass. Bioresour. Technol. Reports 4, 21–28. doi:10.1016/j.biteb.2018.08.014

Burman, N.W., van Dyk, L., Postma, F., Sheridan, C., Simate, G.S., HArding, K.G., 2017. Flow Sheet and Sensitivity Analyses for the Bio-Remediation of Acid Mine Drainage Using Sulfate Reducing Bacteria and South African Grasses, in: 2nd International Conference on Energy, Evironment and Climate Change (ICEECC). Pointe Aux Piments, Mauritius.

Dowe, N., Mcmillan, J.D., 2008. SSF Experimental Protocols — Lignocellulosic Biomass Hydrolysis and Fermentation Laboratory Analytical Procedure. Golden, Co.

E4TECH, RE-CORD, WUR, 2015. From the Sugar Platform to biofuels and biochemicals, Final report for the European Commission Directorate-General Energy. doi:contract No. ENER/C2/423-2012/SI2.673791

Humbird, D., Davis, R., Tao, L., Kinchin, C., Hsu, D., Aden, A., Schoen, P., Lukas, J., Olthof, B., Worley, M., Sexton, D., Dudgeon, D., 2011. Process Design and Economics for Biochemical Conversion of Lignocellulosic Biomass to Ethanol. Golden, Co.

IPCC, 2014. Climate Change 2014: Contribution of Working Groups I, II and III to the Fifth Assessment Report of the Intergovernmental Panel on Climate Change, in: Core Writing Team, Pachauri, R.K., Meyer, L.A. (Eds.), . IPCC, Geneva, Switzerland, p. 151.

Johnson, D.B., Hallberg, K.B., 2005. Biogeochemistry of the compost bioreactor components of a composite acid mine drainage passive remediation system. Sci. Total Environ. 338, 81–93. doi:10.1016/j.scitotenv.2004.09.008

Lange, J., 2007. Lignocellulose conversion : an introduction to chemistry ,. Biofuels, Bioprod. Biorefining 1, 39–48. doi:10.1002/bbb

Lee, D., Ownes, V.N., Boe, A., Jeramyama, P., 2007. Composition of Herbaceous Biomass Feedstocks. Brookings, SD.

Liao, W., Liu, Y., Wen, Z., Frear, C., Chen, S., 2008. Kinetic Modeling of Enzymatic Hydrolysis of Cellulose in Differently Pretreated Fibers From Dairy Manure 101, 441–451. doi:10.1002/bit.21921

Lu, X., Zhang, Y., Angelidaki, I., 2009. Optimization of H2SO4-catalyzed hydrothermal pretreatment of rapeseed straw for bioconversion to ethanol: Focusing on pretreatment at high solids content. Bioresour. Technol. 100, 3048–3053. doi:10.1016/j.biortech.2009.01.008

Magowo, E., Rumbold, K., Sheridan, C., 2015. The Utilization of Cellulosic Biomass in treating AMD and

the Subsequent Generation of Fermentable Sugars, in: 10th International Conference on Acid Rock Drainage and IMWA Anual Conference. pp. 1–12.

Maurya, D.P., Singla, A., Negi, S., 2015. An overview of key pretreatment processes for biological conversion of lignocellulosic biomass to bioethanol. 3 Biotech 5, 597–609. doi:10.1007/s13205-015-0279-4

McCarthy, T.S., 2011. The impact of acid mine drainage in South Africa. S. Afr. J. Sci. 107, 1–7. doi:10.4102/sajs.v107i5/6.712

Mccarthy, T.S., Steyl, G., Maree, J., Zhao, H., 2010. MINE WATER MANAGEMENT IN THE WITWATERSRAND WITH SPECIAL EMPHASIS ON ACID MINE DRAINAGE: Report to the Inter-Ministerial Committee on Acid Mine Drainage 1–128.

Menegol, D., Scholl, A.L., Fontana, R.C., Dillon, A.J.P., Camassola, M., 2014. Increased release of fermentable sugars from elephant grass by enzymatic hydrolysis in the presence of surfactants. Energy Convers. Manag. 88, 1252–1256. doi:10.1016/j.enconman.2014.02.071

Mohapatra, S., Mishra, C., Behera, S.S., Thatoi, H., 2017. Application of pretreatment, fermentation and molecular techniques for enhancing bioethanol production from grass biomass – A review. Renew. Sustain. Energy Rev. 78, 1007–1032. doi:10.1016/j.rser.2017.05.026

Mosier, N., Wyman, C., Dale, B., Elander, R., Lee, Y.Y., Holtzapple, M., Ladisch, M., 2005. Features of promising technologies for pretreatment of lignocellulosic biomass. Bioresour. Technol. 96, 673–686. doi:10.1016/j.biortech.2004.06.025

Olsson, L., Soerensen, H.R., Christensen, H., Ktogh, K.M., Meyer, A.S., 2006. Separate and Simultaneous Enzymatic Hydrolysis and Fermentation of Wheat Hemicellulose With Recombinant Xylose Utilizing Saccharomyces cerevisiae. Appl. Biochem. Biotechnol. 129–132, 117–129.

Philippidis, G.P., Smith, T.K., 1995. Limiting factors in the simultaneous saccharification and fermentation process for conversion of cellulosic biomass to fuel ethanol. Appl. Biochem. Biotechnol. 51, 117–124. doi:10.1007/BF02933416

Ramla, B., Sheridan, C., 2015. The potential utilisation of indigenous South African grasses for acid mine drainage remediation. Water SA 41, 247–252. doi:10.4314/wsa.v41i2.10

Saha, B.C., Iten, L.B., Cotta, M.A., Wu, Y.V., 2005. Dilute Acid Pretreatment , Enzymatic Saccharification , and Fermentation of Rice Hulls to Ethanol. Biotechnol. Prog. 21, 816–822.

Searcy, E., Flynn, P.C., 2008. Processing of Straw / Corn Stover : Comparison of Life Cycle Emissions. Int. J. Green Energy 5, 423–437. doi:10.1080/15435070802498010

Simate, G.S., Ndlovu, S., 2014. Acid mine drainage: Challenges and opportunities. J. Environ. Chem. Eng. 2, 1785–1803. doi:10.1016/j.jece.2014.07.021

Sindhu, R., Binod, P., Pandey, A., 2016. Biological pretreatment of lignocellulosic biomass - An overview. Bioresour. Technol. 199, 76–82. doi:10.1016/j.biortech.2015.08.030

Sluiter, A., Hames, B., Ruiz, R., Scarlata, C., Sluiter, J., Templeton, D., 2008a. Determination of Sugars, Byproducts, and Degradation Products in Liquid Fraction Process Samples. Golden , Co.

Sluiter, A., Hames, B., Ruiz, R., Scarlata, C., Sluiter, J., Templeton, D., Crocker, D., 2008b. Determination of Structural Carbohydrates and Lignin in Biomass.

Sun, Y., Cheng, J., 2002. Hydrolysis of lignocellulosic materials for ethanol production: A review. Bioresour. Technol. 83, 1–11. doi:10.1016/S0960-8524(01)00212-7

Taherzadeh, M.J., Karimi, K., 2008. Pretreatment of lignocellulosic wastes to improve ethanol and biogas production: A review. Int. J. Mol. Sci. 9, 1621–1651. doi:10.3390/ijms9091621

Torget, R., Werdene, P., Himmel, M., Grohmann, K., 1990. Dilute Acid Pretreatment of Short Rotation Woody and Herbaceous Crops. Appl. Biochem. Biotechnol. 24, 115–126. doi:10.1007/BF02920238

Westensee, D.K., Rumbold, K., Harding, K.G., Sheridan, C.M., van Dyk, L.D., Simate, G.S., Postma, F., 2018. The availability of second generation feedstocks for the treatment of acid mine drainage and to improve South Africa's bio-based economy. Sci. Total Environ. 637–638, 132–136. doi:10.1016/j.scitotenv.2018.04.410

Wongwatanapaiboon, J., Kangvansaichol, K., Burapatana, V., Inochanon, R., Winayanuwattikun, P., Yongvanich, T., Chulalaksananukul, W., 2012. The Potential of Cellulosic Ethanol Production from Grasses in Thailand. J. Biomed. Biotechnol. doi:10.1155/2012/303748

Ye, Z., Berson, R.E., 2011. Bioresource Technology Kinetic modeling of cellulose hydrolysis with first order inactivation of adsorbed cellulase. Bioresour. Technol. 102, 11194–11199. doi:10.1016/j.biortech.2011.09.044

Yu, Z., Zhang, H., 2003. Ethanol fermentation of acid-hydrolyzed cellulosic pyrolysate with Saccharomyces cerevisiae. Bioresour. Technol. 90, 95–100. doi:10.1016/S0960-8524(03)00093-2

Zheng, Y., Pan, Z., Zhang, R., Jenkins, B.M., 2009. Kinetic Modeling for Enzymatic Hydrolysis of Pretreated Creeping Wild Ryegrass 102, 1558–1569. doi:10.1002/bit.22197

Chapter 7: Feasibility Assessment of the Production of Bioethanol from Lignocellulosic Biomass Pre-treated with Acid Mine Drainage

(Published in Renewable Energy, 2020) This chapter developed process flowsheets for the enzymatic hydrolysis and fermentation of South African grass pre-treated with AMD to produce bioethanol. Estimates of capital and operating costs were used to determine the feasibility of both SHF and SSF process configurations. Pre-treatment with AMD was compared to pre-treatment using H_2SO_4. This addresses objective d.

Burman, N.W., Sheridan, C.M., Harding, K.G., 2020. Feasibility assessment of the production of bioethanol from lignocellulosic biomass pretreated with acid mine drainage (AMD). Renew. Energy 157, 1148–1155. doi:10.1016/j.renene.2020.05.086

Abstract: A techno-economic evaluation of a lignocellulosic bioethanol facility that uses acid mine drainage for the pre-treatment of Weeping lovegrass (*Eragrostis curvula*) was performed. Both separate hydrolysis and fermentation (SHF) and simultaneous saccharification and fermentation (SSF) reactor configurations were evaluated. Results were compared to an evaluation of the same process with biomass pre-treated with dilute H_2SO_4. Capital and operating costs were estimated, and a simple economic evaluation was conducted. It was found that all scenarios made a loss except for biomass pre-treated with H_2SO_4 in the SHF reactor configuration, although the high capital cost resulted in a payback period of 80.7 years, which is infeasible. SHF was found to produce more ethanol at a lower capital cost than SSF and should be further considered for incorporation into a process that simultaneously remediates AMD. Incorporating the simultaneous remediation of AMD into the process could help improve process economics.

Keywords: Lignocellulosic Bioethanol; Economic Evaluation; Acid Mine Drainage (AMD); Pre-treatment; Separate Hydrolysis and Fermentation (SHF); Simultaneous Saccharification and Fermentation (SSF)

7.1. Introduction

The Intergovernmental Panel on Climate Change has concluded in its 5th Assessment Report that the burning of fossil fuels is "extremely likely" to be the cause of recent increased atmospheric and oceanic temperatures (IPCC, 2014a). Although starch-based bioethanol has been demonstrated to be a renewable alternative to petrol (E4TECH et al., 2015), it has various drawbacks including (amongst others) increases in food prices, net energy losses, a reduction of available land for food production, and land degradation (Lange, 2007).

Lignocellulosic biomass (agricultural waste, forestry residue and energy crops) has been identified as a source of biomass that can potentially be used to produce bioethanol without these drawbacks in an environmentally friendly manner (Searcy and Flynn, 2008). Lignocellulosic biomass consists of three fractions, cellulose fibrils (linearly linked glucose molecules), surrounded by a matrix of hemicellulose, and lignin (Mosier et al., 2005b). In the production of bioethanol, cellulose is hydrolyzed to glucose by cellulase enzymes. Glucose is then fermented to produce bioethanol (Yu and Zhang, 2003).

Unfortunately, the presence of the lignocellulosic matrix prevents cellulase enzymes from accessing cellulose fibrils, hindering enzymatic hydrolysis. To overcome this the hemicellulosic matrix needs to be disrupted in a pre-treatment process. Various pre-treatment processes have been investigated including physical, chemical, biological, and physico-chemical processes. Dilute H_2SO_4 pre-treatment has been found to be the most commercially favorable process (Alvira et al., 2010; Burman et al., 2018b; Maurya et al., 2015; Mosier et al., 2005b; Taherzadeh and Karimi, 2008)

Another drawback to enzymatic hydrolysis is that the glucose produced inhibits cellulase activity. This is most evident in the separate hydrolysis and fermentation (SHF) reactor configuration, in which enzymatic hydrolysis and fermentation occur in separate reactors. To overcome this, various reactor configurations which aim to maintain a low glucose concentration, have been investigated. These include: simultaneous saccharification and fermentation (SSF), in which enzymatic hydrolysis and fermentation occur simultaneously in the same reactor; simultaneous saccharification and co-fermentation (SSCF) in which enzymatic hydrolysis of cellulose, fermentation of glucose and co-fermentation of hemicellulose produced in pre-treatment all occur in the same reactor; and consolidated

bioprocessing (CBP) in which enzyme production, enzymatic hydrolysis, and fermentation all occur in the same reactor, with a host of different micro-organisms.

Recently there have been investigations into the use of acid mine drainage (AMD) for the pre-treatment of lignocellulosic biomass (Burman et al., 2018a; Magowo et al., 2015). The acidity present in the AMD hydrolyzes the hemicellulose, releasing sugars into the AMD, similar to dilute H_2SO_4 pre-treatment.

AMD is formed through a series of geochemical reactions when sulfate rich minerals are exposed to oxygen and water, often through mining activity (Johnson and Hallberg, 2005a). It is highly acidic (pH 1 – 3) with high sulfate (<20 g/L) and heavy metal (<5 g/L) concentration (Johnson and Hallberg, 2005a). AMD has been found to have a negative effect on aquatic and riparian ecosystems due to the toxic effects of increased concentration of acid, sulfate, and heavy metals, on aquatic life. As the pH rises through natural processes dissolved heavy metals precipitate on the ecosystem floor (Simate and Ndlovu, 2014).

There has been a recent study that has determined the optimal pre-treatment times for biomass pre-treated with AMD, as well as the rate of enzymatic hydrolysis, fermentation, and SSF for this optimally pre-treated biomass (Burman et al., 2019).

It has also been shown that the sugars present in AMD after pre-treatment can be used by sulfate-reducing bacteria (SRB) in a process known as dissimilatory sulfate reduction (DSR) (Magowo et al., 2015; Ramla and Sheridan, 2015). This process partially remediates the water through a reduction of sulfate and heavy metal concentrations and an increase in pH. Although various work has been done on the simultaneous production of ethanol and remediation of AMD (Burman et al., 2018a, 2018b, 2017; Magowo et al., 2015; Ramla and Sheridan, 2015; Westensee et al., 2018), there has yet to be a techno-economic evaluation of any aspect of this process.

There have been various techno-economic evaluations performed on the production of bioethanol from lignocellulosic biomass (Gnansounou and Dauriat, 2010). Although all of these processes utilize hydrolysis to produce sugars, which are subsequently fermented to bioethanol, there have been various feedstocks and processes evaluated. Feedstocks evaluated included corn stover (Bals et al., 2011; Humbird et al., 2011; Kazi et al., 2010; Klein-marcuschamer et al., 2010; Sendich et al., 2008), switchgrass (Gnansounou and Dauriat, 2010;

Huang et al., 2009; Laser et al., 2009), hardwoods and softwoods (Gnansounou and Dauriat, 2010; Huang et al., 2009; National Academy of Sciences et al., 2009; Piccolo and Bezzo, 2009), and paper sludge (Robus et al., 2016). There have been various pre-treatments evaluated including, dilute acid pre-treatment (Gnansounou and Dauriat, 2010; Huang et al., 2009; Humbird et al., 2011; Klein-marcuschamer et al., 2010; Piccolo and Bezzo, 2009), ammonia fiber explosion (AFEX) (Bals et al., 2011; Laser et al., 2009; Sendich et al., 2008), and hot water (National Academy of Sciences et al., 2009). Different reactor configurations for the enzymatic hydrolysis and fermentation process have been evaluated, including SHF (Humbird et al., 2011), SSF (Robus et al., 2016), CBP (Laser et al., 2009; Sendich et al., 2008) and SSCF (Sendich et al., 2008).

Most of these techno-economic studies have been performed using a variety of process simulation, flow sheeting and engineering software, *e.g.* Aspen Plus™, Microsoft® Excel, and Capcost. Typically, flowsheets and stream tables are first developed, after which they are used to provide estimates of operating and capital costs which are used in a techno-economic evaluation of the process.

The study presented here investigated the production of bioethanol from *Eragrostis curvula* (Weeping lovegrass), pre-treated with AMD, and for comparison, pre-treated with H_2SO_4. Both SHF and SSF reactor configurations are investigated. The AMD remediation process is not investigated in this study.

The objectives of this study are to develop a process flowsheet for all scenarios; estimate the operating costs; estimate the capital costs; and perform an economic evaluation to determine the feasibility of the process.

7.2. Methods

7.2.1 Process flowsheet development

7.2.1.1 Simulation Basis

The simulation was carried out using Aspen Plus™ V8.4 (www.aspentech.com), with a basis of 90 ton/hr of milled (4 mm) dry *Eragrostis curvula* (Weeping lovegrass) grass with a composition of 37% cellulose, 29% xylan (hemicellulose), 19% acid insoluble lignin, 6% acid soluble lignin, 6% ash and 3% protein (Burman et al., 2019).

Separate simulations were developed for both SHF and SSF, with pre-treatment using AMD, and for comparison, H_2SO_4. There were thus four scenarios considered, *i.e.* AMD pre-treatment with SHF (A-SHF), H_2SO_4 pre-treatment with SHF (H-SHF), AMD pre-treatment with SSF(A-SSF), and H_2SO_4 pre-treatment with SSF (H-SSF).

The model made use of the NREL database for chemical compounds that was used in the DW1102A Aspen Plus™ simulation (Humbird et al., 2011). This study made use of the NRTL equations of state for modeling of vapor-liquid equilibrium.

7.2.1.2 Process description

The process consists of three sections: pre-treatment (Figure 7.1); hydrolysis and fermentation (SHF (Figure 7.2); SSF (Figure 7.3)) and product separation (Figure 7.4).

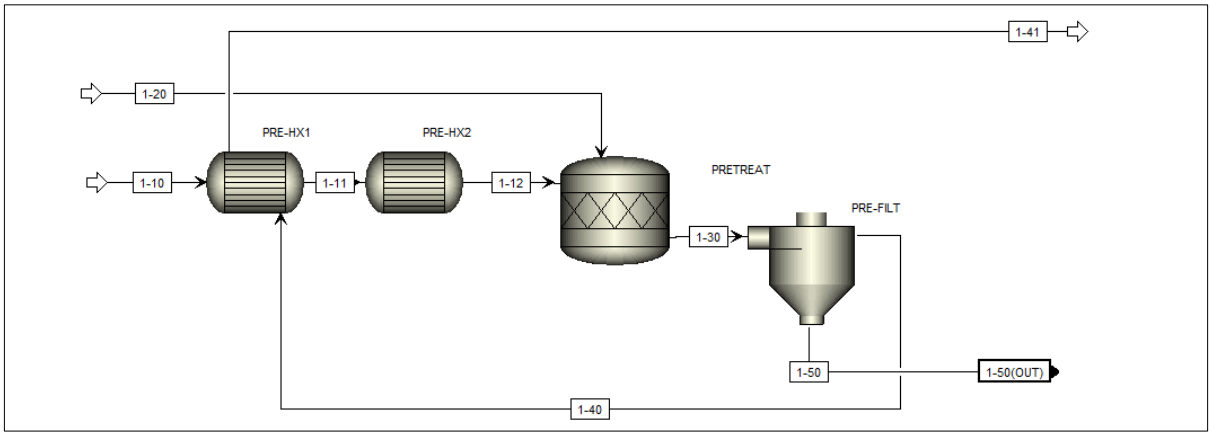

Figure 7.1: Layout of the pre-treatment section used in the Aspen Plus™ simulation

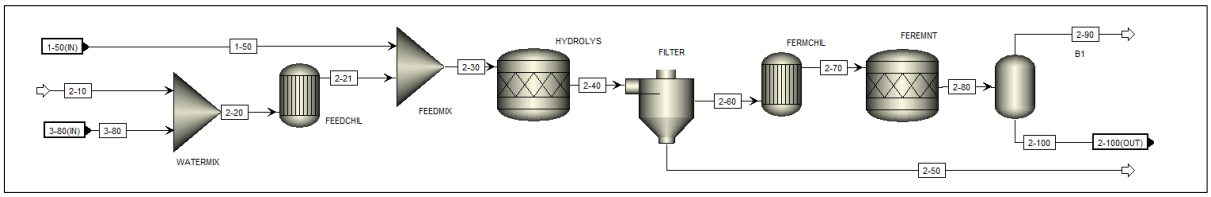

Figure 7.2: Layout of the SHF section used in the Aspen Plus™ simulation

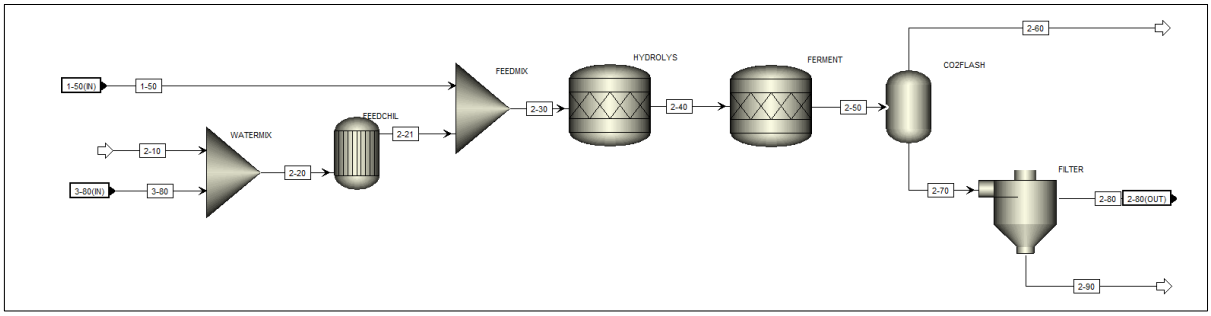

Figure 7.3: Layout of the SSF section used in the Aspen Plus™ simulation

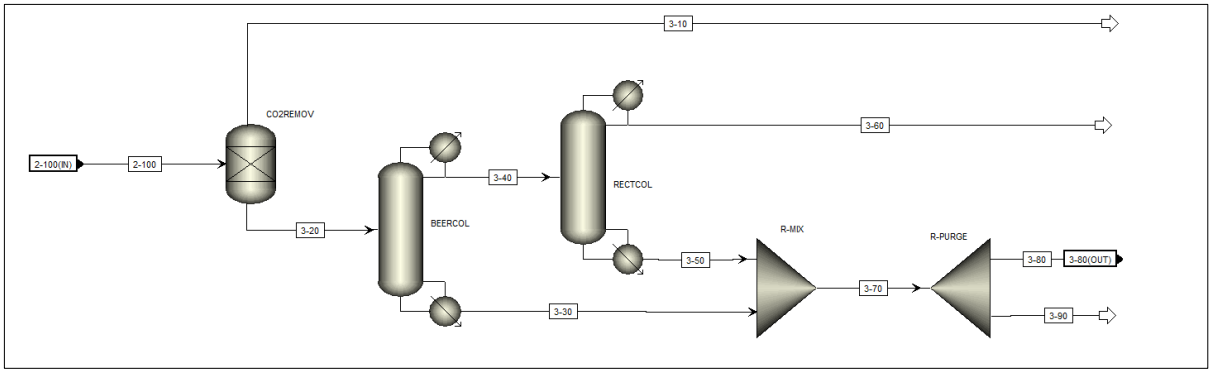

Figure 7.4: Layout of the product separation section used in the Aspen Plus™ simulation

Pre-treatment

In the pre-treatment section, grass is fed into a batch reactor (PRETREAT) where it undergoes pre-treatment by either AMD or H_2SO_4 which has been heated to 90°C (PRE-HX1 & PRE-HX2). In pre-treatment, xylan is hydrolyzed to xylose, breaking up the ligno-hemicellulosic structure, making cellulose more susceptible to enzymatic hydrolysis. The pre-treated biomass is separated from the liquid (PREFILT) and sent to the hydrolysis and fermentation section. The liquid product is first used to heat the incoming liquid stream before going to further treatment/ disposal (not considered in this study).

SHF

In SHF, pre-treated biomass is fed into the batch hydrolysis reactor (HYDROLYS) which is operated at 50°C. Makeup water and water recycled from the product separation section (cooled to 50°C), are fed into this reactor, along with cellulase enzymes, to achieve a solid loading of 20 wt% biomass. Cellulase enzymes catalyze the hydrolysis of cellulose to glucose. After hydrolysis is complete, the liquid fraction of the product stream is separated from the solid fraction (FILTER), cooled to 35°C (FERMCHIL) and fed into the fermenter (FERMENT). An inoculum of *Saccharomyces cerevisiae* is fed into the fermenter. *Saccharomyces cerevisiae* facilitates the conversion of glucose to ethanol and CO_2. Gas phase CO_2 produced in fermentation will leave the top of the fermenter. Solid biomass is then separated from the liquid product stream (FILTER) which goes to the product separation section.

SSF

In SSF, pre-treated biomass is fed into the batch SSF reactor which is operated at 38°C. Make-up water and water recycled from the product separation section are blended and cooled to 38°C before passing into the SSF reactor, together with cellulase enzymes and *Saccharomyces cerevisiae*, to achieve a biomass solid loading of 20 wt%. In this reactor there is the

simultaneous hydrolysis of cellulose to glucose and fermentation of glucose to ethanol. Gas phase CO_2 produced in fermentation will leave the top of the fermenter. Solid biomass is then separated from the liquid product stream (FILTER) which goes to the product separation section.

Product separation

The product separation section consists of two distillation columns. In the 1st distillation column (BEERCOL) the distillate stream contains 40% ethanol, with a 95% recovery of ethanol to the distillate. The second column (RECTCOL) produces a distillate of 90% ethanol with a recovery of 95% ethanol to the distillate. The bottoms stream from both columns is recycled/ purged as necessary.

7.2.1.3 Simulation specifications

All reactors were modeled using an RStoic block with conversions determined in previous experiments (Burman et al., 2019). In SSF the hydrolysis and fermentation sections were modeled using separate blocks for hydrolysis (HDROLYSIS) and fermentation (FERMNET) although this process would occur in one reactor. This was done to increase model understanding and troubleshooting capabilities and is valid as the hydrolysis and fermentation reactions would have occurred in series anyway if they were in the same RStoic block. In both SHF and SSF a Flash2 block (CO2FLASH) has been included after the FERMENT block to model the vapor-liquid equilibrium of CO_2 and ethanol entering the product separation section.

Liquid streams entering/exiting reactors were heated/cooled to appropriate temperatures, by heat exchangers modeled by the Heater block (2 stream heat exchanger) or HeatX block (heat exchanger with a utility) as required. Solid-liquid separation was modeled using the SSplit block. Distillation columns were modeled with DSTWU block, which uses the Winn-Underwood-Gilliland shortcut method to model distillation columns based on the assumptions of constant relative volatilities and constant molar overflow.

The presence of CO_2 made the modeling of distillation with DSTWU blocks technically difficult, and hence it was assumed that there was no CO_2 present. This was accomplished by the incorporation of a Sep block (CO2REMOV) prior to distillation.

A summary of all block design specifications is presented in Table 7.1. A summary of the design specifications that were manipulated by Aspen Plus™ is presented in Table 7.2.

Table 7.1: Summary of block specifications used in Aspen Plus™ simulations

	Block Name	Block Type	Specification
Pre-treatment	FEEDCHILL	Heater	$T_{hot, out}$ = 50°C
	PRE-HX1	HeatX	$T_{hot, out}$ = 30°C
	PRE-HX2	Heater	$T_{cold, out}$ = 90°C
	PRETREAT	RStoic	RX1: Xylan → Xylose = 0.5
	PREFILT	SSPLIT	1-50 = 100% solids 1-41 = 90% liquid
SHF	HYDROLYSIS	RStoic	Time = 168 Hrs RX1: Cellulose → Glucose
	FILTER	SSPLIT	2-50 = 100% solid 2-60 = 95% liquids
	FERMCHILL	HeatX	$T_{cold, out}$ = 35°C
	FERMENT	RStoic	RX1: Glucose → 2CO2 + 2 EtOH X=0.90
	B1	Flash2	T=35°C
SSF	FEEDCHILL	Heater	$T_{hot, out}$ = 38
	HYDROLYSIS	RStoic	time = 168 Hrs RX1: Cellulose → Glucose
	FERMENT	RStoic	RX1: Glucose → 2CO2 + 2 EtOH X=0.90
	CO2FLASH	Flash2	$T_{cold, out}$ = 38°C
	FILTER	SSplit	2-90 = 100% solid 2-80 = 95% liquids
SEP	CO2REMOV	Sep	3-10 = 100% CO2
	BEERCOL	DSTWU	RRATIO = 1.1 times minimum
	RECTCOL	DSTWU	RRATIO = 1.1 times minimum

Table 7.2: Summary of design specifications used in Aspen Plus™ simulation

Design Spec.	Specification	Adjusted variable
DS1	Reaction time = 168 hrs	Glucose conversion in HYDROLYS block
DS2	40% ethanol in BEERCOL distillate	Recovery of water to RECTCOL distillate
DS3	90% ethanol in RECTCOL distillate	Recovery of water RECTCOL to distillate
DS4	Flow rate of water in reactor feed = 20 000 kg/hr	Flow rate of make-up water to FEEDMIX

In hydrolysis, the conversion of cellulose to glucose, and the conversion of glucose to ethanol was modeled using kinetics determined in a previous study (Burman et al., 2019) (Table 7.3). The conversion of cellulose to glucose was varied using a design specification on the total reaction time.

Table 7.3: Summary of empirical equations

Reaction	Equation	
SHF Hydrolysis	$G = (m_{1,M}W + C_{1,M})ln(t) + (m_{1,C}W + C_{1,C})$	
SHF Fermentation	$G = G_0 - r_g \times t_f$	$for\ t_f \in 0{:}6\ hr$
	$G = G_0 - r_{lg} \times 6 - r_s \times (t_f - 6)$	$for\ t_f \in 6{:}12\ hr$
SSF	$E = (m_{2,M}W + C_{2,M})ln(t) + (m_{2,C}ln(W) + C_{2,C})$	

Where G is the glucose concentration (g/L), W is the solid loading fraction of biomass (wt%) t_h, t_f, t_{ssf} are the hydrolysis, fermentation and SSF time respectively (hrs), G_0 is the initial glucose concentration at the start of fermentation (g/L), r_g and r_s are the rates of fermentation in different phases of fermentation (g/L.hr), E is the ethanol concentration in SSF (g/L), and $m_{i,j}$ and $c_{i,j}$ are empirically determined constants (Burman et al., 2019).

The pre-treatment time required for AMD pre-treatment (3 days) and H_2SO_4 pre-treatment (1 day) was based on previous studies (Burman et al., 2019).

7.2.2 Operating costs

Estimation of operating costs was performed using the Aspen Plus™ inbuilt utility and operating cost tools. This was done by defining three utilities and then assigning them to certain operating blocks. The three utilities that were defined are low pressure steam, cooling water and refrigerated water (Table 7.4).

The cost of the utilities was estimated based on the method of Ulrich and Vasudevan (2006), assuming that steam was produced in a natural gas boiler and the electricity used in the production of cooling and refrigeration water was produced in a coal-based power plant. The cost of fuel was assumed to be 3.57 USD/GJ for natural gas and 0.95 USD/GJ for coal (Department of Energy, 2018).

Table 7.4: Summary of the utilities used in the Aspen Plus™ process simulation

	Low pressure steam	Cooling water	Refrigerated water
Cost (USD/GJ)	6.15	1.06	5.08
Tin (°C)	125	30	20
Tout (°C)	124	45	30
Enthalpy change kJ/kg	2191	62.59	41.74
Used at	All reboilers	All condensers, FEEDCHILL (SHF)	FERMCHILL (SHF) FEEDCHILL (SSF)
Pressure (atm)	2.29	1	1
Vapor fraction inlet/ outlet	1/0	0/0	0/0

To minimize operating costs, the inlet and outlet temperature of refrigerated water was assumed to be 20°C and 30°C. Decreasing the temperature of refrigerated water would result in an increase in operating costs but potentially decrease the capital costs, due to decrease in

size of various heat exchangers (FERMCHIL (SHF), FEEDCHILL (SSF)). The optimal temperature of refrigerated water is a parameter that has been identified for future investigation but is not considered in this study.

The DSTWU block does not allow for the allocation of utilities. The utility requirements were thus calculated manually and added to utilities calculated in Aspen Plus™.

The cost of the grass was taken to be 35 USD/ton, as this represents the lowest feedstock cost found in literature. This was based on an investigation into the market value of the feedstock. Due to the lack of physical property data, enzymes were not included in the Aspen Plus™ simulation, however, the cost of enzyme was taken into account. It was assumed enzyme was dosed at 0.25 kg/kg pre-treated biomass. It was assumed that the cost of enzyme was 1.25 USD/kg enzyme. This is once again the cheapest enzyme cost found in literature (Liu et al., 2016). The cost of H_2SO_4 was taken to be 80 USD/ton (Argus Media, 2018).

The market value of the product was taken to be 815.00 USD/ton (E4TECH et al., 2015)

7.2.3 Capital costs

The size of all heat exchangers, columns and pumps were taken from the Aspen Plus™ reactors (PRETREAT, HYDROLYSIS, FERMENT) based on the process flow rates and kinetics of reactions determined by Burman *et al.* (2019) (Chapter 6). All equations used for the determination of reactor volumes are presented in the supplementary data (Appendix C).

An estimation of the capital costs for individual process units was performed using the Capcost2017 program (www.richardturton.faculty.wvu.edu). A summary of the equipment cost is presented in the supplementary data (Appendix C). The cost of the hydrolysis, fermentation, and pre-treatment reactors was estimated using prices from the NREL 2011 design report (Humbird et al., 2011) adjusted to 2017 prices using the Chemical Engineering Price Cost Index (CEPCI). Due to the PRETREAT reactor having similar solid loading, batch time, and temperatures to the HYDROLYSIS reactor, it was assumed that the price per volume of these reactors would be the same. The total installed capital cost was estimated from the total equipment cost using the Lang factor method with a Lang factor of 4.74 (Turton et al., 1998).

7.2.4 Economic evaluation

A simple economic evaluation in which the non-discounted payback period was determined for the process based on the estimated capital costs and annual profit. This evaluation only considered the operating costs mentioned in the operating costs section and did not consider other operating costs such as salaries or tax.

7.3. Results and Discussion

7.3.1 Process flowsheet

A full stream table of all streams can be found in the supplementary data (Appendix C).

Table 7.5: Summary of the raw material costs

	Unit Value	H_2SO_4 Pre-treatment		AMD Pre-treatment	
Raw material	**USD/kg**	**ton/yr**	**MUSD/yr**	**ton/yr**	**MUSD/yr**
Grass	0.035	750 000	25.5	750 000	25.5
Enzyme	1.25	5 500	6.93	5500	6.93
H_2SO_4	0.08	18 000	1.50	0	0
Total			33.9		32.4

The feedstock requirements for scenarios with the same pre-treatment are the same (Table 7.5). This is due to all scenarios have the same basis (90 tons/hr grass) as well as having the same mass balance around the pre-treatment process section, resulting in the same quantity of biomass entering the hydrolysis and fermentation section and hence the same enzyme usage. The cost of H2SO4 was included for scenarios with H_2SO_4 pre-treatment.

Table 7.6: Summary of ethanol yield, volume produced, and revenue from sales for different scenarios.

	Ethanol Yield	Ethanol Volume	Revenue
Scenario*	**L/dry ton**	**ton/Year**	**MUSD/yr**
A-SHF	58.4	44 000	35.7
H-SHF	80.7	60 000	49.3
A-SSF	50.3	38 000	30.7
H-SSF	53.7	40 000	32.8

* A = AMD; H = H_2SO_4

The amount of ethanol produced in different scenarios varies substantially ranging from 38 000 to 60 000 ton/year (Table 7.6). Scenarios with H_2SO_4 pre-treatment produced more ethanol than the scenarios with AMD pre-treatment. The scenarios with SHF reactor configuration produced more ethanol than the scenarios with SSF reactor configuration.

The ethanol yield ranged from 58.4 – 80.7 L/dry ton. This is low in comparison to other techno-economic evaluations which report yields of up to 420 L/dry ton (Huang et al., 2009). One explanation of the comparatively low yield is that other studies are fermenting both C5 and C6 sugars (Humbird et al., 2011), whereas in this study the C5 sugars are required as a carbon source for the SRB. Another explanation is that the yields in this study are based on experiments that were conducted without access to tailored cellulase mixtures, advanced bioreactors, or genetically modified fermentative organisms (Burman et al., 2019).

Table 7.7: Summary of utility duties and utility costs for different scenarios.

Scenario*	Utility Duty TJ/yr	Utility Cost MUSD/yr
A-SHF	2 690	11.4
H-SHF	2 830	11.9
A-SSF	2 340	9.06
H-SSF	2 360	9.13

* A = AMD; H = H2SO4

The heating and cooling duty vary with each scenario from 2 340 to 2 830 TJ/yr (Table 7.7). Total duties required are higher for H_2SO_4 pre-treatment than for AMD pre-treatment, and higher for SHF reactor configuration than SSF reactor configuration. The variation in the heating/cooling duties can mainly be attributed to the different reflux/reboiler requirements in each scenario.

7.3.2 Operating costs and revenue

As can be seen in Table 7.5 the feedstock costs are the same for scenarios with the same pre-treatments (*i.e.* A-SHF & A-SSF; H-SHF & H-SSF). Scenarios with AMD pre-treatment do not require H_2SO_4 and hence have a lower raw material cost. Although there are many other feedstocks, only grass, cellulase enzyme, and H_2SO_4 were accounted for as these are considered to be the most significant costs.

The variation in ethanol revenue (30.7 MUSD/yr – 49.3 MUSD/yr) follows the same trends as the variation in ethanol produced (Table 7.6).

The trends in the utility costs follow the trend in utility duty (Table 7.7), with H-SHF (11.9 MUSD/yr) being the highest, followed by A-SHF (11.4 MUSD/yr), followed by H-SSF (9.13 MUSD/yr), and lastly A-SSF (9.06 MUSD/yr).

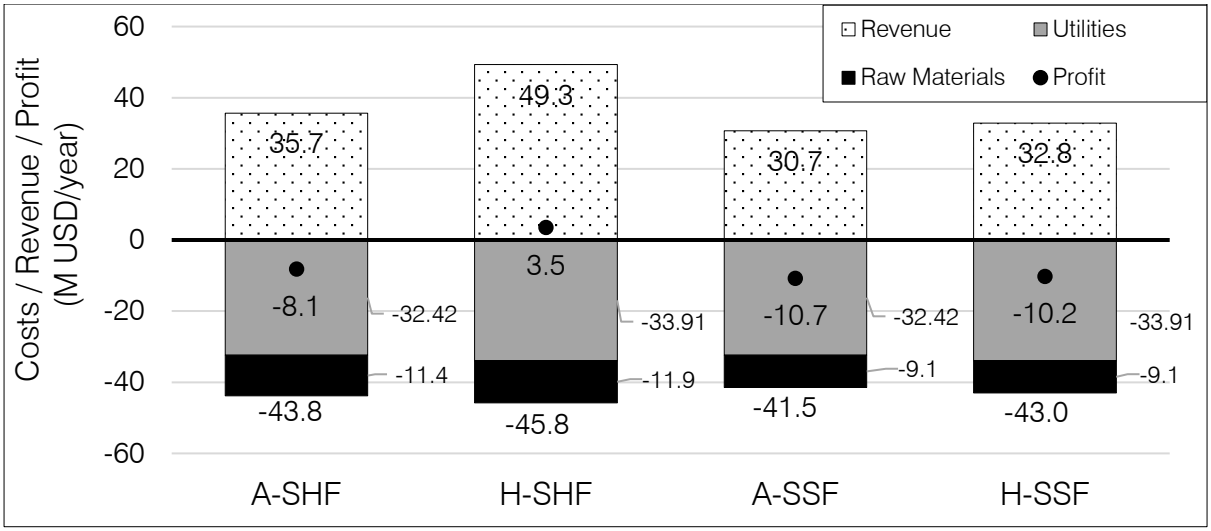

Figure 7.5: Summary of operating costs, revenue, and profit for different scenarios (A = AMD; H = H_2SO_4)

As can be seen in Figure 7.5, for all scenarios except for H-SHF, the operating costs are higher than the revenue and hence not profitable. This is mainly due to low ethanol yield and hence revenue. Although scenario H-SHF makes a profit, it is small (3.5 MUSD/yr). Considering that this evaluation assumes the cheapest raw material costs, favorable ethanol price, and ignores various other operating costs (salaries, tax, *etc.*), it is extremely unlikely that this scenario is feasible. The low revenue achieved in each scenario is due to the product yields achieved in hydrolysis and fermentation.

7.3.3 Capital costs

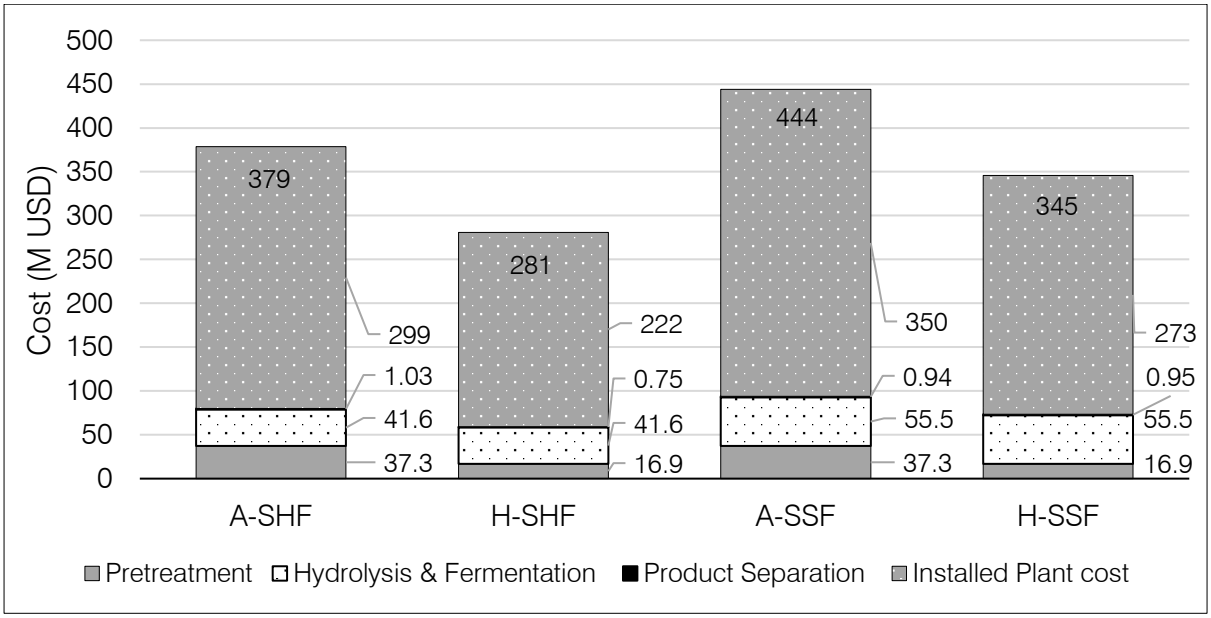

Figure 7.6: Summary of the capital costs for each processes section for the different scenarios (A = AMD; H = H_2SO_4)

As can be seen in Figure 7.6 the capital cost for the product separation section is substantially less than the capital cost for pre-treatment and hydrolysis and fermentation sections. The large capital cost of the pre-treatment and hydrolysis and fermentation sections is due to the large reactor volumes required for both pre-treatment and hydrolysis. The capital cost for pre-treatment is approximately the same for scenarios with the same type of pre-treatment *i.e.* AMD or H_2SO_4. The capital cost for hydrolysis and fermentation is approximately the same for scenarios with the same hydrolysis and fermentation configuration *i.e.* SSF or SHF.

The capital cost for scenarios with H_2SO_4 pre-treatment was found to be lower than scenarios with AMD pre-treatment. This is due to a lower cost for the pre-treatment, which is due to shorter pre-treatment times (and hence smaller reactor volumes) required to achieve the desired level of pre-treatment.

The capital cost for scenarios with SHF was found to be lower than scenarios with SSF. This is due to the hydrolysis reactor having a simpler design, and hence less expensive, than the SHF reactor. Although the SHF scenarios require an additional fermentation reactor, the cost of this is small in comparison to the hydrolysis and SHF reactors due to a significantly shorter batch time, and hence volume.

The installed plant cost was calculated from the total plant cost using the Lang factor method with a factor of 4.74 (Turton et al., 1998). The total installed plat cost ranges from 281 MUSD to 444 MUSD.

A previous techno-economic evaluation (Humbird et al., 2011) determined the total installed plant cost of 232 MUSD, which is the same order of magnitude. The study by Humbird *et al.* (2011) included various process sections such as enzyme production and wastewater remediation that were not included in this evaluation. The total installed plant cost determined in this evaluation is thus significantly higher, even if compared to an inflation-adjusted value. This high installed plant cost can be attributed to the large reactor volumes required for both pre-treatment and hydrolysis, resulting in a large capital cost for these sections.

7.3.4 Economic evaluation

Table 7.8: Summary of operating costs, capital cost and payback period

Scenario Name*	Capital Cost	Operating Cost	Revenue	Profit	Payback Period
	MUSD	MUSD/yr	MUSD/yr	MUSD/yr	yr
A-SHF	378.8	43.83	35.69	-8.14	-
H-SHF	281.0	45.82	49.30	3.48	80.7
A-SSF	444.1	41.47	30.72	-10.75	-
H-SSF	345.3	43.04	32.83	-10.21	-

* A = AMD; H = H_2SO_4

As all scenarios, except H-SHF, make a loss and thus the payback period could not be evaluated (Table 7.8).

The payback period for Scenario H-SHF is extremely long (80.7 years), indicating that this process is not economically feasible. Considering that this evaluation assumed favorable economic conditions and did not take into account various operating costs (tax, salaries) this scenario would be of even less feasibility. The major issue making this process infeasible is the low yield of ethanol from the feedstock. This results in a low revenue as well as a high capital cost as the enzymatic hydrolysis time has been extended to try to achieve a higher product yield.

To reduce the capital cost and hence the payback period, all scenarios were analyzed using a hydrolysis/ SSF reaction time of 84 hours as opposed to 168 hours. This resulted in a slightly lower volume of ethanol produced, and a significantly lower capital cost for the hydrolysis and fermentation section. Although this reduces the capital cost for all scenarios, the decreased ethanol production, and hence revenue, resulted in all scenarios, including H-SHF making a loss.

Although this evaluation clearly indicates that all scenarios are currently infeasible, some insightful observations can be made. The SHF reactor configuration is significantly cheaper and produces more ethanol than the SSF configuration. This is true for both pre-treatment with AMD and pre-treatment with H_2SO_4. The SHF reactor configuration also allows for the production of various products through different biochemical transformations of the glucose intermediary. The production of small quantities of high-value chemicals, in addition to large quantities of biofuels, can contribute towards the economic feasibility of a process (Burman

et al., 2018a) (Chapter 3). It is thus recommended that all future studies into the production of bioethanol using AMD pre-treated biomass should focus on the SHF reactor configuration.

Incorporating the process of bioethanol production into a process that simultaneously remediates AMD could also improve its feasibility. After pre-treatment AMD contains xylose released during pre-treatment, which could be utilized as a carbon source for sulfate-reducing bacteria to remediate the AMD. The integration of the two processes would be financially beneficial to both as the cost of pre-treatment of the biomass could be shared with both processes. As the remediation of AMD already has a cost associated with it any savings on this could be attributed as a profit stream for the integrated process. It is thus recommended that a techno-economic evaluation of this envisioned integrated bioethanol production/AMD remediation process be conducted.

As the product yield was found to be low, it is recommended that further experimental work be carried to determine the optimal conditions of enzymatic hydrolysis in the SHF configuration. Tailored enzyme mixtures should be investigated in conjunction with hydrolysis operating conditions such as temperature, pH and mixing.

7.4. Conclusion

This techno-economic evaluation showed that scenarios A-SHF, A-SSF and H-SHF made a loss while Scenario H-SHF only made a small profit (3.5 MUSD/year). The capital cost for the different scenarios ranged from 281 MUSD – 444 MUSD. The payback period of the H-SHF scenario being 80.7 years which is infeasible. Although all scenarios are infeasible SHF was shown to be more favorable than SSF.

As the pre-treatment of biomass using AMD is not well studied this investigation was limited to the data from Burman *et al*. (2019) (Chapter 6) which was both feedstock (Weeping lovegrass) and product (ethanol) specific and resulted in a low product yield (58.4 – 80.7 L/dry ton). The low product yield decreased the feasibility of the process, especially considering that ethanol is a low-value biochemical.

There are many opportunities to improve the feasibility of the process. Optimization of enzymatic hydrolysis, through improved enzymes and operating conditions, could substantially increase product yield. Dwindling fossil reserves should drive up the prices of

bioethanol, hence generating more revenue. The production of higher value biochemicals should also be considered as this could make the process more profitable.

The feasibility of this process could also be substantially improved if it were to be coupled with an AMD remediation process. AMD remediation has a cost associated with it so any saving could be considered as a source of income. If this process could include the beneficiation of rare earth metals the process economics could improve further.

Although this process is not currently feasible the above recommendations should be considered. This process has the potential to produce environmentally friendly alternatives to fossil fuel products, while simultaneously remediating AMD. This could be highly beneficial for a developing country such as South Africa, as it will help protect the environment and increase both the energy and water security without impacting food production.

7.5. Acknowledgments

This work is based on research supported in part by the National Research Foundation of South Africa (Grant Numbers: 111864). The support of the University of the Witwatersrand, Johannesburg is also acknowledged.

7.6. References

Alvira, P., Tomas-Pejo, E., Ballesteros, M., Negro, M.J., 2010. Pretreatment technologies for an efficient bioethanol production process based on enzymatic hydrolysis: A review. Bioresour. Technol. 101, 4851–4861. doi:10.1016/j.biortech.2009.11.093

Argus Media, 2018. Argus Sulfuric Acid. London.

Bals, B., Wedding, C., Balan, V., Sendich, E., Dale, B., 2011. Evaluating the impact of ammonia fiber expansion (AFEX) pretreatment conditions on the cost of ethanol production. Bioresour. Technol. 102, 1277–1283. doi:10.1016/j.biortech.2010.08.058

Burman, N.W., Harding, K.G., Sheridan, C.M., 2019. Lignocellulosic bioethanol production from grasses pre-treated with acid mine drainage: Modeling and comparison of SHF and SSF Author links open overlay panel. Bioresour. Technol. Reports 7. doi:10.1016/j.biteb.2019.100299

Burman, N.W., Harding, K.G., Sheridan, C.M., Van Dyk, L., 2018a. Evaluation of a combined lignocellulosic / waste water bio-refinery for the simultaneous production of valuable biochemical products and the remediation of acid mine drainage. Biofuels, Bioprod. Biorefining 12, 649–664. doi:10.1002/bbb.1880

Burman, N.W., Sheridan, C., van Dyk, L., Harding, K.G., 2018b. Modelling of low temperature dilute sulfuric acid pre-treatment of South African grass. Bioresour. Technol. Reports 4, 21–28. doi:10.1016/j.biteb.2018.08.014

Burman, N.W., van Dyk, L., Postma, F., Sheridan, C., Simate, G.S., HArding, K.G., 2017. Flow Sheet and Sensitivity Analyses for the Bio-Remediation of Acid Mine Drainage Using Sulfate Reducing Bacteria and South African Grasses, in: 2nd International Conference on Energy, Evironment and Climate Change (ICEECC). Pointe Aux Piments, Mauritius.

Department of Energy, 2018. 2018 Energy Price Report. Pretoria.

E4TECH, RE-CORD, WUR, 2015. From the Sugar Platform to biofuels and biochemicals, Final report for the European Commission Directorate-General Energy. doi:contract No. ENER/C2/423-2012/SI2.673791

Gnansounou, E., Dauriat, A., 2010. Bioresource Technology Techno-economic analysis of lignocellulosic ethanol : A review. Bioresour. Technol. 101, 4980–4991. doi:10.1016/j.biortech.2010.02.009

Huang, H., Ramaswamy, S., Al-dajani, W., Tschirner, U., Cairncross, R.A., 2009. Effect of biomass species and plant size on cellulosic ethanol : A comparative process and economic analysis. Biomass and Bioenergy 33, 234–246. doi:10.1016/j.biombioe.2008.05.007

Humbird, D., Davis, R., Tao, L., Kinchin, C., Hsu, D., Aden, A., Schoen, P., Lukas, J., Olthof, B., Worley, M., Sexton, D., Dudgeon, D., 2011. Process Design and Economics for Biochemical Conversion of Lignocellulosic Biomass to Ethanol. Golden, Co.

IPCC, 2014. Climate Change 2014: Contribution of Working Groups I, II and III to the Fifth Assessment Report of the Intergovernmental Panel on Climate Change, in: Core Writing Team, Pachauri, R.K., Meyer, L.A. (Eds.), . IPCC, Geneva, Switzerland, p. 151.

Johnson, D.B., Hallberg, K.B., 2005. Acid mine drainage remediation options: A review. Sci. Total Environ. 338, 3–14. doi:10.1016/j.scitotenv.2004.09.002

Kazi, F.K., Fortman, J.A., Anex, R.P., Hsu, D.D., Aden, A., Dutta, A., Kothandaraman, G., 2010. Techno-economic comparison of process technologies for biochemical ethanol production from corn stover q. Fuel 89, S20–S28. doi:10.1016/j.fuel.2010.01.001

Klein-marcuschamer, D., Oleskowicz-popiel, P., Simmons, B.A., Blanch, H.W., 2010. Technoeconomic

analysis of biofuels : A wiki-based platform for lignocellulosic biorefineries. Biomass and Bioenergy 34, 1914–1921. doi:10.1016/j.biombioe.2010.07.033

Lange, J., 2007. Lignocellulose conversion : an introduction to chemistry ,. Biofuels, Bioprod. Biorefining 1, 39–48. doi:10.1002/bbb

Laser, M., Larson, E., Dale, B.E., Wang, M., Greene, N., Lynd, L.R., 2009. Comparative analysis of efficiency , environmental impact , and process economics for mature biomass refi ning scenarios. Biofuels, Bioprod. Biorefining 3, 247–270. doi:10.1002/bbb

Liu, G., Zhang, J., Bao, J., 2016. Cost evaluation of cellulase enzyme for industrial-scale cellulosic ethanol production based on rigorous Aspen Plus modeling Cost evaluation of cellulase enzyme for industrial-scale cellulosic ethanol production based on rigorous Aspen Plus modeling. Bioprocess Biosyst. Eng. 39, 133–140. doi:10.1007/s00449-015-1497-1

Magowo, E., Rumbold, K., Sheridan, C., 2015. The Utilization of Cellulosic Biomass in treating AMD and the Subsequent Generation of Fermentable Sugars, in: 10th International Conference on Acid Rock Drainage and IMWA Anual Conference. pp. 1–12.

Maurya, D.P., Singla, A., Negi, S., 2015. An overview of key pretreatment processes for biological conversion of lignocellulosic biomass to bioethanol. 3 Biotech 5, 597–609. doi:10.1007/s13205-015-0279-4

Mosier, N., Wyman, C., Dale, B., Elander, R., Lee, Y.Y., Holtzapple, M., Ladisch, M., 2005. Features of promising technologies for pretreatment of lignocellulosic biomass. Bioresour. Technol. 96, 673–686. doi:10.1016/j.biortech.2004.06.025

National Accademy of Sciences, National Academy of Engineering, National Research Council, 2009. The national academies press, 1st ed. The National Academies Press, Wachington, D.C. doi:10.17226/12620

Piccolo, C., Bezzo, F., 2009. A techno-economic comparison between two technologies for bioethanol production from lignocellulose. Biomass and Bioenergy 33, 478–491. doi:10.1016/j.biombioe.2008.08.008

Ramla, B., Sheridan, C., 2015. The potential utilisation of indigenous South African grasses for acid mine drainage remediation. Water SA 41, 247–252. doi:10.4314/wsa.v41i2.10

Robus, C.L.L., Gottumukkala, L.D., van Rensburg, E., Görgens, J.G., 2016. Feasible process development and techno-economic evaluation of paper sludge to bioethanol conversion : South African paper mills scenario 92, 333–345. doi:10.1016/j.renene.2016.02.017

Searcy, E., Flynn, P.C., 2008. Processing of Straw / Corn Stover : Comparison of Life Cycle Emissions. Int. J. Green Energy 5, 423–437. doi:10.1080/15435070802498010

Sendich, E., Laser, M., Kim, S., Alizadeh, H., Laureano-perez, L., Dale, B., Lynd, L., 2008. Recent process improvements for the ammonia fiber expansion (AFEX) process and resulting reductions in minimum ethanol selling price. Bioresour. Technol. 99, 8429–8435. doi:10.1016/j.biortech.2008.02.059

Simate, G.S., Ndlovu, S., 2014. Acid mine drainage: Challenges and opportunities. J. Environ. Chem. Eng. 2, 1785–1803. doi:10.1016/j.jece.2014.07.021

Taherzadeh, M.J., Karimi, K., 2008. Pretreatment of lignocellulosic wastes to improve ethanol and biogas production: A review. Int. J. Mol. Sci. 9, 1621–1651. doi:10.3390/ijms9091621

Turton, R., Bailie, R.C., Whiting, W.B., Shaeiwitz, J.A., 1998. Analysis, Synthesis, and Design of Chemical Processes, 1st ed. Pretince Hall, Upper Saddle River.

Ulrich, G.D., Vasudevan, P.T., 2006. How to Estimate Utility Costs for a number of utilities. Chem. Eng.

66–69.

Westensee, D.K., Rumbold, K., Harding, K.G., Sheridan, C.M., van Dyk, L.D., Simate, G.S., Postma, F., 2018. The availability of second generation feedstocks for the treatment of acid mine drainage and to improve South Africa's bio-based economy. Sci. Total Environ. 637–638, 132–136. doi:10.1016/j.scitotenv.2018.04.410

Yu, Z., Zhang, H., 2003. Ethanol fermentation of acid-hydrolyzed cellulosic pyrolysate with Saccharomyces cerevisiae. Bioresour. Technol. 90, 95–100. doi:10.1016/S0960-8524(03)00093-2

Chapter 8: Techno-Economic Evaluation of the Incorporation of Biological Acid Mine Drainage Remediation into a Bioethanol Production Process

(To be submitted to Biomass and Bioenergy) This chapter expanded the process flowsheets developed in the previous chapter to include the remediation of AMD. A full techno-economic evaluation was performed to determine the economic feasibility of the process. Sensitivity analyses were performed to evaluate the feasibility of the process under various conditions. This addresses objective e.

Abstract: In a previous study, the production of ethanol from lignocellulosic biomass, through contact of the lignocellulosic biomass with acid mine drainage (AMD), was assessed. In that study, the remediation of the AMD was not considered. Therefore, in the study presented here, a techno-economic evaluation was performed to determine the feasibility of the process to simultaneously produce lignocellulosic bioethanol and remediate AMD. This was done by incorporating an Aspen Plus™ simulation for the remediation of AMD, using dissimilatory sulfate reduction, into the previous simulation, that produced bioethanol from lignocellulosic biomass pre-treated with AMD. Discounted cash flow methods were used to determine the minimum ethanol selling price (MESP), at which the process would be economically feasible. The incorporation of an AMD remediation process section was found to reduce the MESP from 3 355 to 3 114 USD/ton through the potential savings in AMD remediation. Although this is substantially higher than the recent historical ethanol prices, sensitivity analyses revealed that there are opportunities for the MESP to be substantially reduced. The MESP was found to be especially sensitive to the ethanol yield. If the yield were to be increased through optimization of enzymatic hydrolysis the MESP would be reduced to within the range of recent historical prices. An evaluation at reasonable assumptions was found to achieve an MESP of 741 USD/ton, which is in the range of historical prices indicating that the process could be feasible at these conditions.

Keywords: Lignocellulosic Bioethanol; Acid Mine Drainage Remediation; Sulfate-reducing Bacteria; Process Simulation; Economic Evaluation

8.1. Introduction

The effects of anthropogenic greenhouse gas emissions have led to widespread environmental damage (IPCC, 2014a). One way to begin to reduce the global carbon dioxide emissions sustainably is through blending petrol with 2nd generation biofuels, such as bioethanol, produced from lignocellulosic biomass (IPCC, 2014b). Unfortunately, the presence of the ligno-hemicellulosic matrix within the plant, prevents efficient enzymatic hydrolysis of the lignocellulosic biomass, resulting in the need for additional pre-treatment processes. The additional pre-treatment steps increase the processing cost, often preventing the production of lignocellulosic bioethanol from being economically feasible (Mosier et al., 2005b).

One of the most effective pre-treatment technologies is through the use of dilute H_2SO_4 (Alvira et al., 2010; Maurya et al., 2015; Mosier et al., 2005b; Taherzadeh and Karimi, 2008). Recently there have been investigations into using acid mine drainage (AMD) as a source of H_2SO_4 for pre-treatment process (Burman et al., 2019; Magowo et al., 2015; Westensee et al., 2018). As there are vast quantities of AMD in both the Witwatersrand basin and Mpumalanga coalfields in South Africa, AMD can be obtained freely. If a process could be developed to produce bioethanol from biomass pre-treated with AMD, whilst simultaneously remediating AMD, the remediation of AMD could provide an additional revenue stream (Burman et al., 2018a).

AMD is contaminated water that has a low pH (1 – 3), a high concentration of sulfate (<20 g/L) and a high concentration of metals (<5 g/L). It is produced through a series of geochemical reactions when sulfate rich minerals are exposed to oxygen and water (Johnson and Hallberg, 2005a). Both shaft and pit mining can result in favorable conditions for the production of AMD, as has been seen in countries such as the USA, Canada, Australia, Germany, and South Africa amongst others (Mccarthy et al., 2010). In South Africa, the two main regions where AMD is generated are the Witwatersrand basin (shaft mines), and the Mpumalanga and Kwa-Zulu Natal coalfields (pit mines).

Currently, the most common AMD remediation technique is chemical neutralization, using an alkali substance, which increases the pH and results in the formation of salts and metal precipitates (Kefeni et al., 2017). Although effective, this is expensive and not

environmentally sustainable (Moodley et al., 2017). Another AMD remediation technique that has shown promise is biological sulfate reduction, also called dissimilatory sulfate reduction (DSR). This is catalyzed by sulfate-reducing bacteria (SRB) (Sánchez-Andrea et al., 2014).

SRB have been found to be capable of utilizing lignocellulosic biomass as an electron donor for DSR. DSR reduces sulfate to sulfide, effectively transforming strong sulfuric acid into hydrogen sulfide, a weaker acid. This increases the pH, and results (primarily) in the precipitation of metals (Simate and Ndlovu, 2014).

Many studies have found the process of DSR suitable for the remediation of AMD, with the rate of sulfate reduction ranging from 0.12 to 29 g/L.day (Sánchez-Andrea et al., 2014). Various reactor types have been investigated such as continuous stirred tank reactor (CSTR), fluidized bed reactor (FBR), gas lift reactor (GLR), up-flow anaerobic sludge blanket reactor (UASB) and membrane reactors (MB), amongst others (Kaksonen and Puhakka, 2007). The reactors are typically operated at mesophilic temperatures but DSR has been performed at temperatures as high as 65°C (Weijma et al., 2000). There have also been different sources of SRB, operating conditions, and substrate investigated (Sánchez-Andrea et al., 2014). Additionally, there are already two commercially available processes that utilize SRB for the remediation of AMD, namely SULFATEQ™ from Paques (https://en.paques.nl/) and the Biosulfide™ process from BQE Water (https://www.bqewater.com/).

A flowsheet for the remediation of AMD using lignocellulosic biomass has been previously developed (Burman et al., 2017) (Chapter 4). In that flowsheet, three different reactor configurations were evaluated and compared in terms of the total volume required. The reactor configuration that was found to be the best suited consisted of first reacting biomass with AMD at high temperatures, releasing xylose into the AMD. The xylose containing AMD could then undergo DSR in a separate sulfate-reducing bioreactor to produce clean water. This flowsheet was developed with the subsequent use of the pre-treated biomass for the production of bioethanol in mind, however, it was not incorporated in that study.

Previous economic evaluations investigated the feasibility of producing bioethanol from biomass pre-treated with AMD (Burman et al., 2020) (Chapter 7). That study investigated both separate hydrolysis and fermentation (SHF) and simultaneous saccharification and fermentation (SSF) reactor configurations. Although neither reactor configuration was found

to be economically feasible, the SHF reactor configuration was determined to be better suited economically. One of the major recommendations of that study was that AMD remediation be incorporated into the model and the economic feasibility be re-evaluated. This forms the basis of the work presented in this paper.

Other techno-economic evaluations have investigated the feasibility of producing bioethanol using various processes and feedstocks (Humbird et al., 2011). These investigations typically use operating and capital costs of the process to determine the minimum ethanol selling price (MESP), at which ethanol needs to be sold to be considered economically feasible. Determining the MESP makes an evaluation of the feasibility possible when compared to the current and historical ethanol prices. Economies of scale improve process economics and hence the processes investigated are generally large (850 – 5 000 ton/hr biomass). The yield of ethanol from biomass ranges from 125 to 420 L/ton dry biomass, and the MESP has been found to range between 0.63 USD/Gal to 4.58 USD/Gal (211 – 1 535 USD/ton) (Humbird et al., 2011). Although there is a large fluctuation in the ethanol price, (prices between 2013 – 2018 range from 1.21 to 3.58 USD/Gal (405 – 1 200 USD/ton)), it is clear that the production of 2nd generation bioethanol can be economically feasible if the process is well designed.

This study aimed to further develop the techno-economic evaluation by Burman *et al.* (2020) (Chapter 7) by incorporating the remediation of AMD into the design and performing a more detailed economic evaluation. The minimum ethanol price was determined and used as an indicator of economic feasibility. Various sensitivity analyses were performed to determine the effects of various parameters on the feasibility of the process.

8.2. Methods

8.2.1 Process flowsheet development

8.2.1.1 Simulation basis

The current simulation was developed based on the previous study (Burman et al., 2020) (Chapter 7). In Burman *et al.* (2020) a process to produce bioethanol from Weeping lovegrass (*Eragrostis curvula*) that was pre-treated with AMD was simulated. Both SHF and SSF were investigated but as SHF was found to be better suited it was used as the basis for this study. The basis for the previous study was 90 ton/hr dry biomass, with major outputs being ethanol and AMD containing 40 g/L xylose. This xylose rich AMD was used as an input into the

simulation presented here. The current simulation was developed in a separate Aspen Plus™ file, and the simulation in the previous study was not altered except in some of the sensitivity analyses, which investigate various parameters in that simulation.

The simulation was carried out using Aspen Plus™ V8.4 (www.aspentech.com), using the electrolyte template with the ELEC-NRTL equations of state on all blocks. The reaction wizard was used to incorporate both equilibrium and salt formation reactions.

The AMD was assumed to have a pH of 2.0 with the following concentrations of contaminants SO_4^{2-} 12.1 g/L; Fe^{2+} 4.29 g/L; Al^{3+} 0.396 g/L, Mg^2 0.474 g/L; and Ca^{2+} 0.592 g/L.

The concentration of xylose in the xylose rich AMD was taken to be 40 g/L, at a flow rate of 472 ton/hr. This is as a result of the acid hydrolysis of xylan and will serve as a substrate for the sulfate-reducing bacteria in DSR.

8.2.1.2 AMD remediation process section description

The Aspen Plus™ flowsheet that was developed in this study is presented in Figure 8.1.

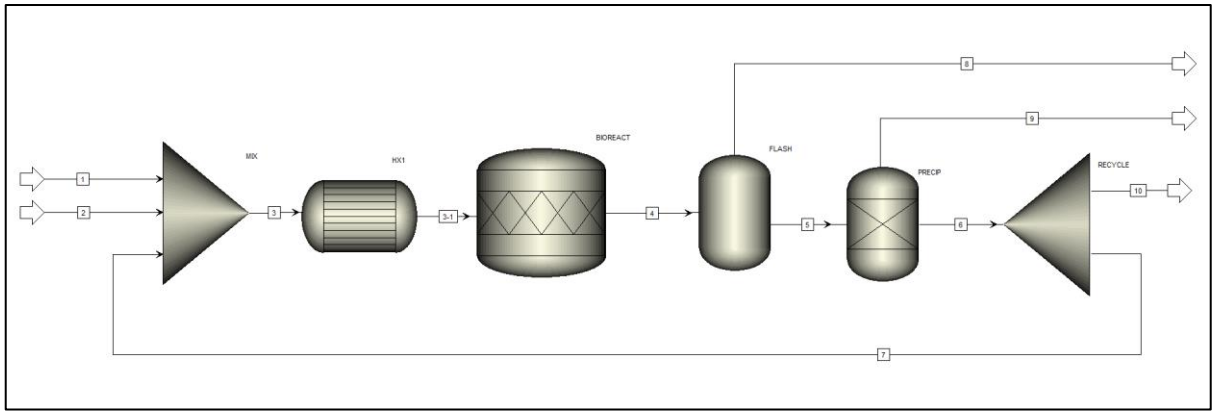

Figure 8.1: Aspen Plus™ flowsheet developed for the remediation of AMD using sulfate-reducing bacteria

Xylose-rich AMD is mixed with pure AMD (to achieve a suitable SO_4^{2-}:COD ratio), and a recycle stream of remediated water, before going to a heat exchanger (HX1) which heats the water to 35°C. This stream enters the sulfate-reducing bioreactor (BIOREACT) in which DSR occurs (rx 8.1). Dissolved metals and sulfides react to form metal sulfides (rx 8.2 – rx 8.5), and various equilibria reactions and salt formation reactions occur (Table 8.1).

Gas phase CO_2 and SO_2 will exit the top of the reactor, while the liquid phase will flow into a mineral precipitate filter (PRECIP) in which all mineral precipitates are removed.

A portion of the remediated water is recycled and mixed with the AMD solution flowing into the bioreactor to control the pH entering the DSR reactor.

8.2.1.3 Simulation specifications

The heat exchanger (HX1) was modeled using the HeatX block.

The sulfate-reducing bioreactor (BIOREACT) was modeled using an RStoic block and was constructed with the following reactions

$$C_5H_{10}O_5 + 2.5SO_4^{2-} \xrightarrow{SRB} 5CO_2 + 5H_2O + 2.5S^{2-} \quad \text{(rx 8.1)}$$

$$\square\square^{2+} + \square^{2-} \rightarrow \square\square\square \quad \text{(rx 8.2)}$$

$$\square\square^{2+} + \square^{2-} \rightarrow \square\square\square \quad \text{(rx 8.3)}$$

$$2\square\square^{3+} + 3\square^{2-} \rightarrow \square\square_2\square_3 \quad \text{(rx 8.4)}$$

$$\square\square^{2+} + \square^{2-} \rightarrow \square\square\square \quad \text{(rx 8.5)}$$

In addition to these reactions, the reactions generated with the reaction wizard were also incorporated in the simulation (Table 8.1).

Table 8.1: Summary of equations generated by the equation wizard in the Aspen Plus™ simulation

#	Equilibrium Reaction	#	Salt Formation reaction
E1	$4H_2O + 2Fe^{2+} \leftrightarrow Fe_2(OH)_2 + 2H_3O^+$	**S1**	$CaSO_4 2H_2O \leftrightarrow Ca^{2+} + SO_4^{2-} + 2H_2O$
E2	$2H_2O + FeOH^{2+} \leftrightarrow Fe(OH)_2^+ + H_3O^+$	**S2**	$2CaSO_4 H_2O \leftrightarrow H_2O + 2Ca^{2+} + 2SO_4^{2-}$
E3	$2H_2O + 2Fe^{3+} \leftrightarrow FeOH^{2+} + H_3O^+$	**S3**	$CaSO_4 \leftrightarrow Ca^{2+} + SO_4^{2-}$
E4	$3OH^- + 2Fe^{2+} \leftrightarrow Fe(OH)_3^-$	**S4**	$Ca(OH)_2 \leftrightarrow CaOH^- + OH$
E5	$CaOH^+ \leftrightarrow Ca^{2+} + OH^-$	**S5**	$FeSO_4 H_2O \leftrightarrow H_2O + Fe^{2+} + SO_4^{2-}$
E6	$MgOH^+ \leftrightarrow Mg^{2+} + OH^-$	**S6**	$FeSO_4 4H_2O \leftrightarrow Fe^{2+} + SO_4^{2-} + 4H_2O$
E7	$H_2O + HSO_4^- \leftrightarrow H_3O^+ + SO_4^{2-}$	**S7**	$FeSO_4 7H_2O \leftrightarrow Fe^{2+} + SO_4^{2-} + 7H_2O$
E8	$H_2O + H_2SO_4 \leftrightarrow HSO_4^- + H_3O^+$	**S8**	$FeSO_4 \leftrightarrow Fe^{2+} + SO_4^{2-}$
E9	$FeOH^+ \leftrightarrow Fe^{2+} + OH^-$	**S9**	$MgSO_4 H_2O \leftrightarrow H_2O + Mg^{2+} + SO_4^{2-}$
E10	$H_2O + HCO_3^- \leftrightarrow CO_3^{2-} + H_3O^+$	**S10**	$MgSO_4 6H_2O \leftrightarrow 6H_2O + Mg^{2+} + SO_4^{2-}$
E11	$2H_2O + CO_2 \leftrightarrow HCO_3^- + H_3O^+$	**S11**	$CaCO_3 \leftrightarrow CO_3^{2-} + Ca^{2+}$
E12	$H_2O + HS^- \leftrightarrow H_3O^+ + S^{2-}$	**S12**	$MgCO_3 3H_2O \leftrightarrow CO_3^{2-} + Mg^{2+} + 3H_2O$
E13	$H_2O + H_2S \leftrightarrow H_3O^+ + HS^-$	**S13**	$MgCO_3 \leftrightarrow CO_3^{2-} + Mg^{2+}$
E14	$2H_2O \leftrightarrow OH^- + H_3O^+$	**S14**	$Fe(OH)_3 \leftrightarrow Fe(OH)_2^+ + OH^-$
		S15	$Fe(OH)_2 \leftrightarrow FeOH^+ + OH^-$
#	**Dissociation Reaction**	**S16**	$Al_2(SO_4)_3\, 7H_2O \leftrightarrow 2Al^{3+} + 3SO_4^{2-} + 6H_2O$
D1	$Fe(OH)_2 \rightarrow FeOH^+ + OH^-$	**S17**	$Salt \leftrightarrow 2Al^{3+} + 3SO_4^{2-} + 6H_2O$
		S18	$Mg(OH)_2 \leftrightarrow OH^- + MgOH^+$
		S19	$AL_2(SO_4)_3 \leftrightarrow 2Al^{3+} + 3SO_4^{2-}$
		S20	$MgSO_4 \leftrightarrow Mg^{2+} + SO_4^{2-}$

The separation of CO_2 and SO_2 was modeled using a Flash2 block (FLASH). The mineral precipitate filter (PRECIP) was modeled using a Sep block. Mixers/Splitters were used as necessary.

A summary of the block specifications is presented in Table 8.2

Table 8.2: Summary of block specifications used in Aspen Plus™ simulation

Block Name	Block Type	Specification
HX1	HeatX	$T_{cold,out}$ = 35°C
BIOREACT	RStoic	T = 35°C P = 1 atm X_1 = 0.9 $X_{2\text{-}5}$ = 0.5
FLASH	Flash2	T = 0.35°C P = 1 atm
PRECIP	Sep	T = 35°C P = 1 atm 100% of all salts and metal sulfides formed removed

Two design specifications were set up in the Aspen Plus™ model. One specification set the concentration of xylose in the stream exiting the sulfate-reducing bioreactor (Stream 4) to 1 g/L by changing the volume of AMD without xylose (Stream 2) entering the process. The second specification set the pH of the stream entering the reactor (Stream 3) to 3.0 by varying the volume of the recycle stream (Stream 7).

8.2.2 Operating costs

The operating costs of the pre-treatment, enzymatic hydrolysis and fermentation, and product separation sections were assumed to be the same as previously determined (43.8 MUSD/yr) for the scenario which considers the AMD pre-treatment with SHF reactor configuration (Burman et al., 2020) (Chapter 7).

Estimation of the operating costs for the AMD remediation section was performed using the Aspen Plus™ inbuilt utility and operating cost tools. The only utility considered was steam which was assumed to be at a temperature of 125°C (2.3 bar). The unit cost of this was assumed to be 6.15 USD/GJ which was estimated based on the method of Ulrich and Vasudevan (2006), assuming that steam was produced in a natural gas boiler with a fuel cost of 3.57 USD/GJ (Department of Energy, 2018). No raw material cost was associated with either the AMD or xylose rich AMD.

8.2.3 Revenue

The revenue of the process was based on the sale of bioethanol and on the savings that could be realized if this process to remediate AMD were to replace another, more expensive, process. It was assumed that this process currently remediates AMD at a cost of 1.47 USD/ton AMD. This cost was calculated based on the previously reported costs (Mccarthy et al., 2010) adjusted to 2018 prices. As this is an assumption in which there is a lot of uncertainty, a sensitivity analysis was performed.

8.2.4 Capital costs

The capital costs of the pre-treatment, enzymatic hydrolysis fermentation, and product separation sections were assumed to be the same as previously determined (379 MUSD) for the scenario which considers the AMD pre-treatment with SHF reactor configuration (Burman et al., 2020)(Chapter 7).

The capital costs for the sulfate-reducing section of the process were determined by first estimating the volume of the sulfate-reducing reactor by assuming a constant rate of sulfate reduction of 30 g/L.day. This rate of sulfate reduction was assumed as it represents the fastest rate of sulfate reduction found in literature (Bijmans et al., 2008b). As there is a lot of uncertainty with the rate of sulfate reduction a sensitivity analysis will be performed on it.

The capital cost of the reactor was then estimated by assuming that the capital cost of the reactor would be the same per unit volume as the fermenter. The cost was assumed to be the same as it would require similar construction, mixing and temperature control. Once the cost of the sulfate-reducing reactor was determined the total installed plant cost was calculated using the Lang factor method (Turton et al., 1998).

8.2.5 Economic evaluation

A discounted cash flow method for the economic evaluation was used to determine the minimum ethanol selling price (MESP) that would achieve a zero net present value (NPV) after 20 years at an internal rate of return of 10%. This was achieved by calculating the discounted cash flow in each year according to (Turton et al., 1998)

$$DCF_n = \frac{CF}{(1+r)^n} \tag{8.1}$$

Where DCF_n is the discounted cash flow in year n (MUSD), CF is the cash flow in year n (MUSD), and r is the internal rate of return (%). The net present value was then determined according to

$$NPV_n = \sum_{n=0}^{n} DCF_n$$

Where NPV_n is the net present value at year n (MUSD).

The tax rate was taken to be 28% as in line with South African commercial tax law (Robus et al., 2016). The capital outlay was assumed to be distributed as follows: the land was purchased in year zero; 66% of the capital was outlaid in the first year; and 34% of capital together with the working capital was outlaid in the second year. Depreciation was assumed to be 50% in the first year following start-up, 30% in the second and 20% in the third year. It was assumed that the plant as salvaged after 20 years for 20% of the original capital cost.

Working capital was taken to be 5% of the capital cost, paid in the third year (Robus et al., 2016).

8.2.6 Sensitivity analyses

Sensitivity analyses investigating the effect of the savings on AMD remediation (in USD/ton of AMD remediated), as well as the ethanol yield (L/ton dry biomass) on the MESP, were performed. Both of these sensitivity analyses were based on the assumption that the capital and operating costs would remain the same, but the revenue would differ as a result of the change in the savings on AMD remediation or volume of ethanol produced. This assumption is made since the majority of the operating cost is the biomass (which would remain the same) and that the only change in capital cost is in the product separation section which is relatively insignificant compared to the other process sections. This assumption was verified with the process simulation and economic evaluation.

As there was uncertainty surrounding the rate of sulfate reduction, a sensitivity analysis was performed, that investigated its effect on the MESP. This was done by assuming that only the capital cost would vary with varying rates of sulfate reduction. The volume of the SRB reactor was calculated at various rates of sulfate reduction which was used to calculate the total capital costs. This was used to estimate the MESP assuming all operating costs were the same.

The effect of the pre-treatment temperature on the MESP was also evaluated. This was performed by determining the equivalent time that would be required to achieve the same level of pre-treatment at a higher temperature, based on hydrolysis kinetics that have been experimentally determined for South African grasses (Burman et al., 2018b) (Chapter 5).

This was performed by evaluating the change in operating cost (utilities) and capital cost (cost of pre-treatment reactor and pre-treatment heat exchangers), with a change in pre-treatment temperature. These were used to evaluate the MESP at different temperatures.

The change in pre-treatment time was evaluated by first determining the xylose remaining at the current pre-treatment conditions (95°C, 3.5 days, 0.98 wt% H_2SO_4,) according to the following equation (Burman et al., 2018b) (Chapter 5).

$$X_r = \alpha \cdot e^{K_f \cdot t} + (1 - \alpha) \tag{8.3}$$

Where X_r is the fraction of xylose remaining, α is the fraction of fast reacting xylan, t is time (min), K_f is the rate of reaction of the fast reacting fraction of xylan (/min) and can be calculated according to

$$K_f = A_0 C a^n e^{\frac{-Ea}{RT}} \quad (8.4)$$

Where A_0 is the preexponential factor (/min), Ca is the concentration of H_2SO_4 (wt%), n is an experimentally determined coefficient, Ea is the activation energy (kJ/mol), R is the universal gas constant (mol/kJ.K) and T is the temperature (K).

The new time (t_n) to achieve the equivalent level of pre-treatment was calculated through rearranging Equation (8.3) according to.

$$t_n = \frac{ln\left(\frac{X_r - 1 + \alpha}{\alpha}\right)}{-K_f} \quad (8.5)$$

This was used to estimate the reactor volume and price according to Burman *et al.* (2020) (Chapter 7).

The change in heat exchanger size and operating costs was determined in Aspen Plus™. The new equipment sizes were used to estimate the new cost in the CAPCOST program (Turton et al., 1998). The new operating and capital costs were then used to determine the MESP at various temperatures.

8.3. Results and Discussion

8.3.1 Process flowsheet

A full stream table is available in the supplementary data (Appendix E).

The model found that the amount of AMD that can be treated daily is 50.4 ML/day. This volume is calculated based on the quantity of xylose that is present, reaction stoichiometry (rx 8.1), and the concentration of xylose exiting the reactor. This volume is similar to the volumes that are currently being treated at the AMD remediation facilities in the Central, Eastern and Western basins in the Witwatersrand mining area in Johannesburg, South Africa (van Niekerk, 2017).

The model predicts that the water quality exiting the process would be substantially better than the water entering the process (Table 8.3).

Table 8.3: Summary of the main contaminants entering/exiting the process

	SO4 g/L	Fe g/L	Ca g/L	Mg g/L	Al g/L	pH
In (stream 1 & 2)	12.1	3.84	0.492	0.474	0.396	2
Out (Stream 10)	1.866	0.498	0.139	0.1339	0.111878	6
% Removal	85%	87%	72%	72%	72%	

The ethanol yield determined in Burman *et al.* (2020) (Chapter 7) was found to be 58.4 L/ton dry biomass. This results in a volume of 44 ton/yr of ethanol being produced. This yield of ethanol is substantially lower than the yields reported in literature (125 – 420 L/ton dry biomass).

One explanation of the comparatively low yield is that other studies are fermenting both C5 and C6 sugars (Humbird et al., 2011), whereas in this study the C5 sugars are required as a carbon source for the SRB. Another explanation is that the yields in this study are based on experiments that were conducted without access to tailored cellulase mixtures, advanced bioreactors or genetically modified fermentative organisms (Burman et al., 2019).

8.3.2 Capital costs and operating costs

The total capital cost was found to be 429.3 MUSD. The hydrolysis and fermentation section was found to have the highest capital cost at 199.7 MUSD. This was followed by the pre-treatment section, (174.2 MUSD) the AMD remediation section (50.5 MUSD) and the product separation section (4.9 MUSD) (Figure 8.2). The hydrolysis and fermentation and pre-treatment section are expensive due to the large reactor volumes as a result of long batch times. In this model, the hydrolysis time is 7 days (168 hrs), which is double the hydrolysis time in previous studies (Humbird et al., 2011; Robus et al., 2016). The previous study found that due to the low product yield, the process would not be profitable with a hydrolysis time of only 3.5 days. The hydrolysis time and yields in this study were based on previously performed experiments, which found a slow rate of hydrolysis (Burman et al., 2019). Further experimental research could be performed to try to optimize the hydrolysis rate of reaction such that higher yields can be achieved in substantially shorter times. This would help to reduce the capital cost.

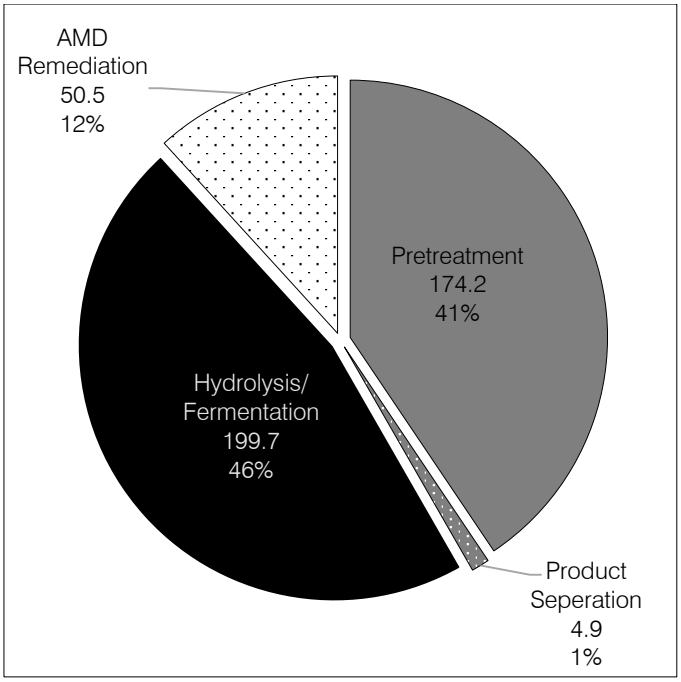

Figure 8.2: Break down of Capital Costs.

Similarly, the capital cost of the pre-treatment section is also high due to a long pre-treatment time. It is thought that the pre-treatment time could be substantially reduced if the pre-treatment reactor is operated at higher temperatures. This has been evaluated in a sensitivity analysis.

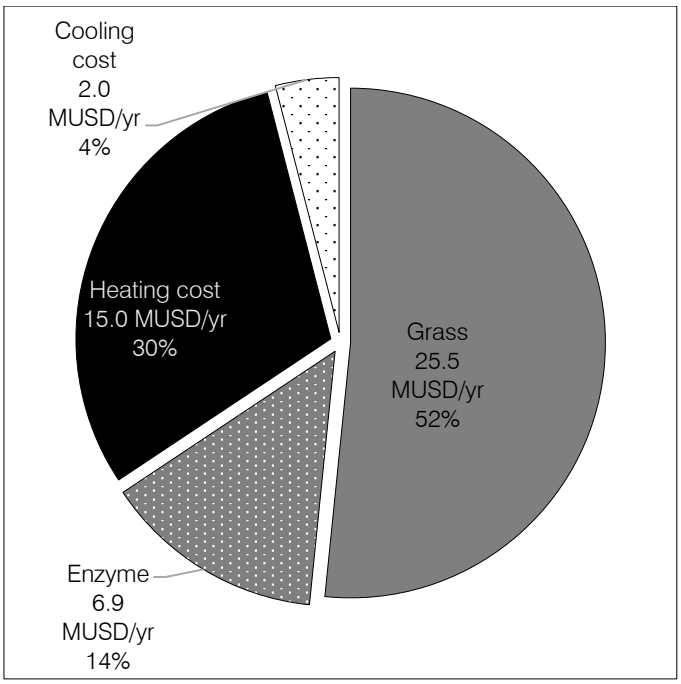

Figure 8.3: Summary of the operating costs

The total operating cost was found to be 49.3 MUSD/yr. The grass feedstock cost was found to be the largest operating cost (25.5 MUSD/yr) followed by the heating utility cost

(15.0 MUSD/yr), the enzyme cost (6.9 MUSD/yr) and the cooling utility cost (2.0 MUSD) (Figure 8.3). Even though the assumed price for grass was very low (35 USD/ton) the cost of the grass was high due to the large volumes required (90 ton/hr). The heating utility cost was high due to the large volumes of AMD being treated.

The operating cost of AMD remediation was found to be 0.33 USD/ton AMD. This resulted in a saving of 1.1 USD/ton AMD, assuming that the current cost of AMD remediation is 1.47 USD/ton AMD (Mccarthy et al., 2010).

8.3.3 Economic evaluation

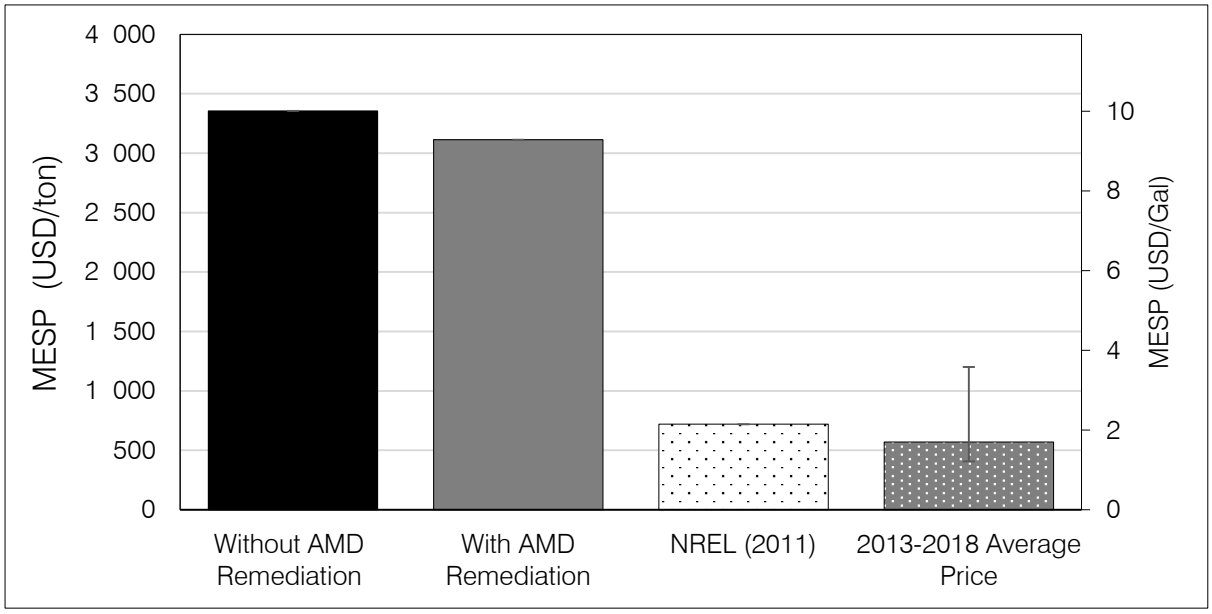

Figure 8.4: Calculated MESP with and without the AMD remediation section

The MESP was calculated with and without the AMD remediation process section (Figure 8.4). The inclusion of AMD remediation decreased the MESP by 240.5 USD/ton (0.71 USD/Gal) from 3 355 USD/ton (10.0 USD/Gal) to 3 114 USD/ton (9.29 USD/Gal). The reduction in MESP realized through the inclusion of AMD remediation was not significant at the operating conditions investigated.

This was compared to the MESP calculated in a techno-economic evaluation performed by the NREL (Humbird et al., 2011) and the average ethanol price between January 2013 – December 2018. The average ethanol price was taken to be the average of the daily opening prices as reported by Markets Insider (https://markets.businessinsider.com) for that timeframe. The error bars indicate the minimum and maximum daily opening price for that

timeframe. This methodology of evaluating the recent historical ethanol prices applies to all of the sensitivity analyses.

Although the inclusion of the AMD remediation process section reduces the MESP it is still significantly higher than the recent historical ethanol prices indicating that the process is currently infeasible.

8.3.4 Sensitivity analyses

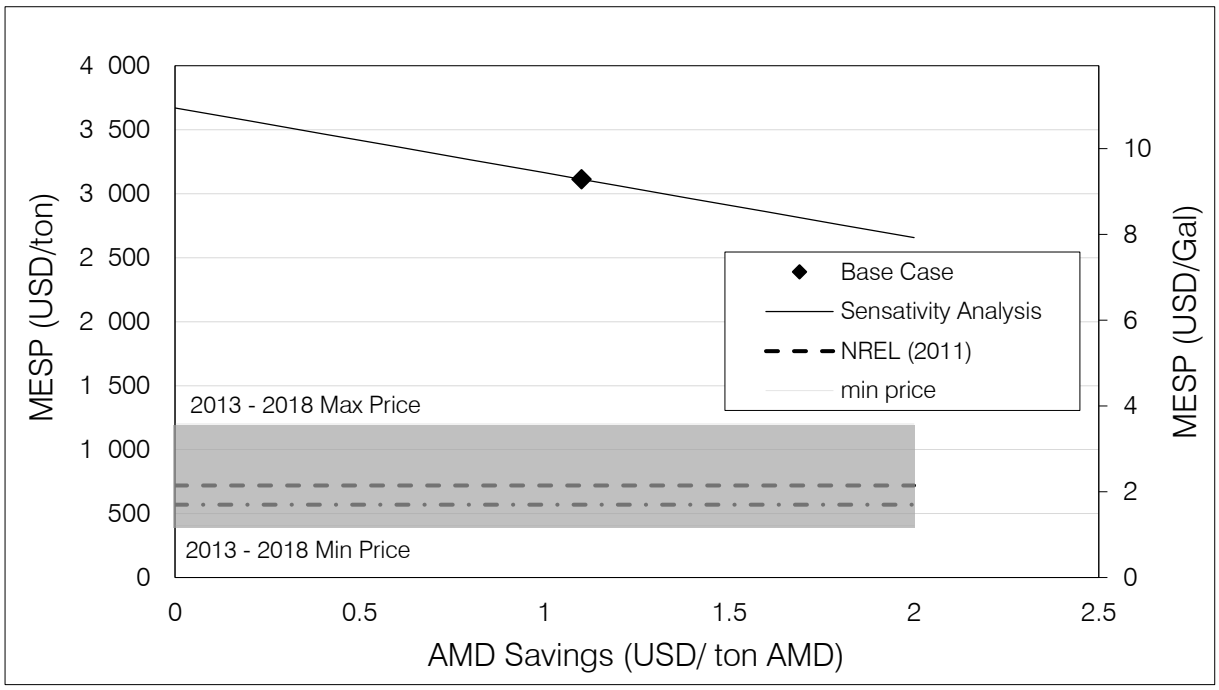

Figure 8.5: Sensitivity Analyses on the effect of the potential AMD remediation saving on the MESP

Increasing the savings on AMD remediation was found to linearly decrease the MESP from 3 671 at a saving of 0.0 USD/ton AMD to 2 656 at a saving of 2.0 USD/ton AMD (Figure 8.5). Although this is a decrease in MESP of 1 015 USD/ton, achieving an AMD saving of 2.0 USD/ton is highly unlikely as this is higher than reported maximum costs for the remediation of AMD (Mccarthy et al., 2010). In the whole range investigated the MESP was still substantially higher than the MESP determined in the 2011 NREL techno-economic evaluation (Humbird et al., 2011), and historical prices between 2013 – 2018. This indicates that even if maximum savings were to be achieved the process would still not be feasible.

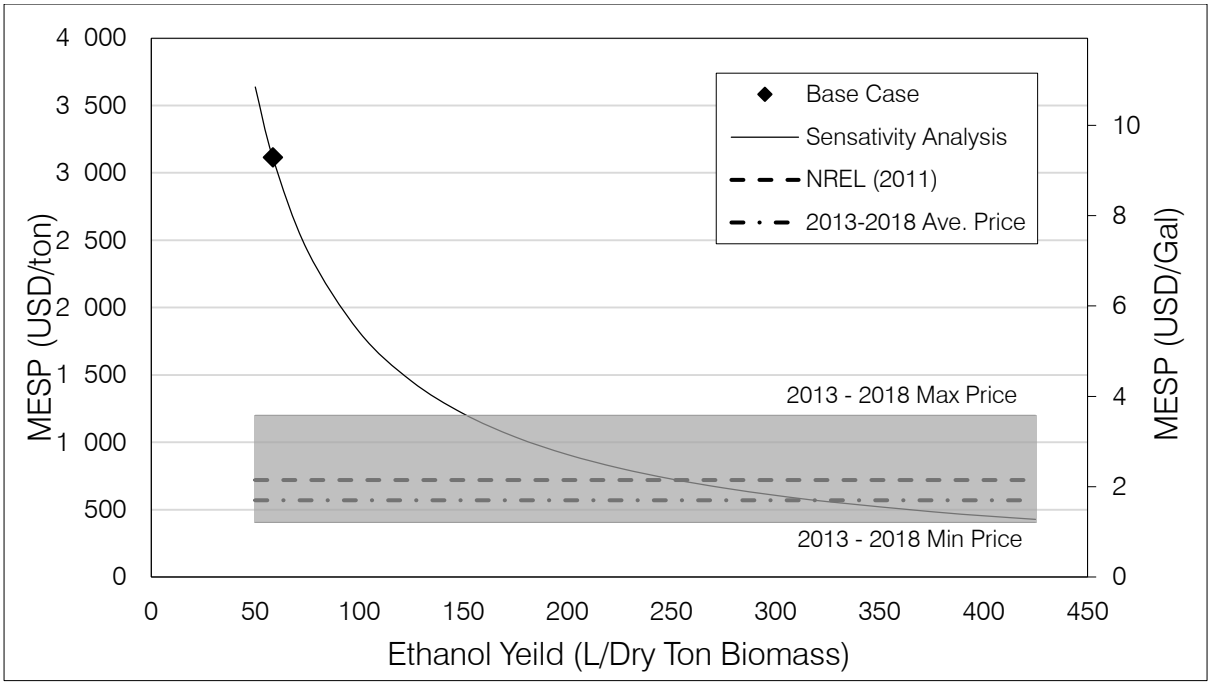

Figure 8.6: Sensitivity analyses on the effect of the ethanol yield on the MESP

Increasing the ethanol yield from biomass was found to decrease the MESP logarithmically from 3 637 USD/ton at a yield of 50 L/ton biomass to 428 USD/ton at a yield of 425 L/ton biomass (Figure 8.6). At yields greater than 150 L/ton biomass the MESP was found to be lower than the highest price in the 2013 – 2018 timeframe (1 200 USD/ton). At a yield of 250 L/ton biomass, the MESP was found to be equal to the MESP determined in the 2011 NREL techno-economic evaluation (Humbird et al., 2011). At a yield above 325 L/ton, the MESP was found to be lower than the average price between 2013 – 2018. This indicates that the process could be feasible at higher ethanol yields. As the pentose sugars released during pre-treatment are utilized by the sulfate-reducing bacteria, achieving yields as high as those reported in literature may not be possible, as previous studies often assume pentose sugars are fermented to ethanol. It is however clear that increasing the ethanol yield would substantially reduce the MESP and increase the feasibility of the process.

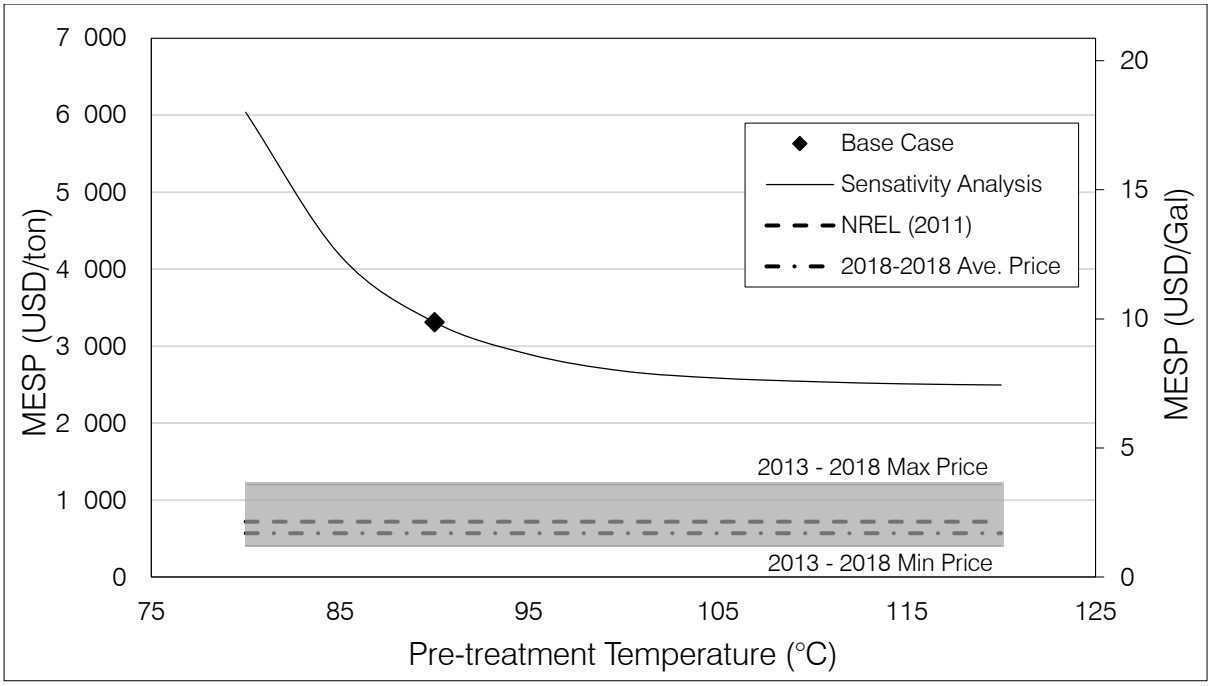

Figure 8.7: Sensitivity analyses on the effect of the pre-treatment temperature on the MESP

The MESP was also found to be very sensitive to variation of the pre-treatment temperature (Figure 8.7). The MESP was found to decrease drastically from 6 037 USD/ton at a pre-treatment temperature of 80°C to 3 309 at 90°C, after which the MESP decrease less rapidly to a minimum of 2 494 USD/ton at 120°C. Increasing the pre-treatment temperature from 90°C (base case), by 20°C would decrease the MESP from 3 309 USD/ton at 90°C to 2 540 USD/ton at 110°C. This is a substantial decrease for such a minor increase in temperature. Although increasing the temperature was found to lower the MESP, even at the highest temperatures investigated the MESP was still greater than the MESP determined in the 2011 NREL techno-economic evaluation (Humbird et al., 2011) and historical prices for the 2013 – 2018 timeframe.

One of the reasons that the decrease in MESP slows down at temperatures above 90°C, is due to the design of the pre-treatment reactor. As the initial pre-treatment reactor was large it was designed as a semi-batch reactor, with grass loaded/ removed after the batch time, and AMD flowing through it continuously. This assumed that there was a long grass loading phase which added to the required reactor volume. At higher pre-treatment temperature the required pre-treatment time is substantially shorter, and the solid loading phase in the reaction cycles starts to account for the majority of the cycle time. If another reactor type was considered, potentially a rotating screw reactor, the capital cost of the pre-treatment section

could potentially be reduced further, hence lowering the MESP. As this was considered to be a major design alteration it was not included in the sensitivity analysis.

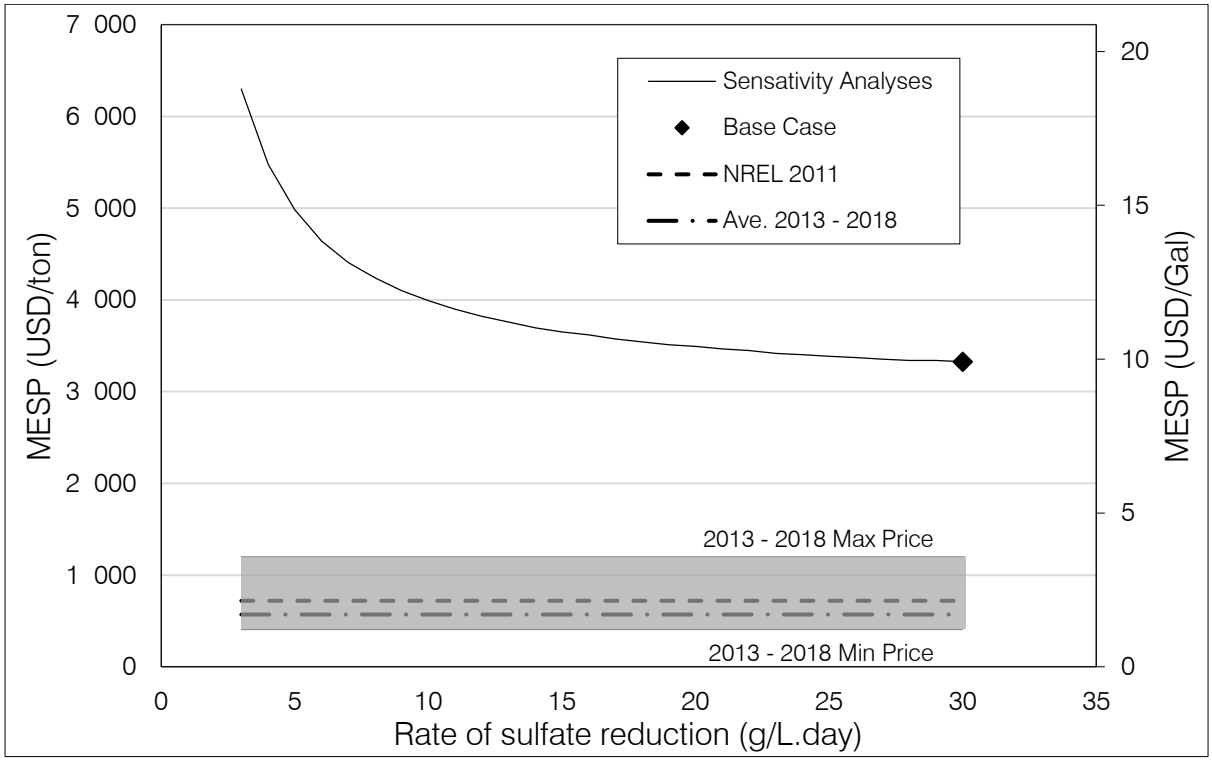

Figure 8.8: Sensitivity analysis in the effect of the rate of sulfate reduction on the MESP.

The MESP was found to decrease drastically with an increasing rate of sulfate reduction, from 6 300 USD/ton at 3.0 g/L.day to 3 990 at 10 g/L.day, the MESP then decreased steadily to 3 324 USD/ton at 30 g/L.day (Figure 8.8). This indicates that the rate of sulfate reduction needs to be maximized to make the processes feasible and unless a rate of reduction of >10 g/L.day can be achieved it is unlikely that the process can be feasible even with optimization of other sections of the process. A sulfate reduction rate of >10 g/L has been demonstrated to be possible in many studies (Bijmans et al., 2009a, 2008b; Houten et al., 2006; Weijma et al., 2000).

A sulfate reduction rate of 30 g/L.day was taken to be the maximum as this was the highest rate that was reported in literature (Sánchez-Andrea et al., 2014). At all rates of sulfate reduction, the MESP was substantially higher than the MESP determined in the 2011 NREL techno-economic evaluation (Humbird et al., 2011) and historical prices for the 2013 – 2018 timeframe, indicating that it is infeasible.

To determine the feasibility of the process at realistically achievable conditions an evaluation was carried out. This assumed that the yield of ethanol was 200 L/ton biomass, the pre-

treatment reactor was operating at 110°C, the rate of sulfate reduction was 30 g/L.day and the savings per ton of AMD remediated was 1.1 USD/ton. Based on these conditions the MESP was found to be 741 USD/ton ethanol (2.21 USD/Gal). This is similar to the MESP calculated by the NREL in its 2011 techno-economic evaluation (Humbird et al., 2011) (720 USD/ton or 2.15 USD/Gal), however, it is higher than the average price for ethanol in the 2013-2018 timeframe (570 USD/ton or 1.7 USD/Gal). It does, however, fall into the range of the ethanol price in the 2013 – 2018 timeframe (405 – 1200 USD/ton or 1.21 – 358 USD/Gal). This indicates that this process could be feasible if operated under the conditions above, with favorable ethanol prices. A move away from cheap fossil fuels due to the national commitments of the Paris Accord should see an increase in the value of biofuels in the future. An increased awareness of the climate crisis has also resulted in many people opting for environmentally friendly alternatives even if they are more expensive than conventional fossil fuel-based products.

There are various opportunities to increase the feasibility of this study through process integration and the production of additional revenue streams. If the CO_2 and SO_2 from the sulfate-reducing bioreactor could be separated and collected they could be upgraded to valuable products. A portion of the glucose from hydrolysis could also be used for the production of high-value biochemicals (Cherubini, 2010). Waste lignin could also be valorized either through the production of valuable lignin-based biochemicals or through combustion for the production of steam.

8.4. Conclusion

The MESP was determined to be 3 355 USD/ton for bioethanol production without AMD and 3 114 USD/ton for bioethanol production with the remediation of AMD. Although the incorporation of AMD remediation was found to reduce the MESP by 240.5 USD/ton, the MESP was still significantly higher than recent historical prices (405 – 1200 USD/ton). One of the main drawbacks to the feasibility of the process was the low ethanol yield (58.4 L/ton dry biomass) which resulted in low ethanol volumes (44 000 ton/yr). The low yield can be attributed to fermenting only C6 sugars and the low experimental yields on which the simulation is based.

Although the process is not feasible in its current form, the sensitivity analyses revealed various opportunities to increase its feasibility. If the operating costs for the remediation of AMD could be reduced this would increase the revenue associated with AMD remediation, decreasing the MESP to as low as 2 656 USD/ton.

Increasing the operating temperature of the pre-treatment reactor from 90°C to 120 °C could also reduce the MESP substantially to 2 494 USD/ton. Increasing the ethanol yield could also substantially reduce the MESP to as little 485 USD/ton at a yield of 375 L/ton dry biomass. At ethanol yields above 150 L/ton Dry biomass, the MESP was found to be lower than historical highs, indicating that this is where the process might start to be feasible. The yield of ethanol was the factor investigated that was found to have the greatest effect on the MESP.

The rate of sulfate reduction was found to substantially affect the MESP. For this process to be economically feasible the rate of sulfate reduction must be >10 g/L.day as the MESP increases sharply at sulfate reduction rates slower than this.

To determine the feasibility of the process at reasonable improvements and minor modifications to the process the MESP was investigated at a sulfate reduction rate of 30 g/L.day, a pre-treatment temperature of 110°C, an ethanol yield of 200 L/ton biomass and a saving on AMD remediation 1.1 USD/ton. Under these conditions, the MESP was found to be 741 USD/ton. This is within the range of the recent historical prices of ethanol indicating that it could be feasible under favorable ethanol prices. There are also further opportunities to increase the feasibility of the process such as process integration and production of additional products.

As this process shows potential for economic feasibility it is recommended that further experimental work be carried out on various process parameters. Attention should be given to improving the yield of ethanol as this was found to be the parameter that had the biggest effect on the MESP.

The study has shown that it is possible to remediate AMD, whilst producing bioethanol. This resonates strongly with the concept of environmentally sustainable remediation. The study has demonstrated that the costs of remediation can be offset through the use of novel and innovative strategies. If successfully developed this process could help reduce anthropogenic greenhouse gas emissions, while simultaneously remediating AMD. This would improve the

quality of the environment, reduces greenhouse gas emissions, and improve energy and water security in South Africa.

8.5. Acknowledgments

This work is based on research supported in part by the National Research Foundation of South Africa (Grant Numbers: 111864). The support of the University of the Witwatersrand, Johannesburg is also acknowledged.

8.6. References

Alvira, P., Tomas-Pejo, E., Ballesteros, M., Negro, M.J., 2010. Pretreatment technologies for an efficient bioethanol production process based on enzymatic hydrolysis: A review. Bioresour. Technol. 101, 4851–4861. doi:10.1016/j.biortech.2009.11.093

Bijmans, M.F.M., Dopson, M., Peeters, T.W.T., Lens, P.N.L., Buisman, C.J.N., 2009. Sulfate Reduction at pH 5 in a High-Rate Membrane Bioreactor : Reactor Performance and Microbial Community Analyses. J. Microbiol. Biotechnol. 19, 698–708. doi:10.4014/jmb.0809.502

Bijmans, M.F.M., Peeters, T.W.T., Lens, P.N.L., Buisman, C.J.N., 2008. High rate sulfate reduction at pH 6 in a pH-auxostat submerged membrane bioreactor fed with formate. Water Res. 42, 2439–2448. doi:10.1016/j.watres.2008.01.025

Burman, N.W., Harding, K.G., Sheridan, C.M., 2019. Lignocellulosic bioethanol production from grasses pre-treated with acid mine drainage: Modeling and comparison of SHF and SSF Author links open overlay panel. Bioresour. Technol. Reports 7. doi:10.1016/j.biteb.2019.100299

Burman, N.W., Sheridan, C.M., Harding, K.G., 2020. Feasibility assessment of the production of bioethanol from lignocellulosic biomass pretreated with acid mine drainage (AMD). Renew. Energy 157, 1148–1155. doi:10.1016/j.renene.2020.05.086

Burman, N.W., Harding, K.G., Sheridan, C.M., Van Dyk, L., 2018a. Evaluation of a combined lignocellulosic / waste water bio-refinery for the simultaneous production of valuable biochemical products and the remediation of acid mine drainage. Biofuels, Bioprod. Biorefining 12, 649–664. doi:10.1002/bbb.1880

Burman, N.W., Sheridan, C., van Dyk, L., Harding, K.G., 2018b. Modelling of low temperature dilute sulfuric acid pre-treatment of South African grass. Bioresour. Technol. Reports 4, 21–28. doi:10.1016/j.biteb.2018.08.014

Burman, N.W., van Dyk, L., Postma, F., Sheridan, C., Simate, G.S., HArding, K.G., 2017. Flow Sheet and Sensitivity Analyses for the Bio-Remediation of Acid Mine Drainage Using Sulfate Reducing Bacteria and South African Grasses, in: 2nd International Conference on Energy, Evironment and Climate Change (ICEECC). Pointe Aux Piments, Mauritius.

Cherubini, F., 2010. The biorefinery concept : Using biomass instead of oil for producing energy and chemicals. Energy Convers. Manag. 51, 1412–1421. doi:10.1016/j.enconman.2010.01.015

Department of Energy, 2018. 2018 Energy Price Report. Pretoria.

Houten, B.H.G.W. Van, Roest, K., Tzeneva, V.A., Dijkman, H., Smidt, H., Stams, A.J.M., 2006. Occurrence of methanogenesis during start-up of a full-scale synthesis gas-fed reactor treating sulfate and metal-rich wastewater. Water Res. 40, 553–560. doi:10.1016/j.watres.2005.12.004

Humbird, D., Davis, R., Tao, L., Kinchin, C., Hsu, D., Aden, A., Schoen, P., Lukas, J., Olthof, B., Worley, M., Sexton, D., Dudgeon, D., 2011. Process Design and Economics for Biochemical Conversion of Lignocellulosic Biomass to Ethanol. Golden, Co.

IPCC, 2014a. Climate Change 2014: Contribution of Working Groups I, II and III to the Fifth Assessment Report of the Intergovernmental Panel on Climate Change, in: Core Writing Team, Pachauri, R.K., Meyer, L.A. (Eds.), . IPCC, Geneva, Switzerland, p. 151.

IPCC, 2014b. Climate Change 2014: Mitigation of Climate Change. Contribution of Working Group III to the Fifth Assessment Report of the Intergovernmental Panel on Climate Change, in: Eickemeier, P., Schlömer, S., Farahani, E., Kadner, S., Brunner, S., Baum, I., Kriemann, B. (Eds.), . Cambridge University Press, Cambridge, United Kingdom and New York, NY, USA.

Johnson, D.B., Hallberg, K.B., 2005. Acid mine drainage remediation options: A review. Sci. Total

Environ. 338, 3–14. doi:10.1016/j.scitotenv.2004.09.002

Kaksonen, A.H., Puhakka, J.A., 2007. Sulfate reduction based bioprocesses for the treatment of acid mine drainage and the recovery of metals. Eng. Life Sci. 7, 541–564. doi:10.1002/elsc.200720216

Kefeni, K.K., Msagati, T.A.M., Mamba, B.B., 2017. Acid mine drainage : Prevention , treatment options , and resource recovery : A review. J. Clean. Prod. 151, 475–493. doi:10.1016/j.jclepro.2017.03.082

Magowo, E., Rumbold, K., Sheridan, C., 2015. The Utilization of Cellulosic Biomass in treating AMD and the Subsequent Generation of Fermentable Sugars, in: 10th International Conference on Acid Rock Drainage and IMWA Anual Conference. pp. 1–12.

Maurya, D.P., Singla, A., Negi, S., 2015. An overview of key pretreatment processes for biological conversion of lignocellulosic biomass to bioethanol. 3 Biotech 5, 597–609. doi:10.1007/s13205-015-0279-4

Mccarthy, T.S., Steyl, G., Maree, J., Zhao, H., 2010. MINE WATER MANAGEMENT IN THE WITWATERSRAND WITH SPECIAL EMPHASIS ON ACID MINE DRAINAGE: Report to the Inter-Ministerial Committee on Acid Mine Drainage 1–128.

Moodley, I., Sheridan, C.M., Kappelmeyer, U., Akcil, A., 2017. Environmentally sustainable acid mine drainage remediation: Research developments with a focus on waste / by-products. Miner. Eng. 126, 207–220. doi:10.1016/j.mineng.2017.08.008

Mosier, N., Wyman, C., Dale, B., Elander, R., Lee, Y.Y., Holtzapple, M., Ladisch, M., 2005. Features of promising technologies for pretreatment of lignocellulosic biomass. Bioresour. Technol. 96, 673–686. doi:10.1016/j.biortech.2004.06.025

Robus, C.L.L., Gottumukkala, L.D., van Rensburg, E., Görgens, J.G., 2016. Feasible process development and techno-economic evaluation of paper sludge to bioethanol conversion : South African paper mills scenario 92, 333–345. doi:10.1016/j.renene.2016.02.017

Sánchez-Andrea, I., Sanz, J.L., Bijmans, M.F.M., Stams, A.J.M., 2014. Sulfate reduction at low pH to remediate acid mine drainage. J. Hazard. Mater. 269, 98–109. doi:10.1016/j.jhazmat.2013.12.032

Simate, G.S., Ndlovu, S., 2014. Acid mine drainage: Challenges and opportunities. J. Environ. Chem. Eng. 2, 1785–1803. doi:10.1016/j.jece.2014.07.021

Taherzadeh, M.J., Karimi, K., 2008. Pretreatment of lignocellulosic wastes to improve ethanol and biogas production: A review. Int. J. Mol. Sci. 9, 1621–1651. doi:10.3390/ijms9091621

Turton, R., Bailie, R.C., Whiting, W.B., Shaeiwitz, J.A., 1998. Analysis, Synthesis, and Design of Chemical Processes, 1st ed. Pretince Hall, Upper Saddle River.

Ulrich, G.D., Vasudevan, P.T., 2006. How to Estimate Utility Costs for a number of utilities. Chem. Eng. 66–69.

van Niekerk, D., 2017. Personal Communication.

Weijma, J., Stams, A.J.M., Pol, L.W.H., Lettinga, G., 2000. Thermophilic Sulfate Reduction and Methanogenesis with Methanol in a High Rate Anaerobic Reactor. Biotechnol. Bioeng. 67, 354–363. doi:10.1002/(SICI)1097-0290(20000205)67:3<354::AID-BIT12>3.0.CO;2-X

Westensee, D.K., Rumbold, K., Harding, K.G., Sheridan, C.M., van Dyk, L.D., Simate, G.S., Postma, F., 2018. The availability of second generation feedstocks for the treatment of acid mine drainage and to improve South Africa's bio-based economy. Sci. Total Environ. 637–638, 132–136. doi:10.1016/j.scitotenv.2018.04.410

Chapter 9: Discussion and Conclusion

This chapter delivers the main findings and the conclusions that can be drawn from those findings. Each objective is considered followed by a discussion of the design, optimization, and feasibility of the process investigated. Finally, recommendations into key areas that require further investigation to develop this process, and conclusions on the entire research will be made.

9.1. Discussion

9.1.1 Discussion of objectives

The main objectives of this study were to perform the following:

a. A desktop study on the simultaneous remediation of AMD and pre-treatment of biomass. This would investigate optimal reactor configuration, estimate reactor sizing, and perform sensitivity analyses on the results;
b. An experimental investigation into the rate of dilute sulfuric acid pre-treatment of indigenous South Africa grass;
c. An experimental investigation into the rate of enzymatic hydrolysis and fermentation in both separate hydrolysis and fermentation (SHF) and simultaneous saccharification and fermentation (SSF), and the optimum conditions for the pre-treatment of grass;
d. A desktop study into the enzymatic hydrolysis of biomass pre-treated with AMD. This would investigate the optimal reactor configuration between SHF and SSF, estimate capital and operating costs, and determine the feasibility of each reactor configuration; and
e. A desktop study into the optimum overall process to simultaneously remediate AMD and produce bioethanol through enzymatic hydrolysis and fermentation of pre-treated biomass. This would entail integrating the two desktop studies performed in (a) and (d) and incorporating all new knowledge and data determined through investigation. The results of this were to recommend a design for a process that maximized both the remediation of AMD and the production of bioethanol and determine the feasibility of such a process.

9.1.1.1 A desktop study on the simultaneous remediation of AMD and pre-treatment of biomass *(Objective a)*

The results of this desktop study are presented in Chapter 4. Three different reactor configurations were investigated, and it was found that the optimum configuration consisted of biomass undergoing pre-treatment in AMD at high temperatures (90°C), followed by remediation of AMD at mesophilic temperatures (35°C). The xylose released in pre-treatment would serve as a carbon source for SRB catalyzed DSR. As the other reactor configurations had simultaneous biomass pre-treatment and AMD remediation in the same reactor, these reactors had to be operated at temperatures that would not harm the SRB (<35°C). The rate of hydrolysis of xylan at these temperatures was substantially slower, resulting in significantly larger reactor volumes.

As there was a large variation in the rate of pre-treatment and DSR found in literature, sensitivity analyses were performed on these parameters. The total reactor volume required was found to be very sensitive to both the rate of pre-treatment and the rate of DSR. All of the kinetic studies found in literature on the rate of pre-treatment were specific to certain types of biomass and at temperatures higher than what was envisioned for this process. The rate of pre-treatment, for the specific biomass used, at the temperatures envisioned for this process, was identified as something that needs to be determined experimentally.

As far as could be ascertained, this was the first time that flowsheets have been developed for the simultaneous remediation of AMD and pre-treatment of lignocellulosic biomass.

9.1.1.2 Experimental investigation into the rate of dilute sulfuric acid pre-treatment of indigenous South Africa grass *(Objective b)*

The results of this experimental investigation are presented in Chapter 5. This study investigated the rate of acid catalyzed hydrolysis of xylan to xylose, at temperatures lower than previously investigated (35 – 90°C). The investigation found that at lower temperatures, instead of xylan consisting of a fast reacting and a slow reacting fraction (as previously determined), the xylan consisted of a reactive and an unreactive fraction, *i.e.* the rate of reaction of the slow reacting fraction was so slow it could be considered negligible. The rates of pre-treatment predicted by the kinetics determined were similar to the rates of reaction predicted by previous studies (Figure 5.5) (Esteghlalian et al., 1997). The proportion of the reactive fraction (50%) was found to be lower than previously determined (55 – 100%). As far as could be determined, these results have not been reported elsewhere in literature.

9.1.1.3 Experimental investigation into the rate of enzymatic hydrolysis and fermentation in SHF and SSF (Objective c)

The results of this experimental investigation are presented in Chapter 6. The results of the experiments of biomass pre-treated with AMD were compared to results from biomass pre-treated with H_2SO_4. The optimum pre-treatment time was found to be 1 day for H_2SO_4 pre-treatment and 3.5 days for AMD pre-treatment. The yield of glucose and ethanol from biomass pre-treated with AMD was found to be 70 – 80% of the yield from biomass pre-treated with H_2SO_4. The discrepancy between the final ethanol concentration achieved in SHF and SSF was higher for biomass pre-treated with H_2SO_4 (22.30 and 19.20 g/L respectively) than for biomass pre-treated with AMD (14.43 and 14.83 g/L respectively).

Empirical equations were then fitted to the data to model the concentration of glucose/ethanol over time in both SHF and SSF configurations. The correlation between the model and the data was found to be high in all cases ($0.86 < r^2 < 0.99$).

As far as could be ascertained this was the first study that quantitatively determined the optimal pre-treatment of biomass using AMD, and quantitatively evaluated and developed empirical models for the performance of enzymatic hydrolysis and fermentation of biomass pre-treated with AMD.

9.1.1.4 A desktop study into the enzymatic hydrolysis of biomass pre-treated with AMD (Objective d)

The results of this desktop study are presented in Chapter 7. This desktop study made use of the kinetics determined in Chapter 6 to develop a process simulation for the process (using Aspen Plus™) as well as estimate capital and operating costs. Flowsheets were developed for both SHF and SSF reactor configurations, with pre-treatment carried out using AMD or H_2SO_4 for comparison. There were thus four different scenarios evaluated, *i.e.* AMD pre-treatment with SHF (A-SHF), H_2SO_4 pre-treatment with SHF (H-SHF); AMD pre-treatment with SSF (A-SSF); and H_2SO_4 pre-treatment with SSF (H-SSF).

The operating costs were found to be higher than the revenue for all processes except H-SHF, with that scenario only making a profit of 3.5 MUSD/year. The capital cost was found to range from 281 – 444 MUSD. The payback period for the H-SHF scenario was found to be 80.5 years indicating that this scenario is also not currently economically feasible. The low revenue generated in all processes is largely attributed to the low product yield and hence revenue. The SHF reactor configuration was found to be better than the SSF configuration, in terms of

profit and capital cost, for both AMD and H_2SO_4 pre-treatment, and hence assumed to be better suited.

As far as could be determined this was the first study that developed process simulations and evaluated the economic feasibility of bioethanol production from biomass pre-treated with AMD.

9.1.1.5 A desktop study into the optimum overall process to simultaneously remediate AMD and produce bioethanol (Objective e)

The results of this desktop study are presented in Chapter 8. This desktop study combined the flowsheets developed previously in Chapters 4 and 7 into a single process simulation that was used to estimate capital and operating costs. Discounted cash flow methods were used to determine the minimum ethanol selling price (MESP) at which ethanol would need to be sold for the process to be feasible. The flowsheet considered only the best reactor configurations developed previously, *i.e.* separate pre-treatment of biomass and remediation of AMD (Chapter 4), and SHF (Chapter 7). It was found that incorporating the remediation of AMD reduced the MESP from 3 355 USD/Gal (10.0 USD/Gal) to 3 114 USD/ton (9.29 USD/Gal), due to the potential saving on AMD remediation. This is significantly higher than recent historical ethanol trading prices (405 – 1 200 USD/ton or 1.21 – 3.58 USD/gal).

The process achieved an 85% reduction of sulfate, an 87% reduction of iron and a 72% reduction in other metals (Ca^{2+}, Mg^{2+}, Al^{3+}), with an increase of pH from 2.0 to 6.1. The volume of AMD that could be treated was found to be 50.4 ML/Day. This is lower than the volumes of AMD being generated daily in the Witwatersrand mining area, indicating that there is a sufficient quantity of AMD being generated, for this process, on this scale.

Sensitivity analyses showed that the MESP could be reduced substantially if the ethanol yield could be improved, and if the operating temperature of the AMD reactor were to be increased. Assuming modest yield increases and operation of the pre-treatment reactor at 110°C, the MESP was found to be 741 USD/ton ethanol (2.21 USD/Gal), which is within the range of recent historical ethanol prices (405 – 1 200 USD/ton or 1.21 – 3.58 USD/gal).

As far as could be determined this was the first techno-economic evaluation of a process to simultaneously remediate AMD and produce bioethanol using lignocellulosic biomass.

9.1.2 Design

The overall design of the process was guided by the findings of Chapter 3 which investigated the best reactor configuration of the process based on the biorefinery complexity index. This showed that the most feasible process would be to produce bioethanol from biomass pre-treated with AMD while remediating the AMD using SRB. Further opportunities for the production of other products from the lignin platform and distillery silage were investigated. The opportunity for the production of additional high-value products from the C6 sugar platform was also noted. Unfortunately, the incorporation of these three additional product streams in the final design was not within the scope of this study.

The main design consideration that was investigated in this dissertation was the reactor configuration for the AMD remediation and biomass pre-treatment reactors and the enzymatic hydrolysis and fermentation reactors.

The following three AMD remediation and biomass pre-treatment reactor configurations were investigated:

- Packed Bed Hydrolysis and SRB Recycle Reactor (Process 1);
- Combined Hydrolysis and DSR Reactor (Process 2); and
- Counter Current Sequential CSTR's (Process 3).

Process 1 was found to have a significantly smaller total reactor volume than Process 2 and 3. In Process 1, pre-treatment is carried out at high temperatures (90°C), ensuring a fast rate of reaction, followed by remediation of AMD in a separate reactor at mesophilic temperatures (<35°C). In Process 2 and 3 both pre-treatment and AMD remediation occur simultaneously in the same reactor at the mesophilic temperatures (<35°C). The rate of pre-treatment at mesophilic temperatures was found to be severely rate-limiting resulting in significantly larger reactor volumes.

Although it is clear that the biomass pre-treatment and AMD remediation bioreactor should be separate, the detailed design of each unit operation is still required. The design of the pre-treatment reactor used in the process simulations presented in Chapters 3 and 7 assumes a semi-continuous reactor in which AMD flows continuously through a packed grass bed which is replaced after a specified pre-treatment time. A sensitivity analysis that was performed in Chapter 8, investigating the effect of the pre-treatment temperature on the required pre-

treatment time, indicated that a small increase in temperature (20°C) could reduce the pre-treatment time substantially. In this case, other types of reactors, such as a rotating screw reactor, could be considered. The design of the SRB reactor also needs further attention, however previous investigation suggests that a continuous reactor would be best suited (Kaksonen and Puhakka, 2007; Sánchez-Andrea et al., 2014).

With regards to the enzymatic hydrolysis and fermentation reactor, both SHF and SSF reactor configurations were investigated (Chapter 7). SHF was found to be better than SSF in terms of capital cost (379 *vs.* 444 MUSD) and revenue (35.7 *vs.* 30.7 MUSD/yr), however, the operating costs using SHF were slightly higher than using SSF (43.8 *vs.* 41.5 MUSD/yr). As the operating costs are higher than the revenue both configurations make a loss, however, the loss made using SHF is less than that made using SSF (-8.1 *vs.* – 10.7 MUSD/yr). The lower capital cost and loss of the SHF configuration indicate that SHF is better suited for the production of bioethanol from biomass pre-treated with AMD (Chapter 7).

The low revenue generated in both SHF and SSF configurations is largely attributed to a low product yield of ethanol from biomass. This was mainly due to a low yield of glucose from biomass, as the yield of ethanol from glucose was found to be relatively good. Further research needs to be considered to increase glucose yield, which can in part be achieved through improved design of the hydrolysis reactor and optimization of enzymatic hydrolysis operating conditions.

Although the purification of the ethanol is an important part of the process, ethanol separation through distillation is a well-studied process. As such the design used in this study was based on previous designs that have been demonstrated to be successful (Humbird et al., 2011). The design consisted of two distillation columns, the first achieving an ethanol concentration of 40% in the distillate, and the second achieving an ethanol concentration of 90% in the distillate. In both columns, the recovery of ethanol to the distillate was set to 95%. The dehydration of ethanol to produce anhydrous alcohol was not included in the study.

In summary, the optimal design of the complete process was found to consist of:

- pre-treatment of biomass with AMD at high temperatures, to produce pre-treated biomass and xylose rich AMD;

- DSR of xylose rich AMD, in a sulfate-reducing bioreactor, to produce remediated water;
- SHF of pre-treated biomass, to produce a dilute ethanol stream; and
- ethanol purification through the use of two distillation columns.

The MESP calculated for the design based on the data obtained experimentally (Chapter 6) was found to be 3 114 USD/ton (9.29 USD/Gal).

9.1.3 Optimization

The sensitivity analyses performed in Chapter 8 identified parameters that could be optimized to increase the economic feasibility of the process. The overall yield of ethanol from biomass and the pre-treatment temperature were found to have the largest effect on the economic feasibility, however, it was also found that it would be difficult for the process to be economically feasible if the rate of sulfate reduction was too slow.

The MESP could be substantially reduced if the ethanol yield were to be increased. The ethanol yield achieved in this study was found to be 58.4 L/ton dry biomass, which is substantially lower than what has been reported in literature (<420 L/ton) (Huang et al., 2009). One of the reasons the ethanol yield is so low is that instead of fermenting xylose to ethanol, it is used as a carbon source for SRB. However, there is still substantial room for improvement in the overall ethanol yield. Various factors could be optimized to increase the glucose yield in enzymatic hydrolysis, including the use of tailored cellulase mixtures; optimizing various operating conditions such as temperature, pH, mixing, and enzyme dosage; and optimizing the design of the hydrolysis reactor.

Although the low overall ethanol yield is mainly due to the low yield of glucose from biomass, increasing the yield of ethanol from glucose would further increase the overall ethanol yield. This could be achieved through the use of genetically modified fermentative organisms, that achieve a lower growth yield and a higher product yield. Recombinant strains of *Zymomomas mobilis* have been demonstrated to have this ability.

A sensitivity analysis performed on the pre-treatment temperature revealed that increasing the pre-treatment temperature from 90°C to 110°C would decrease the MESP from 3 309 USD/ton at 90°C to 2 540 USD/ton at 110°C. This is a substantial reduction in MESP

considering that it is only a temperature increase of 20°C. This is largely due to the rate of acid hydrolysis being highly sensitive to the pre-treatment temperature (Chapter 4).

Originally the pre-treatment reactor was designed as a semi-batch reactor, with grass loaded/ removed after the specified batch time, and AMD flowing through it continuously. This assumed that there was a long grass loading phase which added to the required reactor volume. At higher pre-treatment temperatures the required pre-treatment time is substantially shorter, and the grass loading phase in the reaction cycles starts to account for the majority of the cycle time. If other reactor types, such as a rotating screw reactor, were considered the MESP could be further reduced at higher pre-treatment temperatures.

9.1.4 Feasibility

The MESP of the process under the conditions simulated was found to be 3 114 USD/ton (9.29 USD/Gal). This is substantially higher than recent ethanol prices (405 – 1200 USD/ton or 1.21 – 3.58 USD/gal), indicating that the process is currently not economically feasible. However, if the process were to be optimized the feasibility of the process could be increased. Assuming an ethanol yield of 200 L/ton biomass, and a pre-treatment temperature of 110°C the MESP was calculated to be 741 USD/ton ethanol (2.21 USD/Gal). This is within the range of recent ethanol prices, indicating that the process could be feasible under these conditions. If the ethanol price were to increase above the recent historical prices, the economic feasibility would increase further.

The feasibility of the process could also be further increased through the production of additional products. Various additional products could be produced through the incorporation of additional processing routes (Chapter 3), such as:

- the production of small quantities of high-value biochemicals from glucose;
- the processing of lignin, through gasification or combustion, to produce either bioenergy or biochemicals; and
- the processing of distillery silage to produce feed or fertilizer (Chapter 3).

The feasibility of the process could also be improved if CO_2 and SO_2 from the SRB reactor were to be captured and upgraded to valuable products (Chapter 8).

Although the process is not currently economically feasible it does address two important environmental issues. Firstly, it provides a sustainable solution to the remediation of AMD, increasing the water security of South Africa. Secondly, it produces 2nd generation renewable biofuel, that is carbon negative, without any of the negative effects on food security that are associated with 1st generation biofuel. This not only increases South Africa's energy security but also provides an environmentally sustainable alternative to fossil fuel products, mitigating the effects of anthropogenic climate change.

9.2. Conclusion

The simultaneous remediation of AMD and production of biochemicals is technically possible and could be economically feasible with realistic improvements to the process and favorable economic conditions.

Based on the findings of this work, the optimal process configuration for the simultaneous remediation of AMD and production of bioethanol from indigenous South African grasses consists of a process in which there are separate reactors for biomass pre-treatment, AMD remediation, enzymatic hydrolysis, and fermentation. The separation of bioethanol product is achieved in two distillation columns.

There is, however, further research that is still required to develop this process. The key areas that require further investigation include:

- increasing the yield of bioethanol from biomass;
- verifying the suitability of high temperature pre-treatment with AMD;
- developing a detailed design for a sulfate-reducing bioreactor; and
- integrating the production of additional products into the biorefinery design.

The low yield of bioethanol from biomass can be attributed to the low yield of glucose from biomass. Therefore, further research aiming to increase the bioethanol yield should focus on the enzymatic hydrolysis of biomass pre-treated with AMD. This should investigate the best combination of cellulase enzymes, while also focusing on enzymatic hydrolysis operating conditions, such as temperature, pH, and mixing. Further research into the optimal reactor design should also be performed. Additionally, the operating conditions of fermentation (micro-organisms, temperature, nutrients, *etc.*) should also be optimized to maximize ethanol yields.

The use of high temperature pre-treatment with AMD needs to be investigated. Although high temperature H_2SO_4 pre-treatment is well documented, the effect of the metals present in the AMD is unknown. Therefore, the suitability of high temperature pre-treatment of biomass using AMD, for subsequent enzymatic hydrolysis of biomass, and DSR of xylose rich AMD, needs to be verified. To provide a detailed pre-treatment reactor design, the kinetic parameters are required to model the AMD catalyzed hydrolysis reaction that is specific to the biomass used.

Since the sensitivity analyses have shown that a high rate of sulfate reduction is required for the process to be feasible, further research should be conducted into optimizing the rate of sulfate reduction. A combination of experimental laboratory and design work should be performed to first determine the factors that affect the rate of sulfate reduction and then use these to design a suitable sulfate-reducing bioreactor. The performance of such a reactor then needs to be demonstrated and optimized on a lab scale before it can be scaled up.

Further process simulation, design and evaluation needs to be conducted to determine the feasibility of incorporating the following processing streams: the production of small quantities of high-value biochemicals from glucose; the processing of lignin into biofuels or biochemicals; the processing of distillery silage into feed or fertilizer; and the upgrading of CO_2 and SO_2 released in DSR into valuable products. The findings of these investigations should then be used to develop a design for an integrated biorefinery that valorizes all of the biomass present, and by-products produced, to produce multiple revenue streams. The design of an integrated biorefinery should help increase the feasibility of the process.

Although this process is not currently economically feasible, or technologically ready, further research to develop this process into a commercial operation is encouraged. Water is a scarce and valuable resource in South Africa, and this process provides a sustainable solution to help protect the limited water that South Africa has. The use of 2nd generation biofuels and biochemicals products, as an alternative to fossil fuel-based products, will help reduce anthropogenic carbon emissions and associated climate change. This process will result in increased national water and energy security in South Africa and improve the environment for generations to come. The successful development of this process will also provide economic opportunities and create employment, both of which are much needed in South Africa.

Acid mine drainage is a legacy issue in many parts of the world. It continues to utilize economic and physical resources for treatment, in many cases, long after mining operations have ceased. Unlocking the potential of cellulose for the production of fuels has long been a research priority as a mechanism for reducing the reliance on fossil fuels, and hence minimizing the production of greenhouse gases. In the research presented here, these two challenges have been combined, resulting in positive outcomes for both*, i.e.* the treatment of the AMD and the simultaneous production of 2nd generation biofuel. Whilst this would not be a 'treatment silver bullet' for application at every mine site, this research demonstrates that it is possible to generate income from treating waste, whilst potentially lowering the environmental impacts from the waste generating processes. This resonates strongly with the concept of developing bespoke, complex solutions as a way forward for complex problems.

9.3. References

Esteghlalian, A., Hashimoto, A.G., Fenske, J.J., Penner, M.H., 1997. Modeling and optimization of the dilute-sulfuric-acid pretreatment of corn stover, poplar and switchgrass. Bioresour. Technol. 59, 129–136. doi:10.1016/S0960-8524(97)81606-9

Huang, H., Ramaswamy, S., Al-dajani, W., Tschirner, U., Cairncross, R.A., 2009. Effect of biomass species and plant size on cellulosic ethanol : A comparative process and economic analysis. Biomass and Bioenergy 33, 234–246. doi:10.1016/j.biombioe.2008.05.007

Humbird, D., Davis, R., Tao, L., Kinchin, C., Hsu, D., Aden, A., Schoen, P., Lukas, J., Olthof, B., Worley, M., Sexton, D., Dudgeon, D., 2011. Process Design and Economics for Biochemical Conversion of Lignocellulosic Biomass to Ethanol. Golden, Co.

Kaksonen, A.H., Puhakka, J.A., 2007. Sulfate reduction based bioprocesses for the treatment of acid mine drainage and the recovery of metals. Eng. Life Sci. 7, 541–564. doi:10.1002/elsc.200720216

Sánchez-Andrea, I., Sanz, J.L., Bijmans, M.F.M., Stams, A.J.M., 2014. Sulfate reduction at low pH to remediate acid mine drainage. J. Hazard. Mater. 269, 98–109. doi:10.1016/j.jhazmat.2013.12.032

Appendix A: Supplementary Data for Chapter 4

A.1. Supplementary Data

Table A1: Summary of rate of sulfate reduction in AMD by SRB (Sánchez-Andrea et al., 2014)

Reference	pH	Temp ˚C	Energy Source	Rate mol/m³.hr
(Moosa et al., 2002)	8	35	Acetate and peptone	1.24E-04
(Weijma et al., 2000)	7.5	65	Methanol	6.51E-03
(Houten et al., 2006)	7.3	30	Synthesis gas fed	6.51E-03
(Nagpal et al., 2000)	7	-	Ethanol	2.75E-03
(Lin and Lee, 2001)	7	35	Acetate	1.35E-04
(Chang et al., 2000)	6.8	25	Waste material	5.21E-05
(Wybrant et al., 2002)	6.5	-	Reactive mixture	5.21E-05
(Hiibel et al., 2011)	6.2	(-13)-36	Ethanol, wood chips ,corn stover	1.30E-05
(Bijmans et al., 2008b)	6	30	Formate	1.26E-02
(Bijmans et al., 2009b)	5	30	H_2/CO_2	2.17E-03
(Bijmans et al., 2009a)	5	30	Formate	7.81E-03
(Sánchez-Andrea et al., 2012)	5	30	Domestic water	1.48E-04
(Jong and Parry, 2003)	4.5	25	Lactate	2.08E-04
(Bijmans et al., 2010)	4.5	30	H_2/CO_2	3.26E-03
(Tsukamoto and Miller, 1999)	4.2	23-26	Methanol	6.98E-04
(Kolmert and Johnson, 2001)	4	-	Ethanol, lactate and glycerol	2.17E-04
(Bijmans et al., 2010)	4	30	Formate	2.65E-03
(Bijmans et al., 2010)	4	30	H_2/CO_2	3.47E-03
(Jong and Parry, 2006)	4	23-26	Lactate	5.51E-04
(Montoya et al., 2013)	4	25	Acetate: lactate (9:1)	3.86E-04
(Kaksonen et al., 2004)	3	35	Ethanol	1.87E-03
(Glombitza, 2001)	3	0	Methanol	1.35E-03
(Foucher et al., 2001)	2.5	30	Acetate and H_2/CO_2	2.08E-03
(Kaksonen et al., 2003)	2.5-3	35	Lactate	8.25E-04
(Nancucheo and Johnson, 2012)	2.3	30	Glycerol	5.21E-05
(Moosa et al., 2005)	8	35	Glucose and sodium acetate	9.22E-04

Table A2: Summary of the kinetic data used in sensitivity analysis

Source	A_f /min	Ea_f kJ/mol	n_f	A_s /min	Ea_s kJ/mol	n_s	X_f	Substrate
(Esteghlalian et al., 1997)	1.90E+21	169	0.4	4.20E+23	210.7	2	0.768	Switch Grass
(Yat et al., 2008)	2.48E+13	115	1.75	-	-	-	1	Switch Grass
(Maloney et al., 1985)	2.67E+16	128.1	1	1.63E+19	156	1	0.684	Paper Birch
(Nee and Yee, 1976)	6.40E+05	53	1.02	10.7	23.5	0.36	0.65	Bagasse
(Aguilar et al., 2002)	3.93E+12	99.15	1	-	-	-	1	Bagasse
(Kim et al., 2013)	6.88E+12	89.4	1.74	-	-	-	1	Xylo-oligomers
(Lavarack et al., 2002)	5.86E+09	88.1	0.79	8.76E+07	73.5	0.79	0.58	Bagasse

Table A3: Summary of main process parameters used in model

	Process 1	Process 2	Process 3
Hydrolysis reactor temperature4	95	-	-
Sulfate reducing reactor temperature(˚C)	35	35	35
Rate of sulfate reduction (mol/m^3/hr)	$9.22x10^{-4}$	$9.22x10^{-4}$	$9.22x10^{-4}$
pH entering sulfate reducing reactor	4	-	4
Fraction fast reacting xylan	0.768	0.768	0.768
Fraction slow reacting xylan	0.232	0.232	0.232
Desired Conversion SO4	0.8	0.8	0.8
Desired Conversion Xylan	0.75	.75	.75
Ratio conversion Fe^{2+}:SO_4	1	1	1
Conversion of H^+	0.99	0.99	0.99
Average Flow rate of Grass (Kg/Hr)	11.6	11.6	11.6
Solid liquid loading (θ)	0.1	0.1	0.1
Density of the sludge	1000	1000	1000

A.2. References

Aguilar, R., Ram, J.A., 2002. Kinetic study of the acid hydrolysis of sugar cane bagasse 55, 309–318.

Bijmans, M.F.M., Dopson, M., Peeters, T.W.T., Lens, P.N.L., Buisman, C.J.N., 2009a. Sulfate Reduction at pH 5 in a High-Rate Membrane Bioreactor : Reactor Performance and Microbial Community Analyses. J. Microbiol. Biotechnol. 19, 698–708. doi:10.4014/jmb.0809.502

Bijmans, M.F.M., Helvoort, P. Van, Dar, S.A., Dopson, M., Lens, P.N.L., Buisman, C.J.N., 2009b. Selective recovery of nickel over iron from a nickel – iron solution using microbial sulfate reduction in a gas-lift bioreactor. Water Res. 43, 853–861. doi:10.1016/j.watres.2008.11.023

Bijmans, M.F.M., Peeters, T.W.T., Lens, P.N.L., Buisman, C.J.N., 2008. High rate sulfate reduction at pH 6 in a pH-auxostat submerged membrane bioreactor fed with formate. Water Res. 42, 2439–2448. doi:10.1016/j.watres.2008.01.025

Bijmans, M.F.M., Vries, E. De, Yang, C.-H., Buisman, C.J.N., Lens, P.N.L., Dopson, M., 2010. Sulfate Reduction at pH 4 . 0 for Treatment of Process and Wastewaters. Biotechnol. Prog. 26, 1029–1037. doi:10.1002/btpr.400

Chang, I.S., Shin, P.K., Kim, B.H., 2000. Biological treatment of acid mine drainage under sulphate-reducing conditions with solid waste materials as substrate. Water Res. 34, 1269–1277. doi:10.1016/s0043-1354(99)00268-7

Esteghlalian, A., Hashimoto, A.G., Fenske, J.J., Penner, M.H., 1997. Modeling and optimization of the dilute-sulfuric-acid pretreatment of corn stover, poplar and switchgrass. Bioresour. Technol. 59, 129–136. doi:10.1016/S0960-8524(97)81606-9

Foucher, S., Battaglia-Brunet, F., Ignatiadis, I., Morin, D., 2001. Treatment by sulfate-reducing bacteria of Chessy acid-mine drainage and metals recovery. Chem. Eng. Sci. 56, 1639–1645. doi:10.1016/S0009-2509(00)00392-4

Glombitza, F., 2001. Treatment of acid lignite mine ¯ ooding water by means of microbial sulfate reduction. Waste Manag. 21, 197–203. doi:10.1016/S0956-053X(00)00061-1

Hiibel, S.R., Pereyra, L.P., Breazeal, M.V.R., Reisman, D.J., Reardon, K.F., Pruden, A., 2011. Effect of Organic Substrate on the Microbial Community Structure in Pilot-Scale Sulfate-Reducing Biochemical Reactors Treating Mine Drainage 1. Enviromental Eng. Sci. 28, 563–572. doi:10.1089/ees.2010.0237

Houten, B.H.G.W. Van, Roest, K., Tzeneva, V.A., Dijkman, H., Smidt, H., Stams, A.J.M., 2006.

Occurrence of methanogenesis during start-up of a full-scale synthesis gas-fed reactor treating sulfate and metal-rich wastewater. Water Res. 40, 553–560. doi:10.1016/j.watres.2005.12.004

Jong, T., Parry, D.L., 2006. Microbial sulfate reduction under sequentially acidic conditions in an upflow anaerobic packed bed bioreactor. Water Res. 40, 2561–2571. doi:10.1016/j.watres.2006.05.001

Jong, T., Parry, D.L., 2003. Removal of sulfate and heavy metals by sulfate reducing bacteria in short-term bench scale upflow anaerobic packed bed reactor runs. Water Res. 37, 3379–3389. doi:10.1016/S0043-1354(03)00165-9

Kaksonen, A.H., Franzmann, P.D., Puhakka, J.A., 2004. Effects of Hydraulic Retention Time and Sulfide Toxicity on Ethanol and Acetate Oxidation in Sulfate-Reducing Metal- Precipitating Fluidized-Bed Reactor. Biotechnol. Bioeng. 86, 332–343. doi:10.1002/bit.20061

Kaksonen, A.H., Riekkola-vanhanen, M., Puhakka, J.A., 2003. Optimization of metal sulphide precipitation in fluidized-bed treatment of acidic wastewater. Water Res. 37, 255–266.

Kim, Y., Kreke, T., Ladisch, M.R., 2013. Reaction Mechanisms and Kinetics of Xylo-Oligosaccharide Hydrolysis by Dicarboxylic Acids 59. doi:10.1002/aic

Kolmert, A., Johnson, D.B., 2001. Remediation of acidic waste waters using immobilised , acidophilic sulfate-reducing bacteria. J. Chem. Technol. Biotechnol. 76, 836–843. doi:10.1002/jctb.453

Lavarack, B.P., Gri, G.J., Rodman, D., 2002. The acid hydrolysis of sugarcane bagasse hemicellulose to produce xylose , arabinose , glucose and other products 23, 367–380.

Lin, Y.H., Lee, K.K., 2001. Verification of Anarobic Biofilm Model for Phenol Degradation with Sulfate Reduction. J. Environ. Eng. 127, 119–125. doi:10.1061/(ASCE)0733-9372(2001)127:2(119)

Maloney, M.T., Chapman, T.W., Baker, a J., 1985. Dilute acid hydrolysis of paper birch: kinetics studies of xylan and acetyl-group hydrolysis. Biotechnol. Bioeng. 27, 355–361. doi:10.1002/bit.260270321

Montoya, L., Celis, L.B., Gallegos-Garcia, M., Elias, R.-F., Alpuche-Solis, A., 2013. Consortium diversity of a sulfate-reducing biofilm developed at acidic pH influent conditions in a down-flow fluidized bed reactor. Eng. Life Sci. 13, 302–311. doi:10.1002/elsc.201200047

Moosa, S., Nemati, M., Harrison, S.T.L., 2005. A kinetic study on anaerobic reduction of sulphate , part II : incorporation of temperature effects in the kinetic model. Chem. Eng. Sci. 60, 3517–3524. doi:10.1016/j.ces.2004.11.036

Moosa, S., Nemati, M., Harrison, S.T.L., 2002. A kinetic study on anaerobic reduction of sulphate , Part I : Effect of sulphate concentration. Chem. Eng. Sci. 57, 2773–2780. doi:10.1016/S0009-2509(02)00152-5

Nagpal, S., Chuichulcherm, S., Peeva, L., 2000. Microbial Sulfate Reduction in a Liquid – Solid Fluidized Bed Reactor. Biotechnol. Bioeng. 70, 370–380. doi:10.1002/1097-0290(20001120)70:4<370::AID-BIT2>3.0.CO;2-7

Nancucheo, I., Johnson, D.B., 2012. Selective removal of transition metals from acidic mine waters by novel consortia of acidophilic sulfidogenic bacteria. Microb. Biotechnol. 5, 34–44. doi:10.1111/j.1751-7915.2011.00285.x

Nee, C.I., Yee, W.F., 1976. Hydrolysis of Pentosans in Bagasse Pith 283–287.

Sánchez-Andrea, I., Sanz, J.L., Bijmans, M.F.M., Stams, A.J.M., 2014. Sulfate reduction at low pH to remediate acid mine drainage. J. Hazard. Mater. 269, 98–109. doi:10.1016/j.jhazmat.2013.12.032

Sánchez-Andrea, I., Triana, D., Sanz, J.L., 2012. Bioremediation of acid mine drainage coupled with domestic wastewater treatment. Water Sci. Technol. 66, 2425–2431. doi:10.2166/wst.2012.477

Tsukamoto, T.K., Miller, G.C., 1999. METHANOL AS A CARBON SOURCE FOR MICROBIOLOGICAL TREATMENT OF ACID MINE DRAINAGE. Water Res. 33, 1365–1370. doi:10.1016/S0043-1354(98)00342-X

Weijma, J., Stams, A.J.M., Pol, L.W.H., Lettinga, G., 2000. Thermophilic Sulfate Reduction and Methanogenesis with Methanol in a High Rate Anaerobic Reactor. Biotechnol. Bioeng. 67, 354–363. doi:10.1002/(SICI)1097-0290(20000205)67:3<354::AID-BIT12>3.0.CO;2-X

Wybrant, K.R., Ptacek, C.J., Blowes, D.W., 2002. Treatment of Mine Drainage Using Permeable Reactive Barriers : Column Experiments. Environ. Sci. Technol. 36, 1349–1356. doi:10.1021/es010751g

Yat, S.C., Berger, A., Shonnard, D.R., 2008. Kinetic characterization for dilute sulfuric acid hydrolysis of timber varieties and switchgrass. Bioresour. Technol. 99, 3855–3863. doi:10.1016/j.biortech.2007.06.046

Appendix B: Scilab Code for Fitting Rate of Hydrolysis Determination of Kinetic Parameters in Chapter 5

```
//=========================================================================
// Script to fit a model of the rate of hydrolysis of xylan to experimental,
// data and determine the kinetic parameters. To run model  under the assumption
// that the slow reacting fraction of xylan does not react, replace "mxr1"
// in line 2 of function my myerror with "mxr2"
//=========================================================================

clc; clear ; xdel(winsid())

// Extracting data frim Excel=============================================
datasummary = readxls..
('/Users/nwburman/Dropbox/1.          Doctorate/5.          experiments/1.Hydrolysis
experiments/1.xls')    //Open the excel file with data
data35=datasummary(1)         //get all data for experiments at 35C
data65=datasummary(2)         //get all data for experiments at 65C
data90=datasummary(3)         //get all data for 1st experiment at 90C
data90n=datasummary(4)         //get all data for 2st experiment at 90C
data90c=datasummary(5)        //get all data for 1st and 2nd exp. at 90C
t35=data35(2:13,1)            // time data for 35 C
x135=data35(2:13,2)          //xylose data for pH1 @ 35C
x235=data35(2:13,3)          //xylose data for pH2 @ 35C
x335=data35(2:13,4)          //xylose data for pH3 @ 35C

t65=data65(2:11,1)            // time data for 65C
x165=data65(2:11,2)          //xylose data for pH1 @ 65C
x265=data65(2:11,3)          //xylose data for pH2 @ 65C
x365=data65(2:11,4)          //xylose data for pH3 @ 65C

t90=data90(2:11,1)            // time data for 90C
x190=data90(2:11,2)          //xylose data for pH1 @ 90C
x290=data90(2:11,3)          //xylose data for pH2 @ 90C
x390=data90(2:11,4)          //xylose data for pH3 @ 90C

t90n=data90n(2:14,1)               // time data for 90 C (2nd exp.)
x190n=data90n(2:14,2)              //xylose data for pH1 @ 90C (2nd exp.)

t90c=data90c(2:10,1)               // time data for 90 C (combined)
x190c=data90c(2:10,2)              // xylose data for pH1 @ 90C (combined)

t235=linspace(0,40,1000)            //time vector for model @35C
t265=linspace(0,20,1000)            //time vector for model @65C
t290=linspace(0,20,1000)            //time vector for model @90C

x35=[x135 x235 x335]                 //xylose data for all @ 35C
x65=[x165 x265 x365]                 //xylose data for all @ 65C
x90=[x190 x290 x390]                 //xylose data for all @ 90C

alpha=0.5                             //fraction of fast reacting xylan

//Functions=============================================================================

function y=mxr1(x, c)             //remaining xylan over time with both Kf and Ks
     y=alpha*exp(c(1)*x)+(1-alpha)*exp(c(2)*x)
endfunction

function y=mxr2(x, c)             //remaining xylan over time with both Kf and Ks
    y=alpha*exp(c(1)*x)+(1-alpha)
endfunction

function e=myerror(c, x, y)        // func. to minimize the err of model and data.
    e=mxr1(x,c)-y                // change mxr1 to mxr2 for results without ks
endfunction
```

```
//=============================================================================
// fitting of model to data.
// all fx below is the sum of the square error between model and exp values.
// all xopt below is the values of kf and ks that minimizes the sum of sq. err
//=============================================================================

bsupf=-%inf                     //lower bound for kf
binff=-1/10^%inf                //upper bounds for kf
bsups=-%inf                     //lower bound for ks
binfs=-1/(10^(%inf+1))          //upper bound for ks

c035=[-.1, -.0001];          // initial estimates of kf and ks at 35C
c065=[-.1, -.00000000001];   // initial estimates of kf and ks at 65C
c090=[-.1, -.0001]           // initial estimates of kf and ks at 90C

//iniital estimates and leastsq optimization @ 35=================================

//fitting of kf and ks at pH 1 and 35C
[fx135,xopt135]=leastsq(list(myerror,t35,x135),'b',..
[-%inf,-%inf],[-1/1000000000,-1/10000000000000],c035)
//fitting of kf and ks at pH 2 and 35C
[fx235,xopt235]=leastsq(list(myerror,t35,x235),'b',..
[bsupf,bsups],[binff,binfs],c035)
//fitting of kf and ks at pH 3 and 35C
[fx335,xopt335]=leastsq(list(myerror,t35,x335),'b',..
[bsupf,bsups],[binff,binfs],c035)

xopt35=[xopt135; xopt235; xopt335] //put all kf and ks at 35C in one matrix

//iniital estimates and leastsq optimization 65=================================

//fitting of kf and ks at pH 1 and 65C
[fx165,xopt165]=leastsq(list(myerror,t65,x165),'b',..
[bsupf,bsups],[binff,binfs],c065)
//fitting of kf and ks at pH 2 and 65C
[fx265,xopt265]=leastsq(list(myerror,t65,x265),'b',..
[bsupf,bsups],[binff,binfs],c065)
//fitting of kf and ks at pH 3 and 65C
[fx365,xopt365]=leastsq(list(myerror,t65,x365),'b',..
[bsupf,bsups],[binff,binfs],c065)

xopt65=[xopt165; xopt265; xopt365] //put all kf and ks at 65C in one matrix

//iniital estimates and leastsq optimization 90=================================

//change t90n to t90c and x190n to x190c for combined pH1 90C results
//fitting of kf and ks at pH 1 and 90C
[fx190,xopt190]=leastsq(list(myerror,t90c,x190c),'b',..
[bsupf,bsups],[binff,binfs],c090)
//fitting of kf and ks at pH 1 and 90C
[fx290,xopt290]=leastsq(list(myerror,t90,x290),'b',..
[bsupf,bsups],[binff,binfs],c090)
//fitting of kf and ks at pH 1 and 90C
[fx390,xopt390]=leastsq(list(myerror,t90,x390),'b',..
[bsupf,bsups],[binff,binfs],c090)

xopt90=[xopt190; xopt290; xopt390] //put all kf and ks at 90 C in one matrix

//make sure kf > ks otherwise swop=============================================
if xopt90(1,1)> xopt90 (1,2)
    then op=xopt90(1,1); opp=xopt90(1,2); xopt90(1,1)=opp; xopt90(1,2)=op
    end

xoptf=[xopt35(:,1) xopt65(:,1) xopt90(:,1)] //put all kf in one matrix
xopts=[xopt35(:,2) xopt65(:,2) xopt90(:,2)] //put all ks in one matrix

//plot graphs of model predictions vs exp data for all
```

```
//run models at 35=================================================================
//N.B. replace all mxr1 below to mxr2 to run model under the assumpton that
//slowreacting fraction of xylan does not react.

mx135=mxr1(t235,xopt135) // model predicted xylose remaining at pH 1 and 35C
mx235=mxr1(t235,xopt235) // model predicted xylose remaining at pH 2 and 35C
mx335=mxr1(t235,xopt335) // model predicted xylose remaining at pH 3 and 35C
mx35=[mx135' mx235' mx335'] //model predicted xylose remaining  all pH and 35C

//run models at 65=================================================================
//N.B. replace all mxr1 below to mxr2 to run model under the assumpton that
//slowreacting fraction of xylan does not react.

mx165=mxr1(t265,xopt165) // model predicted xylose remaining at pH 1 and 65C
mx265=mxr1(t265,xopt265) // model predicted xylose remaining at pH 2 and 65C
mx365=mxr1(t265,xopt365) // model predicted xylose remaining at pH 3 and 65C
mx65=[mx165' mx265' mx365'] // model predicted xylose remaining all pH 65C

//run models at 90=================================================================
//N.B. replace all mxr1 below to mxr2 to run model under the assumpton that
//slowreacting fraction of xylan does not react.

mx190=mxr1(t290,xopt190) // model predicted xylose remaining at pH 1 and 90C
mx290=mxr1(t290,xopt290) // model predicted xylose remaining at pH 2 and 90C
mx390=mxr1(t290,xopt390) // model predicted xylose remaining at pH 3 and 90C
mx90=[mx190' mx290' mx390'] // model predicted xylose remaining all pH and 90C

scf(0)
//Plot graphs  35=================================================================
subplot(3,1,1)
//scf(1)
plot(t35,x35,'o')
plot(t235,mx35)
legend("pH1 exp", "pH2 exp", "pH3 exp", "ph1 model", "pH2 Model", "pH3 model")
xtitle("", "Time (t) [days]","% Xylose Remaining [%]")
title("35 xylose")

//Plot graphs  65=================================================================
subplot(3,1,2)
//scf(3)
plot(t65,x65,'o')
plot(t265,mx65)
legend("pH1 exp", "pH2 exp", "pH3 exp", "ph1 model", "pH2 Model", "pH3 model")
xtitle("", "Time (t) [days]","% Xylose Remaining [%]")
title("65 xylose")

//Plot graphs  90=================================================================
subplot(3,1,3)
//scf(5)
//plot(t90n,x190n,t90,x90,'o')
plot(t90n,x190n,'o',t90,x90(:,2:3),'o')
//plot(t290,mx90,t290,mx90s)
plot(t290,mx90)
legend("pH1 exp", "pH2 exp", "pH3 exp", "ph1 model", "pH2 Model", "pH3 model")
xtitle("", "Time (t) [days]","% Xylose Remaining [%]")
title("90 xylose")

// Linear Regression to get kinetic constants=====================================

kf=[-xopt35(:,1) -xopt65(:,1) -xopt90(:,1)]/24// all kf in matrix convert to /hr
ks=[-xopt35(:,2) -xopt65(:,2) -xopt90(:,2)]/24// all ks in matrix convert to /hr

kf(find(kf==0)) = %nan  //remove zero values
ks(find(ks==0)) = %nan  //remove zero values
R=8.314e-3              //universal gas constant [KJ/mol.K]

lnkf=log(kf)            //log of Kf matrix
```

```
lnks=log(ks)              //log of ks matrix

t=[35 65 90]              //different temperatures [C]
T=1'./(t+273.15)          //1/t [1/K]

// fit equations to the line lnKf=Ea/R.1/T+ln(A0)+nln(ca)
//solve the set of linear equations
//Ax=b -> x=A\b
//A (Af) is matrix containing vectors and 1/T's
//b (yf) is matrix containing ln(kf)'s
//x (Xf) is matrix containing the intercepts of the line and gradient

Af=[1 1 1 0 0 0; 0 0 0 1 1 0;0 0 0 0 0 1; ..
T(1) T(2) T(3) T(2) T(3) T(3)]'          //A matrix (fast reacting fraction )
As=[1 0 ;0 1 ; T(1) T(2)]'               //A matrix (slow reacting fraction )
yf=[lnkf(1,:) lnkf(2,2:3) lnkf(3,3)]     //b matrix (fast reacting frac)
ys=[lnks(1,1) lnks(2,2)]                 //b matrix (slow reacting frac)
Xf=Af\yf'                                //x matrix (fast reacting frac)
Xs=As\ys'                                //x matrix (slow reacting frac)

// fit equations to the line C=ln(A0)+nln(ca)
//solve the set of linear equations
//Ax=b -> x=A\b
//A (Anf) is matrix containing vectors vectors and ln(Ca)'s
//b (Bf) is matrix containing C (intercepts from above)
//x (Xnf) is matrix containing the ln(A0) and n

lnca=[-4.337775864 -6.314761665 -9.061739807]  //acid concentrations
Anf=[1 1 1; lnca(1,1) lnca(1,2) lnca(1,3)]'    //A matrix (fast reacting frac)
Ans=[1 1; lnca(1,1) lnca(1,2)]'                //A matrix (slow reacting frac)
Bf=[Xf(1) Xf(2) Xf(3)]'                        //b matrix (fast reacting frac)
Bs=[Xs(1) Xs(2)]'                              //b matrix (slow reacting frac)

Xnf=Anf\Bf                                     //x matrix (fast reacting frac)
Xns=Ans\Bs                                     //x matrix (slow reacting frac)

A0f=exp(Xnf(1,1))         //Pre exp. factor (fast reacting frac) [/min]
A0s=exp(Xns(1,1))         //Pre exp. factor (slow reacting frac) [/min]
Eaf=-Xf(4)*R              //Activation energy (fast reacting frac) [kJ/mol]
Eas=-Xs(3)*R              //Activation energy (slow reacting frac)  [kJ/mol]
nf=Xnf(2,1)               //n (fast reacting frac)
ns=Xns(2,1)               //n (slow reacting frac)
```

Appendix C: Supplementary Data for chapter 7

C.1. Equations for Sizing of Reactors

$$V_{pretreat} = v_1 \times (t_{pretreat} + 24) \times D_f \quad \text{(S1)}$$

Where $V_{pretreat}$ is the volume of the pre-treatment reactor (m^3), $t_{pretreat}$ is the pre-treatment time (hrs), v_1 is the volumentric flow rate of stream 1 (m^3/hr), D_f is an over design factor (assumed to be 1.1). 24 hr have been added to $t_{pretreat}$ to allow for loading, emptying and cleaning of the reactor.

$$V_{hydrolysis} = \frac{M_2 \times t_{batch}}{\rho_2} \times \frac{204}{168} \times D_f \quad \text{(S2)}$$

Where $V_{hydrolysis}$ is the volume of the hydrolysis reactor, M_2 is the mass flow rate of stream 2 (kg/hrs), t_{batch} is the batch time (hrs), ρ_2 is the density of stream 2 (kg/m^3), 204/168 has been included to allow for loading, unloading and cleaning of reactors.

$$t_{ferm} = \frac{(C_{G,5} - r_{lg} \times 6)}{r_s} + 6 \quad \text{(S3)}$$

Where t_{ferm} is the fermentation time (hrs), $C_{G,5}$ is the glucose concentration in stream 5, r_{lg} and r_s are the rate of fermentation in the lag a and stationary phases respectively (g/L.hr)

$$t_{cycle} = t_{ferm} + 6 \quad \text{(S4)}$$

Where t_{cycle} is the time of the total cycle including loading, unloading and cleaning.

$$V_{ferm} = \frac{v_{ferm} \times \rho_8}{\rho_8} \times D_f \quad \text{(S5)}$$

Where V_{ferm} is the volume of the fermentor, v_8 is the volumetric flow rate of stream 8 (m^3/hr) and ρ_8 is the density of stream 8 (kg/m^3).

$$V_{SSF} = \frac{M_2 \times T_{batch}}{\rho_2} \times \frac{204}{168} \times D_f \quad \text{(S6)}$$

Where V_{SSF} is the volume of the SSF reactor, M_2 is the mass flow rate of stream 2 (kg/hrs), t_{batch} is the batch time (hrs), ρ_2 is the density of stream 2 (kg/m^3), 204/168 has been included to allow for loading, unloading and cleaning of reactors.

C.2. Summary of Individual Equipment Costs

Table C1: Summary of capital cost of individual equipment in different scenarios

Item Number	Item	A-SHF (USD)	H-SHF (USD)	A-SSF (USD)	H-SHF (USD)
Heat Exchangers					
E-101	FEEDCHILL	125 000	125 000	143 000	143 000
E-102	FERMCHILL	84 100	84 600		
E-103	PRE-HX1	692 000	692 000	692 000	173 000
E-104	PRE-HX2	65 300	65 300	65 300	65 300
E-105	BEERCOl Reboiler	263 000	134 000	119 000	134 000
E-106	Beercol Condenser	35 900	41 600	36 100	37 100
E-107	RECTCOL Reboiler	35 600	36 600	32 900	36 500
E-108	RECTCOL Condenser	36 800	43 200	37 000	38 200
Distillation Columns					
T-101	BEERCOL	530 000	349 000	599 000	599 000
T-102	RECTCOL	82 100	108 000	79 900	82 100
Flash Tanks					
V-101	Flash Tank (BEERCOL)	28 600	23 800	18 700	16 600
V-102	Flash Tank (RECTCOL)	15 400	18 700	16 600	17 300
Reactors					
Z-101	FERMENT	2 753 229	2 753 229		
Z-102	PRETREAT	36 535 735	16 180 111	36 535 735	16 180 111
Z-103	HYDROLYSIS	38 623 491	38 623 491		
Z-104	SSF			55 325 541	55 325 541
Total Purchased Cost		79 900 000	59 300 000	93 700 000	72 800 000
Lang Factor		4.74	4.74	4.74	4.74
Total Installed cost		379 000 000	281 000 000	444 000 000	345 000 000

C.3. Full Stream Table for Aspen Plus™ Model (H-SHF: Pre-treatment Area)

	Units	1-10	1-11	1-12	1-20	1-30	1-40	1-41	1-50
From			PRE-HX1	PRE-HX2		PRETREAT	PRE-FILT	PRE-HX1	PRE-FILT
To		PRE-HX1	PRE-HX2	PRETREAT	PRETREAT	PRE-FILT	PRE-HX1		$C-3
Substream: ALL									
Temperature	C	20	78.95488	95	20	90	90	30	90
Mass Flow	KG/HR	450000	450000	450000	90000	540000	448431	448431	91569.4
Component Mass Flow									
CELLULOS	KG/HR	0	0	0	33300	33300	0	0	33300
XYLAN	KG/HR	0	0	0	26100	9467.79	0	0	9467.79
LIGNIN	KG/HR	0	0	0	22500	17100	0	0	17100
PROTEIN	KG/HR	0	0	0	2700	2700	0	0	2700
ASH	KG/HR	0	0	0	5400	5400	0	0	5400
H2O	KG/HR	447750	447750	447750	0	445482.1	423208	423208	22274.1
H2SO4	KG/HR	2250	2250	2250	0	2250	2137.5	2137.5	112.5
GLUCOSE	KG/HR	0	0	0	0	0	0	0	0
XYLOSE	KG/HR	0	0	0	0	18900.04	17955.04	17955.04	945
LGNSOL	KG/HR	0	0	0	0	5400	5130	5130	270
ETHANOL	KG/HR	0	0	0	0	0	0	0	0
CO2	KG/HR	0	0	0	0	0	0	0	0
Component Mass Fraction									
CELLULOS		0	0	0	0.37	0.0617	0	0	0.3637
XYLAN		0	0	0	0.29	0.0175	0	0	0.1034
LIGNIN		0	0	0	0.25	0.0317	0	0	0.1867
PROTEIN		0	0	0	0.03	0.005	0	0	0.0295
ASH		0	0	0	0.06	0.01	0	0	0.059
H2O		0.995	0.995	0.995	0	0.825	0.9438	0.9438	0.2432
H2SO4		0.005	0.005	0.005	0	0.0042	0.0048	0.0048	0.0012
GLUCOSE		0	0	0	0	0	0	0	0
XYLOSE		0	0	0	0	0.035	0.04	0.04	0.0103
LGNSOL		0	0	0	0	0.01	0.0114	0.0114	0.0029
ETHANOL		0	0	0	0	0	0	0	0
CO2		0	0	0	0	0	0	0	0

	Units	1-10	1-11	1-12	1-20	1-30	1-40	1-41	1-50
From			PRE-HX1	PRE-HX2		PRETREAT	PRE-FILT	PRE-HX1	PRE-FILT
To		PRE-HX1	PRE-HX2	PRETREAT	PRETREAT	PRE-FILT	PRE-HX1		$C-3
Substream: ALL									
Temperature	C	20	78.95488	95	20	90	90	30	90
Mass Flow	KG/HR	450000	450000	450000	90000	540000	448431	448431	91569.4
Component Mole Flow									
CELLULOS	KMOL/HR	0	0	0	205.38	205.38	0	0	205.38
XYLAN	KMOL/HR	0	0	0	197.55	71.66	0	0	71.66
LIGNIN	KMOL/HR	0	0	0	147.88	112.39	0	0	112.39
PROTEIN	KMOL/HR	0	0	0	118.22	118.22	0	0	118.22
ASH	KMOL/HR	0	0	0	96.3	96.3	0	0	96.3
H2O	KMOL/HR	24853.9	24853.9	24853.9	0	24728.01	23491.61	23491.61	1236.4
H2SO4	KMOL/HR	22.94	22.94	22.94	0	22.94	21.79	21.79	1.15
GLUCOSE	KMOL/HR	0	0	0	0	0	0	0	0
XYLOSE	KMOL/HR	0	0	0	0	125.89	119.6	119.6	6.29
LGNSOL	KMOL/HR	0	0	0	0	35.49	33.72	33.72	1.77
ETHANOL	KMOL/HR	0	0	0	0	0	0	0	0
CO2	KMOL/HR	0	0	0	0	0	0	0	0
Component Mole Fraction									
CELLULOS		0	0	0	0.2684	0.008	0	0	0.111
XYLAN		0	0	0	0.2581	0.0028	0	0	0.0387
LIGNIN		0	0	0	0.1932	0.0044	0	0	0.0608
PROTEIN		0	0	0	0.1545	0.0046	0	0	0.0639
ASH		0	0	0	0.1258	0.0038	0	0	0.0521
H2O		0.9991	0.9991	0.9991	0	0.9691	0.9926	0.9926	0.6685
H2SO4		0.0009	0.0009	0.0009	0	0.0009	0.0009	0.0009	0.0006
GLUCOSE		0	0	0	0	0	0	0	0
XYLOSE		0	0	0	0	0.0049	0.0051	0.0051	0.0034
LGNSOL		0	0	0	0	0.0014	0.0014	0.0014	0.001
ETHANOL		0	0	0	0	0	0	0	0
CO2		0	0	0	0	0	0	0	0

C.4. Full Stream Table for Aspen Plus™ Model (H-SHF: Hydrolysis and Fermentation Area)

	Units	1-50	2-10	2-100	2-20	2-21	2-30	2-40	2-50	2-60	2-70	2-80	2-90	3-80
From		$C-4		B1	WATERMIX	FEEDCHIL	FEEDMIX	HYDROLYS	FILTER	FILTER	FERMCHIL	FEREMNT	B1	$C-6
To		FEEDMIX	WATERMIX	$C-2	FEEDCHIL	FEEDMIX	HYDROLYS	FILTER		FERMCHIL	FEREMNT	B1		WATERMIX
Substream: ALL														
Temperature	C	90.00	25.00	35.00	93.48	50.00	54.06	50.00	50.00	50.00	35.00	35.00	35.00	99.88
Mass Flow	KG/HR	91569.4	29072.54	340339	328203	328203	419784	419784	72940.94	346843	346843	346843	6503.8	299130
Component Mass flow														
CELLULOS	KG/HR	33300	0	0	0	0	33300	20018.26	20018.26	0	0	0	0	0
XYLAN	KG/HR	9467.79	0	0	0	0	9467.79	9467.79	9467.79	0	0	0	0	0
LIGNIN	KG/HR	17100	0	0	0	0	17100	17100	17100	0	0	0	0	0
PROTEIN	KG/HR	2700	0	0	0	0	2700	2700	2700	0	0	0	0	0
ASH	KG/HR	5400	0	0	0	0	5400	5400	5400	0	0	0	0	0
H2O	KG/HR	22274.1	29072.54	321305.5	317564.8	317564.8	339850.8	338375.1	16918.75	321456.3	321456.3	321456.3	150.82	288492.3
H2SO4	KG/HR	112.5	0	737.07	663.36	663.36	775.86	775.86	38.79	737.07	737.07	737.07	0	663.36
GLUCOSE	KG/HR	0	0	2384.67	2146.2	2146.2	2146.13	16903.57	845.18	16058.39	16058.39	2384.67	0	2146.2
XYLOSE	KG/HR	945	0	6191.39	5572.25	5572.25	6517.26	6517.26	325.86	6191.39	6191.39	6191.39	0	5572.25
LGNSOL	KG/HR	270	0	1768.96	1592.07	1592.07	1862.07	1862.07	93.1	1768.96	1768.96	1768.96	0	1592.07
ETHANOL	KG/HR	0	0	7565.86	663.9	663.9	663.94	663.94	33.2	630.74	630.74	7623.89	58.03	663.9
CO2	KG/HR	0	0	385.62	0	0	0	0	0	0	0	6680.57	6294.95	0
Component Mass Fraction														
CELLULOS		0.3637	0	0	0	0	0.0793	0.0477	0.2744	0	0	0	0	0
XYLAN		0.1034	0	0	0	0	0.0226	0.0226	0.1298	0	0	0	0	0
LIGNIN		0.1867	0	0	0	0	0.0407	0.0407	0.2344	0	0	0	0	0
PROTEIN		0.0295	0	0	0	0	0.0064	0.0064	0.037	0	0	0	0	0
ASH		0.059	0	0	0	0	0.0129	0.0129	0.074	0	0	0	0	0
H2O		0.2432	1	0.9441	0.9676	0.9676	0.8096	0.8061	0.232	0.9268	0.9268	0.9268	0.0232	0.9644
H2SO4		0.0012	0	0.0022	0.002	0.002	0.0018	0.0018	0.0005	0.0021	0.0021	0.0021	0	0.0022
GLUCOSE		0	0	0.007	0.0065	0.0065	0.0051	0.0403	0.0116	0.0463	0.0463	0.0069	0	0.0072
XYLOSE		0.0103	0	0.0182	0.017	0.017	0.0155	0.0155	0.0045	0.0179	0.0179	0.0179	0	0.0186
LGNSOL		0.0029	0	0.0052	0.0049	0.0049	0.0044	0.0044	0.0013	0.0051	0.0051	0.0051	0	0.0053
ETHANOL		0	0	0.0222	0.002	0.002	0.0016	0.0016	0.0005	0.0018	0.0018	0.022	0.0089	0.0022
CO2		0	0	0.0011	0	0	0	0	0	0	0	0.0193	0.9679	0

	Units	1-50	2-10	2-100	2-20	2-21	2-30	2-40	2-50	2-60	2-70	2-80	2-90	3-80
From		$C-4		B1	WATERMIX	FEEDCHIL	FEEDMIX	HYDROLYS	FILTER	FILTER	FERMCHIL	FEREMNT	B1	$C-6
To		FEEDMIX	WATERMIX	$C-2	FEEDCHIL	FEEDMIX	HYDROLYS	FILTER		FERMCHIL	FEREMNT	B1		WATERMIX
Substream: ALL														
Temperature	C	90.00	25.00	35.00	93.48	50.00	54.06	50.00	50.00	50.00	35.00	35.00	35.00	99.88
Mass Flow	KG/HR	91569.4	29072.54	340339	328203	328203	419784	419784	72940.94	346843	346843	346843	6503.8	299130
Component Mole flow														
CELLULOS	KMOL/HR	205.38	0	0	0	0	205.38	123.46	123.46	0	0	0	0	0
XYLAN	KMOL/HR	71.66	0	0	0	0	71.66	71.66	71.66	0	0	0	0	0
LIGNIN	KMOL/HR	112.39	0	0	0	0	112.39	112.39	112.39	0	0	0	0	0
PROTEIN	KMOL/HR	118.22	0	0	0	0	118.22	118.22	118.22	0	0	0	0	0
ASH	KMOL/HR	96.3	0	0	0	0	96.3	96.3	96.3	0	0	0	0	0
H2O	KMOL/HR	1236.4	1613.77	17835.16	17627.53	17627.53	18864.58	18782.67	939.13	17843.54	17843.54	17843.54	8.37	16013.76
H2SO4	KMOL/HR	1.15	0	7.52	6.76	6.76	7.91	7.91	0.4	7.52	7.52	7.52	0	6.76
GLUCOSE	KMOL/HR	0	0	13.24	11.91	11.91	11.91	93.83	4.69	89.14	89.14	13.24	0	11.91
XYLOSE	KMOL/HR	6.29	0	41.24	37.12	37.12	43.41	43.41	2.17	41.24	41.24	41.24	0	37.12
LGNSOL	KMOL/HR	1.77	0	11.63	10.46	10.46	12.24	12.24	0.61	11.63	11.63	11.63	0	10.46
ETHANOL	KMOL/HR	0	0	164.23	14.41	14.41	14.41	14.41	0.72	13.69	13.69	165.49	1.26	14.41
CO2	KMOL/HR	0	0	8.76	0	0	0	0	0	0	0	151.8	143.04	0
Component Mole Fraction														
CELLULOS		0.111	0	0	0	0	0.0105	0.0063	0.084	0	0	0	0	0
XYLAN		0.0387	0	0	0	0	0.0037	0.0037	0.0488	0	0	0	0	0
LIGNIN		0.0608	0	0	0	0	0.0057	0.0058	0.0765	0	0	0	0	0
PROTEIN		0.0639	0	0	0	0	0.006	0.0061	0.0804	0	0	0	0	0
ASH		0.0521	0	0	0	0	0.0049	0.0049	0.0655	0	0	0	0	0
H2O		0.6685	1	0.9864	0.9954	0.9954	0.9645	0.9644	0.639	0.9909	0.9909	0.9786	0.0548	0.995
H2SO4		0.0006	0	0.0004	0.0004	0.0004	0.0004	0.0004	0.0003	0.0004	0.0004	0.0004	0	0.0004
GLUCOSE		0	0	0.0007	0.0007	0.0007	0.0006	0.0048	0.0032	0.005	0.005	0.0007	0	0.0007
XYLOSE		0.0034	0	0.0023	0.0021	0.0021	0.0022	0.0022	0.0015	0.0023	0.0023	0.0023	0	0.0023
LGNSOL		0.001	0	0.0006	0.0006	0.0006	0.0006	0.0006	0.0004	0.0006	0.0006	0.0006	0	0.0007
ETHANOL		0	0	0.0091	0.0008	0.0008	0.0007	0.0007	0.0005	0.0008	0.0008	0.0091	0.0083	0.0009
CO2		0	0	0.0005	0	0	0	0	0	0	0	0.0083	0.9369	0

C.5. Full Stream Table for Aspen Plus™ Model (H-SHF: Product Separation Area)

	Units	2-100	3-10	3-20	3-30	3-40	3-50	3-60	3-70	3-80	3-90
From		$C-5	$C-5	CO2REMOV	CO2REMOV	BEERCOL	BEERCOL	RECTCOL	RECTCOL	R-MIX	R-PURGE
To		CO2REMOV	CO2REMOV		BEERCOL	R-MIX	RECTCOL	R-MIX		R-PURGE	$C-1
Substream: ALL											
Temperature	C	35.00	35.00	35.00	100.00	82.91	96.48	78.42	99.88	99.88	99.88
Mass Flow	KG/HR	340339	385.6174	339954	321983	17970.4	10383.72	7586.682	332367	299130	33236.68
Component Mass Flow											
CELLULOS	KG/HR	0	0	0	0	0	0	0	0	0	0
XYLAN	KG/HR	0	0	0	0	0	0	0	0	0	0
LIGNIN	KG/HR	0	0	0	0	0	0	0	0	0	0
PROTEIN	KG/HR	0	0	0	0	0	0	0	0	0	0
ASH	KG/HR	0	0	0	0	0	0	0	0	0	0
H2O	KG/HR	321305.5	0	321305.5	310522.7	10782.78	10024.29	758.49	320547	288492.3	32054.7
H2SO4	KG/HR	737.07	0	737.07	737.07	0	0	0	737.07	663.36	73.71
GLUCOSE	KG/HR	2384.67	0	2384.67	2384.62	0.05	0.05	0	2384.67	2146.2	238.47
XYLOSE	KG/HR	6191.39	0	6191.39	6191.39	0.01	0.01	0	6191.39	5572.25	619.14
LGNSOL	KG/HR	1768.96	0	1768.96	1768.96	0	0	0	1768.96	1592.07	176.9
ETHANOL	KG/HR	7565.86	0	7565.86	378.29	7187.57	359.38	6828.19	737.67	663.9	73.77
CO2	KG/HR	385.62	385.62	0	0	0	0	0	0	0	0
Component Mass Fraction											
CELLULOS		0	0	0	0	0	0	0	0	0	0
XYLAN		0	0	0	0	0	0	0	0	0	0
LIGNIN		0	0	0	0	0	0	0	0	0	0
PROTEIN		0	0	0	0	0	0	0	0	0	0
ASH		0	0	0	0	0	0	0	0	0	0
H2O		0.9441	0	0.9451	0.9644	0.6	0.9654	0.1	0.9644	0.9644	0.9644
H2SO4		0.0022	0	0.0022	0.0023	0	0	0	0.0022	0.0022	0.0022
GLUCOSE		0.007	0	0.007	0.0074	0	0	0	0.0072	0.0072	0.0072
XYLOSE		0.0182	0	0.0182	0.0192	0	0	0	0.0186	0.0186	0.0186
LGNSOL		0.0052	0	0.0052	0.0055	0	0	0	0.0053	0.0053	0.0053
ETHANOL		0.0222	0	0.0223	0.0012	0.4	0.0346	0.9	0.0022	0.0022	0.0022
CO2		0.0011	1	0	0	0	0	0	0	0	0

	Units	2-100	3-10	3-20	3-30	3-40	3-50	3-60	3-70	3-80	3-90
From		$C-5	$C-5	CO2REMOV	CO2REMOV	BEERCOL	BEERCOL	RECTCOL	RECTCOL	R-MIX	R-PURGE
To		CO2REMOV	CO2REMOV		BEERCOL	R-MIX	RECTCOL	R-MIX		R-PURGE	$C-1
Substream: ALL											
Temperature	C	35.00	35.00	35.00	100.00	82.91	96.48	78.42	99.88	99.88	99.88
Mass Flow	KG/HR	340339	385.6174	339954	321983	17970.4	10383.72	7586.682	332367	299130	33236.68
Component Mole Flow											
CELLULOS	KMOL/HR	0	0	0	0	0	0	0	0	0	0
XYLAN	KMOL/HR	0	0	0	0	0	0	0	0	0	0
LIGNIN	KMOL/HR	0	0	0	0	0	0	0	0	0	0
PROTEIN	KMOL/HR	0	0	0	0	0	0	0	0	0	0
ASH	KMOL/HR	0	0	0	0	0	0	0	0	0	0
H2O	KMOL/HR	17835.16	0	17835.16	17236.63	598.54	556.43	42.1	17793.06	16013.76	1779.31
H2SO4	KMOL/HR	7.52	0	7.52	7.52	0	0	0	7.52	6.76	0.75
GLUCOSE	KMOL/HR	13.24	0	13.24	13.24	0	0	0	13.24	11.91	1.32
XYLOSE	KMOL/HR	41.24	0	41.24	41.24	0	0	0	41.24	37.12	4.12
LGNSOL	KMOL/HR	11.63	0	11.63	11.63	0	0	0	11.63	10.46	1.16
ETHANOL	KMOL/HR	164.23	0	164.23	8.21	156.02	7.8	148.22	16.01	14.41	1.6
CO2	KMOL/HR	8.76	8.76	0	0	0	0	0	0	0	0
Component Mole Fraction											
CELLULOS		0	0	0	0	0	0	0	0	0	0
XYLAN		0	0	0	0	0	0	0	0	0	0
LIGNIN		0	0	0	0	0	0	0	0	0	0
PROTEIN		0	0	0	0	0	0	0	0	0	0
ASH		0	0	0	0	0	0	0	0	0	0
H2O		0.9864	0	0.9868	0.9953	0.7932	0.9862	0.2212	0.995	0.995	0.995
H2SO4		0.0004	0	0.0004	0.0004	0	0	0	0.0004	0.0004	0.0004
GLUCOSE		0.0007	0	0.0007	0.0008	0	0	0	0.0007	0.0007	0.0007
XYLOSE		0.0023	0	0.0023	0.0024	0	0	0	0.0023	0.0023	0.0023
LGNSOL		0.0006	0	0.0006	0.0007	0	0	0	0.0007	0.0007	0.0007
ETHANOL		0.0091	0	0.0091	0.0005	0.2068	0.0138	0.7788	0.0009	0.0009	0.0009
CO2		0.0005	1	0	0	0	0	0	0	0	0

C.6. Full Stream Table for Aspen Plus™ Model (A-SHF: Pre-treatment Area)

	Units	1-10	1-11	1-12	1-20	1-30	1-40	1-41	1-50
From			PRE-HX1	PRE-HX2		PRETREAT	PRE-FILT	PRE-HX1	PRE-FILT
To		PRE-HX1	PRE-HX2	PRETREAT	PRETREAT	PRE-FILT	PRE-HX1		$C-3
Substream: ALL									
Temperature	C	20.00	78.95	95.00	20.00	90.00	90.00	30.00	90.00
Mass Flow	KG/HR	450000	450000	450000	90000	540000	448431	448431	91569.4
Component Mass Flow									
CELLULOS	KG/HR	0	0	0	33300	33300	0	0	33300
XYLAN	KG/HR	0	0	0	26100	9467.79	0	0	9467.79
LIGNIN	KG/HR	0	0	0	22500	17100	0	0	17100
PROTEIN	KG/HR	0	0	0	2700	2700	0	0	2700
ASH	KG/HR	0	0	0	5400	5400	0	0	5400
H2O	KG/HR	447750	447750	447750	0	445482.1	423208	423208	22274.1
H2SO4	KG/HR	2250	2250	2250	0	2250	2137.5	2137.5	112.5
GLUCOSE	KG/HR	0	0	0	0	0	0	0	0
XYLOSE	KG/HR	0	0	0	0	18900.04	17955.04	17955.04	945
LGNSOL	KG/HR	0	0	0	0	5400	5130	5130	270
ETHANOL	KG/HR	0	0	0	0	0	0	0	0
CO2	KG/HR	0	0	0	0	0	0	0	0
Component Mass Fraction									
CELLULOS		0	0	0	0.37	0.0617	0	0	0.3637
XYLAN		0	0	0	0.29	0.0175	0	0	0.1034
LIGNIN		0	0	0	0.25	0.0317	0	0	0.1867
PROTEIN		0	0	0	0.03	0.005	0	0	0.0295
ASH		0	0	0	0.06	0.01	0	0	0.059
H2O		0.995	0.995	0.995	0	0.825	0.9438	0.9438	0.2432
H2SO4		0.005	0.005	0.005	0	0.0042	0.0048	0.0048	0.0012
GLUCOSE		0	0	0	0	0	0	0	0
XYLOSE		0	0	0	0	0.035	0.04	0.04	0.0103
LGNSOL		0	0	0	0	0.01	0.0114	0.0114	0.0029
ETHANOL		0	0	0	0	0	0	0	0
CO2		0	0	0	0	0	0	0	0

	Units	1-10	1-11	1-12	1-20	1-30	1-40	1-41	1-50
From			PRE-HX1	PRE-HX2		PRETREAT	PRE-FILT	PRE-HX1	PRE-FILT
To		PRE-HX1	PRE-HX2	PRETREAT	PRETREAT	PRE-FILT	PRE-HX1		$C-3
Substream: ALL									
Temperature	C	20.00	78.95	95.00	20.00	90.00	90.00	30.00	90.00
Mass Flow	KG/HR	450000	450000	450000	90000	540000	448431	448431	91569.4
Component Mole Flow									
CELLULOS	KMOL/HR	0	0	0	205.38	205.38	0	0	205.38
XYLAN	KMOL/HR	0	0	0	197.55	71.66	0	0	71.66
LIGNIN	KMOL/HR	0	0	0	147.88	112.39	0	0	112.39
PROTEIN	KMOL/HR	0	0	0	118.22	118.22	0	0	118.22
ASH	KMOL/HR	0	0	0	96.3	96.3	0	0	96.3
H2O	KMOL/HR	24853.9	24853.9	24853.9	0	24728.01	23491.61	23491.61	1236.4
H2SO4	KMOL/HR	22.94	22.94	22.94	0	22.94	21.79	21.79	1.15
GLUCOSE	KMOL/HR	0	0	0	0	0	0	0	0
XYLOSE	KMOL/HR	0	0	0	0	125.89	119.6	119.6	6.29
LGNSOL	KMOL/HR	0	0	0	0	35.49	33.72	33.72	1.77
ETHANOL	KMOL/HR	0	0	0	0	0	0	0	0
CO2	KMOL/HR	0	0	0	0	0	0	0	0
Component Mole Fraction									
CELLULOS		0	0	0	0.2684	0.008	0	0	0.111
XYLAN		0	0	0	0.2581	0.0028	0	0	0.0387
LIGNIN		0	0	0	0.1932	0.0044	0	0	0.0608
PROTEIN		0	0	0	0.1545	0.0046	0	0	0.0639
ASH		0	0	0	0.1258	0.0038	0	0	0.0521
H2O		0.9991	0.9991	0.9991	0	0.9691	0.9926	0.9926	0.6685
H2SO4		0.0009	0.0009	0.0009	0	0.0009	0.0009	0.0009	0.0006
GLUCOSE		0	0	0	0	0	0	0	0
XYLOSE		0	0	0	0	0.0049	0.0051	0.0051	0.0034
LGNSOL		0	0	0	0	0.0014	0.0014	0.0014	0.001
ETHANOL		0	0	0	0	0	0	0	0
CO2		0	0	0	0	0	0	0	0

C.7. Full Stream Table for Aspen Plus™ Model (A-SHF: Hydrolysis and Fermentation Area)

	Units	1-50	2-10	2-100	2-20	2-21	2-30	2-40	2-50	2-60	2-70	2-80	2-90	3-80
From		$C-4		B1	WATERMIX	FEEDCHIL	FEEDMIX	HYDROLYS	FILTER	FILTER	FERMCHIL	FEREMNT	B1	$C-6
To		FEEDMIX	WATERMIX	$C-2	FEEDCHIL	FEEDMIX	HYDROLYS	FILTER		FERMCHIL	FEREMNT	B1		WATERMIX
Substream: ALL														
Temperature	C	90.00	25.00	35.00	93.68	50.00	54.06	50.00	50.00	50.00	35.00	35.00	35.00	99.96
Mass Flow	KG/HR	91569.4	28450.73	338579	328101	328101	419670	419670	76719.87	342950	342950	342950	4370.86	299650
Component Mass Flow														
CELLULOS	KG/HR	33300	0	0	0	0	33300	24002.08	24002.08	0	0	0	0	0
XYLAN	KG/HR	9467.79	0	0	0	0	9467.79	9467.79	9467.79	0	0	0	0	0
LIGNIN	KG/HR	17100	0	0	0	0	17100	17100	17100	0	0	0	0	0
PROTEIN	KG/HR	2700	0	0	0	0	2700	2700	2700	0	0	0	0	0
ASH	KG/HR	5400	0	0	0	0	5400	5400	5400	0	0	0	0	0
H2O	KG/HR	22274.1	28450.73	321764	317564.9	317564.9	339839	338805.9	16940.3	321865.6	321865.6	321865.6	101.64	289114.2
H2SO4	KG/HR	112.5	0	737.07	663.36	663.36	775.86	775.86	38.79	737.07	737.07	737.07	0	663.36
GLUCOSE	KG/HR	0	0	2497.51	2247.76	2247.76	2247.76	12578.75	628.94	11949.82	11949.82	2497.51	0	2247.76
XYLOSE	KG/HR	945	0	6191.39	5572.25	5572.25	6517.26	6517.26	325.86	6191.39	6191.39	6191.39	0	5572.25
LGNSOL	KG/HR	270	0	1768.96	1592.07	1592.07	1862.07	1862.07	93.1	1768.96	1768.96	1768.96	0	1592.07
ETHANOL	KG/HR	0	0	5243.67	460.13	460.13	460.13	460.13	23.01	437.13	437.13	5271.32	27.65	460.13
CO2	KG/HR	0	0	376.54	0	0	0	0	0	0	0	4618.11	4241.57	0
Component Mass Fraction														
CELLULOS		0.3637	0	0	0	0	0.0793	0.0572	0.3129	0	0	0	0	0
XYLAN		0.1034	0	0	0	0	0.0226	0.0226	0.1234	0	0	0	0	0
LIGNIN		0.1867	0	0	0	0	0.0407	0.0407	0.2229	0	0	0	0	0
PROTEIN		0.0295	0	0	0	0	0.0064	0.0064	0.0352	0	0	0	0	0
ASH		0.059	0	0	0	0	0.0129	0.0129	0.0704	0	0	0	0	0
H2O		0.2432	1	0.9503	0.9679	0.9679	0.8098	0.8073	0.2208	0.9385	0.9385	0.9385	0.0233	0.9648
H2SO4		0.0012	0	0.0022	0.002	0.002	0.0018	0.0018	0.0005	0.0021	0.0021	0.0021	0	0.0022
GLUCOSE		0	0	0.0074	0.0069	0.0069	0.0054	0.03	0.0082	0.0348	0.0348	0.0073	0	0.0075
XYLOSE		0.0103	0	0.0183	0.017	0.017	0.0155	0.0155	0.0042	0.0181	0.0181	0.0181	0	0.0186
LGNSOL		0.0029	0	0.0052	0.0049	0.0049	0.0044	0.0044	0.0012	0.0052	0.0052	0.0052	0	0.0053
ETHANOL		0	0	0.0155	0.0014	0.0014	0.0011	0.0011	0.0003	0.0013	0.0013	0.0154	0.0063	0.0015
CO2		0	0	0.0011	0	0	0	0	0	0	0	0.0135	0.9704	0

	Units	1-50	2-10	2-100	2-20	2-21	2-30	2-40	2-50	2-60	2-70	2-80	2-90	3-80
From		$C-4		B1	WATERMIX	FEEDCHIL	FEEDMIX	HYDROLYS	FILTER	FILTER	FERMCHIL	FEREMNT	B1	$C-6
To		FEEDMIX	WATERMIX	$C-2	FEEDCHIL	FEEDMIX	HYDROLYS	FILTER		FERMCHIL	FEREMNT	B1		WATERMI
Substream: ALL														
Temperature	C	90.00	25.00	35.00	93.68	50.00	54.06	50.00	50.00	50.00	35.00	35.00	35.00	99.96
Mass Flow	KG/HR	91569.4	28450.73	338579	328101	328101	419670	419670	76719.87	342950	342950	342950	4370.86	299650
Component Mole Flow														
CELLULOS	KMOL/HR	205.38	0	0	0	0	205.38	148.03	148.03	0	0	0	0	0
XYLAN	KMOL/HR	71.66	0	0	0	0	71.66	71.66	71.66	0	0	0	0	0
LIGNIN	KMOL/HR	112.39	0	0	0	0	112.39	112.39	112.39	0	0	0	0	0
PROTEIN	KMOL/HR	118.22	0	0	0	0	118.22	118.22	118.22	0	0	0	0	0
ASH	KMOL/HR	96.3	0	0	0	0	96.3	96.3	96.3	0	0	0	0	0
H2O	KMOL/HR	1236.4	1579.26	17860.62	17627.53	17627.53	18863.93	18806.59	940.33	17866.26	17866.26	17866.26	5.64	16048.28
H2SO4	KMOL/HR	1.15	0	7.52	6.76	6.76	7.91	7.91	0.4	7.52	7.52	7.52	0	6.76
GLUCOSE	KMOL/HR	0	0	13.86	12.48	12.48	12.48	69.82	3.49	66.33	66.33	13.86	0	12.48
XYLOSE	KMOL/HR	6.29	0	41.24	37.12	37.12	43.41	43.41	2.17	41.24	41.24	41.24	0	37.12
LGNSOL	KMOL/HR	1.77	0	11.63	10.46	10.46	12.24	12.24	0.61	11.63	11.63	11.63	0	10.46
ETHANOL	KMOL/HR	0	0	113.82	9.99	9.99	9.99	9.99	0.5	9.49	9.49	114.42	0.6	9.99
CO2	KMOL/HR	0	0	8.56	0	0	0	0	0	0	0	104.93	96.38	0
Component Mole Fraction														
CELLULOS		0.111	0	0	0	0	0.0105	0.0076	0.0991	0	0	0	0	0
XYLAN		0.0387	0	0	0	0	0.0037	0.0037	0.048	0	0	0	0	0
LIGNIN		0.0608	0	0	0	0	0.0057	0.0058	0.0752	0	0	0	0	0
PROTEIN		0.0639	0	0	0	0	0.006	0.0061	0.0791	0	0	0	0	0
ASH		0.0521	0	0	0	0	0.0049	0.0049	0.0645	0	0	0	0	0
H2O		0.6685	1	0.9891	0.9957	0.9957	0.9647	0.9646	0.6294	0.9924	0.9924	0.9838	0.055	0.9952
H2SO4		0.0006	0	0.0004	0.0004	0.0004	0.0004	0.0004	0.0003	0.0004	0.0004	0.0004	0	0.0004
GLUCOSE		0	0	0.0008	0.0007	0.0007	0.0006	0.0036	0.0023	0.0037	0.0037	0.0008	0	0.0008
XYLOSE		0.0034	0	0.0023	0.0021	0.0021	0.0022	0.0022	0.0015	0.0023	0.0023	0.0023	0	0.0023
LGNSOL		0.001	0	0.0006	0.0006	0.0006	0.0006	0.0006	0.0004	0.0006	0.0006	0.0006	0	0.0006
ETHANOL		0	0	0.0063	0.0006	0.0006	0.0005	0.0005	0.0003	0.0005	0.0005	0.0063	0.0058	0.0006
CO2		0	0	0.0005	0	0	0	0	0	0	0	0.0058	0.9392	0

C.8. Full Stream Table for Aspen Plus™ Model (A-SHF: Product Separation Area)

	Units	2-100	3-10	3-20	3-30	3-40	3-50	3-60	3-70	3-80	3-90
From		$C-5	$C-5	CO2REMOV	CO2REMOV	BEERCOL	BEERCOL	RECTCOL	RECTCOL	R-MIX	R-PURGE
To		CO2REMOV	CO2REMOV		BEERCOL	R-MIX	RECTCOL	R-MIX		R-PURGE	$C-1
Substream: ALL											
Temperature	C	35.00	35.00	35.00	100.04	82.91	96.48	78.42	99.96	99.96	99.96
Mass Flow	KG/HR	338579	376.5429	338203	325746	12456.59	7198.158	5258.433	332944	299650	33294.42
Component Mass Flow											
CELLULOS	KG/HR	0	0	0	0	0	0	0	0	0	0
XYLAN	KG/HR	0	0	0	0	0	0	0	0	0	0
LIGNIN	KG/HR	0	0	0	0	0	0	0	0	0	0
PROTEIN	KG/HR	0	0	0	0	0	0	0	0	0	0
ASH	KG/HR	0	0	0	0	0	0	0	0	0	0
H2O	KG/HR	321764	0	321764	314288.9	7475.11	6949.08	526.02	321238	289114.2	32123.8
H2SO4	KG/HR	737.07	0	737.07	737.07	0	0	0	737.07	663.36	73.71
GLUCOSE	KG/HR	2497.51	0	2497.51	2497.51	0	0	0	2497.51	2247.76	249.75
XYLOSE	KG/HR	6191.39	0	6191.39	6191.39	0	0	0	6191.39	5572.25	619.14
LGNSOL	KG/HR	1768.96	0	1768.96	1768.96	0	0	0	1768.96	1592.07	176.9
ETHANOL	KG/HR	5243.67	0	5243.67	262.18	4981.48	249.07	4732.41	511.26	460.13	51.13
CO2	KG/HR	376.54	376.54	0	0	0	0	0	0	0	0
Component Mass Fraction											
CELLULOS		0	0	0	0	0	0	0	0	0	0
XYLAN		0	0	0	0	0	0	0	0	0	0
LIGNIN		0	0	0	0	0	0	0	0	0	0
PROTEIN		0	0	0	0	0	0	0	0	0	0
ASH		0	0	0	0	0	0	0	0	0	0
H2O		0.9503	0	0.9514	0.9648	0.6001	0.9654	0.1	0.9648	0.9648	0.9648
H2SO4		0.0022	0	0.0022	0.0023	0	0	0	0.0022	0.0022	0.0022
GLUCOSE		0.0074	0	0.0074	0.0077	0	0	0	0.0075	0.0075	0.0075
XYLOSE		0.0183	0	0.0183	0.019	0	0	0	0.0186	0.0186	0.0186
LGNSOL		0.0052	0	0.0052	0.0054	0	0	0	0.0053	0.0053	0.0053
ETHANOL		0.0155	0	0.0155	0.0008	0.3999	0.0346	0.9	0.0015	0.0015	0.0015
CO2		0.0011	1	0	0	0	0	0	0	0	0

	Units	2-100	3-10	3-20	3-30	3-40	3-50	3-60	3-70	3-80	3-90
From		$C-5	$C-5	CO2REMOV	CO2REMOV	BEERCOL	BEERCOL	RECTCOL	RECTCOL	R-MIX	R-PURGE
To		CO2REMOV	CO2REMOV		BEERCOL	R-MIX	RECTCOL	R-MIX		R-PURGE	$C-1
Substream: ALL											
Temperature	C	35.00	35.00	35.00	100.04	82.91	96.48	78.42	99.96	99.96	99.96
Mass Flow	KG/HR	338579	376.5429	338203	325746	12456.59	7198.158	5258.433	332944	299650	33294.42
Component Mole Flow											
CELLULOS	KMOL/HR	0	0	0	0	0	0	0	0	0	0
XYLAN	KMOL/HR	0	0	0	0	0	0	0	0	0	0
LIGNIN	KMOL/HR	0	0	0	0	0	0	0	0	0	0
PROTEIN	KMOL/HR	0	0	0	0	0	0	0	0	0	0
ASH	KMOL/HR	0	0	0	0	0	0	0	0	0	0
H2O	KMOL/HR	17860.62	0	17860.62	17445.68	414.93	385.73	29.2	17831.42	16048.28	1783.14
H2SO4	KMOL/HR	7.52	0	7.52	7.52	0	0	0	7.52	6.76	0.75
GLUCOSE	KMOL/HR	13.86	0	13.86	13.86	0	0	0	13.86	12.48	1.39
XYLOSE	KMOL/HR	41.24	0	41.24	41.24	0	0	0	41.24	37.12	4.12
LGNSOL	KMOL/HR	11.63	0	11.63	11.63	0	0	0	11.63	10.46	1.16
ETHANOL	KMOL/HR	113.82	0	113.82	5.69	108.13	5.41	102.72	11.1	9.99	1.11
CO2	KMOL/HR	8.56	8.56	0	0	0	0	0	0	0	0
Component Mole Fraction											
CELLULOS		0	0	0	0	0	0	0	0	0	0
XYLAN		0	0	0	0	0	0	0	0	0	0
LIGNIN		0	0	0	0	0	0	0	0	0	0
PROTEIN		0	0	0	0	0	0	0	0	0	0
ASH		0	0	0	0	0	0	0	0	0	0
H2O		0.9891	0	0.9896	0.9954	0.7933	0.9862	0.2213	0.9952	0.9952	0.9952
H2SO4		0.0004	0	0.0004	0.0004	0	0	0	0.0004	0.0004	0.0004
GLUCOSE		0.0008	0	0.0008	0.0008	0	0	0	0.0008	0.0008	0.0008
XYLOSE		0.0023	0	0.0023	0.0024	0	0	0	0.0023	0.0023	0.0023
LGNSOL		0.0006	0	0.0006	0.0007	0	0	0	0.0006	0.0006	0.0006
ETHANOL		0.0063	0	0.0063	0.0003	0.2067	0.0138	0.7787	0.0006	0.0006	0.0006
CO2		0.0005	1	0	0	0	0	0	0	0	0

C.9. Full Stream Table for Aspen Plus™ Model (H-SSF: Pre-treatment Area)

	Units	1-10	1-11	1-12	1-20	1-30	1-40	1-41	1-50
From			PRE-HX1	PRE-HX2		PRETREAT	PRE-FILT	PRE-HX1	PRE-FILT
To		PRE-HX1	PRE-HX2	PRETREAT	PRETREAT	PRE-FILT	PRE-HX1		$C-3
Substream: ALL									
Temperature	C	20.00	81.93	90.00	90.00	90.00	90.00	30.00	90.00
Mass Flow	KG/HR	450000	450000	450000	90000	539999.9	472032.1	472032.1	67967.8
Component Mass Flow									
CELLULOS	KG/HR	0	0	0	33300	33300	0	0	33300
XYLAN	KG/HR	0	0	0	26100	9467.8	0	0	9467.8
LIGNIN	KG/HR	0	0	0	22500	17100	0	0	17100
PROTEIN	KG/HR	0	0	0	2700	2700	0	0	2700
ASH	KG/HR	0	0	0	5400	5400	0	0	5400
H2O	KG/HR	447750	447750	447750	0	445482.1	445482.1	445482.1	0
H2SO4	KG/HR	2250	2250	2250	0	2250	2250	2250	0
GLUCOSE	KG/HR	0	0	0	0	0	0	0	0
XYLOSE	KG/HR	0	0	0	0	18900.03	18900.03	18900.03	0
LGNSOL	KG/HR	0	0	0	0	5400	5400	5400	0
ETHANOL	KG/HR	0	0	0	0	0	0	0	0
CO2	KG/HR	0	0	0	0	0	0	0	0
Component Mass Fraction									
CELLULOS		0	0	0	0.37	0.0617	0	0	0.4899
XYLAN		0	0	0	0.29	0.0175	0	0	0.1393
LIGNIN		0	0	0	0.25	0.0317	0	0	0.2516
PROTEIN		0	0	0	0.03	0.005	0	0	0.0397
ASH		0	0	0	0.06	0.01	0	0	0.0794
H2O		0.995	0.995	0.995	0	0.825	0.9438	0.9438	0
H2SO4		0.005	0.005	0.005	0	0.0042	0.0048	0.0048	0
GLUCOSE		0	0	0	0	0	0	0	0
XYLOSE		0	0	0	0	0.035	0.04	0.04	0
LGNSOL		0	0	0	0	0.01	0.0114	0.0114	0
ETHANOL		0	0	0	0	0	0	0	0
CO2		0	0	0	0	0	0	0	0

	Units	1-10	1-11	1-12	1-20	1-30	1-40	1-41	1-50
From			PRE-HX1	PRE-HX2		PRETREAT	PRE-FILT	PRE-HX1	PRE-FILT
To		PRE-HX1	PRE-HX2	PRETREAT	PRETREAT	PRE-FILT	PRE-HX1		$C-3
Substream: ALL									
Temperature	C	20.00	81.93	90.00	90.00	90.00	90.00	30.00	90.00
Mass Flow	KG/HR	450000	450000	450000	90000	539999.9	472032.1	472032.1	67967.8
Component Mole Flow									
CELLULOS	KMOL/HR	0	0	0	205.38	205.38	0	0	205.38
XYLAN	KMOL/HR	0	0	0	197.55	71.66	0	0	71.66
LIGNIN	KMOL/HR	0	0	0	147.88	112.39	0	0	112.39
PROTEIN	KMOL/HR	0	0	0	118.22	118.22	0	0	118.22
ASH	KMOL/HR	0	0	0	96.3	96.3	0	0	96.3
H2O	KMOL/HR	24853.9	24853.9	24853.9	0	24728.01	24728.01	24728.01	0
H2SO4	KMOL/HR	22.94	22.94	22.94	0	22.94	22.94	22.94	0
GLUCOSE	KMOL/HR	0	0	0	0	0	0	0	0
XYLOSE	KMOL/HR	0	0	0	0	125.89	125.89	125.89	0
LGNSOL	KMOL/HR	0	0	0	0	35.49	35.49	35.49	0
ETHANOL	KMOL/HR	0	0	0	0	0	0	0	0
CO2	KMOL/HR	0	0	0	0	0	0	0	0
Component Mole Fraction									
CELLULOS		0	0	0	0.2684	0.008	0	0	0.3401
XYLAN		0	0	0	0.2581	0.0028	0	0	0.1187
LIGNIN		0	0	0	0.1932	0.0044	0	0	0.1861
PROTEIN		0	0	0	0.1545	0.0046	0	0	0.1957
ASH		0	0	0	0.1258	0.0038	0	0	0.1594
H2O		0.9991	0.9991	0.9991	0	0.9691	0.9926	0.9926	0
H2SO4		0.0009	0.0009	0.0009	0	0.0009	0.0009	0.0009	0
GLUCOSE		0	0	0	0	0	0	0	0
XYLOSE		0	0	0	0	0.0049	0.0051	0.0051	0
LGNSOL		0	0	0	0	0.0014	0.0014	0.0014	0
ETHANOL		0	0	0	0	0	0	0	0
CO2		0	0	0	0	0	0	0	0

C.10. Full Stream Table for Aspen Plus™ Model (H-SSF: Hydrolysis and Fermentation Area)

	Units	1-50	2-10	2-20	2-21	2-30	2-40	2-50	2-60	2-70	2-80	2-90	3-80
From		$C-4		WATERMIX	FEEDCHIL	FEEDMIX	HYDROLYS	FERMENT	CO2FLASH	CO2FLASH	FILTER	FILTER	$C-6
To		FEEDMIX	WATERMIX	FEEDCHIL	FEEDMIX	HYDROLYS	FERMENT	CO2FLASH		FILTER	$C-1		WATERMIX
Substream: ALL													
Temperature	C	90.00	20.00	88.58	35.00	37.02	38.00	38.00	38.00	38.00	38.00	38.00	99.86
Mass Flow	KG/HR	67967.8	50615.79	341643.8	341643.8	409611.6	409611.6	409611.6	4257.31	405354.3	328546.4	76807.9	291028
Component Mass Flow													
CELLULOS	KG/HR	33300	0	0	0	33300	24848.18	24848.18	0	24848.18	0	24848.18	0
XYLAN	KG/HR	9467.8	0	0	0	9467.8	9467.8	9467.8	0	9467.8	0	9467.8	0
LIGNIN	KG/HR	17100	0	0	0	17100	17100	17100	0	17100	0	17100	0
PROTEIN	KG/HR	2700	0	0	0	2700	2700	2700	0	2700	0	2700	0
ASH	KG/HR	5400	0	0	0	5400	5400	5400	0	5400	0	5400	0
H2O	KG/HR	0	50615.79	339839	339839	339839	338899.9	338899.9	117.85	338782.1	321843	16939.1	289223.2
H2SO4	KG/HR	0	0	0	0	0	0	0	0	0	0	0	0
GLUCOSE	KG/HR	0	0	1381.57	1381.57	1381.57	10772.45	1615.87	0	1615.87	1535.07	80.79	1381.57
XYLOSE	KG/HR	0	0	0	0	0	0	0	0	0	0	0	0
LGNSOL	KG/HR	0	0	0	0	0	0	0	0	0	0	0	0
ETHANOL	KG/HR	0	0	423.22	423.22	423.2	423.2	5106.15	29.34	5076.81	4822.97	253.84	423.22
CO2	KG/HR	0	0	0	0	0	0	4473.63	4110.12	363.5	345.33	18.18	0
Component Mass Fraction													
CELLULOS		0.4899	0	0	0	0.0813	0.0607	0.0607	0	0.0613	0	0.3235	0
XYLAN		0.1393	0	0	0	0.0231	0.0231	0.0231	0	0.0234	0	0.1233	0
LIGNIN		0.2516	0	0	0	0.0417	0.0417	0.0417	0	0.0422	0	0.2226	0
PROTEIN		0.0397	0	0	0	0.0066	0.0066	0.0066	0	0.0067	0	0.0352	0
ASH		0.0794	0	0	0	0.0132	0.0132	0.0132	0	0.0133	0	0.0703	0
H2O		0	1	0.9947	0.9947	0.8297	0.8274	0.8274	0.0277	0.8358	0.9796	0.2205	0.9938
H2SO4		0	0	0	0	0	0	0	0	0	0	0	0
GLUCOSE		0	0	0.004	0.004	0.0034	0.0263	0.0039	0	0.004	0.0047	0.0011	0.0047
XYLOSE		0	0	0	0	0	0	0	0	0	0	0	0
LGNSOL		0	0	0	0	0	0	0	0	0	0	0	0
ETHANOL		0	0	0.0012	0.0012	0.001	0.001	0.0125	0.0069	0.0125	0.0147	0.0033	0.0015
CO2		0	0	0	0	0	0	0.0109	0.9654	0.0009	0.0011	0.0002	0

	Units	1-50	2-10	2-20	2-21	2-30	2-40	2-50	2-60	2-70	2-80	2-90	3-80
From		$C-4		WATERMIX	FEEDCHIL	FEEDMIX	HYDROLYS	FERMENT	CO2FLASH	CO2FLASH	FILTER	FILTER	$C-6
To		FEEDMIX	WATERMIX	FEEDCHIL	FEEDMIX	HYDROLYS	FERMENT	CO2FLASH		FILTER	$C-1		WATERMIX
Substream: ALL													
Temperature	C	90.00	20.00	88.58	35.00	37.02	38.00	38.00	38.00	38.00	38.00	38.00	99.86
Mass Flow	KG/HR	67967.8	50615.79	341643.8	341643.8	409611.6	409611.6	409611.6	4257.31	405354.3	328546.4	76807.9	291028
Component Mole Flow													
CELLULOS	KMOL/HR	205.38	0	0	0	205.38	153.25	153.25	0	153.25	0	153.25	0
XYLAN	KMOL/HR	71.66	0	0	0	71.66	71.66	71.66	0	71.66	0	71.66	0
LIGNIN	KMOL/HR	112.39	0	0	0	112.39	112.39	112.39	0	112.39	0	112.39	0
PROTEIN	KMOL/HR	118.22	0	0	0	118.22	118.22	118.22	0	118.22	0	118.22	0
ASH	KMOL/HR	96.3	0	0	0	96.3	96.3	96.3	0	96.3	0	96.3	0
H2O	KMOL/HR	0	2809.6	18863.93	18863.93	18863.93	18811.81	18811.81	6.54	18805.26	17865	940.26	16054.33
H2SO4	KMOL/HR	0	0	0	0	0	0	0	0	0	0	0	0
GLUCOSE	KMOL/HR	0	0	7.67	7.67	7.67	59.79	8.97	0	8.97	8.52	0.45	7.67
XYLOSE	KMOL/HR	0	0	0	0	0	0	0	0	0	0	0	0
LGNSOL	KMOL/HR	0	0	0	0	0	0	0	0	0	0	0	0
ETHANOL	KMOL/HR	0	0	9.19	9.19	9.19	9.19	110.84	0.64	110.2	104.69	5.51	9.19
CO2	KMOL/HR	0	0	0	0	0	0	101.65	93.39	8.26	7.85	0.41	0
Component Mole Fraction													
CELLULOS		0.3401	0	0	0	0.0105	0.0079	0.0078	0	0.0079	0	0.1023	0
XYLAN		0.1187	0	0	0	0.0037	0.0037	0.0037	0	0.0037	0	0.0478	0
LIGNIN		0.1861	0	0	0	0.0058	0.0058	0.0057	0	0.0058	0	0.075	0
PROTEIN		0.1957	0	0	0	0.0061	0.0061	0.006	0	0.0061	0	0.0789	0
ASH		0.1594	0	0	0	0.0049	0.005	0.0049	0	0.0049	0	0.0643	0
H2O		0	1	0.9991	0.9991	0.9681	0.9681	0.9605	0.065	0.9651	0.9933	0.6275	0.999
H2SO4		0	0	0	0	0	0	0	0	0	0	0	0
GLUCOSE		0	0	0.0004	0.0004	0.0004	0.0031	0.0005	0	0.0005	0.0005	0.0003	0.0005
XYLOSE		0	0	0	0	0	0	0	0	0	0	0	0
LGNSOL		0	0	0	0	0	0	0	0	0	0	0	0
ETHANOL		0	0	0.0005	0.0005	0.0005	0.0005	0.0057	0.0063	0.0057	0.0058	0.0037	0.0006
CO2		0	0	0	0	0	0	0.0052	0.9286	0.0004	0.0004	0.0003	0

C.11. Full Stream Table for Aspen Plus™ Model (H-SSF: Product Separation Area)

	Units	2-80	3-10	3-20	3-30	3-40	3-50	3-60	3-70	3-80	3-90
From		$C-5	CO2REMOV	CO2REMOV	BEERCOL	BEERCOL	RECTCOL	RECTCOL	R-MIX	R-PURGE	R-PURGE
To		CO2REMOV		BEERCOL	R-MIX	RECTCOL	R-MIX		R-PURGE	$C-2	
Substream: ALL											
Temperature	C	38.00	38.00	38.00	99.94	83.78	97.24	78.42	99.86	99.86	99.86
Mass Flow	KG/HR	328546.4	345.33	328201	314727.1	13473.94	8637.35	4836.6	323364.4	291028	32336.44
Component Mass Flow											
CELLULOS	KG/HR	0	0	0	0	0	0	0	0	0	0
XYLAN	KG/HR	0	0	0	0	0	0	0	0	0	0
LIGNIN	KG/HR	0	0	0	0	0	0	0	0	0	0
PROTEIN	KG/HR	0	0	0	0	0	0	0	0	0	0
ASH	KG/HR	0	0	0	0	0	0	0	0	0	0
H2O	KG/HR	321843	0	321843	312950.9	8892.12	8408.26	483.86	321359.1	289223.2	32135.91
H2SO4	KG/HR	0	0	0	0	0	0	0	0	0	0
GLUCOSE	KG/HR	1535.07	0	1535.07	1535.07	0	0	0	1535.07	1381.57	153.51
XYLOSE	KG/HR	0	0	0	0	0	0	0	0	0	0
LGNSOL	KG/HR	0	0	0	0	0	0	0	0	0	0
ETHANOL	KG/HR	4822.97	0	4822.97	241.15	4581.82	229.09	4352.73	470.24	423.22	47.02
CO2	KG/HR	345.33	345.33	0	0	0	0	0	0	0	0
Component Mass Fraction											
CELLULOS		0	0	0	0	0	0	0	0	0	0
XYLAN		0	0	0	0	0	0	0	0	0	0
LIGNIN		0	0	0	0	0	0	0	0	0	0
PROTEIN		0	0	0	0	0	0	0	0	0	0
ASH		0	0	0	0	0	0	0	0	0	0
H2O		0.9796	0	0.9806	0.9944	0.6599	0.9735	0.1	0.9938	0.9938	0.9938
H2SO4		0	0	0	0	0	0	0	0	0	0
GLUCOSE		0.0047	0	0.0047	0.0049	0	0	0	0.0047	0.0047	0.0047
XYLOSE		0	0	0	0	0	0	0	0	0	0
LGNSOL		0	0	0	0	0	0	0	0	0	0
ETHANOL		0.0147	0	0.0147	0.0008	0.3401	0.0265	0.9	0.0015	0.0015	0.0015
CO2		0.0011	1	0	0	0	0	0	0	0	0

	Units	2-80	3-10	3-20	3-30	3-40	3-50	3-60	3-70	3-80	3-90
From		$C-5	CO2REMOV	CO2REMOV	BEERCOL	BEERCOL	RECTCOL	RECTCOL	R-MIX	R-PURGE	R-PURGE
To		CO2REMOV		BEERCOL	R-MIX	RECTCOL	R-MIX		R-PURGE	$C-2	
Substream: ALL											
Temperature	C	38.00	38.00	38.00	99.94	83.78	97.24	78.42	99.86	99.86	99.86
Mass Flow	KG/HR	328546.4	345.33	328201	314727.1	13473.94	8637.35	4836.6	323364.4	291028	32336.44
Component Mole Flow											
CELLULOS	KMOL/HR	0	0	0	0	0	0	0	0	0	0
XYLAN	KMOL/HR	0	0	0	0	0	0	0	0	0	0
LIGNIN	KMOL/HR	0	0	0	0	0	0	0	0	0	0
PROTEIN	KMOL/HR	0	0	0	0	0	0	0	0	0	0
ASH	KMOL/HR	0	0	0	0	0	0	0	0	0	0
H2O	KMOL/HR	17865	0	17865	17371.41	493.59	466.73	26.86	17838.14	16054.33	1783.81
H2SO4	KMOL/HR	0	0	0	0	0	0	0	0	0	0
GLUCOSE	KMOL/HR	8.52	0	8.52	8.52	0	0	0	8.52	7.67	0.85
XYLOSE	KMOL/HR	0	0	0	0	0	0	0	0	0	0
LGNSOL	KMOL/HR	0	0	0	0	0	0	0	0	0	0
ETHANOL	KMOL/HR	104.69	0	104.69	5.23	99.46	4.97	94.48	10.21	9.19	1.02
CO2	KMOL/HR	7.85	7.85	0	0	0	0	0	0	0	0
Component Mole Fraction											
CELLULOS		0	0	0	0	0	0	0	0	0	0
XYLAN		0	0	0	0	0	0	0	0	0	0
LIGNIN		0	0	0	0	0	0	0	0	0	0
PROTEIN		0	0	0	0	0	0	0	0	0	0
ASH		0	0	0	0	0	0	0	0	0	0
H2O		0.9933	0	0.9937	0.9992	0.8323	0.9895	0.2213	0.999	0.999	0.999
H2SO4		0	0	0	0	0	0	0	0	0	0
GLUCOSE		0.0005	0	0.0005	0.0005	0	0	0	0.0005	0.0005	0.0005
XYLOSE		0	0	0	0	0	0	0	0	0	0
LGNSOL		0	0	0	0	0	0	0	0	0	0
ETHANOL		0.0058	0	0.0058	0.0003	0.1677	0.0105	0.7787	0.0006	0.0006	0.0006
CO2		0.0004	1	0	0	0	0	0	0	0	0

C.12. Full Stream Table for Aspen Plus™ Model (A-SSF: Pre-treatment Area)

	Units	1-10	1-11	1-12	1-20	1-30	1-40	1-41	1-50
From			PRE-HX1	PRE-HX2		PRETREAT	PRE-FILT	PRE-HX1	PRE-FILT
To		PRE-HX1	PRE-HX2	PRETREAT	PRETREAT	PRE-FILT	PRE-HX1		$C-3
Substream: ALL									
Temperature	C	20.00	81.93	90.00	90.00	90.00	90.00	30.00	90.00
Mass Flow	KG/HR	450000	450000	450000	90000	539999.9	472032.1	472032.1	67967.8
Component Mass Flow									
CELLULOS	KG/HR	0	0	0	33300	33300	0	0	33300
XYLAN	KG/HR	0	0	0	26100	9467.8	0	0	9467.8
LIGNIN	KG/HR	0	0	0	22500	17100	0	0	17100
PROTEIN	KG/HR	0	0	0	2700	2700	0	0	2700
ASH	KG/HR	0	0	0	5400	5400	0	0	5400
H2O	KG/HR	447750	447750	447750	0	445482.1	445482.1	445482.1	0
H2SO4	KG/HR	2250	2250	2250	0	2250	2250	2250	0
GLUCOSE	KG/HR	0	0	0	0	0	0	0	0
XYLOSE	KG/HR	0	0	0	0	18900.03	18900.03	18900.03	0
LGNSOL	KG/HR	0	0	0	0	5400	5400	5400	0
ETHANOL	KG/HR	0	0	0	0	0	0	0	0
CO2	KG/HR	0	0	0	0	0	0	0	0
Component Mass Fraction									
CELLULOS		0	0	0	0.37	0.0617	0	0	0.4899
XYLAN		0	0	0	0.29	0.0175	0	0	0.1393
LIGNIN		0	0	0	0.25	0.0317	0	0	0.2516
PROTEIN		0	0	0	0.03	0.005	0	0	0.0397
ASH		0	0	0	0.06	0.01	0	0	0.0794
H2O		0.995	0.995	0.995	0	0.825	0.9438	0.9438	0
H2SO4		0.005	0.005	0.005	0	0.0042	0.0048	0.0048	0
GLUCOSE		0	0	0	0	0	0	0	0
XYLOSE		0	0	0	0	0.035	0.04	0.04	0
LGNSOL		0	0	0	0	0.01	0.0114	0.0114	0
ETHANOL		0	0	0	0	0	0	0	0
CO2		0	0	0	0	0	0	0	0

	Units	1-10	1-11	1-12	1-20	1-30	1-40	1-41	1-50
From			PRE-HX1	PRE-HX2		PRETREAT	PRE-FILT	PRE-HX1	PRE-FILT
To		PRE-HX1	PRE-HX2	PRETREAT	PRETREAT	PRE-FILT	PRE-HX1		$C-3
Substream: ALL									
Temperature	C	20.00	81.93	90.00	90.00	90.00	90.00	30.00	90.00
Mass Flow	KG/HR	450000	450000	450000	90000	539999.9	472032.1	472032.1	67967.8
Component Mole Flow									
CELLULOS	KMOL/HR	0	0	0	205.38	205.38	0	0	205.38
XYLAN	KMOL/HR	0	0	0	197.55	71.66	0	0	71.66
LIGNIN	KMOL/HR	0	0	0	147.88	112.39	0	0	112.39
PROTEIN	KMOL/HR	0	0	0	118.22	118.22	0	0	118.22
ASH	KMOL/HR	0	0	0	96.3	96.3	0	0	96.3
H2O	KMOL/HR	24853.9	24853.9	24853.9	0	24728.01	24728.01	24728.01	0
H2SO4	KMOL/HR	22.94	22.94	22.94	0	22.94	22.94	22.94	0
GLUCOSE	KMOL/HR	0	0	0	0	0	0	0	0
XYLOSE	KMOL/HR	0	0	0	0	125.89	125.89	125.89	0
LGNSOL	KMOL/HR	0	0	0	0	35.49	35.49	35.49	0
ETHANOL	KMOL/HR	0	0	0	0	0	0	0	0
CO2	KMOL/HR	0	0	0	0	0	0	0	0
Component Mole Fraction									
CELLULOS		0	0	0	0.2684	0.008	0	0	0.3401
XYLAN		0	0	0	0.2581	0.0028	0	0	0.1187
LIGNIN		0	0	0	0.1932	0.0044	0	0	0.1861
PROTEIN		0	0	0	0.1545	0.0046	0	0	0.1957
ASH		0	0	0	0.1258	0.0038	0	0	0.1594
H2O		0.9991	0.9991	0.9991	0	0.9691	0.9926	0.9926	0
H2SO4		0.0009	0.0009	0.0009	0	0.0009	0.0009	0.0009	0
GLUCOSE		0	0	0	0	0	0	0	0
XYLOSE		0	0	0	0	0.0049	0.0051	0.0051	0
LGNSOL		0	0	0	0	0.0014	0.0014	0.0014	0
ETHANOL		0	0	0	0	0	0	0	0
CO2		0	0	0	0	0	0	0	0

C.13. Full Stream Table for Aspen Plus™ Model (A-SSF: Hydrolysis and Fermentation Area)

	Units	1-50	2-10	2-20	2-21	2-30	2-40	2-50	2-60	2-70	2-80	2-90	3-80
From		$C-4		WATERMIX	FEEDCHIL	FEEDMIX	HYDROLYS	FERMENT	CO2FLASH	CO2FLASH	FILTER	FILTER	$C-6
To		FEEDMIX	WATERMIX	FEEDCHIL	FEEDMIX	HYDROLYS	FERMENT	CO2FLASH		FILTER	$C-1		WATERMIX
Substream: ALL													
Temperature	C	90.00	20.00	88.61	35.00	37.02	38.00	38.00	38.00	38.00	38.00	38.00	99.87
Mass Flow	KG/HR	67967.8	50528.65	341527.7	341527.7	409495.7	409495.7	409495.7	3958.71	405537	328203.4	77333.55	290999
Component Mass Flow													
CELLULOS	KG/HR	33300	0	0	0	33300	25391.89	25391.89	0	25391.89	0	25391.89	0
XYLAN	KG/HR	9467.8	0	0	0	9467.8	9467.8	9467.8	0	9467.8	0	9467.8	0
LIGNIN	KG/HR	17100	0	0	0	17100	17100	17100	0	17100	0	17100	0
PROTEIN	KG/HR	2700	0	0	0	2700	2700	2700	0	2700	0	2700	0
ASH	KG/HR	5400	0	0	0	5400	5400	5400	0	5400	0	5400	0
H2O	KG/HR	0	50528.65	339838.9	339838.9	339839	338960.4	338960.4	109.63	338850.7	321908.2	16942.54	289310.2
H2SO4	KG/HR	0	0	0	0	0	0	0	0	0	0	0	0
GLUCOSE	KG/HR	0	0	1292.65	1292.65	1292.65	10079.42	1511.91	0	1511.91	1436.32	75.6	1292.65
XYLOSE	KG/HR	0	0	0	0	0	0	0	0	0	0	0	0
LGNSOL	KG/HR	0	0	0	0	0	0	0	0	0	0	0	0
ETHANOL	KG/HR	0	0	396.16	396.16	396.19	396.19	4777.87	25.62	4752.25	4514.64	237.61	396.16
CO2	KG/HR	0	0	0	0	0	0	4185.82	3823.47	362.36	344.24	18.12	0
Component Mass Fraction													
CELLULOS		0.4899	0	0	0	0.0813	0.062	0.062	0	0.0626	0	0.3283	0
XYLAN		0.1393	0	0	0	0.0231	0.0231	0.0231	0	0.0233	0	0.1224	0
LIGNIN		0.2516	0	0	0	0.0418	0.0418	0.0418	0	0.0422	0	0.2211	0
PROTEIN		0.0397	0	0	0	0.0066	0.0066	0.0066	0	0.0067	0	0.0349	0
ASH		0.0794	0	0	0	0.0132	0.0132	0.0132	0	0.0133	0	0.0698	0
H2O		0	1	0.9951	0.9951	0.8299	0.8278	0.8278	0.0277	0.8356	0.9808	0.2191	0.9942
H2SO4		0	0	0	0	0	0	0	0	0	0	0	0
GLUCOSE		0	0	0.0038	0.0038	0.0032	0.0246	0.0037	0	0.0037	0.0044	0.001	0.0044
XYLOSE		0	0	0	0	0	0	0	0	0	0	0	0
LGNSOL		0	0	0	0	0	0	0	0	0	0	0	0
ETHANOL		0	0	0.0012	0.0012	0.001	0.001	0.0117	0.0065	0.0117	0.0138	0.0031	0.0014
CO2		0	0	0	0	0	0	0.0102	0.9658	0.0009	0.001	0.0002	0

	Units	1-50	2-10	2-20	2-21	2-30	2-40	2-50	2-60	2-70	2-80	2-90	3-80
From		$C-4		WATERMIX	FEEDCHIL	FEEDMIX	HYDROLYS	FERMENT	CO2FLASH	CO2FLASH	FILTER	FILTER	$C-6
To		FEEDMIX	WATERMIX	FEEDCHIL	FEEDMIX	HYDROLYS	FERMENT	CO2FLASH		FILTER	$C-1		WATERMIX
Substream: ALL													
Temperature	C	90.00	20.00	88.61	35.00	37.02	38.00	38.00	38.00	38.00	38.00	38.00	99.87
Mass Flow	KG/HR	67967.8	50528.65	341527.7	341527.7	409495.7	409495.7	409495.7	3958.71	405537	328203.4	77333.55	290999
Component Mole Flow													
CELLULOS	KMOL/HR	205.38	0	0	0	205.38	156.6	156.6	0	156.6	0	156.6	0
XYLAN	KMOL/HR	71.66	0	0	0	71.66	71.66	71.66	0	71.66	0	71.66	0
LIGNIN	KMOL/HR	112.39	0	0	0	112.39	112.39	112.39	0	112.39	0	112.39	0
PROTEIN	KMOL/HR	118.22	0	0	0	118.22	118.22	118.22	0	118.22	0	118.22	0
ASH	KMOL/HR	96.3	0	0	0	96.3	96.3	96.3	0	96.3	0	96.3	0
H2O	KMOL/HR	0	2804.77	18863.92	18863.92	18863.93	18815.16	18815.16	6.09	18809.07	17868.62	940.45	16059.16
H2SO4	KMOL/HR	0	0	0	0	0	0	0	0	0	0	0	0
GLUCOSE	KMOL/HR	0	0	7.18	7.18	7.18	55.95	8.39	0	8.39	7.97	0.42	7.18
XYLOSE	KMOL/HR	0	0	0	0	0	0	0	0	0	0	0	0
LGNSOL	KMOL/HR	0	0	0	0	0	0	0	0	0	0	0	0
ETHANOL	KMOL/HR	0	0	8.6	8.6	8.6	8.6	103.71	0.56	103.16	98	5.16	8.6
CO2	KMOL/HR	0	0	0	0	0	0	95.11	86.88	8.23	7.82	0.41	0
Component Mole Fraction													
CELLULOS		0.3401	0	0	0	0.0105	0.0081	0.008	0	0.008	0	0.1043	0
XYLAN		0.1187	0	0	0	0.0037	0.0037	0.0037	0	0.0037	0	0.0477	0
LIGNIN		0.1861	0	0	0	0.0058	0.0058	0.0057	0	0.0058	0	0.0748	0
PROTEIN		0.1957	0	0	0	0.0061	0.0061	0.006	0	0.0061	0	0.0787	0
ASH		0.1594	0	0	0	0.0049	0.005	0.0049	0	0.0049	0	0.0641	0
H2O		0	1	0.9992	0.9992	0.9682	0.9681	0.9611	0.0651	0.9654	0.9937	0.6263	0.999
H2SO4		0	0	0	0	0	0	0	0	0	0	0	0
GLUCOSE		0	0	0.0004	0.0004	0.0004	0.0029	0.0004	0	0.0004	0.0004	0.0003	0.0004
XYLOSE		0	0	0	0	0	0	0	0	0	0	0	0
LGNSOL		0	0	0	0	0	0	0	0	0	0	0	0
ETHANOL		0	0	0.0005	0.0005	0.0004	0.0004	0.0053	0.0059	0.0053	0.0054	0.0034	0.0005
CO2		0	0	0	0	0	0	0.0049	0.929	0.0004	0.0004	0.0003	0

C.14. Full Stream Table for Aspen Plus™ Model (A-SSF: Product Separation Area)

	Units	2-80	3-10	3-20	3-30	3-40	3-50	3-60	3-70	3-80	3-90
From		$C-5	CO2REMOV	CO2REMOV	BEERCOL	BEERCOL	RECTCOL	RECTCOL	R-MIX	R-PURGE	R-PURGE
To		CO2REMOV		BEERCOL	R-MIX	RECTCOL	R-MIX		R-PURGE	$C-2	
Substream: ALL											
Temperature	C	38.00	38.00	38.00	99.95	83.77	97.23	78.42	99.87	99.87	99.87
Mass Flow	KG/HR	328203.4	344.24	327859.2	315279.1	12580.1	8053.2	4526.9	323332.3	290999	32333.23
Component Mole Flow											
CELLULOS	KMOL/HR	0	0	0	0	0	0	0	0	0	0
XYLAN	KMOL/HR	0	0	0	0	0	0	0	0	0	0
LIGNIN	KMOL/HR	0	0	0	0	0	0	0	0	0	0
PROTEIN	KMOL/HR	0	0	0	0	0	0	0	0	0	0
ASH	KMOL/HR	0	0	0	0	0	0	0	0	0	0
H2O	KMOL/HR	17868.62	0	17868.62	17408.39	460.23	435.12	25.11	17843.51	16059.16	1784.35
H2SO4	KMOL/HR	0	0	0	0	0	0	0	0	0	0
GLUCOSE	KMOL/HR	7.97	0	7.97	7.97	0	0	0	7.97	7.18	0.8
XYLOSE	KMOL/HR	0	0	0	0	0	0	0	0	0	0
LGNSOL	KMOL/HR	0	0	0	0	0	0	0	0	0	0
ETHANOL	KMOL/HR	98	0	98	4.9	93.1	4.65	88.44	9.55	8.6	0.96
CO2	KMOL/HR	7.82	7.82	0	0	0	0	0	0	0	0
Component Mole Fraction											
CELLULOS		0	0	0	0	0	0	0	0	0	0
XYLAN		0	0	0	0	0	0	0	0	0	0
LIGNIN		0	0	0	0	0	0	0	0	0	0
PROTEIN		0	0	0	0	0	0	0	0	0	0
ASH		0	0	0	0	0	0	0	0	0	0
H2O		0.9937	0	0.9941	0.9993	0.8317	0.9894	0.2211	0.999	0.999	0.999
H2SO4		0	0	0	0	0	0	0	0	0	0
GLUCOSE		0.0004	0	0.0004	0.0005	0	0	0	0.0004	0.0004	0.0004
XYLOSE		0	0	0	0	0	0	0	0	0	0
LGNSOL		0	0	0	0	0	0	0	0	0	0
ETHANOL		0.0054	0	0.0055	0.0003	0.1683	0.0106	0.7789	0.0005	0.0005	0.0005
CO2		0.0004	1	0	0	0	0	0	0	0	0

	Units	2-80	3-10	3-20	3-30	3-40	3-50	3-60	3-70	3-80	3-90
From		$C-5	CO2REMOV	CO2REMOV	BEERCOL	BEERCOL	RECTCOL	RECTCOL	R-MIX	R-PURGE	R-PURGE
To		CO2REMOV		BEERCOL	R-MIX	RECTCOL	R-MIX		R-PURGE	$C-2	
Substream: ALL											
Temperature	C	38.00	38.00	38.00	99.95	83.77	97.23	78.42	99.87	99.87	99.87
Mass Flow	KG/HR	328203.4	344.24	327859.2	315279.1	12580.1	8053.2	4526.9	323332.3	290999	32333.23
Component Mole Flow											
CELLULOS	KMOL/HR	0	0	0	0	0	0	0	0	0	0
XYLAN	KMOL/HR	0	0	0	0	0	0	0	0	0	0
LIGNIN	KMOL/HR	0	0	0	0	0	0	0	0	0	0
PROTEIN	KMOL/HR	0	0	0	0	0	0	0	0	0	0
ASH	KMOL/HR	0	0	0	0	0	0	0	0	0	0
H2O	KMOL/HR	17868.62	0	17868.62	17408.39	460.23	435.12	25.11	17843.51	16059.16	1784.35
H2SO4	KMOL/HR	0	0	0	0	0	0	0	0	0	0
GLUCOSE	KMOL/HR	7.97	0	7.97	7.97	0	0	0	7.97	7.18	0.8
XYLOSE	KMOL/HR	0	0	0	0	0	0	0	0	0	0
LGNSOL	KMOL/HR	0	0	0	0	0	0	0	0	0	0
ETHANOL	KMOL/HR	98	0	98	4.9	93.1	4.65	88.44	9.55	8.6	0.96
CO2	KMOL/HR	7.82	7.82	0	0	0	0	0	0	0	0
Component Mole Fraction											
CELLULOS		0	0	0	0	0	0	0	0	0	0
XYLAN		0	0	0	0	0	0	0	0	0	0
LIGNIN		0	0	0	0	0	0	0	0	0	0
PROTEIN		0	0	0	0	0	0	0	0	0	0
ASH		0	0	0	0	0	0	0	0	0	0
H2O		0.9937	0	0.9941	0.9993	0.8317	0.9894	0.2211	0.999	0.999	0.999
H2SO4		0	0	0	0	0	0	0	0	0	0
GLUCOSE		0.0004	0	0.0004	0.0005	0	0	0	0.0004	0.0004	0.0004
XYLOSE		0	0	0	0	0	0	0	0	0	0
LGNSOL		0	0	0	0	0	0	0	0	0	0
ETHANOL		0.0054	0	0.0055	0.0003	0.1683	0.0106	0.7789	0.0005	0.0005	0.0005
CO2		0.0004	1	0	0	0	0	0	0	0	0

Appendix D: Aspen Plus™ Input Summaries for Simulations Used in Chapter 7

D.1. SHF Input Summary

```
;Input Summary created by Aspen Plus Rel. 30.0 at 10:29:55 Wed Oct 30, 2019
;Directory C:\Users\1474213.STUDENTS\Desktop\SHF - SSF aspen models v1\Main Files\168hrs  Filename
C:\Users\147421~1.STU\AppData\Local\Temp\~apc6d5.txt
;

TITLE 'A-SHF: Bioethanol Production with AMD pretreated Biomass'

;

IN-UNITS MET ENTHALPY='J/kg' ENTROPY='J/kg-K' VOLUME-FLOW=ACFM  &
      ENTHALPY-FLO='MJ/hr' MOLE-HEAT-CA='J/kmol-K'  &
      HEAT-TRANS-C='J/sec-sqm-K' ENERGY-PRICE='$/kJ'  &
      MOLE-ENTHALP='J/kmol' MASS-ENTHALP='J/kg'  &
      MOLE-ENTROPY='J/kmol-K' MASS-ENTROPY='J/kg-K'  &
      MASS-HEAT-CA='J/kg-K' UA='J/sec-K' HEAT=kJ  &
      VOL-HEAT-CAP='J/cum-K' HEAT-FLUX='J/sec-m'  &
      INVERSE-HT-C='sec-sqm-K/J' VOL-ENTHALPY='J/cum'

DEF-STREAMS MIXCISLD ALL

DIAGNOSTICS
   HISTORY SYS-LEVEL=4 SIM-LEVEL=4 PROP-LEVEL=2 STREAM-LEVEL=4
   TERMINAL SIM-LEVEL=0 CONV-LEVEL=0 COST-LEVEL=0 PROP-LEVEL=0  &
      ECON-LEVEL=0 STREAM-LEVEL=0 SYS-LEVEL=0
   MAX-PRINT SIM-LIMIT=1000

;

SIM-OPTIONS MASS-BAL-CHE=YES FLASH-TOL=1.0000E-07  &
      PROP-DERIV=NUMERICAL PACK-FLOW=1.0000E-15  &
      PACK-FRAC=1.0000E-15

MODEL-OPTION

SYS-OPTIONS INTERPRET=YES

RUN-CONTROL MAX-TIME=20000.0 MAX-ERRORS=4000 MAX-FORT-ERR=200

;


DATABANKS 'APV84 PURE28' / 'APV84 SOLIDS' / 'APV84 ASPENPCD' /  &
      'NISTV84 NIST-TRC' / 'APV84 POLYMER'

PROP-SOURCES 'APV84 PURE28' / 'APV84 SOLIDS' / 'APV84 ASPENPCD' &
       / 'NISTV84 NIST-TRC' / 'APV84 POLYMER'

;=============================================================================
;                        Components
```

```
;=============================================================================
;


COMPONENTS
   H2O H2O /
   ETHANOL C2H6O-2 /
   GLUCOSE C6H12O6 /
   XYLOSE C5H10O5 /
   EXTRACT C6H12O6 /
   LGNSOL C8H8O3-D1 /
   HMF C6H6O3-U /
   H2SO4 H2SO4 /
   CO2 CO2 /
   CELLULOS CELLULOSE /
   XYLAN C5H8O4-U /
   LIGNIN C8H8O3-D1 /
   PROTEIN CHONS-U3 /
   ASH CAO /
   ENZYME CHONS-U3

CISOLID-COMPS CELLULOS XYLAN LIGNIN PROTEIN ASH ENZYME

FORMULA HMF C6H6O3-U / XYLAN C5H8O4-U / PROTEIN CHONS-U3 /  &
      ENZYME CHONS-U3

COMP-GROUP OTHRSOLS SUBSTREAM=MIXED COMPS=LGNSOL EXTRACT

COMP-GROUP SUGARS SUBSTREAM=MIXED COMPS=GLUCOSE XYLOSE

;

HENRY-COMPS HC CO2

SOLVE
   RUN-MODE MODE=SIM

;
;THIS FLOWSHEET MODELS THE DISTILLATION/DEHYDRATION AREA.
;   BLOCK H506+    IN=596 QH506  OUT=597 QH506EX          ;
;   BLOCK H502     IN=592 QRD502 OUT=593 QH504EX          ;
;   BLOCK H501     IN=594 QRD501 OUT=595 QRD501EX         ;
;     ADDED SEPARATE MIXER AND SPLITTER SO WE CAN SEE TOTAL CONDENSATE
;     VENT SCRUBBER
;     Stream Definitions:  524 WATER, 550 VENT, 551 WASTE WATER
;     PNEUMAPRESS UNIT

FLOWSHEET A500
   HIERARCHY B1
   CONNECT $C-3 IN="B1.1-50" OUT=1-50
   HIERARCHY B2
   CONNECT $C-6 IN=S2 OUT="B2.3-80"
   CONNECT $C-4 IN=1-50 OUT="B2.1-50"
   CONNECT $C-2 IN="B2.2-100" OUT=2-100
   HIERARCHY B3
   CONNECT $C-5 IN=2-100 OUT="B3.2-100"
   CONNECT $C-1 IN="B3.3-80" OUT=S2
```

```
;
;

PROPERTIES NRTL HENRY-COMPS=HC
   PROPERTIES NRTL A500 HENRY-COMPS=HC FREE-WATER=STEAM-TA  &
      SOLU-WATER=3 TRUE-COMPS=YES
   PROPERTIES NRTL-HOC
   PROPERTIES SYSOP12

PROP-REPLACE SYSOP12 STEAM-TA

PROP-DATA
   PROP-LIST ATOMNO / NOATOM
   PVAL ENZYME 6 1 8 7 16 / 1. 1.59 0.42 0.24 0.01

PROP-DATA
   PROP-LIST ATOMNO / NOATOM
   PVAL PROTEIN 6 1 8 7 16 / 1. 1.57 0.31 0.29 0.007

PROP-DATA
   PROP-LIST ATOMNO / NOATOM
   PVAL XYLAN 6 1 8 / 5. 8. 4.

STRUCTURES
   STRUCTURES XYLOSE C2 O1 S / C2 C3 S / C3 C4 S / C4  &
      C5 S / C5 C6 S / C6 O1 S / O10 C3 S / C4 O9  &
      S / C5 O8 S / C6 O7 S

PROP-DATA
   PROP-LIST ATOMNO / NOATOM
   PVAL XYLOSE 6 1 8 / 5. 10. 5.

PROP-DATA PCES-1
   IN-UNITS MET TEMPERATURE=C
   PROP-LIST ZC / VB / VLSTD
   PVAL HMF .2950480100 / 75.44034060 / 56.60831900
   PROP-LIST VB / OMEGA / DHVLB / RGYR
   PVAL H2SO4 65.75890000 / -.5549676020 / 13890.79966 /  &
      2.5372000E-10
   PROP-LIST VB / RKTZRA / VLSTD / DGFORM
   PVAL XYLOSE 157.8481910 / .0792980740 / 94.27630000 /  &
      -1.5306678E+5
   PROP-LIST DHVLB / VLSTD / TC
   PVAL PROTEIN 0 / 0.0 / -226.7884
   PVAL XYLAN 0.0 / 0.0 / -244.0887200
   PROP-LIST RKTZRA / VLSTD
   PVAL CELLULOS .2060436120 / 146.9770000
   PVAL ASH .2917660970 / 866.9275910
   PVAL GLUCOSE .0715398735 / 152.6100000
   PVAL EXTRACT .0715398735 / 152.6100000
   PVAL LGNSOL .2200963440 / 126.9050000

;
; Use water's dipole moment and radius of gyration,
; these properties are important for the vapor fugacity
; calculation in one block using Hayden & O'Connell.
```

```
; These particular components will not be in the vapor
; phase so their values are unimportant.

PROP-DATA PURE-1
  IN-UNITS SI
  PROP-LIST MUP / RGYR
  PVAL XYLOSE 5.849340E-25 / 6.1500000E-11
  PVAL PROTEIN 5.849340E-25 / 6.1500000E-11
  PVAL HMF 5.849340E-25 / 6.1500000E-11

PROP-DATA REVIEW-1
  IN-UNITS MET TEMPERATURE=C
  PROP-LIST DHSFRM / RKTZRA / VLSTD
  PVAL LIGNIN -108247.86 / .2200963440 / 126.9050000

PROP-DATA USRDEF
  IN-UNITS MET PRESSURE=Pa TEMPERATURE=K MOLE-VOLUME='cum/kmol'  &
    PDROP=atm
  PROP-LIST MW / TB / DHSFRM
  PVAL PROTEIN 22.8396 / 0 / -17618
  PVAL XYLAN 132.117 / 0 / -182099.93
  PROP-LIST MW / DHSFRM
  PVAL ENZYME 24.0156 / -17900.07
  PROP-LIST MW / DHFORM / TB / TC / PC / OMEGA / VC /  &
    RKTZRA
  PVAL HMF 126.11 / -79774.53 / 532.7 / 731.012 / 5235810 / &
    .9936467100 / .3425 / .1981779740

PROP-DATA USRDEF2
  IN-UNITS MET TEMPERATURE=C
  PROP-LIST DHFORM
  PVAL XYLOSE -216752.65
  PROP-LIST DHSFRM
  PVAL CELLULOS -233200.06

PROP-DATA CPIG-1
  IN-UNITS MET TEMPERATURE=C
  PROP-LIST CPIG
  PVAL XYLOSE 37.26888724 .1399898460 -1.5496537E-4  &
    7.36799009E-8 0.0 0.0 6.850000000 826.8500000  &
    8.605426579 6.32086902E-3 1.500000000

PROP-DATA CPIG-1
  IN-UNITS MET MOLE-HEAT-CA='J/kmol-K' TEMPERATURE=K
  PROP-LIST CPIG
  PVAL HMF -23327.1 706.431 -.611538 .000204391 0 0 280  &
    1100 36029.2 20.2733 1.5

PROP-DATA CPSPO1-1
  IN-UNITS MET MOLE-HEAT-CA='J/kmol-K' TEMPERATURE=K
  PROP-LIST CPSPO1
  PVAL XYLAN -9529.9 547.25 0 0 0 0 298.15
  PVAL LIGNIN 39752.8 498.84 0 0 0 0 298.15
  PVAL ENZYME 35533 0 0 0 0 0 298.15

PROP-DATA DHVLWT-1
  IN-UNITS MET TEMPERATURE=C
```

```
   PROP-LIST DHVLWT
   PVAL ASH 71498.34122 3396.850000 .4439946020 -.1498359780  &
      3396.850000
   PVAL XYLAN 0.0 -273.1500000 .3800000000 0.0 -273.1500000
   PVAL LIGNIN 0.0 -273.1500000 .3800000000 0.0 -273.1500000

PROP-DATA DHVLWT-1
   IN-UNITS MET TEMPERATURE=K MOLE-ENTHALP='J/kmol'
   PROP-LIST DHVLWT
   PVAL HMF 80550000 335.1

PROP-DATA KLDIP-1
   IN-UNITS MET TEMPERATURE=C
   PROP-LIST KLDIP
   PVAL ASH -.6218197112 7.78300188E-4 -2.8775749E-7  &
      4.5627261E-11 -2.727830E-15 3396.850000 5686.650000
   PVAL XYLAN -728.6887817 -11.16357334 -.0641578256  &
      -1.6391764E-4 -1.5706055E-7 -273.1500000 -244.3793328
   PVAL LIGNIN -1177.842559 -17.94273624 -.1025248260  &
      -2.6041378E-4 -2.4805952E-7 -273.1500000 -247.9915656
   PVAL HMF -.1886406576 3.82214409E-3 -1.8525171E-5  &
      3.78628761E-8 -2.927970E-11 259.5500000 450.5518800

PROP-DATA MULAND-1
   IN-UNITS MET TEMPERATURE=K
   PROP-LIST MULAND
   PVAL ASH 74.47732598 -27259.04230 -8.432322050 3670.000000  &
      5959.800000

PROP-DATA MULAND-1
   IN-UNITS MET TEMPERATURE=C
   PROP-LIST MULAND
   PVAL CELLULOS 81.25737378 -12127.32210 -10.25255770  &
      1126.850000 1706.850000
   PVAL XYLOSE -15.55079002 7559.999980 -3.0401358E-8  &
      441.8500000 547.1020000

;
; Needed for Tray sizing in RADFRAC

PROP-DATA MULDIP-1
   IN-UNITS MET VOLUME-FLOW='cum/hr' ENTHALPY-FLO='MMkcal/hr'  &
      HEAT-TRANS-C='kcal/hr-sqm-K' PRESSURE=bar TEMPERATURE=C  &
      VOLUME=cum DELTA-T=C HEAD=meter MOLE-DENSITY='kmol/cum'  &
      MASS-DENSITY='kg/cum' MOLE-ENTHALP='kcal/mol'  &
      MASS-ENTHALP='kcal/kg' HEAT=MMkcal MOLE-CONC='mol/l'  &
      PDROP=bar
   PROP-LIST MULDIP
   PVAL PROTEIN -2267.40 138910.0 320.550 0.0 0.0 323.0  &
      418.0

PROP-DATA NATOM-1
   IN-UNITS MET TEMPERATURE=C
   PROP-LIST NATOM
   PVAL XYLAN 5 8 4
   PVAL CELLULOS 6 10 5 0
   PVAL HMF 6 6 3
```

```
PROP-DATA PLXANT-1
   IN-UNITS MET TEMPERATURE=C
   PROP-LIST PLXANT
   PVAL ASH 37.52683375 -48457.53140 0.0 0.0 -2.964795110  &
      4.6976791E-24 6.000000000 3396.850000 5746.850000
   PVAL HMF 114.8702885 -15309.61940 0.0 0.0 -13.73341590  &
      3.8123288E-18 6.000000000 259.5500000 457.8620000
   PVAL PROTEIN -1E20

PROP-DATA SIGDIP-1
   IN-UNITS MET TEMPERATURE=C
   PROP-LIST SIGDIP
   PVAL ASH 139.2135830 1.222222220 -2.171954E-10  &
      2.3955375E-10 -9.673330E-11 3396.850000 5626.450000
   PVAL XYLOSE 291.3517280 1.222222220 -4.7621659E-9  &
      5.32741828E-9 -2.0439985E-9 441.8500000 599.4616000
   PVAL HMF 138.4682720 1.222222220 -1.3987173E-9  &
      1.57302497E-9 -6.210389E-10 259.5500000 443.2417600

PROP-DATA VSPOLY-1
   IN-UNITS MET TEMPERATURE=K MOLE-VOLUME='cum/kmol'
   PROP-LIST VSPOLY
   PVAL XYLAN .0864 0 0 0 0 298.15
   PVAL ENZYME .0152 0 0 0 0 298.15

PROP-DATA HOCETA-1
   IN-UNITS ENG
   PROP-LIST HOCETA
   BPVAL ETHANOL ETHANOL 1.40
   BPVAL ETHANOL H2O 1.550
   BPVAL ETHANOL CO2 .30
   BPVAL H2O ETHANOL 1.550
   BPVAL H2O H2O 1.70
   BPVAL H2O CO2 .30
   BPVAL CO2 ETHANOL .30
   BPVAL CO2 H2O .30
   BPVAL CO2 CO2 .160

;=============================================================================
;  Henry component parameters (Non-condensible <==> solvent)
;   New Parameters for N2 and O2 taken from version 9.2 to improve
;   the calculations involving these two components.
;=============================================================================
;
;
;  Using ethanol Henry's for FURFURAL & HMF
;

PROP-DATA HENRY-1
   IN-UNITS MET PRESSURE=bar TEMPERATURE=C PDROP=atm
   PROP-LIST HENRY
   BPVAL CO2 ETHANOL 89.583080 -5018.80 -11.8910 0.0 10.0  &
      40.0 0.0
   BPVAL CO2 H2O 181.18610 -8982.0 -25.8460 .0121280  &
      .20000610 74.70 0.0
   BPVAL CO2 HMF 89.583080 -5018.80 -11.8910 0.0 10.0 40.0  &
```

```
      0.0

;
;============================================================================
; NRTL Binary Parameters generated by Aspen Plus Release 9.1-3
;============================================================================
;
; Added in W9806C 6/15/98 - "Lit." values from ASPEN 9.2
;

PROP-DATA NRTL-1
   IN-UNITS MET VOLUME-FLOW='cum/hr' ENTHALPY-FLO='MMkcal/hr'  &
      HEAT-TRANS-C='kcal/hr-sqm-K' PRESSURE=bar TEMPERATURE=C  &
      VOLUME=cum DELTA-T=C HEAD=meter MOLE-DENSITY='kmol/cum'  &
      MASS-DENSITY='kg/cum' MOLE-ENTHALP='kcal/mol'  &
      MASS-ENTHALP='kcal/kg' HEAT=MMkcal MOLE-CONC='mol/l'  &
      PDROP=bar
   PROP-LIST NRTL
   BPVAL ETHANOL H2O 0.0 -55.16980 .30310 0.0 0.0 0.0 75.0  &
      100.0
   BPVAL H2O ETHANOL 0.0 670.44420 .30310 0.0 0.0 0.0 75.0  &
      100.0
   BPVAL H2O HMF .3791796770 1788.4839660 .2372956960 0.0 0.0  &
      0.0 90.0 140.0
   BPVAL HMF H2O -.9418711160 -288.70228150 .2372956960 0.0  &
      0.0 0.0 90.0 140.0
   BPVAL ETHANOL HMF 0.0 405.27147860 .30 0.0 0.0 0.0 75.0  &
      135.0
   BPVAL HMF ETHANOL 0.0 -218.05936270 .30 0.0 0.0 0.0 75.0  &
      135.0

PROP-SET CLIQ MOLEFLC UNITS='kmol/hr' SUBSTREAM=MIXED

PROP-SET COD CODMX BODMX UNITS='fraction' SUBSTREAM=ALL

PROP-SET COMP1 MASSFLOW SUBSTREAM=MIXED

PROP-SET COMP2 MASSFLOW SUBSTREAM=CISOLID

PROP-SET CSOL MOLEFLC UNITS='kmol/hr' SUBSTREAM=CISOLID

PROP-SET FRAC MOLEFLOW SUBSTREAM=MIXED PHASE=L V

PROP-SET HREF HFLMX UNITS='MMkcal/hr' SUBSTREAM=ALL  &
      TEMP=298.1500000

;

HIERARCHY B1


SOLVE
   PARAM METHOD=SM
   RUN-MODE MODE=SIM

;
;THIS FLOWSHEET MODELS THE DISTILLATION/DEHYDRATION AREA.
```

```
;   BLOCK H506+    IN=596 QH506  OUT=597 QH506EX          ;
;   BLOCK H502     IN=592 QRD502 OUT=593 QH504EX          ;
;   BLOCK H501     IN=594 QRD501 OUT=595 QRD501EX         ;
;     ADDED SEPARATE MIXER AND SPLITTER SO WE CAN SEE TOTAL CONDENSATE
;     VENT SCRUBBER
;     Stream Definitions:  524 WATER, 550 VENT, 551 WASTE WATER
;     PNEUMAPRESS UNIT

FLOWSHEET A500
   BLOCK PRETREAT IN=1-20 1-12 OUT=1-30
   BLOCK PRE-FILT IN=1-30 OUT=1-40 1-50
   BLOCK PRE-HX1 IN=1-40 1-10 OUT=1-41 1-11
   BLOCK PRE-HX2 IN=1-11 OUT=1-12

PROPERTIES NRTL HENRY-COMPS=HC FREE-WATER=STEAM-TA SOLU-WATER=3  &
      TRUE-COMPS=YES
   PROPERTIES NRTL-HOC / SYSOP12

STREAM 1-10
   SUBSTREAM MIXED TEMP=20. <C> PRES=1. MASS-FLOW=450000.
   MASS-FRAC H2O 0.995 / H2SO4 0.005

STREAM 1-20
   SUBSTREAM CISOLID TEMP=20. <C> PRES=1. MASS-FLOW=90000.
   MASS-FRAC CELLULOS 0.37 / XYLAN 0.29 / LIGNIN 0.25 /  &
      PROTEIN 0.03 / ASH 0.06

BLOCK PRE-HX1 HEATX
   PARAM T-HOT=30. <C> CALC-TYPE=DESIGN U-OPTION=PHASE  &
      F-OPTION=CONSTANT CALC-METHOD=SHORTCUT
   FEEDS HOT=1-40 COLD=1-10
   OUTLETS-HOT 1-41
   OUTLETS-COLD 1-11
   HOT-SIDE DP-OPTION=CONSTANT
   COLD-SIDE DP-OPTION=CONSTANT

BLOCK PRE-HX2 HEATX
   PARAM T-COLD=95. <C> CALC-TYPE=DESIGN U-OPTION=PHASE  &
      F-OPTION=CONSTANT CALC-METHOD=SHORTCUT
   FEEDS COLD=1-11
   OUTLETS-COLD 1-12
   HOT-SIDE DP-OPTION=CONSTANT
   COLD-SIDE DP-OPTION=CONSTANT
   REFERENCE HOT-UTIL=U-2

BLOCK PRETREAT RSTOIC
   PARAM TEMP=95. <C> PRES=1.
   STOIC 1 CISOLID XYLAN -1. / MIXED H2O -1. / XYLOSE 1.
   STOIC 2 CISOLID LIGNIN -1. / MIXED LGNSOL 1.
   CONV 1 CISOLID XYLAN 0.63724934
   CONV 2 CISOLID LIGNIN 0.24

BLOCK PRE-FILT SSPLIT
   FRAC MIXED 1-40 0.95
   FRAC CISOLID 1-40 0.

ENDHIERARCHY B1
```

```
HIERARCHY B2


SOLVE
   PARAM METHOD=SM
   RUN-MODE MODE=SIM

;
;THIS FLOWSHEET MODELS THE DISTILLATION/DEHYDRATION AREA.
;   BLOCK H506+    IN=596 QH506  OUT=597 QH506EX          ;
;   BLOCK H502     IN=592 QRD502 OUT=593 QH504EX          ;
;   BLOCK H501     IN=594 QRD501 OUT=595 QRD501EX         ;
;     ADDED SEPARATE MIXER AND SPLITTER SO WE CAN SEE TOTAL CONDENSATE
;     VENT SCRUBBER
;     Stream Definitions:  524 WATER, 550 VENT, 551 WASTE WATER
;     PNEUMAPRESS UNIT

FLOWSHEET A500
   BLOCK HYDROLYS IN=2-30 OUT=2-40
   BLOCK FILTER IN=2-40 OUT=2-60 2-50
   BLOCK FEREMNT IN=2-70 OUT=2-80
   BLOCK WATERMIX IN=2-10 3-80 OUT=2-20
   BLOCK FEEDMIX IN=2-21 1-50 OUT=2-30
   BLOCK FEEDCHIL IN=2-20 OUT=2-21
   BLOCK FERMCHIL IN=2-60 OUT=2-70
   BLOCK B1 IN=2-80 OUT=2-90 2-100

PROPERTIES NRTL HENRY-COMPS=HC FREE-WATER=STEAM-TA SOLU-WATER=3  &
      TRUE-COMPS=YES
   PROPERTIES NRTL-HOC / SYSOP12

STREAM 2-10
   SUBSTREAM MIXED TEMP=298.1500000 PRES=1.000000000  &
      MASS-FLOW=25001.00000
   MASS-FRAC H2O 1.
   SUBSTREAM CISOLID TEMP=321.1500000 PRES=1.000000000

BLOCK FEEDMIX MIXER
   PARAM

BLOCK WATERMIX MIXER
   PARAM

BLOCK B1 FLASH2
   PARAM TEMP=35. <C> PRES=1.

BLOCK FEEDCHIL HEATX
   PARAM T-HOT=50. <C> CALC-TYPE=DESIGN MIN-TAPP=5. <K>  &
      U-OPTION=PHASE F-OPTION=CONSTANT CALC-METHOD=SHORTCUT
   FEEDS HOT=2-20
   OUTLETS-HOT 2-21
   HOT-SIDE DP-OPTION=CONSTANT
   COLD-SIDE DP-OPTION=CONSTANT
   REFERENCE COLD-UTIL=U-1

BLOCK FERMCHIL HEATX
```

```
   PARAM T-HOT=35. <C> CALC-TYPE=DESIGN U-OPTION=PHASE  &
      F-OPTION=CONSTANT CALC-METHOD=SHORTCUT
   FEEDS HOT=2-60
   OUTLETS-HOT 2-70
   HOT-SIDE DP-OPTION=CONSTANT
   COLD-SIDE DP-OPTION=CONSTANT
   REFERENCE COLD-UTIL=U-3

BLOCK FEREMNT RSTOIC
   PARAM TEMP=35. <C> PRES=1.000000000
   STOIC 1 MIXED GLUCOSE -1. / ETHANOL 2. / CO2 2.
   CONV 1 MIXED GLUCOSE 0.791

BLOCK HYDROLYS RSTOIC
   PARAM TEMP=50. <C> PRES=1.000000000 HEAT-OF-REAC=NO
   STOIC 1 CISOLID CELLULOS -1. / MIXED H2O -1. / GLUCOSE  &
      1.
   CONV 1 CISOLID CELLULOS 0.51228379

BLOCK FILTER SSPLIT
   FRAC MIXED 2-60 0.95
   FRAC CISOLID 2-50 1.

ENDHIERARCHY B2

HIERARCHY B3


SOLVE
   PARAM METHOD=SM
   RUN-MODE MODE=SIM

;
;THIS FLOWSHEET MODELS THE DISTILLATION/DEHYDRATION AREA.
;   BLOCK H506+    IN=596 QH506  OUT=597 QH506EX          ;
;   BLOCK H502     IN=592 QRD502 OUT=593 QH504EX          ;
;   BLOCK H501     IN=594 QRD501 OUT=595 QRD501EX         ;
;     ADDED SEPARATE MIXER AND SPLITTER SO WE CAN SEE TOTAL CONDENSATE
;     VENT SCRUBBER
;     Stream Definitions:  524 WATER, 550 VENT, 551 WASTE WATER
;     PNEUMAPRESS UNIT

FLOWSHEET A500
   HIERARCHY B10
   CONNECT $C-2 IN=H-3 OUT="B10.S3"
   CONNECT $C-1 IN=H-1 OUT="B10.S4"
   CONNECT $C-4 IN=H-4 OUT="B10.S1"
   CONNECT $C-3 IN=H-2 OUT="B10.S2"
   BLOCK CO2REMOV IN=2-100 OUT=3-10 3-20
   BLOCK BEERCOL IN=3-20 OUT=3-40 3-30 H-1 H-4
   BLOCK RECTCOL IN=3-40 OUT=3-60 3-50 H-3 H-2
   BLOCK R-MIX IN=3-50 3-30 OUT=3-70
   BLOCK R-PURGE IN=3-70 OUT=3-90 3-80

PROPERTIES NRTL HENRY-COMPS=HC FREE-WATER=STEAM-TA SOLU-WATER=3  &
      TRUE-COMPS=YES
   PROPERTIES NRTL-HOC / SYSOP12
```

```
DEF-STREAMS HEAT H-1

DEF-STREAMS HEAT H-2

DEF-STREAMS HEAT H-3

DEF-STREAMS HEAT H-4

BLOCK R-MIX MIXER
   PARAM

BLOCK R-PURGE FSPLIT
   FRAC 3-90 0.1

BLOCK CO2REMOV SEP
   PARAM
   FRAC STREAM=3-20 SUBSTREAM=MIXED COMPS=CO2 FRACS=0.

BLOCK BEERCOL DSTWU
   PARAM LIGHTKEY=ETHANOL RECOVL=0.95 HEAVYKEY=H2O  &
      RECOVH=0.002 PTOP=1.000000000 PBOT=1.000000000 RR=-1.1  &
      PLOT=YES

BLOCK RECTCOL DSTWU
   PARAM LIGHTKEY=ETHANOL RECOVL=0.95 HEAVYKEY=H2O RECOVH=0.1  &
      PTOP=1.000000000 PBOT=1.000000000 RR=-1.1 PLOT=YES

HIERARCHY B10

CLIST-REF COMLIST=GLOBAL


SOLVE
   PARAM METHOD=SM
   RUN-MODE MODE=SIM

;
;THIS FLOWSHEET MODELS THE DISTILLATION/DEHYDRATION AREA.
;   BLOCK H506+    IN=596 QH506  OUT=597 QH506EX          ;
;   BLOCK H502     IN=592 QRD502 OUT=593 QH504EX          ;
;   BLOCK H501     IN=594 QRD501 OUT=595 QRD501EX         ;
;     ADDED SEPARATE MIXER AND SPLITTER SO WE CAN SEE TOTAL CONDENSATE
;     VENT SCRUBBER
;     Stream Definitions:  524 WATER, 550 VENT, 551 WASTE WATER
;     PNEUMAPRESS UNIT

FLOWSHEET A500
   BLOCK B4 IN=S3 S4 OUT=S5
   BLOCK B5 IN=S1 S2 OUT=S6
   BLOCK B6 IN=S7 S6 OUT=S8
   BLOCK B7 IN=S9 S5 OUT=S10
   BLOCK B8 IN=S10 OUT=S11
   BLOCK B9 IN=S8 OUT=S12

PROPERTIES NRTL HENRY-COMPS=HC FREE-WATER=STEAM-TA SOLU-WATER=3  &
      TRUE-COMPS=YES
```

```
   PROPERTIES NRTL-HOC / SYSOP12

STREAM S7
   SUBSTREAM MIXED TEMP=368.1500000 PRES=1.000000000  &
      MOLE-FLOW=1.00000000E+5
   MASS-FRAC H2O 1.

STREAM S9
   SUBSTREAM MIXED TEMP=338.1500000 PRES=1.000000000  &
      MOLE-FLOW=1.00000000E+5
   MASS-FRAC H2O 1.

DEF-STREAMS HEAT S1

DEF-STREAMS HEAT S2

DEF-STREAMS HEAT S3

DEF-STREAMS HEAT S4

DEF-STREAMS HEAT S5

DEF-STREAMS HEAT S6

BLOCK B4 MIXER

BLOCK B5 MIXER

BLOCK B6 HEATER
   PARAM PRES=1.000000000

BLOCK B7 HEATER
   PARAM PRES=1.000000000

BLOCK B8 HEATX
   PARAM T-HOT=65. <C> CALC-TYPE=DESIGN U-OPTION=PHASE  &
      F-OPTION=CONSTANT CALC-METHOD=SHORTCUT
   FEEDS HOT=S10
   OUTLETS-HOT S11
   HOT-SIDE DP-OPTION=CONSTANT
   COLD-SIDE DP-OPTION=CONSTANT
   REFERENCE COLD-UTIL=U-1

BLOCK B9 HEATX
   PARAM T-COLD=95. <C> CALC-TYPE=DESIGN U-OPTION=PHASE  &
      F-OPTION=CONSTANT CALC-METHOD=SHORTCUT
   FEEDS COLD=S8
   OUTLETS-COLD S12
   HOT-SIDE DP-OPTION=CONSTANT
   COLD-SIDE DP-OPTION=CONSTANT
   REFERENCE HOT-UTIL=U-2

ENDHIERARCHY B10

ENDHIERARCHY B3

STREAM-PRICE
```

```
   STREAM-PRICE STREAM="B3.3-60" MASS-PRICE=.6140000000 /  &
      STREAM="B2.2-10" MASS-PRICE=1.69 <$/ton> /  &
      STREAM="B2.2-10" MASS-PRICE=1.69 <$/ton> /  &
      STREAM="B3.3-60" MASS-PRICE=.6140000000

UTILITY U-1 GENERAL
   DESCRIPTION "Cooling Water, Inlet Temp=20 C, Outlet Temp=25 C"
   COST ENERGY-PRICE=1.1E-006
   PARAM UTILITY-TYPE=WATER PRES=1.000000000  &
      PRES-OUT=1.000000000 TIN=303.1500000 TOUT=318.1500000  &
      CALOPT=FLASH MIN-TAPP=5.000000000 HTC=3750.000000

UTILITY U-2 GENERAL
   DESCRIPTION  &
      "Low Pressure Steam, Inlet Temp=125 C, Outlet Temp=124 C"
   COST ENERGY-PRICE=6.2E-006
   PARAM UTILITY-TYPE=STEAM TIN=398.1500000 TOUT=397.1500000  &
      VFRAC=1. VFR-OUT=0. CALOPT=FLASH MIN-TAPP=10.00000000  &
      CALCCO2=YES FACTORSOURCE="US-EPA-Rule-E9-5711" FUELSOURCE= &
      "Natural_gas" CO2FACTOR=2.34000000E-7 EFFICIENCY=0.85  &
      HTC=6000.000000

UTILITY U-3 GENERAL
   DESCRIPTION "Cooling Water, Inlet Temp=20 C, Outlet Temp=25 C"
   COST ENERGY-PRICE=4.9E-006
   PARAM UTILITY-TYPE=WATER PRES=1.000000000  &
      PRES-OUT=1.000000000 TIN=293.1500000 TOUT=303.1500000  &
      CALOPT=FLASH MIN-TAPP=5.000000000 HTC=3750.000000

DESIGN-SPEC DS-1
   DEFINE BATT PARAMETER 8 PHYS-QTY=USR-DUMMY0 UOM="base-units"
   SPEC "BATT" TO "168"
   TOL-SPEC "0.001"
   VARY BLOCK-VAR BLOCK="B2.HYDROLYS" VARIABLE=CONV  &
      SENTENCE=CONV ID1=1
   LIMITS "0.01" "0.7"

DESIGN-SPEC DS-2
   DEFINE ETOHFINA MASS-FRAC STREAM="B3.3-40" SUBSTREAM=MIXED  &
      COMPONENT=ETHANOL
   SPEC "ETOHFINA" TO "0.4"
   TOL-SPEC "0.0001"
   VARY BLOCK-VAR BLOCK="B3.BEERCOL" VARIABLE=RECOVH  &
      SENTENCE=PARAM
   LIMITS "0.001" "0.05"

DESIGN-SPEC DS-3
   DEFINE ETOHFIN MASS-FRAC STREAM="B3.3-60" SUBSTREAM=MIXED  &
      COMPONENT=ETHANOL
   SPEC "ETOHFIN" TO "0.9"
   TOL-SPEC "0.0001"
   VARY BLOCK-VAR BLOCK="B3.RECTCOL" VARIABLE=RECOVH  &
      SENTENCE=PARAM
   LIMITS "0.0001" "0.1"

DESIGN-SPEC DS-4
   DEFINE FEEDH2O MASS-FLOW STREAM="B2.2-30" SUBSTREAM=MIXED  &
```

```
      COMPONENT=H2O UOM="kg/hr"
   SPEC "FEEDH2O" TO "339839"
   TOL-SPEC "1"
   VARY STREAM-VAR STREAM="B2.2-10" SUBSTREAM=MIXED  &
      VARIABLE=MASS-FLOW UOM="kg/hr"
   LIMITS "0" "400000"

EO-CONV-OPTI

CALCULATOR C-PRETRE
   DEFINE VOL11MIX STREAM-VAR STREAM="B1.1-10" SUBSTREAM=MIXED  &
      VARIABLE=STDVOL-FLOW UOM="l/hr"
   DEFINE VOL12SOL STREAM-VAR STREAM="B1.1-20"  &
      SUBSTREAM=CISOLID VARIABLE=STDVOL-FLOW UOM="l/hr"
   DEFINE MAS11MIX STREAM-VAR STREAM="B1.1-10" SUBSTREAM=MIXED  &
      VARIABLE=MASS-FLOW UOM="kg/hr"
   DEFINE MAS12SOL STREAM-VAR STREAM="B1.1-20"  &
      SUBSTREAM=CISOLID VARIABLE=MASS-FLOW UOM="kg/hr"
   DEFINE PREVOL PARAMETER 61 PHYS-QTY=VOLUME UOM="cum"
F    MASS=MAS11MIX+MAS12SOL
F    VOL=VOL11MIX+VOL12SOL
F    t=3.5
F    T=t*24
F    PREVOL=T*VOL*1.1*(T+24)/T/1000
F
   READ-VARS VOL11MIX VOL12SOL MAS11MIX MAS12SOL
   WRITE-VARS PREVOL

CALCULATOR FERMVOL
   IN-UNITS MET ENTHALPY-FLO='MMkcal/hr' TEMPERATURE=C  &
      HEAT=MMkcal HEAT-FLUX='Gcal/hr-m'
   DEFINE VOL8 STREAM-VAR STREAM="B3.2-100" SUBSTREAM=MIXED  &
      VARIABLE=STDVOL-FLOW UOM="l/hr"
   DEFINE DENS8 STREAM-VAR STREAM="B3.2-100" SUBSTREAM=MIXED  &
      VARIABLE=MASS-DENSITY UOM="kg/cum"
   DEFINE FERMVOL PARAMETER 3 PHYS-QTY=VOLUME UOM="cum"
   DEFINE EFERMVOL PARAMETER 4 PHYS-QTY=VOLUME UOM="cum"
   DEFINE ETOHPROD PARAMETER 7 PHYS-QTY=USR-DUMMY0 UOM= &
      "base-units" INIT-VAL=1.
   DEFINE BATCHT PARAMETER 21 PHYS-QTY=USR-DUMMY0 UOM= &
      "base-units"
   DEFINE G5 MASS-FLOW STREAM="B2.2-60" SUBSTREAM=MIXED  &
      COMPONENT=GLUCOSE UOM="kg/hr"
   DEFINE VOL5 STREAM-VAR STREAM="B2.2-60" SUBSTREAM=MIXED  &
      VARIABLE=STDVOL-FLOW UOM="l/hr"
   DEFINE CG5 PARAMETER 22 PHYS-QTY=USR-DUMMY0 UOM="base-units"
F    CG5=G5*1000/VOL5

c ======== VALUES FOR H2SO4 ==========
F    r11=1.0282
F    r21=7.1231
c     BATCHT=(CG5-r11*6)/r21+6+6
c ======== VALUES FOR AMD==========
F    r12=0.7723
F    r22=5.4772
F    BATCHT=(CG5-r12*6)/r22+6+6
```

```
F    BATCHS=BATCHT*VOL8
F    BATCHVOL=BATCHS/DENS8
F    FERMVOL=BATCHVOL * 1.1
F
F
F
   READ-VARS DENS8 VOL8 ETOHPROD G5 VOL5
   WRITE-VARS FERMVOL EFERMVOL BATCHT CG5

CALCULATOR HYDVOL
   IN-UNITS MET ENTHALPY-FLO='MMkcal/hr' TEMPERATURE=C  &
      HEAT=MMkcal HEAT-FLUX='Gcal/hr-m'
   DEFINE HYDVOL PARAMETER 1 PHYS-QTY=VOLUME UOM="cum"
   DEFINE BATT PARAMETER 8 PHYS-QTY=USR-DUMMY0 UOM="base-units"
   DEFINE G3 MASS-FLOW STREAM="B2.2-40" SUBSTREAM=MIXED  &
      COMPONENT=GLUCOSE UOM="kg/hr"
   DEFINE VOL3 STREAM-VAR STREAM="B2.2-40" SUBSTREAM=MIXED  &
      VARIABLE=STDVOL-FLOW UOM="l/hr"
   DEFINE GPROD PARAMETER 9 PHYS-QTY=USR-DUMMY0 UOM="base-units"  &
      INIT-VAL=0.0015
   DEFINE CG PARAMETER 10 PHYS-QTY=USR-DUMMY0 UOM="base-units"
   DEFINE RATIORR PARAMETER 20 PHYS-QTY=USR-DUMMY0 UOM= &
      "base-units" INIT-VAL=0.2
   DEFINE MASS2MIX STREAM-VAR STREAM="B2.2-20" SUBSTREAM=MIXED  &
      VARIABLE=MASS-FLOW UOM="kg/hr"
   DEFINE VOL2MIX STREAM-VAR STREAM="B2.2-20" SUBSTREAM=MIXED  &
      VARIABLE=STDVOL-FLOW UOM="l/hr"
   DEFINE MASS2SOL STREAM-VAR STREAM="B2.2-20"  &
      SUBSTREAM=CISOLID VARIABLE=MASS-FLOW UOM="kg/hr"
   DEFINE VOL2SOL STREAM-VAR STREAM="B2.2-20" SUBSTREAM=CISOLID  &
      VARIABLE=STDVOL-FLOW UOM="l/hr"
   DEFINE C PARAMETER 33 PHYS-QTY=USR-DUMMY0
   DEFINE M PARAMETER 34 PHYS-QTY=USR-DUMMY0
F    CG=G3*1000/VOL3
F    MASS2=MASS2MIX+MASS2SOL
F    VOL2=(VOL2MIX+VOL2SOL)
F    DENS2= MASS2/ VOL2
F    wt=RATIORR*100
F
c ==============VALUES FOR H2SO4 ==============
F    a1=0.2224
F    b1=0.4858
F    c1=1.0071
F    d1=1.4986
c     M=a1*wt+b1
c     C=c1*wt+d1
F
c ==============VALUES FOR AMD==============
F    a2=0.2432
F    b2=0.3535
F    c2=0.3625
F    d2=1.2735
F    M=a2*wt+b2
F    C=c2*wt+d2
F
F
F    BATT=EXP((CG-C)/M)
```

```
F
F    BATS=BATT *MASS2
F    BATVOL = BATS/DENS2
F    HYDVOL=BATVOL*1.1*204/168/1000
   READ-VARS G3 VOL3 GPROD RATIORR MASS2MIX VOL2MIX MASS2SOL  &
      VOL2SOL
   WRITE-VARS HYDVOL BATT CG C M

CALCULATOR TOTVOL
   IN-UNITS MET ENTHALPY-FLO='MMkcal/hr' TEMPERATURE=C  &
      HEAT=MMkcal HEAT-FLUX='Gcal/hr-m'
   DEFINE HYDVOL PARAMETER 1 PHYS-QTY=VOLUME UOM="cum"
   DEFINE FERMVOL PARAMETER 3 PHYS-QTY=VOLUME UOM="cum"
   DEFINE TOTVOL PARAMETER 5 PHYS-QTY=VOLUME UOM="cum"
   DEFINE PREVOL PARAMETER 61 PHYS-QTY=VOLUME UOM="cum"
F    TOTVOL=HYDVOL+FERMVOL

   READ-VARS HYDVOL FERMVOL PREVOL
   WRITE-VARS TOTVOL


CONV-OPTIONS
   PARAM TOL=.00010 CHECKSEQ=NO VARITERHIST=NO
   WEGSTEIN MAXIT=100 QMAX=.50
   SECANT BRACKET=YES

REPORT REPORT

;              NODESCRIPTION
;
;  NODESCRIPTION Eliminates the Convergence Summary, but also gets rid of th
;              flowsheet connectivity
;
;
; Use EXCL-STREAMS = or INCL-STREAMS = to reduce the number of blocks report
; With Ion Exchange need to eliminate 10 streams from the report
;  EXCL-STREAMS = 905 909   &
;              922 923

STREAM-REPOR NOZEROFLOW MOLEFLOW MASSFLOW MOLEFRAC MASSFRAC  &
      NOATTR-DESC NOSUBS-ATTR PROPERTIES=FRAC COMP1 COMP2 HREF  &
      COD CSOL CLIQ

FLOWSHEET-RE NOTOTBAL NOCOMPBAL

;REPORT NOPROPERTIES

PROPERTY-REP PARAMS PCES NOPARAM-PLUS
;
```

D.2. SSF Input Summary

```
;Input Summary created by Aspen Plus Rel. 30.0 at 10:55:22 Wed Oct 30, 2019
;Directory C:\Users\1474213.STUDENTS\Desktop\SHF - SSF aspen models v1\Main Files\168hrs  Filename
C:\Users\147421~1.STU\AppData\Local\Temp\~ap12cc.txt
;



TITLE 'A-SSF : Bioethanol Production With AMD Pretreated Biomass'

;

IN-UNITS MET ENTHALPY='J/kg' ENTROPY='J/kg-K' VOLUME-FLOW=ACFM  &
      ENTHALPY-FLO='MJ/hr' MOLE-HEAT-CA='J/kmol-K'  &
      HEAT-TRANS-C='J/sec-sqm-K' ENERGY-PRICE='$/kJ'  &
      MOLE-ENTHALP='J/kmol' MASS-ENTHALP='J/kg'  &
      MOLE-ENTROPY='J/kmol-K' MASS-ENTROPY='J/kg-K'  &
      MASS-HEAT-CA='J/kg-K' UA='J/sec-K' HEAT=kJ  &
      VOL-HEAT-CAP='J/cum-K' HEAT-FLUX='J/sec-m'  &
      INVERSE-HT-C='sec-sqm-K/J' VOL-ENTHALPY='J/cum'

DEF-STREAMS MIXCISLD ALL

DIAGNOSTICS
   HISTORY SYS-LEVEL=4 SIM-LEVEL=4 PROP-LEVEL=2 STREAM-LEVEL=4
   TERMINAL SIM-LEVEL=0 CONV-LEVEL=0 COST-LEVEL=0 PROP-LEVEL=0  &
      ECON-LEVEL=0 STREAM-LEVEL=0 SYS-LEVEL=0
   MAX-PRINT SIM-LIMIT=1000

;

SIM-OPTIONS MASS-BAL-CHE=YES FLASH-TOL=1.0000E-07  &
      PROP-DERIV=NUMERICAL PACK-FLOW=1.0000E-15  &
      PACK-FRAC=1.0000E-15

MODEL-OPTION

SYS-OPTIONS INTERPRET=YES

RUN-CONTROL MAX-TIME=20000.0 MAX-ERRORS=4000 MAX-FORT-ERR=200

;


DATABANKS 'APV84 PURE28' / 'APV84 SOLIDS' / 'APV84 ASPENPCD' /  &
      'NISTV84 NIST-TRC' / 'APV84 POLYMER'

PROP-SOURCES 'APV84 PURE28' / 'APV84 SOLIDS' / 'APV84 ASPENPCD' &
       / 'NISTV84 NIST-TRC' / 'APV84 POLYMER'

;=============================================================================
;                       Components
;=============================================================================
;
```

```
COMPONENTS
   H2O H2O /
   ETHANOL C2H6O-2 /
   GLUCOSE C6H12O6 /
   XYLOSE C5H10O5 /
   EXTRACT C6H12O6 /
   LGNSOL C8H8O3-D1 /
   H2SO4 H2SO4 /
   NH4SO4 "(NH4)2SO4" /
   CO2 CO2 /
   CELLULOS CELLULOSE /
   XYLAN C5H8O4-U /
   LIGNIN C8H8O3-D1 /
   PROTEIN CHONS-U3 /
   ASH CAO /
   ENZYME CHONS-U3

CISOLID-COMPS CELLULOS XYLAN LIGNIN PROTEIN ASH ENZYME

FORMULA XYLAN C5H8O4-U / PROTEIN CHONS-U3 / ENZYME CHONS-U3

COMP-GROUP OTHRSOLS SUBSTREAM=MIXED COMPS=LGNSOL EXTRACT NH4SO4

COMP-GROUP SUGARS SUBSTREAM=MIXED COMPS=GLUCOSE XYLOSE

;

HENRY-COMPS HC CO2

SOLVE
   RUN-MODE MODE=SIM

;
;THIS FLOWSHEET MODELS THE DISTILLATION/DEHYDRATION AREA.
;   BLOCK H506+    IN=596 QH506  OUT=597 QH506EX          ;
;   BLOCK H502     IN=592 QRD502 OUT=593 QH504EX          ;
;   BLOCK H501     IN=594 QRD501 OUT=595 QRD501EX         ;
;     ADDED SEPARATE MIXER AND SPLITTER SO WE CAN SEE TOTAL CONDENSATE
;     VENT SCRUBBER
;     Stream Definitions:  524 WATER, 550 VENT, 551 WASTE WATER
;     PNEUMAPRESS UNIT

FLOWSHEET A500
   HIERARCHY B1
   CONNECT $C-3 IN="B1.1-50" OUT=1-50
   HIERARCHY B2
   CONNECT $C-6 IN=3-80 OUT="B2.3-80"
   CONNECT $C-4 IN=1-50 OUT="B2.1-50"
   CONNECT $C-1 IN="B2.2-80" OUT=2-80
   HIERARCHY B3
   CONNECT $C-5 IN=2-80 OUT="B3.2-80"
   CONNECT $C-2 IN="B3.3-80" OUT=3-80

;
;
```

```
PROPERTIES NRTL HENRY-COMPS=HC
   PROPERTIES NRTL A500 HENRY-COMPS=HC FREE-WATER=STEAM-TA  &
      SOLU-WATER=3 TRUE-COMPS=YES
   PROPERTIES NRTL-HOC
   PROPERTIES SYSOP12

PROP-REPLACE SYSOP12 STEAM-TA

PROP-DATA
   PROP-LIST ATOMNO / NOATOM
   PVAL ENZYME 6 1 8 7 16 / 1. 1.59 0.42 0.24 0.01

PROP-DATA
   PROP-LIST ATOMNO / NOATOM
   PVAL PROTEIN 6 1 8 7 16 / 1. 1.57 0.31 0.29 0.007

PROP-DATA
   PROP-LIST ATOMNO / NOATOM
   PVAL XYLAN 6 1 8 / 5. 8. 4.

STRUCTURES
   STRUCTURES XYLOSE C2 O1 S / C2 C3 S / C3 C4 S / C4  &
      C5 S / C5 C6 S / C6 O1 S / O10 C3 S / C4 O9  &
      S / C5 O8 S / C6 O7 S

PROP-DATA
   PROP-LIST ATOMNO / NOATOM
   PVAL XYLOSE 6 1 8 / 5. 10. 5.

PROP-DATA PCES-1
   IN-UNITS MET TEMPERATURE=C
   PROP-LIST VB / OMEGA / DHVLB / RGYR
   PVAL H2SO4 65.75890000 / -.5549676020 / 13890.79966 /  &
      2.5372000E-10
   PROP-LIST VB / RKTZRA / VLSTD / DGFORM
   PVAL XYLOSE 157.8481910 / .0792980740 / 94.27630000 /  &
      -1.5306678E+5
   PROP-LIST DHVLB / VLSTD / TC
   PVAL PROTEIN 0 / 0.0 / -226.7884
   PVAL XYLAN 0.0 / 0.0 / -244.0887200
   PROP-LIST RKTZRA / VLSTD
   PVAL CELLULOS .2060436120 / 146.9770000
   PVAL ASH .2917660970 / 866.9275910
   PVAL NH4SO4 .2918596200 / 298.9063450
   PVAL GLUCOSE .0715398735 / 152.6100000
   PVAL EXTRACT .0715398735 / 152.6100000
   PVAL LGNSOL .2200963440 / 126.9050000

;
; Use water's dipole moment and radius of gyration,
; these properties are important for the vapor fugacity
; calculation in one block using Hayden & O'Connell.
; These particular components will not be in the vapor
; phase so their values are unimportant.

PROP-DATA PURE-1
   IN-UNITS SI
```

```
   PROP-LIST MUP / RGYR
   PVAL XYLOSE 5.849340E-25 / 6.1500000E-11
   PVAL PROTEIN 5.849340E-25 / 6.1500000E-11

PROP-DATA REVIEW-1
   IN-UNITS MET TEMPERATURE=C
   PROP-LIST DHSFRM / RKTZRA / VLSTD
   PVAL LIGNIN -108247.86 / .2200963440 / 126.9050000

PROP-DATA USRDEF
   IN-UNITS MET TEMPERATURE=K
   PROP-LIST MW / TB / DHSFRM
   PVAL PROTEIN 22.8396 / 0 / -17618
   PVAL XYLAN 132.117 / 0 / -182099.93
   PROP-LIST MW / DHSFRM
   PVAL ENZYME 24.0156 / -17900.07

PROP-DATA USRDEF2
   IN-UNITS MET TEMPERATURE=C
   PROP-LIST DHFORM
   PVAL XYLOSE -216752.65
   PROP-LIST DHSFRM
   PVAL CELLULOS -233200.06

PROP-DATA CPIG-1
   IN-UNITS MET TEMPERATURE=C
   PROP-LIST CPIG
   PVAL XYLOSE 37.26888724 .1399898460 -1.5496537E-4  &
      7.36799009E-8 0.0 0.0 6.850000000 826.8500000  &
      8.605426579 6.32086902E-3 1.500000000

PROP-DATA CPSPO1-1
   IN-UNITS MET MOLE-HEAT-CA='J/kmol-K' TEMPERATURE=K
   PROP-LIST CPSPO1
   PVAL XYLAN -9529.9 547.25 0 0 0 0 298.15
   PVAL LIGNIN 39752.8 498.84 0 0 0 0 298.15
   PVAL ENZYME 35533 0 0 0 0 0 298.15

PROP-DATA DHVLWT-1
   IN-UNITS MET TEMPERATURE=C
   PROP-LIST DHVLWT
   PVAL ASH 71498.34122 3396.850000 .4439946020 -.1498359780  &
      3396.850000
   PVAL XYLAN 0.0 -273.1500000 .3800000000 0.0 -273.1500000
   PVAL LIGNIN 0.0 -273.1500000 .3800000000 0.0 -273.1500000
   PVAL CELLULOS 0 -273.15

PROP-DATA KLDIP-1
   IN-UNITS MET TEMPERATURE=C
   PROP-LIST KLDIP
   PVAL ASH -.6218197112 7.78300188E-4 -2.8775749E-7  &
      4.5627261E-11 -2.727830E-15 3396.850000 5686.650000
   PVAL XYLAN -728.6887817 -11.16357334 -.0641578256  &
      -1.6391764E-4 -1.5706055E-7 -273.1500000 -244.3793328
   PVAL LIGNIN -1177.842559 -17.94273624 -.1025248260  &
      -2.6041378E-4 -2.4805952E-7 -273.1500000 -247.9915656
   PVAL PROTEIN -242.2721830 -3.811665784 -.0225151720  &
```

```
      -5.9168403E-5 -5.8321342E-8 -273.1500000 -227.2520160

PROP-DATA MULAND-1
   IN-UNITS MET TEMPERATURE=K
   PROP-LIST MULAND
   PVAL ASH 74.47732598 -27259.04230 -8.432322050 3670.000000  &
      5959.800000

PROP-DATA MULAND-1
   IN-UNITS MET TEMPERATURE=C
   PROP-LIST MULAND
   PVAL NH4SO4 81.15506718 -12127.32210 -10.25255770  &
      1126.850000 1706.850000
   PVAL CELLULOS 81.25737378 -12127.32210 -10.25255770  &
      1126.850000 1706.850000
   PVAL XYLOSE -15.55079002 7559.999980 -3.0401358E-8  &
      441.8500000 547.1020000

;
; Needed for Tray sizing in RADFRAC

PROP-DATA MULDIP-1
   IN-UNITS MET VOLUME-FLOW='cum/hr' ENTHALPY-FLO='MMkcal/hr'  &
      HEAT-TRANS-C='kcal/hr-sqm-K' PRESSURE=bar TEMPERATURE=C  &
      VOLUME=cum DELTA-T=C HEAD=meter MOLE-DENSITY='kmol/cum'  &
      MASS-DENSITY='kg/cum' MOLE-ENTHALP='kcal/mol'  &
      MASS-ENTHALP='kcal/kg' HEAT=MMkcal MOLE-CONC='mol/l'  &
      PDROP=bar
   PROP-LIST MULDIP
   PVAL PROTEIN -2267.40 138910.0 320.550 0.0 0.0 323.0  &
      418.0

PROP-DATA NATOM-1
   IN-UNITS MET TEMPERATURE=C
   PROP-LIST NATOM
   PVAL XYLAN 5 8 4
   PVAL CELLULOS 6 10 5 0

PROP-DATA PLXANT-1
   IN-UNITS MET TEMPERATURE=C
   PROP-LIST PLXANT
   PVAL ASH 37.52683375 -48457.53140 0.0 0.0 -2.964795110  &
      4.6976791E-24 6.000000000 3396.850000 5746.850000
   PVAL PROTEIN -1E20

PROP-DATA SIGDIP-1
   IN-UNITS MET TEMPERATURE=C
   PROP-LIST SIGDIP
   PVAL ASH 139.2135830 1.222222220 -2.171954E-10  &
      2.3955375E-10 -9.673330E-11 3396.850000 5626.450000
   PVAL XYLOSE 291.3517280 1.222222220 -4.7621659E-9  &
      5.32741828E-9 -2.0439985E-9 441.8500000 599.4616000

PROP-DATA VSPOLY-1
   IN-UNITS MET TEMPERATURE=K MOLE-VOLUME='cum/kmol'
   PROP-LIST VSPOLY
   PVAL XYLAN .0864 0 0 0 0 298.15
```

```
   PVAL ENZYME .0152 0 0 0 0 298.15

PROP-DATA HOCETA-1
   IN-UNITS ENG
   PROP-LIST HOCETA
   BPVAL ETHANOL ETHANOL 1.40
   BPVAL ETHANOL H2O 1.550
   BPVAL ETHANOL CO2 .30
   BPVAL H2O ETHANOL 1.550
   BPVAL H2O H2O 1.70
   BPVAL H2O CO2 .30
   BPVAL CO2 ETHANOL .30
   BPVAL CO2 H2O .30
   BPVAL CO2 CO2 .160

;=============================================================================
;  Henry component parameters (Non-condensible <==> solvent)
;   New Parameters for N2 and O2 taken from version 9.2 to improve
;   the calculations involving these two components.
;=============================================================================
;
;
;  Using ethanol Henry's for FURFURAL & HMF
;

PROP-DATA HENRY-1
   IN-UNITS MET PRESSURE=bar TEMPERATURE=C PDROP=atm
   PROP-LIST HENRY
   BPVAL CO2 ETHANOL 89.583080 -5018.80 -11.8910 0.0 10.0  &
      40.0 0.0
   BPVAL CO2 H2O 181.18610 -8982.0 -25.8460 .0121280  &
      .20000610 74.70 0.0

;
;=============================================================================
; NRTL Binary Parameters generated by Aspen Plus Release 9.1-3
;=============================================================================
;
; Added in W9806C 6/15/98 - "Lit." values from ASPEN 9.2
;

PROP-DATA NRTL-1
   IN-UNITS MET VOLUME-FLOW='cum/hr' ENTHALPY-FLO='MMkcal/hr'  &
      HEAT-TRANS-C='kcal/hr-sqm-K' PRESSURE=bar TEMPERATURE=C  &
      VOLUME=cum DELTA-T=C HEAD=meter MOLE-DENSITY='kmol/cum'  &
      MASS-DENSITY='kg/cum' MOLE-ENTHALP='kcal/mol'  &
      MASS-ENTHALP='kcal/kg' HEAT=MMkcal MOLE-CONC='mol/l'  &
      PDROP=bar
   PROP-LIST NRTL
   BPVAL ETHANOL H2O 0.0 -55.16980 .30310 0.0 0.0 0.0 75.0  &
      100.0
   BPVAL H2O ETHANOL 0.0 670.44420 .30310 0.0 0.0 0.0 75.0  &
      100.0

PROP-SET CLIQ MOLEFLC UNITS='kmol/hr' SUBSTREAM=MIXED

PROP-SET COD CODMX BODMX UNITS='fraction' SUBSTREAM=ALL
```

```
PROP-SET COMP1 MASSFLOW SUBSTREAM=MIXED

PROP-SET COMP2 MASSFLOW SUBSTREAM=CISOLID

PROP-SET CSOL MOLEFLC UNITS='kmol/hr' SUBSTREAM=CISOLID

PROP-SET FRAC MOLEFLOW SUBSTREAM=MIXED PHASE=L V

PROP-SET HREF HFLMX UNITS='MMkcal/hr' SUBSTREAM=ALL  &
      TEMP=298.1500000

;

HIERARCHY B1


SOLVE
   PARAM METHOD=SM
   RUN-MODE MODE=SIM

;
;THIS FLOWSHEET MODELS THE DISTILLATION/DEHYDRATION AREA.
;   BLOCK H506+    IN=596 QH506  OUT=597 QH506EX          ;
;   BLOCK H502     IN=592 QRD502 OUT=593 QH504EX          ;
;   BLOCK H501     IN=594 QRD501 OUT=595 QRD501EX         ;
;     ADDED SEPARATE MIXER AND SPLITTER SO WE CAN SEE TOTAL CONDENSATE
;     VENT SCRUBBER
;     Stream Definitions:  524 WATER, 550 VENT, 551 WASTE WATER
;     PNEUMAPRESS UNIT

FLOWSHEET A500
   BLOCK PRETREAT IN=1-20 1-12 OUT=1-30
   BLOCK PRE-HX IN=1-40 1-10 OUT=1-41 1-11
   BLOCK PRE-HEAT IN=1-11 OUT=1-12
   BLOCK PRE-FILT IN=1-30 OUT=1-50 1-40

PROPERTIES NRTL HENRY-COMPS=HC FREE-WATER=STEAM-TA SOLU-WATER=3  &
      TRUE-COMPS=YES
   PROPERTIES NRTL-HOC / SYSOP12

STREAM 1-10
   SUBSTREAM MIXED TEMP=20. <C> PRES=1. MASS-FLOW=450000.
   MASS-FRAC H2O 0.995 / H2SO4 0.005

STREAM 1-20
   SUBSTREAM CISOLID TEMP=90. <C> PRES=1. MASS-FLOW=90000.
   MASS-FRAC CELLULOS 0.37 / XYLAN 0.29 / LIGNIN 0.25 /  &
      PROTEIN 0.03 / ASH 0.06

BLOCK PRE-HEAT HEATX
   PARAM T-COLD=90. <C> CALC-TYPE=DESIGN U-OPTION=PHASE  &
      F-OPTION=CONSTANT CALC-METHOD=SHORTCUT
   FEEDS COLD=1-11
   OUTLETS-COLD 1-12
   HOT-SIDE DP-OPTION=CONSTANT
   COLD-SIDE DP-OPTION=CONSTANT
```

```
   REFERENCE HOT-UTIL=U-2

BLOCK PRE-HX HEATX
   PARAM T-HOT=30. <C> CALC-TYPE=DESIGN U-OPTION=PHASE  &
      F-OPTION=CONSTANT CALC-METHOD=SHORTCUT
   FEEDS HOT=1-40 COLD=1-10
   OUTLETS-HOT 1-41
   OUTLETS-COLD 1-11
   HOT-SIDE DP-OPTION=CONSTANT
   COLD-SIDE DP-OPTION=CONSTANT

BLOCK PRETREAT RSTOIC
   PARAM TEMP=90. <C> PRES=1.
   STOIC 1 CISOLID XYLAN -1. / MIXED H2O -1. / XYLOSE 1.
   STOIC 2 CISOLID LIGNIN -1. / MIXED LGNSOL 1.
   CONV 1 CISOLID XYLAN 0.637249
   CONV 2 CISOLID LIGNIN 0.24

BLOCK PRE-FILT SSPLIT
   FRAC CISOLID 1-50 1.
   FRAC MIXED 1-40 1.

ENDHIERARCHY B1

HIERARCHY B2


SOLVE
   PARAM METHOD=SM
   RUN-MODE MODE=SIM

;
;THIS FLOWSHEET MODELS THE DISTILLATION/DEHYDRATION AREA.
;   BLOCK H506+    IN=596 QH506  OUT=597 QH506EX          ;
;   BLOCK H502     IN=592 QRD502 OUT=593 QH504EX          ;
;   BLOCK H501     IN=594 QRD501 OUT=595 QRD501EX         ;
;     ADDED SEPARATE MIXER AND SPLITTER SO WE CAN SEE TOTAL CONDENSATE
;     VENT SCRUBBER
;     Stream Definitions:  524 WATER, 550 VENT, 551 WASTE WATER
;     PNEUMAPRESS UNIT

FLOWSHEET A500
   BLOCK FILTER IN=2-70 OUT=2-90 2-80
   BLOCK FERMENT IN=2-40 OUT=2-50
   BLOCK HYDROLYS IN=2-30 OUT=2-40
   BLOCK CO2FLASH IN=2-50 OUT=2-60 2-70
   BLOCK WATERMIX IN=2-10 3-80 OUT=2-20
   BLOCK FEEDMIX IN=2-21 1-50 OUT=2-30
   BLOCK FEEDCHIL IN=2-20 OUT=2-21

PROPERTIES NRTL HENRY-COMPS=HC FREE-WATER=STEAM-TA SOLU-WATER=3  &
      TRUE-COMPS=YES
   PROPERTIES NRTL-HOC / SYSOP12

STREAM 2-10
   SUBSTREAM MIXED TEMP=293.1500000 PRES=1. MASS-FLOW=45546.
   MASS-FRAC H2O 1.
```

```
BLOCK FEEDMIX MIXER
   PARAM

BLOCK WATERMIX MIXER
   PARAM PRES=1.

BLOCK CO2FLASH FLASH2
   PARAM TEMP=311.1500000 PRES=1.

BLOCK FEEDCHIL HEATX
   PARAM T-HOT=35. <C> CALC-TYPE=DESIGN U-OPTION=PHASE  &
      F-OPTION=CONSTANT CALC-METHOD=SHORTCUT
   FEEDS HOT=2-20
   OUTLETS-HOT 2-21
   HOT-SIDE DP-OPTION=CONSTANT
   COLD-SIDE DP-OPTION=CONSTANT
   REFERENCE COLD-UTIL=U-1

BLOCK FERMENT RSTOIC
   PARAM TEMP=311.1500000 PRES=1. HEAT-OF-REAC=YES
   STOIC 1 MIXED GLUCOSE -1. / ETHANOL 2. / CO2 2.
   CONV 1 MIXED GLUCOSE 0.85
   HEAT-RXN REACNO=1 CID=GLUCOSE

BLOCK HYDROLYS RSTOIC
   PARAM TEMP=311.1500000 PRES=1. HEAT-OF-REAC=YES
   STOIC 1 CISOLID CELLULOS -1. / MIXED H2O -1. / GLUCOSE  &
      1.
   CONV 1 CISOLID CELLULOS 0.3
   HEAT-RXN REACNO=1 CID=CELLULOS

BLOCK FILTER SSPLIT
   FRAC CISOLID 2-90 1.
   FRAC MIXED 2-80 0.95

ENDHIERARCHY B2

HIERARCHY B3


SOLVE
   PARAM METHOD=SM
   RUN-MODE MODE=SIM

;
;THIS FLOWSHEET MODELS THE DISTILLATION/DEHYDRATION AREA.
;    BLOCK H506+    IN=596 QH506  OUT=597 QH506EX          ;
;    BLOCK H502     IN=592 QRD502 OUT=593 QH504EX          ;
;    BLOCK H501     IN=594 QRD501 OUT=595 QRD501EX         ;
;      ADDED SEPARATE MIXER AND SPLITTER SO WE CAN SEE TOTAL CONDENSATE
;      VENT SCRUBBER
;      Stream Definitions:  524 WATER, 550 VENT, 551 WASTE WATER
;      PNEUMAPRESS UNIT

FLOWSHEET A500
   HIERARCHY B10
```

```
   CONNECT $C-3 IN=H-1 OUT="B10.H-1"
   CONNECT $C-4 IN=H-3 OUT="B10.H-3"
   CONNECT $C-1 IN=H-4 OUT="B10.H-4"
   CONNECT $C-2 IN=H-2 OUT="B10.H-2"
   BLOCK BEERCOL IN=3-20 OUT=3-40 3-30 H-1 H-4
   BLOCK CO2REMOV IN=2-80 OUT=3-20 3-10
   BLOCK RECTCOL IN=3-40 OUT=3-60 3-50 H-3 H-2
   BLOCK R-MIX IN=3-30 3-50 OUT=3-70
   BLOCK R-PURGE IN=3-70 OUT=3-90 3-80

PROPERTIES NRTL HENRY-COMPS=HC FREE-WATER=STEAM-TA SOLU-WATER=3  &
      TRUE-COMPS=YES
   PROPERTIES NRTL-HOC / SYSOP12

DEF-STREAMS HEAT H-1

DEF-STREAMS HEAT H-2

DEF-STREAMS HEAT H-3

DEF-STREAMS HEAT H-4

BLOCK R-MIX MIXER
   PARAM

BLOCK R-PURGE FSPLIT
   FRAC 3-90 0.1

BLOCK CO2REMOV SEP
   PARAM
   FRAC STREAM=3-10 SUBSTREAM=MIXED COMPS=H2O ETHANOL  &
      GLUCOSE CO2 FRACS=0. 0. 0. 1.

BLOCK BEERCOL DSTWU
   PARAM LIGHTKEY=ETHANOL RECOVL=0.95 HEAVYKEY=H2O  &
      RECOVH=0.002 PTOP=1. PBOT=1. RR=-1.1 PLOT=YES

BLOCK RECTCOL DSTWU
   PARAM LIGHTKEY=ETHANOL RECOVL=0.95 HEAVYKEY=H2O RECOVH=0.1  &
      PTOP=1. PBOT=1. RR=-1.1 PLOT=YES
   PLOT LOWER=10 UPPER=40

HIERARCHY B10

CLIST-REF COMLIST=GLOBAL


SOLVE
   PARAM METHOD=SM
   RUN-MODE MODE=SIM

;
;THIS FLOWSHEET MODELS THE DISTILLATION/DEHYDRATION AREA.
;   BLOCK H506+    IN=596 QH506  OUT=597 QH506EX          ;
;   BLOCK H502     IN=592 QRD502 OUT=593 QH504EX          ;
;   BLOCK H501     IN=594 QRD501 OUT=595 QRD501EX         ;
;     ADDED SEPARATE MIXER AND SPLITTER SO WE CAN SEE TOTAL CONDENSATE
```

```
;     VENT SCRUBBER
;     Stream Definitions:  524 WATER, 550 VENT, 551 WASTE WATER
;     PNEUMAPRESS UNIT

FLOWSHEET A500
   BLOCK B1 IN=H-1 H-3 OUT=S9
   BLOCK B8 IN=S3 S9 OUT=S4
   BLOCK B9 IN=S4 OUT=S6
   BLOCK B4 IN=H-4 H-2 OUT=S8
   BLOCK B10 IN=S12 S8 OUT=S13
   BLOCK B11 IN=S13 OUT=S14

PROPERTIES NRTL HENRY-COMPS=HC FREE-WATER=STEAM-TA SOLU-WATER=3  &
      TRUE-COMPS=YES
   PROPERTIES NRTL-HOC / SYSOP12

STREAM S3
   SUBSTREAM MIXED TEMP=338.1500000 PRES=1. MOLE-FLOW=100000.
   MOLE-FRAC H2O 1.

STREAM S12
   SUBSTREAM MIXED TEMP=368.1500000 PRES=1. MOLE-FLOW=100000.
   MASS-FRAC H2O 1.

DEF-STREAMS HEAT H-1

DEF-STREAMS HEAT H-2

DEF-STREAMS HEAT H-3

DEF-STREAMS HEAT H-4

DEF-STREAMS HEAT S8

DEF-STREAMS HEAT S9

BLOCK B1 MIXER

BLOCK B4 MIXER

BLOCK B8 HEATER
   PARAM PRES=1.

BLOCK B10 HEATER
   PARAM PRES=1.

BLOCK B9 HEATX
   PARAM T-HOT=65. <C> CALC-TYPE=DESIGN U-OPTION=PHASE  &
      F-OPTION=CONSTANT CALC-METHOD=SHORTCUT
   FEEDS HOT=S4
   OUTLETS-HOT S6
   HOT-SIDE DP-OPTION=CONSTANT
   COLD-SIDE DP-OPTION=CONSTANT
   REFERENCE COLD-UTIL=U-1

BLOCK B11 HEATX
   PARAM T-COLD=95. <C> CALC-TYPE=DESIGN U-OPTION=PHASE  &
```

```
      F-OPTION=CONSTANT CALC-METHOD=SHORTCUT
   FEEDS COLD=S13
   OUTLETS-COLD S14
   HOT-SIDE DP-OPTION=CONSTANT
   COLD-SIDE DP-OPTION=CONSTANT
   REFERENCE HOT-UTIL=U-2

ENDHIERARCHY B10

ENDHIERARCHY B3

STREAM-PRICE
   STREAM-PRICE STREAM="B3.3-60" MASS-PRICE=.8150000000 /  &
      STREAM="B3.3-60" MASS-PRICE=.8150000000

UTILITY U-1 GENERAL
   DESCRIPTION "Cooling Water, Inlet Temp=20 C, Outlet Temp=25 C"
   COST ENERGY-PRICE=1.1E-006
   PARAM UTILITY-TYPE=WATER PRES=1. PRES-OUT=1. TIN=303.1500000  &
      TOUT=318.1500000 CALOPT=FLASH MIN-TAPP=5.000000000  &
      HTC=3750.000000

UTILITY U-2 GENERAL
   DESCRIPTION  &
      "Low Pressure Steam, Inlet Temp=125 C, Outlet Temp=124 C"
   COST ENERGY-PRICE=6.2E-006
   PARAM UTILITY-TYPE=STEAM TIN=398.1500000 TOUT=397.1500000  &
      VFRAC=1. VFR-OUT=0. CALOPT=FLASH MIN-TAPP=10.00000000  &
      CALCCO2=YES FACTORSOURCE="US-EPA-Rule-E9-5711" FUELSOURCE= &
      "Natural_gas" CO2FACTOR=2.34000000E-7 EFFICIENCY=0.85  &
      HTC=6000.000000

UTILITY U-3 GENERAL
   DESCRIPTION "Cooling Water, Inlet Temp=20 C, Outlet Temp=25 C"
   COST ENERGY-PRICE=5.1E-006
   PARAM UTILITY-TYPE=WATER PRES=1.000000000  &
      PRES-OUT=1.000000000 TIN=293.1500000 TOUT=303.1500000  &
      CALOPT=FLASH MIN-TAPP=5.000000000 HTC=3750.000000

DESIGN-SPEC DS-1
   DEFINE BATT PARAMETER 33 PHYS-QTY=USR-DUMMY0
   SPEC "BATT" TO "168"
   TOL-SPEC "0.10"
   VARY BLOCK-VAR BLOCK="B2.HYDROLYS" VARIABLE=CONV  &
      SENTENCE=CONV ID1=1
   LIMITS "0.01" "1"

DESIGN-SPEC DS-2
   DEFINE ETOHFINA MASS-FRAC STREAM="B3.3-40" SUBSTREAM=MIXED  &
      COMPONENT=ETHANOL
   SPEC "ETOHFINA" TO "0.34"
   TOL-SPEC "0.001"
   VARY BLOCK-VAR BLOCK="B3.BEERCOL" VARIABLE=RECOVH  &
      SENTENCE=PARAM
   LIMITS "0.0001" "0.1"

DESIGN-SPEC DS-3
```

```
   DEFINE ETOHFIN MASS-FRAC STREAM="B3.3-60" SUBSTREAM=MIXED  &
      COMPONENT=ETHANOL
   SPEC "ETOHFIN" TO "0.9"
   TOL-SPEC "0.0001"
   VARY BLOCK-VAR BLOCK="B3.RECTCOL" VARIABLE=RECOVH  &
      SENTENCE=PARAM
   LIMITS "0.01" "0.2"

DESIGN-SPEC DS-4
   DEFINE FEEDH2O MASS-FLOW STREAM="B2.2-30" SUBSTREAM=MIXED  &
      COMPONENT=H2O UOM="kg/hr"
   SPEC "FEEDH2O" TO "339839"
   TOL-SPEC "1"
   VARY STREAM-VAR STREAM="B2.2-10" SUBSTREAM=MIXED  &
      VARIABLE=MASS-FLOW UOM="kg/hr"
   LIMITS "0" "400000"

EO-CONV-OPTI

CALCULATOR FERMVOL
   IN-UNITS MET ENTHALPY-FLO='MMkcal/hr' TEMPERATURE=C  &
      HEAT=MMkcal HEAT-FLUX='Gcal/hr-m'
   DEFINE E4 MASS-FLOW STREAM="B2.2-50" SUBSTREAM=MIXED  &
      COMPONENT=ETHANOL UOM="kg/hr"
   DEFINE FERMVOL PARAMETER 1 PHYS-QTY=VOLUME UOM="cum"
   DEFINE EFERMVOL PARAMETER 2 PHYS-QTY=USR-DUMMY0 UOM= &
      "base-units"
   DEFINE ETOHPROD PARAMETER 3 PHYS-QTY=USR-DUMMY0 UOM= &
      "base-units" INIT-VAL=0.5
   DEFINE RATIORR PARAMETER 20 PHYS-QTY=USR-DUMMY0 UOM= &
      "base-units" INIT-VAL=0.2
   DEFINE BATT PARAMETER 33 PHYS-QTY=USR-DUMMY0
   DEFINE VOL2SOL STREAM-VAR STREAM="B2.2-30" SUBSTREAM=CISOLID  &
      VARIABLE=STDVOL-FLOW UOM="l/hr"
   DEFINE MASS2SOL STREAM-VAR STREAM="B2.2-30"  &
      SUBSTREAM=CISOLID VARIABLE=MASS-FLOW UOM="kg/hr"
   DEFINE VOL2MIX STREAM-VAR STREAM="B2.2-30" SUBSTREAM=MIXED  &
      VARIABLE=STDVOL-FLOW UOM="l/hr"
   DEFINE MASS2MIX STREAM-VAR STREAM="B2.2-30" SUBSTREAM=MIXED  &
      VARIABLE=MASS-FLOW UOM="kg/hr"
   DEFINE VOL4 STREAM-VAR STREAM="B2.2-50" SUBSTREAM=MIXED  &
      VARIABLE=STDVOL-FLOW UOM="l/hr"
   DEFINE CE PARAMETER 41 PHYS-QTY=USR-DUMMY0
F    CE=E4*1000/VOL4
F    MASS2=MASS2MIX+MASS2SOL
F    VOL2=(VOL2MIX+VOL2SOL)
F    DENS2= MASS2/ VOL2
F
F    wt=RATIORR*100
F
c ==========VALUES FOR H2SO4 ==================
F    a1=0.1437
F    b1=0.0135
F    c1=1.8872
F    d1=-1.4286
c     M=a1*wt+b1
c     C=c1*ALOG(wt)+d1
```

```
F
c ==========VALUES FOR AMD=================
F    a2=0.0973
F    b2=0.0865
F    c2=1.3983
F    d2=-0.8637
F    M=a2*wt+b2
F    C=c2*ALOG(wt)+d2
F
F
F    BATT=EXP((CE-C)/M)
F
F    BATS=BATT*MASS2
F    BATVOL=BATS/DENS2
F    FERMVOL=BATVOL * 1.1 * 204/168/1000
   READ-VARS E4 ETOHPROD RATIORR VOL2SOL MASS2SOL VOL2MIX  &
      MASS2MIX VOL4
   WRITE-VARS EFERMVOL FERMVOL BATT CE

CALCULATOR PRETREA
   DEFINE VOL11MIX STREAM-VAR STREAM="B1.1-10" SUBSTREAM=MIXED  &
      VARIABLE=STDVOL-FLOW UOM="l/hr"
   DEFINE VOL12SOL STREAM-VAR STREAM="B1.1-20"  &
      SUBSTREAM=CISOLID VARIABLE=STDVOL-FLOW UOM="l/hr"
   DEFINE MAS11MIX STREAM-VAR STREAM="B1.1-10" SUBSTREAM=MIXED  &
      VARIABLE=MASS-FLOW UOM="kg/hr"
   DEFINE MAS12SOL STREAM-VAR STREAM="B1.1-20"  &
      SUBSTREAM=CISOLID VARIABLE=MASS-FLOW UOM="kg/hr"
   DEFINE PREVOL PARAMETER 61 PHYS-QTY=VOLUME UOM="cum"
F    MASS=MAS11MIX+MAS12SOL
F    VOL=VOL11MIX+VOL12SOL
F    t=3.5
F    T=t*24
F    PREVOL=T*VOL*1.1*(T+24)/T/1000
F
   READ-VARS VOL11MIX VOL12SOL MAS11MIX MAS12SOL
   WRITE-VARS PREVOL


CONV-OPTIONS
   PARAM TOL=.00010 CHECKSEQ=NO VARITERHIST=NO
   WEGSTEIN MAXIT=100 QMAX=.50
   SECANT BRACKET=YES

;              NODESCRIPTION
;
;  NODESCRIPTION Eliminates the Convergence Summary, but also gets rid of th
;             flowsheet connectivity
;
; Use EXCL-STREAMS = or INCL-STREAMS = to reduce the number of blocks report
; With Ion Exchange need to eliminate 10 streams from the report
;  EXCL-STREAMS = 905 909   &
;              922 923

STREAM-REPOR REPORT SORT MOLEFLOW MASSFLOW MOLEFRAC MASSFRAC  &
      NOATTR-DESC NOSUBS-ATTR PROPERTIES=FRAC COMP1 COMP2 HREF  &
      COD CSOL CLIQ
```

```
FLOWSHEET-RE NOTOTBAL NOCOMPBAL

;REPORT NOPROPERTIES

PROPERTY-REP PARAMS PCES NOPARAM-PLUS

REACTIONS R-1 GENERAL
   REAC-DATA 1 NAME=HYDROLYS REAC-CLASS=POWERLAW PHASE=LS  &
      STATUS=ON CBASIS=MASSCONC RBASIS=REAC-VOL RATE-UNITV= &
      "KMOL/CUM-HR"
   RATE-CON 1 PRE-EXP=1E+020 ACT-ENERGY=0.0 TEMP-EXPONEN=0.
   STOIC 1 CISOLID CELLULOS -1. / MIXED H2O -1. / GLUCOSE  &
      1.
   REAC-ACT 1
```

Appendix E: Supplementary Data for Chapter 8

E.1. Full Stream Table for Aspen Plus™ Model (Remediation of AMD Using Sulfate-reducing Bacteria)

		1	2	3	3-1	4	5	6	7	8	9	10
From				MIX	HX1	BIOREACT	FLASH	PRECIP	RECYCLE	FLASH	PRECIP	RECYCLE
To		MIX	MIX	HX1	BIOREACT	FLASH	PRECIP	RECYCLE	MIX			
Temperature K		303.1	293.1	303.6	308.1	308.1	308.1	308.1	308.1	308.1	308.1	308.1
Mass Flow	KG/HR	472032	1626030	5805060	5805060	5805060	5783400	5768190	3707000	21664.28	15208.82	2061190
Component Mass Flow												
H2O	KG/HR	444958.4	1595300	5726360	5726390	5735440	5734910	5734910	3685610	529.631		2049300
H3O+	KG/HR	124.089	536.667	542.67	503.784	0.394	0.394	0.394	0.253			0.141
XYLOSE	KG/HR	18295.17		23848.9	23848.9	8641.753	8641.753	8641.753	5553.729	< 0.001		3088.024
CO2	KG/HR			4558.835	4558.72	25532.21	5778.256	5778.256	3713.467	19753.96		2064.789
HCO3-	KG/HR			1.297	1.456	1825.718	1825.704	1825.704	1173.311			652.393
CO3--	KG/HR			trace	trace	0.078	0.078	0.078	0.05			0.028
H2SO4	KG/HR	trace	trace	trace	trace	trace	trace	trace	trace	trace		trace
HSO4-	KG/HR	1455.967	4564.248	4558.45	4757.235	2.034	2.034	2.034	1.307			0.727
SO4--	KG/HR	4786.695	17396.24	30604.8	30408.08	10787.42	10787.42	10787.42	6932.665			3854.75
S--	KG/HR			trace	trace	trace	trace	trace	trace			trace
H2S	KG/HR			844.929	844.919	2617.474	1236.775	1236.775	794.829	1380.69		441.946
HS-	KG/HR			0.042	0.052	75.71	75.718	75.718	48.661			27.057
FE2+	KG/HR	1756.345	6139.39	9781.615	9781.578	2881.174	2881.175	2881.175	1851.623			1029.553
FE+++	KG/HR											
FES	KG/HR					10778.76	10778.76				10778.76	
FEOH+	KG/HR	0.005	0.007	0.104	0.152	69.684	69.682	69.682	44.782			24.9
FE(OH)3-	KG/HR	trace	trace	trace	trace	trace	trace	trace	trace			trace
OH-	KG/HR	trace	trace	trace	trace	0.001	0.001	0.001	0.001			< 0.001
CA++	KG/HR	225.131	847.208	1605.46	1605.46	802.73	802.73	802.73	515.884			286.846
CALCI-01	KG/HR					1445.026	1445.026				1445.026	
AL+++	KG/HR	162.124	566.713	1073.923	1073.923	536.961	536.961	536.961	345.085			191.877
ALUMI-01	KG/HR					1494.274	1494.274				1494.274	
MG++	KG/HR	194.058	678.339	1285.453	1285.453	642.726	642.726	642.726	413.056			229.67
MAGNE-02	KG/HR					1490.754	1490.754				1490.754	
MGOH+	KG/HR	trace	trace	trace	trace	0.001	0.001	0.001	0.001			0.001
CAOH+	KG/HR	trace	trace	trace	trace	< 0.001	< 0.001	< 0.001	< 0.001			< 0.001
SALT13	KG/HR	74.052										

		1	2	3	3-1	4	5	6	7	8	9	10
From				MIX	HX1	BIOREACT	FLASH	PRECIP	RECYCLE	FLASH	PRECIP	RECYCLE
To		MIX	MIX	HX1	BIOREACT	FLASH	PRECIP	RECYCLE	MIX			
Temperature K		303.1	293.1	303.6	308.1	308.1	308.1	308.1	308.1	308.1	308.1	308.1
Mass Flow	KG/HR	472032	1626030	5805060	5805060	5805060	5783400	5768190	3707000	21664.28	15208.82	2061190
Component Mass Fraction												
H2O		0.943	0.981	0.986	0.986	0.988	0.992	0.994	0.994	0.024		0.994
H3O+		263 PPM	330 PPM	93 PPM	87 PPM	68 PPB	68 PPB	68 PPB	68 PPB			68 PPB
XYLOSE		0.039		0.004	0.004	0.001	0.001	0.001	0.001	trace		0.001
CO2				785 PPM	785 PPM	0.004	999 PPM	0.001	0.001	0.912		0.001
HCO3-				223 PPB	251 PPB	315 PPM	316 PPM	317 PPM	317 PPM			317 PPM
CO3--				trace	trace	14 PPB	14 PPB	14 PPB	14 PPB			14 PPB
H2SO4		trace	trace	trace	trace	trace	trace	trace	trace	trace		trace
HSO4-		0.003	0.003	785 PPM	819 PPM	350 PPB	352 PPB	353 PPB	353 PPB			353 PPB
SO4--		0.01	0.011	0.005	0.005	0.002	0.002	0.002	0.002			0.002
S--				trace	trace	trace	trace	trace	trace			trace
H2S				146 PPM	146 PPM	451 PPM	214 PPM	214 PPM	214 PPM	0.064		214 PPM
HS-				7 PPB	9 PPB	13 PPM	13 PPM	13 PPM	13 PPM			13 PPM
FE2+		0.004	0.004	0.002	0.002	496 PPM	498 PPM	499 PPM	499 PPM			499 PPM
FE+++												
FES						0.002	0.002				0.709	
FEOH+		11 PPB	4 PPB	18 PPB	26 PPB	12 PPM	12 PPM	12 PPM	12 PPM			12 PPM
FE(OH)3-		trace	trace	trace	trace	trace	trace	trace	trace			trace
OH-		trace	trace	trace	trace	trace	trace	trace	trace			trace
CA++		477 PPM	521 PPM	277 PPM	277 PPM	138 PPM	139 PPM	139 PPM	139 PPM			139 PPM
CALCI-01						249 PPM	250 PPM				0.095	
AL+++		343 PPM	349 PPM	185 PPM	185 PPM	92 PPM	93 PPM	93 PPM	93 PPM			93 PPM
ALUMI-01						257 PPM	258 PPM				0.098	
MG++		411 PPM	417 PPM	221 PPM	221 PPM	111 PPM	111 PPM	111 PPM	111 PPM			111 PPM
MAGNE-02						257 PPM	258 PPM				0.098	
MGOH+		trace	trace	trace	trace	trace	trace	trace	trace			trace
CAOH+		trace	trace	trace	trace	trace	trace	trace	trace			trace
SALT13		157 PPM										

		1	2	3	3-1	4	5	6	7	8	9	10
From				MIX	HX1	BIOREACT	FLASH	PRECIP	RECYCLE	FLASH	PRECIP	RECYCLE
To		MIX	MIX	HX1	BIOREACT	FLASH	PRECIP	RECYCLE	MIX			
Temperature K		303.1	293.1	303.6	308.1	308.1	308.1	308.1	308.1	308.1	308.1	308.1
Mass Flow	KG/HR	472032	1626030	5805060	5805060	5805060	5783400	5768190	3707000	21664.28	15208.82	2061190
Component Mole Flow												
H2O	KMOL/HR	24698.94	88552.82	317861.1	317863.1	318365.2	318335.8	318335.8	204582.4	29.399		113753.4
H3O+	KMOL/HR	6.523	28.212	28.528	26.483	0.021	0.021	0.021	0.013			0.007
XYLOSE	KMOL/HR	121.861		158.853	158.853	57.561	57.561	57.561	36.992	trace		20.569
CO2	KMOL/HR			103.587	103.584	580.148	131.295	131.295	84.378	448.854		46.917
HCO3-	KMOL/HR			0.021	0.024	29.921	29.921	29.921	19.229			10.692
CO3--	KMOL/HR			trace	trace	0.001	0.001	0.001	0.001			< 0.001
H2SO4	KMOL/HR	trace	trace	trace	trace	trace	trace	trace	trace	trace		trace
HSO4-	KMOL/HR	14.999	47.019	46.959	49.007	0.021	0.021	0.021	0.013			0.007
SO4--	KMOL/HR	49.828	181.089	318.585	316.537	112.293	112.293	112.293	72.167			40.127
S--	KMOL/HR			trace	trace	trace	trace	trace	trace			trace
H2S	KMOL/HR			24.791	24.791	76.8	36.288	36.288	23.321	40.511		12.967
HS-	KMOL/HR			0.001	0.002	2.289	2.289	2.289	1.471			0.818
FE2+	KMOL/HR	31.45	109.934	175.154	175.153	51.592	51.592	51.592	33.156			18.436
FE+++	KMOL/HR											
FES	KMOL/HR					122.607	122.607				122.607	
FEOH+	KMOL/HR	< 0.001	< 0.001	0.001	0.002	0.956	0.956	0.956	0.615			0.342
FE(OH)3-	KMOL/HR	trace	trace	trace	trace	trace	trace	trace	trace			trace
OH-	KMOL/HR	trace	trace	trace	trace	< 0.001	< 0.001	< 0.001	< 0.001			< 0.001
CA++	KMOL/HR	5.617	21.14	40.059	40.059	20.03	20.03	20.03	12.872			7.157
CALCI-01	KMOL/HR					20.03	20.03				20.03	
AL+++	KMOL/HR	6.009	21.005	39.805	39.805	19.902	19.902	19.902	12.79			7.112
ALUMI-01	KMOL/HR					9.951	9.951				9.951	
MG++	KMOL/HR	7.985	27.911	52.891	52.891	26.445	26.445	26.445	16.995			9.45
MAGNE-02	KMOL/HR					26.445	26.445				26.445	
MGOH+	KMOL/HR	trace	trace	trace	trace	< 0.001	< 0.001	< 0.001	< 0.001			< 0.001
CAOH+	KMOL/HR	trace	trace	trace	trace	trace	trace	trace	trace			trace
SALT13	KMOL/HR	0.43										

Appendix F: Aspen Plus™ Input Summary for Simulation Used in Chapter 8

```
;
;Input Summary created by Aspen Plus Rel. 30.0 at 11:08:54 Wed Oct 30, 2019
;Directory C:\Users\1474213.STUDENTS\Desktop\SHF - SSF aspen models v1\Main Files\SRB  Filename
C:\Users\147421~1.STU\AppData\Local\Temp\~ap77e0.txt
;


DYNAMICS
   DYNAMICS RESULTS=ON

IN-UNITS MET

DEF-STREAMS CONVEN ALL

SIM-OPTIONS MASS-BAL-CHE=YES

DESCRIPTION "
   Electrolytes Simulation with English Units :
   F, psi, lb/hr, lbmol/hr, Btu/hr, cuft/hr.

   Property Method: ELECNRTL

   Flow basis for input: Mass

   Stream report composition: Mass flow
   "

DATABANKS 'APV84 ASPENPCD' / 'APV84 AQUEOUS' / 'APV84 SOLIDS' &
       / 'APV84 INORGANIC' / 'NISTV84 NIST-TRC' /  &
      'APV84 ELECPURE' / 'APV84 PURE28'

PROP-SOURCES 'APV84 ASPENPCD' / 'APV84 AQUEOUS' / 'APV84 SOLIDS' &
       / 'APV84 INORGANIC' / 'NISTV84 NIST-TRC' /  &
      'APV84 ELECPURE' / 'APV84 PURE28'

COMPONENTS
   H2O H2O /
   H3O+ H3O+ /
   XYLOSE C5H10O5 /
   CO2 CO2 /
   HCO3- HCO3- /
   CO3-- CO3-2 /
   H2SO4 H2SO4 /
   HSO4- HSO4- /
   SO4-- SO4-2 /
   S-- S-2 /
   H2S H2S /
   HS- HS- /
   IRON FE /
   FE2+ FE+2 /
   FE+++ FE+3 /
   FES FES /
```

```
   O2 O2 /
   FEO FEO /
   FE2O3 FE2O3 /
   MAGNE-01 FE3O4 /
   IRON--01 "FE(OH)2" /
   "FEO(O-01" FEO2H /
   "FE2(OH)2" "FE2(OH)2+4" /
   FEOH++ FEOH+2 /
   "FE(OH)2+" "FE(OH)2+" /
   FEOH+ FEOH+ /
   "IRON-(S)" "FE(OH)2" /
   SALT1 "FE(OH)3" /
   "FESO4(S)" FESO4 /
   SALT2 "FESO4*7W" /
   SALT3 "FESO4*4W" /
   SALT4 "FESO4*W" /
   "FE(OH)3-" "FE(OH)3-" /
   OH- OH- /
   CA++ CA+2 /
   CALCI-01 CAS /
   AL+++ AL+3 /
   ALUMI-01 AL2S3 /
   MG++ MG+2 /
   MAGNE-02 MGS /
   MGOH+ MGOH+ /
   CAOH+ CAOH+ /
   "CALCI(S)" "CA(OH)2" /
   "MGSO4(S)" MGSO4 /
   "ALUMI(S)" "AL2(SO4)3" /
   "MAGNE(S)" "MG(OH)2" /
   SALT5 "MGSO4*7W" /
   SALT6 "AL2S3O12*6W" /
   "MGCO3(S)" MGCO3 /
   SALT7 NESQUEHONITE /
   "CACO3(S)" CACO3 /
   SALT8 "MGSO4*6W" /
   SALT9 "MGSO4*W" /
   "CASO4(S)" CASO4 /
   SALT12 "CASO4*1:2W:A" /
   SALT13 "CASO4*2H2O"

CISOLID-COMPS FES "IRON-(S)" SALT1 "FESO4(S)" SALT2 SALT3  &
      SALT4 CALCI-01 ALUMI-01 MAGNE-02 "CALCI(S)" "MGSO4(S)"  &
      "ALUMI(S)" "MAGNE(S)" SALT5 SALT6 "MGCO3(S)" SALT7  &
      "CACO3(S)" SALT8 SALT9 "CASO4(S)" SALT12 SALT13

ADA-SETUP
   ADA-SETUP PROCEDURE=REL9

HENRY-COMPS GLOBAL CO2 H2S O2

SOLVE
   RUN-MODE MODE=SIM

CHEMISTRY GLOBAL
   PARAM GAMMA-BASIS=UNSYMMETRIC
   DISS IRON--01 FEOH+ 1 / OH- 1
```

```
STOIC 1 H2O -4 / FE+++ -2 / "FE2(OH)2" 1 / H3O+ 2
STOIC 2 H2O -2 / FEOH++ -1 / "FE(OH)2+" 1 / H3O+ 1
STOIC 3 H2O -2 / FE+++ -1 / FEOH++ 1 / H3O+ 1
STOIC 4 OH- -3 / FE2+ -1 / "FE(OH)3-" 1
STOIC 5 CAOH+ -1 / CA++ 1 / OH- 1
STOIC 6 MGOH+ -1 / OH- 1 / MG++ 1
STOIC 7 H2O -1 / HSO4- -1 / H3O+ 1 / SO4-- 1
STOIC 8 H2SO4 -1 / H2O -1 / H3O+ 1 / HSO4- 1
STOIC 9 FEOH+ -1 / FE2+ 1 / OH- 1
STOIC 10 H2O -1 / HCO3- -1 / CO3-- 1 / H3O+ 1
STOIC 11 H2O -2 / CO2 -1 / HCO3- 1 / H3O+ 1
STOIC 12 H2O -1 / HS- -1 / H3O+ 1 / S-- 1
STOIC 13 H2O -1 / H2S -1 / H3O+ 1 / HS- 1
STOIC 14 H2O -2 / OH- 1 / H3O+ 1
K-STOIC 1 A=-10.717564 B=0 C=0 D=0
K-STOIC 2 A=-14.585564 B=0 C=0 D=0
K-STOIC 3 A=-10.532563 B=0 C=0 D=0
K-STOIC 9 A=-19.535563 B=0 C=0 D=0
K-STOIC 10 A=216.050446 B=-12431.700195 C=-35.481899 D=0
K-STOIC 11 A=231.465439 B=-12092.099609 C=-36.781601 D=0
K-STOIC 12 A=-9.741963 B=-8585.469727 C=0 D=0
K-STOIC 13 A=214.582443 B=-12995.400391 C=-33.5471 D=0
K-STOIC 14 A=132.89888 B=-13445.900391 C=-22.477301 D=0
SALT SALT13 CA++ 1 / SO4-- 1 / H2O 2
SALT SALT12 H2O 0.5 / CA++ 1 / SO4-- 1
SALT "CASO4(S)" CA++ 1 / SO4-- 1
SALT "CALCI(S)" CAOH+ 1 / OH- 1
SALT SALT4 H2O 1 / FE2+ 1 / SO4-- 1
SALT SALT3 FE2+ 1 / SO4-- 1 / H2O 4
SALT SALT2 FE2+ 1 / SO4-- 1 / H2O 7
SALT "FESO4(S)" FE2+ 1 / SO4-- 1
SALT SALT9 H2O 1 / MG++ 1 / SO4-- 1
SALT SALT8 MG++ 1 / SO4-- 1 / H2O 6
SALT "CACO3(S)" CO3-- 1 / CA++ 1
SALT SALT7 CO3-- 1 / MG++ 1 / H2O 3
SALT "MGCO3(S)" CO3-- 1 / MG++ 1
SALT SALT1 "FE(OH)2+" 1 / OH- 1
SALT "IRON-(S)" FEOH+ 1 / OH- 1
SALT SALT6 AL+++ 2 / SO4-- 3 / H2O 6
SALT SALT5 MG++ 1 / SO4-- 1 / H2O 7
SALT "MAGNE(S)" OH- 1 / MGOH+ 1
SALT "ALUMI(S)" AL+++ 2 / SO4-- 3
SALT "MGSO4(S)" MG++ 1 / SO4-- 1
K-SALT SALT13 A=354.905609 B=-14056.379883 C=-59.450218  &
   D=0.042882
K-SALT SALT4 A=1723.050049 B=-52834.378906 C=-292.391815  &
   D=0.363675
K-SALT SALT3 A=2139.059082 B=-64624.421875 C=-365.817291  &
   D=0.500447
K-SALT SALT2 A=-1023.346008 B=22212.589844 C=182.535202  &
   D=-0.350806
K-SALT SALT9 A=462.093811 B=-19508.289063 C=-72.651291  &
   D=0.019189
K-SALT SALT8 A=-161.838593 B=-602.626282 C=32.31744  &
   D=-0.110798
K-SALT SALT5 A=-438.810211 B=5068.070801 C=83.042549  &
   D=-0.215346
```

```
FLOWSHEET
   BLOCK BIOREACT IN=3-1 OUT=4
   BLOCK MIX IN=1 2 7 OUT=3
   BLOCK RECYCLE IN=6 OUT=10 7
   BLOCK PRECIP IN=5 OUT=9 6
   BLOCK FLASH IN=4 OUT=8 5
   BLOCK HX1 IN=3 OUT=3-1

PROPERTIES ELECNRTL HENRY-COMPS=GLOBAL CHEMISTRY=GLOBAL  &
      TRUE-COMPS=YES
   PROPERTIES ENRTL-HF / NRTL

SP-ROUTE DHVMX01 DHVMX 1 DHVMX01
   MODEL ESRK

MP-ROUTE PHIVMX01 PHIVMX 1 PHIVMX01
   MODEL ESRK

MP-ROUTE VVMX01 VVMX 1 VVMX01
   MODEL ESRK

ESTIMATE ALL

PROP-DATA PCES-1
   IN-UNITS MET
   PROP-LIST DGAQHG / DHAQHG / S25HG / OMEGHG / DHVLB /  &
      VB / RGYR / VLSTD
   PVAL H2SO4 -1.7782794E+5 / -2.1717541E+5 / 4.800802522 /  &
      26729.66466 / 13890.79966 / 65.75890000 / 2.5372000E-10 / &
      53.46030000
   PROP-LIST DGAQHG / DHAQHG / S25HG / OMEGHG / VB / RGYR / &
      VLSTD
   PVAL SALT1 -1.5747110E+5 / -1.7401020E+5 / 71.35961498 /  &
      -74067.00081 / 140.9030000 / 3.1820000E-10 / 0.0
   PVAL "MGSO4(S)" -2.8953138E+5 / -3.2387504E+5 /  &
      -1.695805866 / 36568.12840 / 140.9030000 /  &
      3.1820000E-10 / 0.0
   PROP-LIST VLSTD / RKTZRA
   PVAL XYLOSE 82.21587830 / .1973153540
   PVAL FES 298.9063450 / .2918596200
   PVAL FEO 298.9063450 / .2918596200
   PVAL FE2O3 298.9063450 / .2918596200
   PVAL MAGNE-01 298.9063450 / .2918596200
   PVAL "CALCI(S)" 298.9063450 / .2918596200
   PVAL "MAGNE(S)" 298.9063450 / .2918596200
   PVAL "MGCO3(S)" 298.9063450 / .2918596200
   PVAL "CACO3(S)" 298.9063450 / .2918596200
   PVAL "CASO4(S)" 298.9063450 / .2918596200

PROP-DATA MULAND-1
   IN-UNITS MET
   PROP-LIST MULAND
   PVAL XYLOSE 233.1213903 -17221.59180 -32.14621760  &
      575.2930000 763.2900000
   PVAL FES 80.95127588 -12127.32210 -10.25255770 1400.000000  &
      1980.000000
```

```
   PVAL FEO 80.85039868 -12127.32210 -10.25255770 1400.000000  &
      1980.000000
   PVAL FE2O3 81.24975968 -12127.32210 -10.25255770  &
      1400.000000 1980.000000
   PVAL MAGNE-01 81.43551038 -12127.32210 -10.25255770  &
      1400.000000 1980.000000

PROP-DATA MULAND-1
   IN-UNITS MET
   PROP-LIST MULAND
   PVAL "CALCI(S)" 80.86581028 -12127.32210 -10.25255770  &
      1400.000000 1980.000000
   PVAL "MAGNE(S)" 80.74610878 -12127.32210 -10.25255770  &
      1400.000000 1980.000000
   PVAL "MGCO3(S)" 80.93045408 -12127.32210 -10.25255770  &
      1400.000000 1980.000000
   PVAL "CACO3(S)" 81.01616808 -12127.32210 -10.25255770  &
      1400.000000 1980.000000
   PVAL "CASO4(S)" 81.16998398 -12127.32210 -10.25255770  &
      1400.000000 1980.000000

PROP-DATA SIGDIP-1
   IN-UNITS MET
   PROP-LIST SIGDIP
   PVAL XYLOSE 112.1969930 1.222222220 1.31487342E-9  &
      -1.4789984E-9 5.8066956E-10 575.2930000 755.5800000

PROP-DATA HOCETA-1
   IN-UNITS ENG
   PROP-LIST HOCETA
   BPVAL H2O H2O 1.700000000
   BPVAL H2O H2S .7000000000
   BPVAL H2O CO2 .3000000000
   BPVAL H2S H2O .7000000000
   BPVAL H2S CO2 .1000000000
   BPVAL CO2 H2O .3000000000
   BPVAL CO2 H2S .1000000000
   BPVAL CO2 CO2 .1600000000

PROP-DATA HENRY-1
   IN-UNITS ENG PRESSURE=psi PDROP=psi
   PROP-LIST HENRY
   BPVAL H2S H2O 381.6601370 -23826.24000 -55.05510000  &
      .0330916666 31.73000000 301.7300000 0.0
   BPVAL CO2 H2O 174.7803680 -15259.87980 -21.95743000  &
      3.21152667E-3 31.73000000 440.3300000 0.0
   BPVAL O2 H2O 157.8962298 -13995.10800 -18.39740000  &
      -5.2464111E-3 33.53000000 166.7300000 0.0

PROP-DATA NRTL-1
   IN-UNITS ENG
   PROP-LIST NRTL
   BPVAL H2O H2S -3.674000000 2080.620000 .2000000000 0.0 0.0  &
      0.0 32.00000000 302.0000000
   BPVAL H2S H2O -3.674000000 2080.620000 .2000000000 0.0 0.0  &
      0.0 32.00000000 302.0000000
   BPVAL H2O CO2 10.06400000 -5882.643000 .2000000000 0.0 0.0  &
```

```
      0.0 32.00000000 392.0000000
   BPVAL CO2 H2O 10.06400000 -5882.643000 .2000000000 0.0 0.0  &
      0.0 32.00000000 392.0000000

PROP-DATA VLCLK-1
   IN-UNITS ENG
   PROP-LIST VLCLK
   BPVAL H3O+ HSO4- .8778750658 .3242692828

PROP-DATA GMELCC-1
   IN-UNITS ENG
   PROP-LIST GMELCC
   PPVAL H2O ( H3O+ HS- ) 8.045000000
   PPVAL ( H3O+ HS- ) H2O -4.072000000
   PPVAL H2O ( H3O+ HCO3- ) 8.045000000
   PPVAL ( H3O+ HCO3- ) H2O -4.072000000
   PPVAL H2O ( H3O+ HSO4- ) 6.362000000
   PPVAL ( H3O+ HSO4- ) H2O -3.749000000
   PPVAL H2O ( H3O+ S-- ) 8.045000000
   PPVAL ( H3O+ S-- ) H2O -4.072000000
   PPVAL H2O ( H3O+ CO3-- ) 8.045000000
   PPVAL ( H3O+ CO3-- ) H2O -4.072000000
   PPVAL H2O ( H3O+ SO4-- ) 8.000000000
   PPVAL ( H3O+ SO4-- ) H2O -4.000000000
   PPVAL H2SO4 ( H3O+ HSO4- ) 12.99200000
   PPVAL ( H3O+ HSO4- ) H2SO4 -2.981000000
   PPVAL H2SO4 ( H3O+ SO4-- ) 8.000000000
   PPVAL ( H3O+ SO4-- ) H2SO4 -4.000000000
   PPVAL H2S ( H3O+ HS- ) 15.00000000
   PPVAL ( H3O+ HS- ) H2S -8.000000000
   PPVAL H2S ( H3O+ HCO3- ) 15.00000000
   PPVAL ( H3O+ HCO3- ) H2S -8.000000000
   PPVAL H2S ( H3O+ S-- ) 15.00000000
   PPVAL ( H3O+ S-- ) H2S -8.000000000
   PPVAL H2S ( H3O+ CO3-- ) 15.00000000
   PPVAL ( H3O+ CO3-- ) H2S -8.000000000
   PPVAL CO2 ( H3O+ HS- ) 15.00000000
   PPVAL ( H3O+ HS- ) CO2 -8.000000000
   PPVAL CO2 ( H3O+ HCO3- ) 15.00000000
   PPVAL ( H3O+ HCO3- ) CO2 -8.000000000
   PPVAL CO2 ( H3O+ S-- ) 15.00000000
   PPVAL ( H3O+ S-- ) CO2 -8.000000000
   PPVAL CO2 ( H3O+ CO3-- ) 15.00000000
   PPVAL ( H3O+ CO3-- ) CO2 -8.000000000
   PPVAL H2O ( FE2+ SO4-- ) 7.745000000
   PPVAL ( FE2+ SO4-- ) H2O -3.912000000
   PPVAL H2O ( H3O+ OH- ) 8.045000000
   PPVAL ( H3O+ OH- ) H2O -4.072000000
   PPVAL CO2 ( H3O+ OH- ) 15.00000000
   PPVAL ( H3O+ OH- ) CO2 -8.000000000
   PPVAL H2S ( H3O+ OH- ) 15.00000000
   PPVAL ( H3O+ OH- ) H2S -8.000000000
   PPVAL H2O ( MG++ SO4-- ) 8.017000000
   PPVAL ( MG++ SO4-- ) H2O -4.031000000

PROP-DATA GMELCD-1
   IN-UNITS ENG
```

```
    PROP-LIST GMELCD
    PPVAL H2O ( H3O+ HSO4- ) 3524.760000
    PPVAL ( H3O+ HSO4- ) H2O -1049.760000
    PPVAL H2O ( H3O+ SO4-- ) 0.0
    PPVAL ( H3O+ SO4-- ) H2O 0.0
    PPVAL H2SO4 ( H3O+ HSO4- ) -3119.220000
    PPVAL ( H3O+ HSO4- ) H2SO4 -292.1400000
    PPVAL H2SO4 ( H3O+ SO4-- ) 0.0
    PPVAL ( H3O+ SO4-- ) H2SO4 0.0
    PPVAL H2S ( H3O+ HS- ) 0.0
    PPVAL ( H3O+ HS- ) H2S 0.0
    PPVAL H2S ( H3O+ HCO3- ) 0.0
    PPVAL ( H3O+ HCO3- ) H2S 0.0
    PPVAL H2S ( H3O+ S-- ) 0.0
    PPVAL ( H3O+ S-- ) H2S 0.0
    PPVAL H2S ( H3O+ CO3-- ) 0.0
    PPVAL ( H3O+ CO3-- ) H2S 0.0
    PPVAL CO2 ( H3O+ HS- ) 0.0
    PPVAL ( H3O+ HS- ) CO2 0.0
    PPVAL CO2 ( H3O+ HCO3- ) 0.0
    PPVAL ( H3O+ HCO3- ) CO2 0.0
    PPVAL CO2 ( H3O+ S-- ) 0.0
    PPVAL ( H3O+ S-- ) CO2 0.0
    PPVAL CO2 ( H3O+ CO3-- ) 0.0
    PPVAL ( H3O+ CO3-- ) CO2 0.0
    PPVAL CO2 ( H3O+ OH- ) 0.0
    PPVAL ( H3O+ OH- ) CO2 0.0
    PPVAL H2S ( H3O+ OH- ) 0.0
    PPVAL ( H3O+ OH- ) H2S 0.0

PROP-DATA GMELCE-1
    IN-UNITS ENG
    PROP-LIST GMELCE
    PPVAL H2O ( H3O+ HSO4- ) -4.599000000
    PPVAL ( H3O+ HSO4- ) H2O 4.472000000
    PPVAL H2SO4 ( H3O+ HSO4- ) -30.12600000
    PPVAL ( H3O+ HSO4- ) H2SO4 .8060000000
    PPVAL H2S ( H3O+ HS- ) 0.0
    PPVAL ( H3O+ HS- ) H2S 0.0
    PPVAL H2S ( H3O+ HCO3- ) 0.0
    PPVAL ( H3O+ HCO3- ) H2S 0.0
    PPVAL H2S ( H3O+ S-- ) 0.0
    PPVAL ( H3O+ S-- ) H2S 0.0
    PPVAL H2S ( H3O+ CO3-- ) 0.0
    PPVAL ( H3O+ CO3-- ) H2S 0.0
    PPVAL CO2 ( H3O+ HS- ) 0.0
    PPVAL ( H3O+ HS- ) CO2 0.0
    PPVAL CO2 ( H3O+ HCO3- ) 0.0
    PPVAL ( H3O+ HCO3- ) CO2 0.0
    PPVAL CO2 ( H3O+ S-- ) 0.0
    PPVAL ( H3O+ S-- ) CO2 0.0
    PPVAL CO2 ( H3O+ CO3-- ) 0.0
    PPVAL ( H3O+ CO3-- ) CO2 0.0
    PPVAL CO2 ( H3O+ OH- ) 0.0
    PPVAL ( H3O+ OH- ) CO2 0.0
    PPVAL H2S ( H3O+ OH- ) 0.0
    PPVAL ( H3O+ OH- ) H2S 0.0
```

```
PROP-DATA GMELCN-1
  IN-UNITS ENG
  PROP-LIST GMELCN
  PPVAL H2O ( H3O+ HSO4- ) .2000000000
  PPVAL H2SO4 ( H3O+ HSO4- ) .2000000000
  PPVAL H2S ( H3O+ HS- ) .1000000000
  PPVAL H2S ( H3O+ HCO3- ) .1000000000
  PPVAL H2S ( H3O+ S-- ) .1000000000
  PPVAL H2S ( H3O+ CO3-- ) .1000000000
  PPVAL CO2 ( H3O+ HS- ) .1000000000
  PPVAL CO2 ( H3O+ HCO3- ) .1000000000
  PPVAL CO2 ( H3O+ S-- ) .1000000000
  PPVAL CO2 ( H3O+ CO3-- ) .1000000000
  PPVAL CO2 ( H3O+ OH- ) .1000000000
  PPVAL H2S ( H3O+ OH- ) .1000000000

PROP-SET COD CODMX UNITS='ppm' SUBSTREAM=MIXED

PROP-SET MASSCONC MASSCONC UNITS='gm/l' SUBSTREAM=MIXED PHASE=L
;  "Mass concentration (component mass/liquid volume)"


PROP-SET PH PH SUBSTREAM=MIXED PHASE=L
;  "pH at current temperature"


STREAM 1
  SUBSTREAM MIXED TEMP=303.1500000 PRES=1.000000000  &
    MASS-FLOW=4.72032002E+5 SOLVENT=H2O FREE-WATER=NO  &
    NPHASE=1 PHASE=L
  MASS-CONC H3O+ 1. / XYLOSE 40. / SO4-- 12.10000000 /  &
    FE2+ 4.29 / CA++ 0.592 / AL+++ 0.396 / MG++ 0.474

STREAM 2
  SUBSTREAM MIXED TEMP=293.1500000 PRES=1.000000000  &
    MASS-FLOW=2000000. SOLVENT=H2O FREE-WATER=NO NPHASE=1  &
    PHASE=L
  MASS-CONC H3O+ 1.000000000 / SO4-- 12.10000000 / FE2+  &
    4.290000000 / CA++ 0.592 / AL+++ 0.396 / MG++ 0.474

BLOCK MIX MIXER
  PARAM PRES=1.000000000
  PROPERTIES ELECNRTL HENRY-COMPS=GLOBAL CHEMISTRY=GLOBAL  &
    FREE-WATER=STEAM-TA SOLU-WATER=3 TRUE-COMPS=YES

BLOCK RECYCLE FSPLIT
  FRAC 10 0.2

BLOCK PRECIP SEP
  PARAM
  FRAC STREAM=9 SUBSTREAM=MIXED COMPS=IRON FES FEO FE2O3  &
    MAGNE-01 IRON--01 "FEO(O-01" "IRON-(S)" SALT1 "FESO4(S)"  &
    SALT2 SALT3 SALT4 CALCI-01 ALUMI-01 MAGNE-02 "CALCI(S)"  &
    "MGSO4(S)" "ALUMI(S)" "MAGNE(S)" SALT5 SALT6 "MGCO3(S)"  &
    SALT7 "CACO3(S)" SALT8 SALT9 "CASO4(S)" SALT12 SALT13  &
    FRACS=1. 1. 1. 1. 1. 1. 1. 1. 1. 1. 1. 1. 1. 1.  &
```

```
      1. 1. 1. 1. 1. 1. 1. 1. 1. 1. 1. 1. 1. 1. 1.  &
      1.

BLOCK FLASH FLASH2
   PARAM TEMP=35. <C> PRES=1.

BLOCK HX1 HEATX
   PARAM T-COLD=35. <C>
   FEEDS COLD=3
   OUTLETS-COLD 3-1
   REFERENCE HOT-UTIL=U-1

BLOCK BIOREACT RSTOIC
   PARAM TEMP=308.1500000 PRES=1.000000000 SERIES=YES  &
      HEAT-OF-REAC=NO
   STOIC 1 MIXED HSO4- -1. / H2O -1. / SO4-- 1. / H3O+  &
      1.
   STOIC 2 MIXED XYLOSE -1. / SO4-- -2.5 / CO2 5. / H2O  &
      5. / S-- 2.5
   STOIC 3 MIXED FE2+ -1. / S-- -1. / FES 1.
   STOIC 4 MIXED CA++ -1. / S-- -1. / CALCI-01 1.
   STOIC 5 MIXED AL+++ -2. / S-- -3. / ALUMI-01 1.
   STOIC 6 MIXED MG++ -1. / S-- -1. / MAGNE-02 1.
   CONV 1 MIXED HSO4- 0.
   CONV 2 MIXED SO4-- 0.8
   CONV 3 MIXED FE2+ 0.7
   CONV 4 MIXED CA++ 0.5
   CONV 5 MIXED AL+++ 0.5
   CONV 6 MIXED MG++ 0.5

UTILITY U-1 GENERAL
   DESCRIPTION  &
      "Low Pressure Steam, Inlet Temp=125 C, Outlet Temp=124 C"
   COST ENERGY-PRICE=6.15 <$/GJ>
   PARAM UTILITY-TYPE=STEAM TIN=398.1500000 TOUT=397.1500000  &
      VFRAC=1. VFR-OUT=0. CALOPT=FLASH MIN-TAPP=10.00000000  &
      CALCCO2=YES FACTORSOURCE="US-EPA-Rule-E9-5711" FUELSOURCE= &
      "Natural_gas" CO2FACTOR=2.34000000E-7 EFFICIENCY=0.85  &
      HTC=.1433075380

DESIGN-SPEC DS-1
   DEFINE XYLOSE MASS-FRAC STREAM=4 SUBSTREAM=MIXED  &
      COMPONENT=XYLOSE
   SPEC "XYLOSE" TO "0.001"
   TOL-SPEC "0.0005"
   VARY STREAM-VAR STREAM=2 SUBSTREAM=MIXED VARIABLE=MASS-FLOW  &
      UOM="kg/hr"
   LIMITS "1e6" "3e6"

DESIGN-SPEC DS-2
   DEFINE PH3 STREAM-PROP STREAM=3-1 PROPERTY=PH
   SPEC "PH3" TO "3"
   TOL-SPEC "0.6"
   VARY BLOCK-VAR BLOCK=RECYCLE SENTENCE=FRAC VARIABLE=FRAC  &
      ID1=10
   LIMITS "0.05" "0.95"
```

```
EO-CONV-OPTI

CALCULATOR SRB
   DEFINE SO43 MASS-FLOW STREAM=3 SUBSTREAM=MIXED  &
      COMPONENT=SO4-- UOM="kg/hr"
   DEFINE HSO43 MASS-FLOW STREAM=3 SUBSTREAM=MIXED  &
      COMPONENT=HSO4- UOM="kg/hr"
   DEFINE SO44 MASS-FLOW STREAM=4 SUBSTREAM=MIXED  &
      COMPONENT=SO4-- UOM="kg/hr"
   DEFINE HSO44 MASS-FLOW STREAM=4 SUBSTREAM=MIXED  &
      COMPONENT=HSO4- UOM="kg/hr"
   DEFINE V3 STREAM-VAR STREAM=3 SUBSTREAM=MIXED  &
      VARIABLE=MASS-FLOW UOM="kg/hr"
   DEFINE RSO4 PARAMETER 1 PHYS-QTY=USR-DUMMY0 INIT-VAL=30.
   DEFINE SRBT PARAMETER 2 PHYS-QTY=TIME UOM="day"
   DEFINE SRBVOL PARAMETER 3 PHYS-QTY=VOLUME UOM="cum"
   DEFINE SO4OUT PARAMETER 4 PHYS-QTY=USR-DUMMY0
   DEFINE SO4IN PARAMETER 5 PHYS-QTY=USR-DUMMY0
   DEFINE DSO4 PARAMETER 6 PHYS-QTY=USR-DUMMY0
F    SO4IN=SO43+HSO43*96/97
F    SO4OUT=SO44+HSO44*96/97
F    DSO4=(SO4IN-SO4OUT)*1000/V3
F    SRBT=(DSO4)/RSO4
F    SRBVOL=SRBT*V3*24/1000
F
F
F
c     V6=MASS6/DENS6
c     C6=SO4OUT/V6
c     C3=C6/(1-XSO4)
c     DC=C3-C6
c     SRBT=DC/RSO4
c     SRBVOL=SRBT*(V6*24)
   READ-VARS RSO4 SO43 SO44 HSO43 HSO44 V3
   WRITE-VARS SRBT SRBVOL SO4OUT SO4IN DSO4

SENSITIVITY S-1
   DEFINE SRBVOL PARAMETER 3 PHYS-QTY=VOLUME UOM="cum"
   TABULATE 1 "SRBVOL"
   VARY PARAMETER 1 PHYS-QTY=USR-DUMMY0
   RANGE LOWER="3" UPPER="30" INCR="1.000000"

CONV-OPTIONS
   WEGSTEIN MAXIT=41

STREAM-REPOR MOLEFLOW MASSFLOW MASSFRAC PROPERTIES=PH COD  &
      MASSCONC

PROPERTY-REP PCES NOPROP-DATA NODFMS NOPARAM-PLUS
;
;
;
;
;
```